867

A Proposal to Continue the Study of Hidden Charm and Beauty States by Triggering on High Transverse Momentum Single Muons and High Mass Dimuons in 800 GeV/c pN Interactions

September 3, 1992

T.Alexopoulos[20], L.Antoniazzi[13], M.Arenton[19], A.Asmolov[3], S.Bagdasarov[21], C.Ballagh[1], H.Bingham[1], A. Blankman[15], M.Block[12], A.Boden[2], G.Bonomi[13], J.Budagov[3], Z.L. Cao[19], D.Chapman[1], T.Y.Chen[11], G.Chlachidze[8], K.Clark[16], D.Cline[2], S.Conetti[19], M.Cooper[18], G.Corti[19], B.Cox[19], P.Creti[9], D.Djincharadze[8], C.Dukes[19], C. Durandet[20], V. Elia[9], A.Erwin[20], V.Flyagine[7], L.Fortney[4], V.Geger[3], V.Glagolev[3], V.Golovatyuk[19], E.Gorini[9], F.Grancagnolo[9], M.Haire[14], K.Hagan-Ingram[19], P.Hanlet[19], M.Jenkins[16], J.Jennings[20], M.He[17], G.Introzzi[13], D.J.Judd[14], W.Kononeko[15], W.Kowald[4], A.Kurilin[7], V.Kushpil[3], A.Lanza[13], K.Lau[6], T.Lawry[19], A.Ledovskoy[19], G.Liguori[13], J.Lys[1], N.Malakhov[3], S.Maliukov[3], P.O.Mazur[5], A.McManus[19], G.Mescheriakov[3], I.Minashivili[8], S.Misawa[1], G.H.Mo[6], C.T.Murphy[5], K.S.Nelson[19], M.Panareo[9], P.Pistilli[9], V.Pogosian[19], S.Ramachadran[2], S.Ratti[13], M. Recagni[19], M.Reynolds[19], J.Rhoades[2], W.J.Robertson[4], V.Rumiantsev[7], W.Selove[15], J.Segal[19], R.P.Smith[5], L.Spiegel[5], J.G.Sun[19], S.Tokar[3], P.Torre[13], J.Trischuk[10], E.Tsyganov[3], L.Turnbull[14], I.Tzamouranis[19], A.Vaganov[3], A.Volodko[3], W.Yang[5], N.Yao[11], D.E.Wagoner[14], C.R.Wang[17], C.Wei[4], N.J.Zhang[17], B.Zou[4]

(1) University of California at Berkeley, Berkeley, CA 94720
(2) University of California at Los Angeles, Los Angeles, CA 90024
(3) Joint Institute for Nuclear Research, Dubna, Russia
(4) Duke University, Durham, NC 27706
(5) Fermilab, Batavia, IL 60510
(6) University of Houston, Houston, TX 77204-5504
(7)Institute of Physics, Belorussia Academy of Science, Minsk, Belorussia
(8) IHEP, Tbilisi State University, Tbilisi, Georgia
(9) University of Lecce/INFN, Lecce, Italy
(10) McGill University, Montreal, Canada, PQ H3A 2T8
(11) Nanking University, PRC
(12) Northwestern University, Evanston, IL 60208
(13) University of Pavia/INFN, Pavia, Italy
(14) Prairie View A&M University, Prairie View, TX 77446-0355
(15) University of Pennsylvania, Philadelphia, PA 19104
(16) University of South Alabama, Mobile AL 36688
(17) Shandong University, PRC
(18) Vanier College, Montreal, Canada PQ H3A 2T8
(19) University of Virginia, Charlottesville, VA 22901
(20) University of Wisconsin, Madison, WI 53706
(21)Yerevan State University, Yerevan, Armenia

Contact: B. Cox Dept. of Physics
Univ. of Virginia
804-982-5377

Table of Contents

I. Introduction

In a short data taking run of Fermilab Experiment E771 in 1991, we began the process of studying hadronic interactions which contain either a high p_t single muon or a high mass dimuon pair in our large aperture, open geometry spectrometer shown in Fig.1. Such interactions contain a significant number of B->J/Ψ and B->μ decays as well as hidden charm states decaying into J/Ψ and Ψ'. With the much larger data sample that can be obtained in the 1994 Fermilab fixed target run as outlined in Section III, B total and differential cross sections, B lifetimes for the various B species ($B_{u,d,s}$), b->u transitions, B_d and B_s mixing and oscillations and Λ_b production and decay can be studied. The physics that becomes accessible with our projected yields is discussed in more detail in Section IV.

Our projections for the expected yields of B decays discussed in this proposal are based, to a large extent, on extrapolations from a very short run, approximately 6.6×10^5 seconds of beam in a three week period at the end of the 1991 Fermilab fixed target period, where we obtained approximately 60 million single muon triggers with $p_t > 0.8$ GeV/c and 110 million dimuon triggers. A preliminary examination of the small fraction (0.2%) of the dimuon triggers processed to date is presented in Appendix A.

In addition to beauty physics, the physics of hidden charm states that decay into Ψ or Ψ' (followed by a subsequent decay into dimuons) can be studied with much greater statistics than heretofore possible. In Section IV.B and Appendix B, we discuss our tentative observations[1] of the $^1P_1$ and $^3D_2$ charmonium states in E705 which could be confirmed by a high statistics 1994 run. In addition, the study of production and decay of the charmonium χ->$\gamma\Psi$ can be continued with better resolution and higher statistics. We propose in the 1994 run to continue the study[2] of such final states.

We expect to obtain much more data than previously accumulated in either E705 or E771 because of the following factors:

1. Longer data taking time anticipated in the 1994 fixed target run; 5.1×10^6 seconds of beam in 1994 versus 6.6×10^5 seconds in 1991, a factor of 8 increase.

2. Better trigger efficiency and acceptance; 21.2% for dimuons and 15.6% for single muons in the 1994 run versus 8.2% and 5.3% in the 1991 run, a factor of 2.9 and 2.6 for single and dimuons respectively; See Appendix D for more detail.

3. Operation at rates $\geq 5 \times 10^6$ int/sec as compared to an average of $2\text{-}3 \times 10^6$ ints/sec in the 1991 run, a factor of two increase.

4. Better reconstruction efficiencies of muons and other decay products from either beauty or charm decay due to the completion of the instrumentation of all planes of the E771 silicon beam/microvertex detector and the optimization of the efficiencies of all other wire planes. The details of the 1994 improvements of the silicon microvertex detector and the muon Resistive Plate Chamber systems are given in Appendix C and D respectively. Increases averaging approximately 1.5 to 3 are expected in overall reconstruction efficiency for the selected B decays.

5. More powerful trigger system leading to greater live time for the data acquisition system (80% live time in 1994 vs. 60% in 1991, a factor of 1.3).

Finally, there has been discussion of operation of the Fermilab fixed target program at a higher energy, (900 GeV/c vs. 800 GeV/c in 1991). If that were to come to pass, the yields of B events would increase by a factor of 1.3 due to the expected rise in the B hadroproduction cross section. However, for purposes of this proposal we have estimated all yields assuming operation at 800 GeV/c in 1994.

Combining factors one through five together and considering other improvements planned for the 1994 run, we expect to accumulate ≥100 and ≥110 times as much dimuon and single muon data respectively in the 1994 as we were able to obtain in the very short 1991 run. The spectrometer as shown in Fig. 1 below remains essentially the same as in the 1991 run with the possible addition of a Ring Imaging Cerenkov counter. As discussed in Section IV, most of the physics outlined here can be accomplished to some level without a RICH. However, it will both enhance statistics by making more modes accessible and reduce backgrounds to several B_S modes, thereby enhancing our capability of measuring B_S physics.

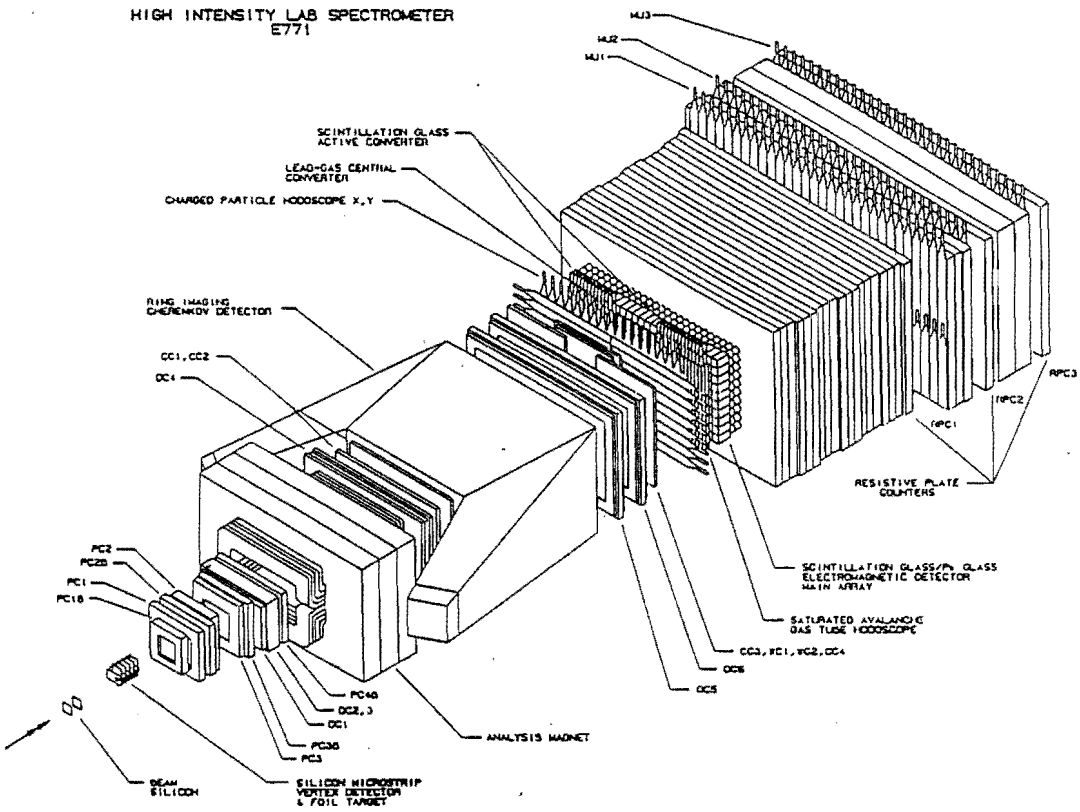

Fig. 1
1994 Spectrometer Configuration

II. 1994 Operating Conditions

Table II.A.1 summarizes the running conditions which we anticipate for the 1994 run in comparison to the conditions of the 1991 run. For purposes of this proposal, we have used an interaction length for the 12 silicon target foils calculated from the inelastic total cross section, σ_T(pN), of 32 mb at 800 GeV/c. We have used an A dependence of $A^{0.71}$ from A. Carroll et al.[3] to scale to a σ_T(pSi) ≈ 342 mb. This results in the 4.10% target interaction length given in Table II.

Table II
1991/1994 Run Conditions

	1991 Run	1994 Run
Proton Beam Momentum	800 GeV/c	800 GeV/c
Running Time	6.6×10^5 seconds*	5.1×10^6 seconds**
Spill Length	≈22 sec. every 57 sec.	≈22 sec. every 57 sec.
Target Material	2 mm Si foils (12)	2 mm Si foils (12)
Target Radiation Length	25.6%	25.6%
Target Interaction Length from σ_T(pSi)	4.10%	4.10%
Average Interactions/Second in Target	1.9×10^6	$\geq5\times10^6$
Beam/Second	4.6×10^7	$\geq1.2\times10^8$
Beam σ_x,σ_y	2.3 mm, 1.8 mm	4.0 mm, 4.0 mm
Total "Usable" Integrated Beam	3.0×10^{13}	$\geq6.1\times10^{14}$
Total Integrated Beam/cm^2 ($<\pm\sigma_{x,y}$)	$\approx3.3\times10^{14}$/cm^2***	$\geq8.2\times10^{14}$/cm^2
Total Integrated Interactions in Target	1.2×10^{12}	$\geq2.5\times10^{13}$

* In the 1991 run, the silicon electronics installation and threshold setting were completed (save for beam silicon detector installation) on approximately Dec. 4, 1991. Various silicon and trigger studies were complete and stable running conditions were achieved on the weekend of December 20th. We have assumed in our summation of "usable" beam for the 1991 run that we can utilize almost all beam taken between December 4th and January 4th when special running and calibrations began. The percentage of the integrated beam which was live is introduced into the yield calculations in the trigger discussion in Section III.B below.

** Based on a 10 month run as indicated on the July 1992 Fermilab long range schedule; Scaling from our 1991 run experience, this amount would require 7.5 months out of the ten months of scheduled time leaving 2.5 months for tune up of the spectrometer and electronics.

*** In estimating the amount of exposure of the silicon detector to beam during the 1991 run, we have used the total exposure, not just the beam that we presume to be usable for physics.

III. 1994 Beauty and Hidden Charm Yields in the 1994 Run

Our objective for the 1994 run is to accumulate the maximum numbers of inclusive and exclusive B decays of the types B->J/Ψ + x->μμ +x, semi-muonic B->μ and double semi-muonic BB->μμ, and hidden charm states-> J/Ψ or Ψ', as detected by the presence of high p_t single muon or high mass muon pairs. In the following pages, we estimate the numbers of several interesting inclusive and exclusive B modes produced (Section III.A), triggered on and logged to tape (Section III.B), fully accepted (Section III.C) and reconstructed (Section III.D). In Section III.E, we summarize the yields of reconstructed B and hidden charm decays obtained in each

category together with the fractions of the events produced in each decay modes which survive the trigger, acceptance and reconstruction losses.

As discussed in Appendix B, there have been tentative low statistics observations[1,4] of the $^1P_1$ and $^3D_2$ of hidden charm via their decay into J/Ψ and pions. Since the 1994 run will result in approximately two orders of magnitude more J/Ψ's than have been accumulated in the highest statistics experiments to date (Fermilab Experiment E705[5] and CERN Experiment WA11[6] with 24,000 and 45,000 reconstructed J/Ψ->μμ decays, respectively), it will be important to examine the 1994 J/Ψ and Ψ' data to see if these observations are confirmed. We summarize in Table III.F.1, reconstructed yields of the various interesting hidden charm final states expected in the 1994 run, obtained by scaling the numbers of events for the $^3D_2$ and $^1P_1$ candidates, the Ψ' and various χ states reconstructed in E705 at 300 GeV/c^2 (See Section IV.B.1 and IV.B.2). Since each of the final states in question is associated with a J/Ψ->μμ decay, this method takes into account A dependence and increase of cross sections due to increased beam energy, provided the ratio of production of the various states to overall J/Ψ production does not change. Additional yields which could be expected because of increases in reconstruction efficiencies have not been included in our charm estimates.

III.A. Production of J/Ψ-μμ, B->J/Ψ and B->μ Inclusive and Exclusive Decays

Our determination of the sensitivity for beauty and charmonium physics achievable in the 1994 run begins with an evaluation of the numbers of J/Ψ and B's produced and the number of decays into the selected inclusive and exclusive charm and beauty channels to be used in accomplishing the physics objectives outlined in Section IV.

III.A.1. Direct J/Ψ Production

We have used the Lyons parameterization[7] for J/Ψ production by protons

$$\sigma(pN\text{->}J/\Psi + x) = 1985\ e^{-17\sqrt{\tau}}\ \text{nb}$$

corrected to take into account a new measurement[8], 0.0591± 0.0011±0.0020, for the J/Ψ->μμ branching ratio. In addition, we use an A dependence of $A^{0.92}$ to estimate pSi ->J/Ψ+x cross sections at 800 GeV/c ($\sqrt{\tau}$=0.080) as given in Table III.A.1 below.

Table III.A.1
Production of J/Ψ->μμ Decays per Run

	1991	1994
J/Ψ Production Cross Section per Nucleon	509 nb	509 nb
J/Ψ Production Cross Section per Si Nucleus	11.0 μb	11.0 μb
Number of J/Ψ	4.0×10^7	8.0×10^8
Number of J/Ψ->μμ	2.4×10^6	4.8×10^7

III.A.2. Beauty Production

We have used the B hadroproduction cross section calculations of Berger[9] and an assumed A dependence of $A^{1.0}$ to estimate and compare the number of B's expected to be produced in the 1991 and 1994 runs. In estimating the number of the exclusive B decays from a particular state of the B mesons, we assume hadronization ratios for u/d/s of 2/2/1.

Table III.A.2
Production per Run of B Pairs

	1991	1994
B Pair Cross Section for pN	17 nb	17 nb
B Pair Production Cross Section for pSi	478 nb	478 nb
Number of B Pairs	1.7×10^6	$\geq3.5\times10^7$
Number of $B^{\pm}_u$	1.4×10^6	$\geq2.8\times10^7$
Number of B^0_d	1.4×10^6	$\geq2.8\times10^7$
Number of B^0_s	6.8×10^5	$\geq1.4\times10^7$

III.A.3. Production of Inclusive and Exclusive B-> J/Ψ->μμ +x Decays

The inclusive and exclusive B-> J/Ψ modes are very interesting since they are both relatively easy to trigger on and are less vulnerable to backgrounds than other B decays. We have estimated the numbers of several inclusive and exclusive B-> J/Ψ decays produced in the 1991 run and expected from a 1994 run, from which various B physics issues including cross sections, lifetimes and branching ratios can be addressed (see Section IV).

Measurements of the cross sections and lifetimes can be accomplished in a way which averages over the B species by studies of the inclusive B-> J/Ψ->μμ decays themselves. In estimating the number of B->J/Ψ inclusive decays produced per run, we have used 1.12% for the branching ratio[10] for B–>J/Ψ and 5.91% for the J/Ψ->μμ decay leading to a composite branching ratio of 6.62×10^{-4}. It should be kept in mind that this value for the inclusive B->J/Ψ rate could be different in our case due to contributions from B^0_s decays not present in the ARGUS and CLEO experiments.

For the studies of the B^0_d, we have selected, as examples of accessible J/Ψ exclusive decay modes, B^0_d->ΨK^0_s, B^0_d->ΨKπ and B^0_d->Ψ'K^*(890). To estimate the production of the B^0_d->ΨK^0_s decay, we use a branching ratio[11] of 6.5×10^{-4} in combination with 68.6% for the K^0_s->$\pi^+\pi^-$ decay[12] giving a composite branching ratio of 2.6×10^{-5} for the sequence B^0_d->ΨK^0_s->μμ$\pi^+\pi^-$. A larger yield of B^0_d can be obtained using the B^0_d->Ψ$K^+\pi^-$ which has a branching ratio of 1.0×10^{-3} resulting in a composite branching ratio of 5.9×10^{-5} for the final state μμ$K^+\pi^-$ Finally, we should also be able to observe some B->Ψ' modes. As an example, we consider B^0_d->Ψ'K^*(890)->Ψ'$K^+\pi^-$ which has a branching ratio[13] of 1.4×10^{-3} leading to a composite branching ratio of 1.1×10^{-5} for the μμKπ final state (when the Ψ'->μμ) and 2.7×10^{-5} for the μμππKπ (when the Ψ'->Ψππ->ππμμ) .

We can search for B^0_s via its decay into Ψφ. We are able to estimate our sensitivity for this mode even though it has not yet been observed since the branching ratio for the B^0_s->Ψφ decay should be approximately equal[14] to that of the $B^{\pm}_u$->ΨK^* decay, measured[15] to be 1.4×10^{-3}. Using this and the φ->K^+K^- decay branching ratio[16] of 49.1%, we obtain a composite branching ratio of 4.1×10^{-5} for the B^0_s->Ψφ->μμK^+K^- sequence. We point out that the B^0_s should also

have decay modes analogous to the B^0_d->Ψ $K^{\pm}$ plus charged pion. We intend to search for such modes of the B^0_s and expect to completely reconstruct a considerable number of such decays to add to the $\Psi\phi$ observation and allow relative branching ratio determinations.

For studies of the $B^{\pm}_u$ we have chosen the B->$\Psi K^{\pm}$ and $\Psi K^{\pm}\pi^+\pi^-$ modes to demonstrate the sensitivity to $B^{\pm}$ physics issues such as lifetime determination using J/Ψ exclusive modes. To estimate the production of $B^{\pm}_u$->$\Psi K^{\pm}$->$\mu\mu K^{\pm}$, we use the branching ratio[17] 7.7×10^{-4} for the $B^{\pm}_u$->$\Psi K^{\pm}$ decay, resulting in a composite branching ratio of 4.55×10^{-5} for the entire chain. For the $B^{\pm}_u$->$\Psi K^{\pm}\pi^+\pi^-$->$\mu\mu K^{\pm}\pi^+\pi^-$, we use 1.1×10^{-3} for the $B^{\pm}_u$->$\Psi K^{\pm}\pi^+\pi^-$ decay[18] giving 6.5×10^{-5} for the chain.

Collecting the information about these modes, we give their expected production in Table III.A.3.

Table III.A.3
Production per Run of Inclusive and Exclusive
B->J/Ψ->$\mu\mu$ Decays and B->J/Ψ Exclusive Decays

	Composite BR	1991	1994
Number of B Pairs	-	1.7×10^6	$\geq3.5\times10^7$
B->J/Ψ	1.12×10^{-2}	3.8×10^4	$\geq7.8\times10^5$
B->J/Ψ->$\mu\mu$	6.6×10^{-4}	≈2,250	≥46,000
B^0_d->ΨK^0_s->$\mu\mu\pi^+\pi^-$	2.6×10^{-5}	≈35	≥730
B^0_d->$\Psi K^+\pi^-$->$\mu\mu K^+\pi^-$	5.9×10^{-5}	≈80	≥1660
B^0_d->$\Psi' K^*(890)$->$\mu\mu K^+\pi^-$	1.1×10^{-5}	≈15	≥310
B^0_d->$\Psi' K^*(890)$->$\Psi\pi^+\pi^- K^+\pi^-$ ->$\mu\mu\pi^+\pi^- K^+\pi^-$	2.7×10^{-5}	≈35	≥760
B^0_s->$\Psi\phi$->$\mu\mu K^+K^-$	4.1×10^{-5}	≈30	≥570
$B^{\pm}_u$->$\Psi K^{\pm}$->$\mu\mu K^{\pm}$	4.6×10^{-5}	≈60	≥1,300
$B^{\pm}_u$->$\Psi K^{\pm}\pi^+\pi^-$->$\mu\mu K^{\pm}\pi^+\pi^-$	6.5×10^{-5}	≈90	≥1,800

III.A.4. Production of Inclusive and Exclusive B->μ +x Semi-Muonic B Decays

We have estimated the number of semi-muonic and double semi-muonic B decays using the branching ratio[19] for B->μ+x of 10.3%. The composite branching ratio of double semi-muonic decays is given by the square of the semi-muonic branching ratio, 1.06%.

The two exclusive semi-muonic modes B^0_d->$\pi^-\mu^+\nu$ and $B^{\pm}_u$->$\rho^0\mu^{\pm}\nu$->$\pi^+\pi^-\mu^{\pm}\nu$ are evaluated below as channels in which to made a determination of V_{ub} as described in Section IV.A. The ARGUS collaboration has reported[20] a branching ratio of 1.03×10^{-3} but the CLEO collaboration has obtained[21] an upper limit $\leq4\times10^{-4}$ for the $B^{\pm}_d$->$\rho^0\mu^{\pm}\nu$ decay. We choose to use 4×10^{-4} which is the mid range of the theoretical estimates[22] of this branching ratio. Since the B^0_d->$\pi^-\mu^+\nu$ decay has not yet been observed, we use a theoretical expectation[22] of 10^{-4} to determine the yields of this mode.

Finally, we have selected the semi-inclusive decay mode B^0_s->$D^+_s\,\mu^-\nu$->$\pi^+K^+K^-\mu^-\nu$ as another candidate for searching for B^0_s. A preliminary measurement[23] of the inclusive BR(B_s -> $D_s\,\mu$ x) = 8% has been reported. This measurement, which is obtained from B's produced in e^+e^- interactions, assumes a hadronization fraction of 0.2 for the B_s. If we take the vector-to-pseudoscalar decay ratio to be ≈3 and the fraction of the semileptonic rate into either $D_s l\nu$ or $D^*_s l\nu$

to be 64% (similar[24] to B^0_d->D^{*+} $\mu^-\nu$ to B^0_d->D^+ $\mu^-\nu$), then 16% of the B_s->$D_s\mu x$ branching ratio should be due to the exclusive mode B_s -> D_s $\mu\nu$. This means an overall branching ratio of 1.28% for B_s -> D_s $\mu\nu$. Finally, using a branching ratio[25] of 3.9% for the D^+_s->$\pi^+K^+K^-$ decay, we obtain a composite branching ratio of 5.0×10^{-4} for the entire sequence.

Gathering the information on the inclusive and semi-inclusive B->μ decays together, we estimate the production of the selected modes shown in Table III.A.4

Table III.A.4
Production per Run of B->μ and BB->$\mu\mu$ Semi-muonic Inclusive and Exclusive Decays

	Composite BR	1991	1994
Number of B Pairs	-	1.7×10^6	$\geq3.5\times10^7$
B->μ	1.03×10^{-1}	3.5×10^5	$\geq7.2\times10^6$
BB->$\mu\mu$ double Semi-muonic Decays	1.06×10^{-2}	1.8×10^4	$\geq3.7\times10^5$
B^0_d->$\pi^-\mu^+\nu$	1.0×10^{-4}	≈140	≥2,800
$B^\pm_u$->$\rho^0\mu^\pm\nu$ ->$\pi^+\pi^-\mu^\pm\nu$	4.0×10^{-4}	≈560	≥11,200
B^0_s->D^+_s $\mu^-\nu$->$\pi^+K^+K^-\mu^-\nu$	5.0×10^{-4}	≈340	≥7,000

III.A.5. Joint Production of B->μ Inclusive Decays and Selected B Decays

In this section, we estimate the numbers of decays produced in various interesting quasi-exclusive decay modes that are produced in conjunction with an inclusive semi-muonic decay which provides the trigger of the detector. Since b->c modes have relatively large branching ratios, they present some of the better opportunities for measuring cross sections, lifetimes and mixing for both the B^0_d and B^0_s. These modes are selected from the general interactions using the high p_t single muon trigger where we trigger on the inclusive B->μ decay and attempt to at least partially reconstruct a b->c decay of the other B in the event. The charge of the trigger muon gives a tag (allowing for the dilution factor due to the mixing and b->c->μ decays of the trigger B itself) to separate B from anti-B distributions when investigating B^0_d or B^0_s mixing.

We plan to use the inclusive decay channel, B^0_d ->D^-_d+X^+ where the D^-_d decays completely into charged particles to contribute to the measurements of production cross sections, hadronization, lifetimes and, most particularly, mixing. The identification of the charged D forms the heart of these measurements. Using the measurement[26] of the $B_{u,d}$->$D^\pm$+x branching ratio (22.7%) in which the charge of the $B_{u,d}$ is not determined and, taking into account that the $B^\pm_u$ strongly prefers to decay into D^0_u or D^{*0}_u as compared to the B^0_d which decays predominately into $D^\pm_d$ or $D^{*\pm}_d$, we infer an inclusive branching ratio for B^0_d->$D^\pm_d$ + anything of approximately 45%. Summing over several $D^\pm$ modes[27], we obtain a branching ratio for $D^\pm_d$-> all charged of approximately 10%. If we include the semi-leptonic decay, $D^\pm_d$->Kπlν, which is identifiable as a $D^\pm_d$, the total "usable" $D^\pm_d$ branching ratio goes up to 17.6%, resulting in a composite branching ratio of 7.9%. As a subset of these various all-charged decays, we have also considered B^0_d ->$D^-_d X^+$ where the D^-_d->$K^-\pi^+\pi^-$. Once again using a B^0_d->->$D^\pm_d$ + anything ≈ 45% and the measured branching ratio[27] of 8.0% for the D^-->$K^-\pi^+\pi^-$ mode, we obtain an overall branching ratio of 3.6%.

In a similar manner, we also have estimated the rate for the inclusive B^0_s ->$D^-_s X^+$ decays where the D^-_s-> all charged modes are considered to include semi-leptonic modes containing a ϕ. To estimate yields, we assume that the branching ratio for B^0_s ->$D^-_s X^+$ is the same as B^0_d ->D^-

dX^+, i.e., 45%. Summing over several D^-_S all charged exclusive modes and the $D^-_S \to \phi l\nu$ mode (see Section IV, Table IV.A.4 and Ref. 28), we obtain a branching ratio of 7.5% for the "usable" D^-_S decays, leading to a composite branching ratio of 3.4%. In addition, once again, we have considered a specific decay channel of the D^-_S as an option. Using the measured branching ratio[28] of 3.9%, for the $D^-_S \to K^-K^+\pi^-$ decay, we get a composite branching ratio of 1.8% for the decay chain $B^0_S \to D^-_S X^+ \to K^-K^+\pi^-X^+$.

Using these composite branching ratios, we obtain the production yields of the various $B \to \mu \bullet B \to D+x$ modes shown in Table III.A.5.

Table III.A.5
Joint Production per Run of $B \to \mu \bullet$ Exclusive B Decay Modes

	Composite BR*	1991	1994
Number of B Pairs	-	1.7×10^6	$\geq3.5\times10^7$
$B \to \mu$	1.03×10^{-1}	3.5×10^5	$\geq7.2\times10^6$
$\bar{B}B \to \mu \bullet B^0_d \to D^-_d + X^+ \to$ all chrg$+X^+$	8.1×10^{-3}**	≈5500	$\geq113{,}000$
$\bar{B}B \to \mu \bullet B^0_S \to D^-_S + X^+ \to$ all chrg$+X^+$	3.4×10^{-3}**	≈1200	$\geq25{,}000$
$\bar{B}B \to \mu \bullet B^0_d \to D^-_d X^+ \to K^-\pi^+\pi^-+X^+$	3.7×10^{-3}	≈2500	$\geq51{,}500$
$\bar{B}B \to \mu \bullet B^0_S \to D^-_S X^+ \to K^-K^+\pi^+ + X^+$	1.9×10^{-3}	≈650	$\geq13{,}400$

*Including the branching ratio for the other $B \to \mu$ decay where appropriate
** Includes the semi-leptonic modes

III.B. Single and Dimuon Trigger Acceptances/Efficiencies for Retention of Signal

The single and dimuon triggers which form the heart of the E771 experiment are composed of several levels, each level imposing several conditions. They also include the geometric acceptances for the muons. Briefly the conditions which had to be satisfied to generate a dimuon trigger in the 1991 run were:

Level 1A: One or two muons had to penetrate a thickness of steel and shielding concrete equivalent to between 6 and 10 GeV/c. The muons which penetrated the steel and concrete must generate triple coincidences between combinations of pads (called Super ORs) in three planes of Resistive Plate Counters[29] (RPC's) which are positioned at varying depths in the steel.

Level 1B: Upon satisfaction of the Level 1A muon condition, coincidences indexed on the observed RPC triple coincidences were formed between certain collections of pads in two layers of pad chambers (called CC2 and CC3 chambers) between the E771 analysis magnet and the muon detector as shown schematically in Fig. 2. These possible coincidences, about 40,000 in number, span the allowed trajectories for charged tracks with $p_t > 0.8$ GeV/c. The implementation of this large number of coincidences was accomplished with Programmable Array Logic chips as explained in Ref. 30. The effect of the Level 1B trigger on the muon momentum spectrum is shown in Fig. D1 of Appendix D.

As explained in Appendix D, there are several improvements that can be made to enhance the acceptance and efficiency of the high p_t single muon and high mass dimuon triggers. In particular, a Level 2 trigger[31] will be implemented using associative memories to detect the presence of secondary vertices in the interaction. This level of trigger is completely independent of the muon triggers.

Signal retention is but one half of the story since the trigger rates for single muon and dimuons must be considered along with beam structure and event size to evaluate losses due to dead times in the data acquisition process. The single and dimuon trigger rates at various trigger levels for the 1991 and 1994 runs are given in Tables D.3 and D.4 in Appendix D, along with an evaluation of the dead time associated with such rates assuming no major changes in the data acquisition system for the 1994 run. Based on the discussion of Appendix D, we estimate that we can operate at $5x10^6$ interactions per second with 80% live time using the Level 1A • Level 1B• Level 2 trigger system and the E771 data acquisition system.

Using muon detector and trigger efficiencies experienced in 1991 run and extrapolated to the 1994 configuration and the live time estimate as discussed in Appendix D, Table III.B.1 and III.B.2 have been compiled. They compare the predicted and observed fractions of single muons and dimuons from direct J/Ψ->μμ, B->J/Ψ-μμ and B->μ decays retained by the 1991 trigger and give the expected performance of the 1994 run.

Table III.B.1*
Diμ Trigger Signal Retention Experienced in the 1991 vs. Expected in 1994

Trigger Level	1991	1994
Level 1A Dimuon Trigger Acceptance•Efficiency	8%	33%
Level 1B Dimuon Trigger Acceptance•Efficiency	-	70%
Level 2 Trigger Acceptance•Efficiency	-	90%
Live Time	61%	80%
Overall Trigger Acceptance•Efficiency	5%	17%

Table III.B.2*
Single μ Trigger Signal Retention as Experienced in the 1991 vs. Expected in the 1994

	1991	1994
Level 1A Single μ Trigger Acceptance • Efficiency	25%	54%
Level 1B Single μ Trigger Acceptance • Efficiency	21%	41%
Level 2 Trigger Acceptance • Efficiency	-	70%
Live Time	61%	80%
Overall Trigger Acceptance • Efficiency	3.2%	12.5%

*See Appendix D for details of the Levels 1A, 1B and 2 triggers and the estimate of live time.

III.C. Yields of Accepted Beauty Events Written to Tape

The acceptances for the other required B decay products for several interesting B decays, have been calculated using PYTHIA and a GEANT simulations of the spectrometer. These acceptances, the trigger efficiencies and live time estimates have been used to calculate the yields of B decays which are written to tape and are useful to accomplish our physics objectives if they can be reconstructed. These acceptances and yields are given in Table II.C.1 below:

Table III.C.1
Yields of B Decays Triggered on/Recorded/Accepted

Selected Decay Channels	Relative Acceptance of Tracks Other than Trigger μ's	1991 Trigger• Recording Efficiency	1994 Trigger• Recording Efficiency	1991 # of Triggered• Recorded• Accepted Events	1994 # of Triggered• Recorded• Accepted Events
$J/\Psi \to \mu\mu$	-	0.05	0.057	1.2×10^5	2.7×10^6
$B \to J/\Psi \to \mu\mu$	-	0.05	0.17	110	7,800
$B^0_d \to \Psi K^0_s \to \mu\mu\pi^+\pi^-$	30%	0.05	0.17	NA	≈35
$B^0_d \to \Psi K^+\pi^- \to \mu\mu K^+\pi^-$	42%	0.05	0.17	≈2	≈120
$B^0_d \to \Psi' K^*(890) \to \mu\mu K^+\pi^-$	50%	0.05	0.17	NA	≈25
$B^0_d \to \Psi' K^*(890) \to \Psi\pi^+\pi^- K^+\pi^-$. $\to \mu\mu\pi^+\pi^- K^+\pi^-$	23%	0.05	0.17	≈1	≈30
$B^0_s \to \Psi\phi \to \mu\mu K^+K^-$	50%	0.05	0.17	NA	≈50
$B^\pm_u \to \Psi K^\pm \to \mu\mu K^\pm$	60%	0.05	0.17	≈2	≈130
$B^\pm_u \to \Psi K^\pm \pi^+\pi^- \to \mu\mu K^\pm \pi^+\pi^-$	27%	0.05	0.17	≈1	≈80
$B \to \mu$	-	0.032	0.125	1.1×10^4	9×10^5
$BB \to \mu\mu$	-	0.05	0.17	≈900	6.3×10^4
$B^0_d \to \pi^-\mu^+\nu$	64%	0.032	0.125	≈3	≈220
$B^\pm_u \to \rho^0\mu^\pm\nu \to \pi^+\pi^-\mu^\pm\nu$	40%	0.032	0.125	≈7	≈560
$B^0_s \to D^+_s \mu^-\nu \to \pi^+K^+K^-\mu^-\nu$	28%	0.032	0.125	≈3	≈250
$\bar{B}B \to \mu\bullet B^0_d \to D^-_d + X^+ \to$ all chrg$+X^+$	22%**	0.032	0.125	≈37	3,100
$\bar{B}B \to \mu\bullet B^0_s \to D^-_s + X^+ \to$ all chrg$+X^+$	22%**	0.032	0.125	≈9	690
$\bar{B}B \to \mu\bullet B^0_d \to D^-_d X^+ \to K^-\pi^+\pi^- + X^+$	20%**	0.032	0.125	≈16	1300
$\bar{B}B \to \mu\bullet B^0_s \to D^-_s X^+ \to K^-K^+\pi^+ + X^+$	20%**	0.032	0.125	≈4	330

*The NA entry in Table III.C.1 means that the mode is not accessible at that level of analysis.
** The multiplicities of the ensemble of modes summed over averages to approximately three; Therefore, the acceptance for the B->DX decays which require all D charged decay products plus one charged decay product from the original B decay are very similar to the acceptance for the D->Kππ or KKπ decay modes.

The acceptances given above are the relative acceptances for tracks other than the trigger muons in events in which the muon trigger conditions have been satisfied (the muons are in the trigger acceptance of the spectrometer, have penetrated the muon detector absorber and have satisfied the other muon trigger conditions imposed by the 1A and 1B logic). Losses due to small differences between the muon trigger acceptances and the spectrometer tracking system acceptances

have been taken into account (for example, approximately 95% of the dimuons which satisfy the trigger are in the tracking acceptance of the spectrometer). In addition, losses due to the interactions and decays of the hadrons from the B decays are taken into account in these relative acceptances. To calculate the acceptances for the non leptonic inclusive B->D decays, we ask that all D decay products and one charged particle from X^+ must be in the acceptance of the spectrometer for the use of the modes described in Section IV.A.6. Finally, a requirement of a minimum number of track measurements has been applied to each charged decay product including pions from K^0_S decays.

III.D. Reconstruction Efficiencies and Yields Of Reconstructed Beauty Decays

The next step in estimating the yields of the 1994 run is the determination of the reconstruction efficiencies for the interesting inclusive and exclusive B decays. These efficiencies include detector, track pattern recognition and reconstruction efficiencies (in both the drift chamber/PWC system and the silicon vertex detector) and, where appropriate, the particle identification efficiencies (RICH efficiency, muon detector, electromagnetic detector efficiency, etc.). Moreover, the part of the silicon vertexing efficiencies dealing with the efficiency for associating a specific silicon track to a given primary, secondary or tertiary vertex must be accounted for. However, we do not yet at this stage include in these efficiencies the losses experienced when applying separation criteria between primary, secondary or tertiary vertices. Specific details of these vertex criteria are left to the discussion of particular B physics topics in Section IV since these requirements vary not only according to the mode but also according to the use of the mode in the extraction of a specific piece of B physics. Our estimates given in Tables III.D.1 and 2 are based on the use of various single track reconstruction efficiencies to approximately compute the reconstruction efficiencies for multiprong decay channels. Eventually, just as we have done with the $J/\Psi \to \mu\mu$ decays discussed below, we plan to determine the efficiencies from superimposing detailed GEANT simulations of each selected mode, incorporating observed detector efficiencies, on 800 GeV/c interactions from the 1991 run. We point out that this is may be a worst case procedure since the normal dimuon trigger will be due to high multiplicity, rather messy events which generate double π or K semimuonic decays which satisfy our trigger. The single muon triggers are somewhat cleaner but suffer from the same syndrome. It has been observed that events with J/Ψ's are considerably cleaner than an average dimuon trigger and a single muon trigger has only 60% of the multiplicity of a dimuon trigger. It may be that B events will, in general, be cleaner than the average muon trigger we use in this technique. However, this procedure is quite realistic in other aspects and takes into account correlations between tracks and actual noise in various spectrometer components.

The experience of the short 1991 run of E771 has provided essential information to allow a realistic estimate of the reconstruction efficiencies. To determine the reconstruction efficiencies for particular combinations of charged decay products from B's and hidden charm states, we have employed two techniques. First, we have used the $J/\Psi \to \mu\mu$ signal from the small portion of the 1991 data that we have been able to analyze thus far to obtain an experimental estimate of various reconstruction, track matching, vertexing and muon identification efficiencies. Second, we have superimposed tracks (at the hit level) from GEANT Monte Carlo simulations of $J/\Psi \to \mu\mu$ events (which include delta rays, charge sharing, and multiple scattering in the silicon detector as well as observed 1991 efficiencies and other resolution degrading effects for all detector components) on actual 800 GeV/c dimuon and single muon triggers and have determined with what efficiency we

can reconstruct tracks. We have extrapolated from these studies to the 1994 run based on expected improvements in equipment such as those outlined in Appendix C, D and E.

We find that in our 1991 data we are able to pattern recognize and reconstruct single tracks in the acceptance of the spectrometer in the front and rear wire chamber sets and match these segments successfully at the center of the analysis magnet with an overall efficiency of 82% . This tracking efficiency is consistent with the observed yields of J/Ψ's in the 1991 data analyzed to date (see Appendix A). As an indication of the success we have had in obtaining estimates of these efficiencies, the preliminary cross section for J/Ψ->μμ production in the 1991 run which uses tracking efficiencies quoted above agrees with the expectation for 800 GeV/c pN interactions obtained from the Lyons parameterization.

There were two major contributions to the 18% loss of tracks in the spectrometer wire chamber system in 1991 data. First the code is not yet entirely optimized for reconstruction of the tracks. It can be improved. Second, we experienced lower than expected efficiencies in some of the wire chamber planes due to rate effects. These effects can be eliminated by minor tuning of the drift chamber electronics. We expect to raise these efficiencies to the level which has been observed in the 1991 calibration electron beam runs and which has been achieved with these same chambers in previous runs at $\geq 10^6$ int/sec. With the expected improved chamber and code efficiencies for the 1994 run, we estimate our track reconstruction efficiency to be ≥95% per track.

We must also include the efficiency for matching a track found in our wire chamber system to the proper track in the silicon microvertex detector. Our preliminary estimate based on our J/Ψ->μμ events indicates that we are able to match wire chamber spectrometer tracks to silicon microvertex detector tracks approximately 85% of the time. Note this efficiency includes the reconstruction efficiency for tracks in the silicon detector. Our improvements in the silicon vertex detector tracker in 1994 not only will allow us to match ≥95% but also permit us to tighten cuts and reduce by a significant factor the tracks (real and fake) that cause improper track matching.

In Appendix A, we discuss the resolutions of the silicon MVD from the experience of the 1991 run. We have used both the J/Ψ->μμ events and the superimposed Monte Carlo simulated J/Ψ->μμ to determine these resolutions. In general these techniques agree. We observe an impact parameter resolution (individual track resolution) of 25 microns and a primary vertex resolution of 18 microns in the 800 GeV/c 1991 data for the transverse dimensions (x,y). In the 1994 run we expect better primary vertex resolution since we will be able to rely on a completely instrumented and greatly enhanced beam detector to provide primary vertex positions in the transverse coordinates to ≤10 microns over the entire beam profile. From the 1991 data we have also determined the z resolution along the beam direction (z) to be 350 microns for the twelve Si foils. In all case the overlaid J/Ψ agree with the resolutions extracted from the J/Ψ data.

We use the vertex resolutions to set reasonable criteria and determine efficiencies for reconstructing secondary vertices and to estimate the efficiencies of reconstructing the J/Ψ->μμ vertices. Based on the 1991 resolutions, we estimate the efficiency in the 1991 run for the Ψ->μμ pairs to have a distance of closest approach less than our 1991 criterion for forming a vertex to be ≈85%. The improved resolutions expected with the complete instrumentation of the silicon microvertex tracker together with the other improvements described in Appendix C should increase this efficiency. Extrapolating from the 1991 J/Ψ->μμ study, we estimate a range of efficiencies between 90 and 95% for the 1994 run for associating each track with multiprong vertices (taking into account that the efficiency of association of each track increases with the number of tracks already associated with the vertex).

In addition to the efficiency for associating charged tracks with a secondary vertex, there is another vertex efficiency due to the requirement for minimum primary-secondary vertex separation or minimum impact parameter. In Appendix A, based on the primary and secondary resolutions and the average B lifetime of 1.40 ps as recently reported[32] by the LEP experiments , we argue the separation criteria needed to insure distinguishable primary and secondary vertices in 1994 are $\Delta r=\sqrt{\Delta x^2+\Delta y^2} \geq 60$ microns ($\approx 3\sigma$) or $\Delta z \geq 1.2$ mm ($\approx 3\sigma$). The criteria for adequate impact parameters is somewhat greater ($\Delta r \geq 100$ microns) because of slightly poorer single track resolution. We defer imposition of these specific requirements on the selected decays modes of Table III.D.2 to the discussion of individual strategies for extraction of the various B physics parameters in Section IV.

Finally, there are efficiencies associated with charged K/π/μ/e identification. The efficiency of the RICH detector, discussed in Appendix E, has been estimated for the spectrum of the K's from the various decay modes of interest to be approximately 90% on average. The muon identification efficiency is already incorporated in the trigger efficiencies. The efficiencies for the electrons will be addressed later in the physics discussions. No efficiency is incorporated for charged π's since the standard assumption that a charged particle is a pion if it does not satisfy the restrictions for a K or a lepton loses very little since the K/lepton tracks sample is quite small compared to the pion sample.

Using all these efficiencies, we give in Table III.D.1 the overall reconstruction efficiencies and yields of reconstructed events in the 1991 run for several varieties of B inclusive final states of interest for which we have enough data to extract physics.

Table III.D.1
Reconstruction Efficiencies and Yields of Accessible B Inclusive Decays in the 1991 Run

Selected Decay Channels	1991 Overall Recon. Eff.	1991 Yields of Recon. Events
J/Ψ->μμ	49%	5.9×10^4
B->J/Ψ->μμ	35%	≈40
B->μ	70%	7.7×10^3
BB->μμ	48%	≈430

*We require the presence of the silicon portion of the tracks to improve mass resolutions

In Table III.D.2 we give efficiencies for both inclusive and selected exclusive B channels for the 1994 run since the greatly increased statistics gives us the opportunity to investigate exclusive modes. For comparisons, we have included in Table III.D.2 the estimated reconstruction efficiencies for the 1991 data so that the expected improvements due to the upgrades of the spectrometer are manifest. Overall, we expect to improve our reconstruction efficiencies by factors that vary from 1.2 to over five for modes of high multiplicity where individual track efficiencies cut the hardest.

The other obvious conclusion based just on the selected modes given in Table II.D.2 is that many channels are accessible with reasonable numbers of events reconstructed to the level required for the physics extraction discussed in Section IV.

Table III.D.2
Estimated 1994 Yields of Reconstructed B Inclusive and Selected Exclusive Decays

Selected Decay Channels	1994 Track Recon. Eff.*	1994 Particle ID Eff.	1991 Overall Recon. Eff.	1994 Overall Recon. Eff.	1994 Yields of Recon. Events
$J/\Psi \to \mu\mu$	81%	-	49%	81%	2.2×10^6
$B \to J/\Psi \to \mu\mu$	66%	-	35%	66%	≈5200
$B^0_d \to \Psi K^0_s \to \mu\mu\pi^+\pi^-$	63%	-	29%	63%	≈20
$B^0_d \to \Psi K^+\pi^- \to \mu\mu K^+\pi^-$	43%	90%	12%	39%	≈45
$B^0_d \to \Psi' K^*(890) \to \mu\mu K^+\pi^-$	43%	90%	12%	39%	≈10
$B^0_d \to \Psi' K^*(890) \to \Psi\pi^+\pi^- K^+\pi^- \to \mu\mu\pi^+\pi^- K^+\pi^-$	30%	90%	4%	27%	≈8
$B^0_s \to \Psi\phi \to \mu\mu K^+K^-$	43%	-	12%	43%	≈20
$B^\pm_u \to \Psi K^\pm \to \mu\mu K^\pm$	54%	90%	20%	49%	≈65
$B^\pm_u \to \Psi K^\pm \pi^+\pi^- \to \mu\mu K^\pm \pi^+\pi^-$	35%	90%	7%	31%	≈25
$B \to \mu$	91%	-	70%	91%	8.2×10^5
$BB \to \mu\mu$	82%	-	48%	82%	5.2×10^4
$B^0_d \to \pi^-\mu^+\nu$	66%	-	35%	66%	≈145
$B^\pm_u \to \rho^0\mu^\pm\nu \to \pi^+\pi^-\mu^\pm\nu$	54%	-	20%	54%	≈300
$B^0_s \to D^+_s \mu^-\nu \to \pi^+K^+K^-\mu^-\nu$	44%	88%	12%	39%	≈100
$\bar{B}B \to \mu \cdot B^0_d \to D^-_d + X^+ \to$ all chrg$+X^+$	47%	81%	10%	38%	1,180
$\bar{B}B \to \mu \cdot B^0_s \to D^-_s + X^+ \to$ all chrg$+X^+$	47%	94%	10%	45%	310
$\bar{B}B \to \mu \cdot B^0_d \to D^-_d X^+ \to K^-\pi^+\pi^- + X^+$	47%	81%	10%	38%	585
$\bar{B}B \to \mu \cdot B^0_s \to D^-_s X^+ \to K^-K^+\pi^+ + X^+$	47%	94%	10%	45%	150

*Includes PWC tracking and, where appropriate, silicon system tracking including the distance of closest approach cut for tracks from a common vertex. No impact parameter or vertex separation cuts are yet included. They are addressed on a physics topic by topic basis in Section IV. We include silicon vertex tracking for all $J/\Psi \to \mu\mu$ to obtain better mass resolution.

The various efficiencies for the B->D+X decays are averaged over many charged modes. They also include the requirement of observing and reconstructing at least one charged particle as well as the muon from the tagging B decay. The Cerenkov requirements, where needed, are averaged over these modes in a way such as to reduce backgrounds to an acceptable level. In the case of $D_s \to \phi$ decays, the Cerenkov is not required. For other, smaller modes such as $D_s \to KK\pi$, we use Cerenkov identification of the two K's in the event to reduce $D_d \to K\pi\pi$ backgrounds. Even though the analogous $D_s \to KK\pi$ background for $D_d \to K\pi\pi$ is not so serious, we have required positive Cerenkov K/π id for the $D_d \to K\pi\pi$ final state.

Based on the previous sections, the composite yields of final states reconstructed to the level appropriate and useful for the extraction of the beauty physics outlined in Section IV, are given in Table III.D.3 together with the overall recovery fraction due to the several levels of the event selection. Our recovery fractions are typically one percent to a few percent for these very different decay signatures.

Table III.D.3
Summary of Overall 1994 Yields for Selected B Decays

Selected Decay Modes	Produced	Triggered• Recorded• Accepted	Totally Recnsted	Fraction of Mode Recovered
$J/\Psi \to \mu\mu$	4.8×10^{7}	2.7×10^{6}	2.2×10^{6}	4.6×10^{-2}
$B \to J/\Psi \to \mu\mu$	46,000	7,800	≈5200	1.1×10^{-1}
$B^0_d \to \Psi K^0_s \to \mu\mu\pi^+\pi^-$	730	≈35	≈20	2.7×10^{-2}
$B^0_d \to \Psi K^+\pi^- \to \mu\mu K^+\pi^-$	1660	≈140	≈45	2.7×10^{-2}
$B^0_d \to \Psi' K^*(890) \to \mu\mu K^+\pi^-$	310	≈25	≈10	3.2×10^{-2}
$B^0_d \to \Psi' K^*(890) \to \Psi\pi^+\pi^- K^+\pi^- \to \mu\mu\pi^+\pi^- K^+\pi^-$	760	≈65	≈7	1.0×10^{-2}
$B^0_s \to \Psi\phi \to \mu\mu K^+K^-$	570	≈50	≈25	4.4×10^{-2}
$B^\pm_u \to \Psi K^\pm \to \mu\mu K^\pm$	1,300	≈130	≈65	5.0×10^{-2}
$B^\pm_u \to \Psi K^\pm \pi^+\pi^- \to \mu\mu K^\pm \pi^+\pi^-$	1,800	≈80	≈25	1.4×10^{-2}
$B \to \mu$	7.2×10^{6}	9×10^{5}	8.2×10^{5}	1.1×10^{-1}
$B\bar{B} \to \mu\mu$	3.7×10^{5}	6.3×10^{4}	5.2×10^{4}	1.4×10^{-1}
$B^0_d \to \pi^-\mu^+\nu$	2,800	≈220	≈145	5.2×10^{-2}
$B^\pm_u \to \rho^0\mu^\pm\nu \to \pi^+\pi^-\mu^\pm\nu$	11,200	≈560	≈300	2.7×10^{-2}
$B^0_s \to D^+_s\, \mu^-\nu \to \pi^+K^+K^-\mu^-\nu$	7,000	≈250	≈100	1.4×10^{-2}
$\bar{B}B \to \mu\bullet B^0_d \to D^-_d + X^+ \to$ all chrg$+X^+$	113,000	3,100	1,180	1.0×10^{-2}
$\bar{B}B \to \mu\bullet B^0_s \to D^-_s + X^+ \to$ all chrg$+X^+$	25,000	690	310	1.2×10^{-2}
$\bar{B}B \to \mu\bullet B^0_d \to D^-_d X^+ \to K^-\pi^+\pi^- + X^+$	51,500	1300	585	1.1×10^{-3}
$\bar{B}B \to \mu\bullet B^0_s \to D^-_s X^+ \to K^-K^+\pi^+ + X^+$	13,400	330	150	1.1×10^{-2}

III.E. Yields of Reconstructed Hidden Charm Final States

We have also estimated the yields of the hidden charm final states in the 1994 run by scaling from the observations made in E705.

Table III.E
Yields of Reconstructed Hidden Charm States

	E705 Yields	1994 Yields
$J/\Psi \to \mu\mu$	2.4×10^{4}*	2.2×10^{6}
3.837 GeV/$c^2 \to J/\Psi\pi^+\pi^- \to \mu\mu\pi\pi$	74±22**	1.3×10^{4}
3.525 GeV/$c^2 \to J/\Psi\pi^0 \to \mu\mu\pi$	42±17***	3.8×10^{3}
$\Psi' \to \mu\mu$	540±48	4.9×10^{4}
$\Psi' \to J/\Psi\pi^+\pi^- \to \mu\mu\pi^+\pi^-$	68±16**	1.2×10^{4}
$\chi \to J/\Psi\gamma \to \mu\mu\gamma$	1140±85***	1.0×10^{5}

*Sum of $\pi^\pm$ and proton beam data.
**Signal from π^- beam data (12,470 $J/\Psi \to \mu\mu$)
***Signal from sum of all beam types

The details of scaling are discussed in Section IV.B and the results are shown in Table III.E. As well as estimating the yields of "new" states, such as the two enhancements observed in E705, we will have large numbers of Ψ' and χ decays of the varieties indicated in the table. The physics that can be extracted with these higher statistics is discussed in Section IV.B.2 and Appendix B.

IV. Beauty and Hidden Charm Physics in the 1994 Run

Given the increase in yields of beauty and charm events expected in the 1994 run, the sensitivity to the physics of charm and beauty is greatly increased over what was respectively possible in E705 and the 1991 run. In particular, many B decay sequences become accessible to experimental study. Among the beauty physics issues that can be addressed in the 1994 run are:

- determination of the cross sections for beauty production using all information from the modes B->J/Ψ->$\mu\mu$ or B->μ. The B->J/Ψ exclusive decay modes offer a lower statistics but more direct and lower background method of measuring the total and differential cross sections.

- determination of the average lifetime of beauty using global fits to all available decay length distributions.

- determination of the lifetimes of the $B^{\pm}$ and B^0 decay by measurement of the semi-inclusive B->J/Ψ+charge particles->$\mu\mu$ + charged particles decays where all charged decay products are observed.

- determination of the lifetimes of the $B^{\pm}$ and B^0 decay by measurement of the exclusive all charged decays.

- measurement of various relative exclusive branching ratios (such as those for B->J/Ψ+x) with higher precision than measurements presently available.

- determination of the average mixing of the neutral B's using the double semi-muonic decays of the B pairs.

- observation of B^0_S via the inclusive channel, B^0_S->D^-_S + all-charged ->$\pi^+K^-K^-$ + all-charged modes or via various B->J/Ψ channels such as B->$\Psi\phi$. We use these modes in the determination of B^0_S production cross sections and hadronization ratios together with lifetimes and mixing.

- determination of V_{ub} from observation of semi-muonic decay modes $B^{\pm}_u$->$\rho^0\mu\nu$, and B^0_d->$\pi^{\pm}\mu\nu$.

- measurement of B baryon (in particular Λ_b) production and lifetimes.

The hidden charm sector (accessible via observation of charmed states decaying into final states containing J/Ψ or Ψ) contains many interesting physics issues, including:

- measurements with much higher statistics and better resolutions (at 800 GeV/c) the production of Ψ, Ψ' and χ total and differential cross sections to extract information about the heavy flavor production processes.

- confirmation of tentatively observed charmonium states such as the $^3D_2$ and $^1P_1$ states of the $c\bar{c}$ system.

- possible observation of four quark or exotic states.

IV.A. Beauty Physics

In the section that follows, we discuss the techniques for extracting the B physics and determining the backgrounds using various decay modes. At the time of the preparation of this proposal, we have only just made a beginning in evaluating the backgrounds to the various decay modes discussed in this section. The determination of these backgrounds is quite complex since they must be discussed in the context of not only the mode but also the specific use of that mode in the various physics measurements. At this point, even the identification of the major backgrounds is tentative and so any listing of backgrounds must be considered to be representative, not inclusive. In addition, work is continuing on deciding on the best strategies for rejecting backgrounds and retaining signal in the contexts of the various modes and physics objectives. In so far as time has permitted, some obvious backgrounds have been considered and have been subjected to the same detector efficiencies, acceptances, trigger and reconstruction criteria as the signal. In rejecting these backgrounds and retaining the signals, various resolutions have been used as determined, in the main, from the E771 data extrapolated to the 1994 conditions. In particular, silicon track and vertex resolutions, as discussed in Appendix A, have been inferred from 1991 data. In addition, we have estimated the mass resolutions both from the experience of E705 (substantiated by detailed Monte Carlos) and the preliminary results from E771. In general, the mass resolutions for two body modes are to expected to be less than $\sigma \equiv 45$ MeV/c^2 as observed for the J/Ψ->μμ. We have taken this to be a worst case since we not only expect in the 1994 run to improve the two body mass resolution by use of the better angular resolution of tracks possible with a fully instrumented silicon detector but also anticipate that three, four and five body mass resolutions will be better than the two body in any case.

IV.A.1. Measurements of Beauty Cross Sections in 800 GeV/c pN Interactions

We can extract differential and total cross sections for B production from all the classes of B decay that we observe, using both exclusive and inclusive single and dimuon decays. Each class of event will have its own statistics and backgrounds, but each type must give consistent answers to the level of the knowledge of the branching ratios. We discuss below the extraction of these cross sections from the inclusive and exclusive decays.

IV.A.1.a. Cross Sections from Inclusive B->J/Ψ-> μμ and B->μ Decays

Total and differential cross sections for B production in 800 GeV/c pN interactions averaged over the B species can be obtained with good statistical accuracy from the B->J/Ψ->μμ

inclusive decays using the inclusive branching ratio (1.12±0.0016) for $B_{u,d}$->J/Ψ (there will be corrections due to B_s and beauty baryon contributions and perhaps due to B_u/B_d ratios different form e^+e^- interactions). The backgrounds to this determination can be made relatively small since observation of a J/Ψ originating at a secondary vertex is unambiguous evidence for a B event. With the reasonably large statistics, hard cuts can be made on primary and secondary vertex separation to minimize backgrounds.

The experimental error in the total cross section for B production will have contributions among which are the measurement of the beam flux, the uncertainties in the efficiencies and the acceptances of the various cuts necessary to isolate a sample of secondary vertex J/Ψ's, and the level of the surviving backgrounds. The error in measurement of the beam flux (performed by a combination of four beam monitors, two ion chambers and a beam silicon detector consisting of a set of x silicon planes and a set of y silicon planes which independently count the number of beam tracks per bucket) is expected to be the largest of these contributions based on previous experience. All four beam monitors have the capability of taking into account multiple beam tracks in a bucket. In addition, the silicon planes directly count the beam and veto's can be applied to this count in a bucket by bucket manner. We expect to have less than a 5% error due to the measurement of the proton beam flux.

The second experimental error due to uncertainties in the evaluation of trigger and detector efficiencies will be evaluated by studies of direct J/Ψ->μμ production which provides a very significant signal with which to study trigger, detector and reconstruction efficiencies of various types. The narrow peak and the small background for the J/Ψ (observed to be ≈1/10 in the 1991 data; see Fig. A.1) plus the similarity to the B->J/Ψ mode from which we intend to determine the cross section, gives us a direct way to evaluate track reconstruction efficiencies and vertexing efficiencies.

In addition to studies based directly on the data, we use the technique, mentioned above and employed in E705, of superposition of GEANT Monte Carlo simulated J/Ψ->μμ on actual 800 GeV/c dimuon triggers to extract reconstruction efficiencies in a second way. Using both of these techniques, we expect a contribution to the error in the cross sections considerably less than 5% .

The technique for extraction of the differential cross sections in x_F and p_t is indirect since we only observed the J/Ψ->μμ decay in this class of events. To extract the parameters of the x_F and p_t distributions we use the x_F and p_t distributions of the J/Ψ->μμ decays from B decay candidates. The technique will be to Monte Carlo B->J/Ψ decays with different choices for the shapes of the x_F and p_t distributions of the B's. By comparing the resulting x_F and p_t of the daughter J/Ψ to the data, we can extract the parameters of the parent distributions. While this indirect method might be thought to contribute some error in the shape parameters of the p_t and x_F distributions, previous experience[33] indicates that such errors are negligible in the extraction of parameters such as the exponent α of gluon structure function, $xG(x)=\beta\cdot(1-x)^{\alpha}$. Overall, based on our previous experience, we expect to be able to make a 10% measurement of the various cross sections.

The backgrounds for this determination of cross section arise from mismeasured or multiple scattered dimuons from J/Ψ production at the primary which appear to form a secondary vertex still managing to satisfy the three criteria:

- reconstruct to a J/Ψ mass

• have a suitably small distance of closest approach to each other
($\leq$15 microns in $r=\sqrt{x^2 + y^2}$; $\approx 2\sigma$)

• appear to originate at a distance from the primary vertex consistent with a secondary vertex
($\Delta r = \sqrt{\Delta x^2 + \Delta y^2} \geq$ 100 microns $\approx 5\sigma$ and $\Delta z \geq$2000 microns $\approx 5\sigma$)

Monte Carlo estimates of the fraction of directly produced J/Ψ->μμ decays which satisfy the three criteria listed above and are a background to the B->J/Ψ->μμ decays give $\leq 1/10^4$ while retaining ≈58% of the B->J/Ψ->μμ inclusive decays. With a ratio of produced B->J/Ψ->μμ decays to directly produced J/Ψ->μμ decays of ≈1/1000, the signal to background at this stage of analysis is already 10/1. Furthermore, in each J/Ψ->μμ event the association of additional charged particles to the J/Ψ->μμ can be used to further reduce the backgrounds, if needed, with very little decrease loss in statistics.

Finally, the large sample of B->μ inclusive decays can also be used to extract the cross sections. However, this data is much more prone to backgrounds. The three background rejection cuts mentioned above for the B->J/Ψ modes are replaced by a very hard cut on the p_t of the single muon (≥2 GeV/c). This should be enough to eliminate charm backgrounds to the level of $\geq 1/10^5$ while retaining approximately 35% of the 820,000 reconstructed single muons of Table III.D.3. If additional suppression of background is needed, we can, once again, take the subset of single muon decays in which a second charged particle is associated with the B decay vertex. A visible mass cut can then be applied to these data.

The differential cross sections for the B production must be inferred in the case of the inclusive B->μ decay from the momentum and direction of the single muon in much the same way that the differential distributions were inferred from the B->J/Ψ decays from the momentum and direction of the μ pair.

As a final note, in both the B->J/Ψ and B->μ inclusive decays, a separation of the data into charged and neutral subsets can be done to the level that we are able to make the assignment of proper tracks to the B decay vertex. Monte Carlo studies are under way to determine our ability to accomplish this feat which is also directly applicable to the charge and neutral B lifetime extraction for the inclusive B decay data.

IV.A.1.b. Cross Sections from Exclusive B->J/Ψ-> μμ and B->μ Decays

We will have much more limited reconstructed data samples in the various exclusive modes with which to determine the cross sections. In this case, to preserve statistics, we do not cut as hard on the vertex separation to purify the sample. The observation of a peak in a mass spectrum (for the J/Ψ modes) or a large visible mass or a reconstructed tertiary D in the case of the semi-exclusive semi-muonic modes will reject backgrounds quite well. We are in the process of evaluating this on a mode by mode basis. We estimate in a preliminary way that we can relax the vertex separation cut to 3σ in Δr and Δz.

It is quite worthwhile to pursue the exclusive modes of Tables III.F because separate cross sections can be obtained for the different specie of B (u,d,s). If this is possible, then to the level that various branching ratios are known, it will be possible to estimate the hadronization fractions for the three B types. In addition, the exclusive modes have the advantage that the B is totally reconstructed and the x_f and p_t distributions are directly observable (modulo efficiency corrections).

Summing over several modes in each specie, we expect to be able to make measurements of cross sections using a few tens to a few hundreds of events in the various semi-inclusive and exclusive categories.

IV.A.2. Measurements of Exclusive Branching Ratios

The discussion of chapter III singled out several exclusive channels of Bd, Bu and Bs decays, showing the projected number of events we would hope to reconstruct in each decay mode. As a general guideline, the Chapter III results show that our projected sensitivity is, for B decays containing primary muon(s), at the level of about 1 event for a combined branching ratio of 10^{-6}, while it is about a factor of ten weaker for muonless decays. These figures by themselves show that we are able to improve the statistical error on a large number of previously observed B decays, while also lowering the existing limits on many others. As an example, Section IV.A.5 gives a more detailed discussion of the potential for observing a b->u transition of the type B -> ρ μ ν; in addition to this, one could put more stringent limits on hadronic decays of the type $B^0 \to \pi^+ \pi^-$ or $B^0 \to p \bar{p} \pi^+ \pi^-$ (both unmistakable signatures, especially if a RICH is available), with current limits in the 10^{-4} range or on flavor changing neutral currents of the type $B \to \mu^+ \mu^- + X$, with limits currently at the 10^{-5} level.

The determination of any given exclusive branching ratio for B decays, in addition to the systematic error due to the knowledge of combined acceptance and efficiency for the given mode, which can be determined to 10% or better, will also require as an input the knowledge of the total cross section for B production as well as the u/d/s hadronization ratio. Section IV.A discussed the determination of the cross section, by analysis of the relatively background free B->Ψ channel. The same sample, as discussed in section IV.A.3.b dealing with neutral and charged lifetime, will allow us to determine the charged to neutral ratios of B production, providing essentially the absolute yield of B_u's. Concerning the neutral B's, there will remain an ambiguity between B_d and B_s production (even so, this is a small price to pay to be allowed entry to the extremely rich field of B_s physics !). Among the various possibilities for resolving the ambiguity, one could study the ratio of exclusive decays of the type $B_d \to D \mu \nu \to K \pi \pi \mu \nu$ (combined branching ratio 1.4×10^{-3}) with respect to $B_s \to D_s \mu \nu \to K K \pi \mu \nu$ (combined branching ratio 0.5×10^{-3}) both of which should be identifiable with sufficient statistics: the d/s hadronization ratio could then be derived within a small theoretical uncertainty.

IV.A.3 Beauty Lifetimes

We have considered the potential of the 1994 run for measuring the average B lifetime and separately the lifetimes of $B^{\pm}_u$, B^0_d and B^0_s mesons. We can achieve precision comparable to or better than those of both the PEP and LEP experiments with quite different backgrounds and systematic errors. There are several ways of accomplishing these measurements. Some methods use most of the available B candidates, but are subject to larger systematic errors than methods which use smaller B decay samples (for example, exclusive B decays) which have smaller systematic errors. In all of these strategies, the strength of the fixed target hadroproduction configuration is the ability of the silicon microvertex detector to make direct measurements of decay lengths (see Appendix A) which will have a resolution for the separation of primary and secondary vertices of $\sigma_r \approx 20$ microns in the plane transverse to the beam and $\sigma \approx 400$ microns in the beam direction. The average of the decay lengths for B's in 800 GeV/c pN interactions (using the LEP

lifetime measurements of 1.40 ps) are 150 microns and 9100 microns respectively (see Fig. A.5 in Appendix A.

IV.A.3.a Average B Lifetimes from B->J/Ψ->μμ and B->μ Inclusive Decays

The average B lifetime (where the charge of the parent $B^{\pm}u$, B^0_d or B^0_s is not determined) can be obtained with good statistical error from the inclusive B->J/Ψ->μμ and B->μ decays. As was the case in the measurement of total cross section, this is an indirect technique. Distributions of the observed quantities, e.g., the primary to decay vertex distance, the visible momentum of the B decay products, the visible invariant mass of the decay, the largest impact parameter of any decay track with respect to the primary vertex etc. are compared with predictions of the detailed Monte Carlos calculated using a range of values of the average lifetime of the B's.

In this method, all decays identified as being due to B's can be used, whether completely reconstructed or not. It has the disadvantage of being dependent on the assumptions put into the Monte Carlo, e.g., the B differential production distributions, the branching ratios to the particular modes as well as the detection efficiencies, resolutions and misassignment probabilities of the charged decay products, including the vertex resolutions and detection efficiencies.

Therefore, this method will have the smaller statistical error and the larger systematic error of the two methods that we plan to use. However, preliminary evaluations of the systematic errors involved in this technique indicate both that they can be reduced and that the lifetime determinations are not particularly sensitive to the majority of the effects mentioned above. For example, subsets of all B decays can be defined (such as separating the μμ and single μ decays) to evaluate the sensitivity to the exact choices of decay branching ratios and dynamics. Also, while the B production differential distributions will matter to some extent (although the details of the production process tend to wash out when integrated over a large number of decay modes), $d\sigma/dx_F$ and $d\sigma/dp_t$ are constrained by the observed distributions of charged particles. Finally, with the number of events available in the 1994 run, the event selection criteria can be tuned to minimize improper assignments of tracks to vertices, and to eliminate events where the missing neutrals carry most of the momentum or mass, etc. We estimate that cuts can be made such as to reduce the level of systematic errors below the statistical error.

Even more importantly, the large numbers of events available in the 1994 run allow us to address the problem of elimination of backgrounds due to light hadron and charm decay and the determination of the effect of resolution effects such as multiple scattering, measurement error, electronic noise, delta rays, etc. (all of which are in our GEANT simulations of the detector and are tuned to the observed data). With the order of two million reconstructed primary J/Ψ->μμ decays, one million reconstructed B->μ inclusive decays and several thousand reconstructed inclusive B->J/Ψ->μμ decays, we expect to be able to select event samples in which the backgrounds mentioned above are reduced to a level less than 10% of the signal. Like all background issues in this proposal, this one is under more complete evaluation at the time of this writing.

The experience of other experiments that have reported indirect measurements of charm and beauty lifetimes convinces us that we can measure the average B lifetimes to better than 10% with the 1994 data. Such a measurement will serve as an interesting contrast to the measurements made at e^+e^- colliders (or hadron colliders provided that lifetime measurements at this level are within the scope of their technical capabilities). Discrepancies could yield interesting information on the relative contributions of B^0_S, B^0_C, or B baryons to the indirect measurements at each energy in each experimental configuration.

IV.A.3.b. $B^{\pm}$ and B^0 Lifetimes from B->J/Ψ->μμ and B->μ Inclusive Decays

The statistics of the 1994 run and our precision of track reconstruction in the silicon microvertex detector will permit the event selection to be refined to the point that a large fraction of the B->J/Ψ->μμ and B->μ inclusive decays can be separated into those with a charged ($B^{\pm}_u$) and those with a neutral ($B^0_{d,s}$) parent, i.e., those with an odd number of outgoing charged particles can be separated from those with an even number. Monte Carlo studies are underway to determine how well this can be done. To the level that it can be done properly, charged and neutral lifetimes can be determined. The proper assignment of outgoing charged particles to a decay vertex will also allow separate measurements of the B^+ and B^- lifetimes.

Cuts on the visible momentum, missing transverse momentum, and visible mass will be used to reject backgrounds, mismeasurements, and improperly assembled events. In addition, clean subsamples of nearly fully reconstructed events are available as monitors of the effectiveness of the procedure. Moreover, these almost fully reconstructed samples can also be used in a manner similar to that possible for exclusive decays (see Section IV.A.3.c) to measure the charged and neutral lifetimes. Specifically, we estimate that ≈10% of the B->J/Ψ->μμ + $x_{charged}$ +$x_{neutral}$ (several hundred events) will be missing at most a soft π^0 or photon. For these, the proper flight time can be estimated well by the quantity:

$$\tau_{effective} = L_{effective} \cdot M_{visible} / (c \cdot p_{visible})$$

where $L_{effective}$ is the distance between the decay point and the point along the potential flight path where an event of this topology and configuration would have first passed all our cuts, $M_{visible}$ is the invariant mass of all the observed decay particles, $p_{visible}$ is the vector sum of their momenta and c is the speed of light. How good an estimate $\tau_{effective}$ is of the true proper flight time will be determined by a comparison of Monte Carlo with the data. Experience from previous experiments[33,34] suggests that we can take out any bias in $\tau_{effective}$ well enough to measure the separate lifetimes to better than 10%. This is true even when only the outgoing muons are identified, i.e., all outgoing charged particles are considered to be pions.

Similarly, we estimate that an unbiased sample of several thousand B->μ+ $x_{charged}$ +$x_{neutral}$, where there is only a neutrino or a neutrino accompanied by a soft π^0 or photon, can be selected. The same technique should permit a second determination of the separate lifetimes to a few percent.

At the present time, detailed Monte Carlos of this technique are being undertaken. In particular, the backgrounds due to the feeding of lower multiplicity topologies into higher B decay topologies by improper addition of tracks or, conversely, the feeding of particular topologies by loss of a track from higher multiplicity topologies are being considered. More precise evaluations of these backgrounds and the associated errors will be forthcoming.

IV.A.3.c. $B^{\pm}_u$ and Neutral B^0_d and B^0_s Lifetimes from B Exclusive Decays

The most direct measurement and the one with the minimum corrections is, of course, the method which uses completely reconstructed exclusive B decays. This method is also much less prone to background contamination since it requires the actual observation of a peak in the reconstructed mass spectrum at the B mass. As discussed elsewhere, the evaluation of the backgrounds to these exclusive channels is ongoing but is expected to be small (less than a few percent in most cases).

For these fully reconstructed events, the proper flight time is measured directly from the decay length (suitably corrected for efficiency and resolution of the measurement of the secondary vertex) and the momentum of the B as determined from its decay products. All completely reconstructed decay modes of particular varieties of B (B^0_d, B^0_s, $B^{\pm}_u$, etc.) can be summed to get the lifetimes of individual B species. Table III.D.2 shows that order of a hundred each of B^0_d and $B^{\pm}_u$ exclusive decays will be completely reconstructed in the selected modes thus far considered. Thus far we have considered only a few possibilities for the various B_d exclusive decays and only one exclusive B_s decay. As the single B_s example, twenty or so decays will be completely reconstructed in the one channel ($B^0_s \rightarrow \Psi\phi$) thus far considered. However, much in the manner of the CLEO and ARGUS experiments, we expect many other decay chains to contribute to the sum of totally reconstructed final states. Even with only the modes listed in Table III.D.3, we expect to obtain the individual B^0_d and $B^{\pm}_u$ lifetimes to 15% and the B^0_s to 25%.

IV.A.4. Observation of B^0_s Decays and B^0_s Lifetime Measurements

In this section, we describe two basic strategies for observation of B^0_s, either by the observation of $B_s \rightarrow D_d$ decays (obtained by either triggering on the semi-muonic decay of the other B in the event and or directly obtained as in the case of selected $B^0_s \rightarrow D^+\mu$ semimuonic decays) or by observation of exclusive B^0_s decays such as $B_s \rightarrow J/\Psi\ \phi$ decays.

IV.A.4.a Observation of $B^0_s \rightarrow D^+_s + x$

The observation of the B^0_s by the detection of $B^0_s \rightarrow D$ decays as described in this section relies on our ability to reconstruct D_s mesons. We have considered in what follows only all charged D^+_s decay modes. In specifying the D^+_s decay chains resulting in ϕ and K^{*0}, we consider only $\phi \rightarrow K^+K^-$ and $\overline{K}^{*0} \rightarrow K^-\pi^+$ with branching ratios of 0.5 and 0.667 respectively.

Table IV.A.4
D_s Decay modes

D_s Decay Mode	Composite BR	Topology*
$D^+_s \rightarrow \pi^+\pi^-\pi^+$	1.2%	3 prong
$D^+_s \rightarrow \phi\pi^+ \rightarrow K^+K^-\pi^+$	1.4%	2 prong
$D^+_s \rightarrow \phi\pi^+\pi^-\pi^+ \rightarrow K^+K^-\pi^+\pi^-\pi^+$	0.6%	4 prong
$D^+_s \rightarrow \phi\mu^+\nu \rightarrow K^+K^-\mu^+\nu$	0.8%	2 prong
$D^+_s \rightarrow \phi e^+\nu \rightarrow K^+K^-\mu^+\nu$	0.8%	2 prong
$D^+_s \rightarrow K^+\overline{K}^{*0} \rightarrow K^+K^-\pi^+$	1.7%	3 prong
$D^+_s \rightarrow K^+K^-\pi^+$	0.8%	3 prong

* The ϕ decays will show up as a one prong.

Since any ϕ candidate track pair would be required to come from a secondary vertex, it may be possible that the first five modes could be reconstructed without particle identification. For example, at LEP, where particle identification is presently done by dE/dx, a $D_s \rightarrow \phi\pi$ (where $\phi \rightarrow K^+K^-$) signal has been seen[23,35] in a sample of secondary vertices without requiring particle identification on the tracks (the track separation is too small). In situations of higher multiplicity and/or ambiguous vertex assignments, K/π particle identification may become necessary. The Tagged Photon Laboratory Spectrometer has found[36,37] particle identification to be crucial in the

study of charm decays containing the ϕ. By making strict vertex cuts, E687 has found[38] ϕ ->KK and D->K+nπ (n=1,2,3) using a topological analysis without resorting to particle identification. In this sense particle id is used more for reducing background than initially finding signals. However, for the last two modes, particle identification would be necessary to distinguish them from the analogous D^+_d decays (e.g. D^+_d-> $\overline{K}^{*0}\pi^+$) and to reduce the combinatorial background.

It should be noted that the above modes are not unimpeachable D_S decays by particle composition alone since D^+_d decays into the same final states with a factor of approximately five (Cabibbo) suppression in all three cases. Thus a mass cut will be required to distinguish the D^+_d from the D^+_S. The mass resolution for a two body state in our spectrometer is of order σ=45 MeV/c^2 to be compared to the D^+_d - D^+_S mass difference of 1969-1864 ≈ 100 MeV/c^2. Since we expect the mass resolution for ≥ 2 prong topologies to be better than the two body resolutions, the mass resolutions of the E771 spectrometer should be adequate to the task of separation.

We have considered two alternative strategies for analyzing events containing B^0_Ss. Either the B_S may decay directly into muon(s) and provide the trigger (self triggered) or, alternatively, the trigger muons may come from the accompanying B. We evaluate our ability to observe B^0_S in three different decay modes: the two which are self triggered are discussed in the following sections, while the third is covered in the Bs mixing discussion (Section IV.A.5.c)

IV.A.4.b Observation of B^0_S -> $D^+_S \mu^- \nu$

In addition to providing clear evidence of B_S production and allowing a determination of its lifetime, decays in which the triggering muon comes from the B under study are also useful for mixing measurements because the charge of the muon identifies the flavor of the B_S at the time of its decay. Of course to take advantage of this, a tag of the B_S flavor at production is also required. In addition to the lepton tagging, if a K/π particle id is available, then another method of tagging the B_S at t=0 is possible. As described in Ref.39, B_S production at this energy should be accompanied by a strange particle, e.g. K or Λ, nearby in phase space which carries the partner strange quark. Thus, a primary K^+ nearby in rapidity to B_S should tag to some level that it was a B_S at t=0. A Cerenkov counter (See Appendix E) would be essential to take advantage of this correlation.

We anticipate that the primary source of background will be from B-> $D_S \overline{D}$ +X where $\overline{D}$-> μ^- + X. The background can be reduced by making a cut on the visible mass at the secondary vertex and requiring a muon p_t higher than the one already applied by the trigger. A detailed Monte Carlo is in progress. At this point, we estimate that the B_S signal will be retained with an efficiency of 70% or better.

As discussed in Section III, we expect to reconstruct a total sample of about 85 B^0_S -> $D^+_S \mu^- \nu$ events when just considering the single exclusive D^+_S decay into $K^+K^-\pi^-$. Inclusion of all the other $D^\pm_S$ decay modes listed above would approximately double the size of the sample. For these decays, the B momentum (which is needed to determine the proper time of the decay) is ambiguous due to the unobserved neutrino. However, since the D_S carries a large fraction of the B_S momentum, one can correct by the appropriate Monte Carlos the visible momentum at the secondary vertex. As discussed in Section IV.A.2, even with incomplete knowledge of the parent B momentum, a sample containing ≈100 events will allow a lifetime determination to ≈15%.

IV.A.4.c Observation of B_S -> J/Ψ ϕ

As one example of an exclusive decay mode which can be used to observe the B^0_S, we have examined B^0_S -> J/Ψ ϕ. This decay is self conjugate, so, in the absence of CP violation, it

cannot be used for a mixing measurement. In the future, a non-zero measurement of CP violation in this mode would be a signature for physics beyond the standard model. As discussed in Section III, for a composite branching ratio of $4x10^{-5}$, we expect to observe about 20 fully reconstructed B^0_S -> J/Ψ φ->μμKK decays. In analogy with the observed $B_{u,d}$ decays, we also expect to fully reconstruct several other B^0_S->J/Ψ exclusive decays, yielding data samples of the same magnitude. The sum of these completely reconstructed modes will yield the most unambiguous determination of the B_S lifetimes.

As in the case with the D_S decay, we will be able to reconstruct the φ without particle id by using tracks from a resolvable secondary vertex. The signal would consist of a secondary vertex containing the two J/Ψ muons and an additional track. The small Q value of the φ decay would produce only one track in front of the magnet matching to two tracks in the bend plane in the rear of the analysis magnet.

IV.A.5. Measurement of B^0 Mixing

We plan in the 1994 run to measure B mixing in several ways. In the sections below, we first consider a determination of the average mixing of all neutral B's from a measurement of the ratio of same sign dimuons from double semileptonic B decay to the opposite sign dimuon signal. Two different approaches (vertex and non-vertex method) to the measurement of the average neutral B mixing are discussed in Section IV.A.5.a.

We have also investigated a method of determining the B^0_S mixing using the sample of muon-tagged B^0_S inclusive decays into D_S, followed by the decay of the D_S into either all charged states or into a lepton, a φ and an unobserved neutrino, as discussed in Section IV.A.4 above.

IV.A.5.a. Average B^0 Mixing from Double Semileptonic Decays

The 1994 run should produce $3.5x10^7$ B pairs. Of these, $3.7x10^5$ should undergo semileptonic decay into μ pairs. A 17% trigger•recording efficiency will result in $6.3x10^4$ of these pairs logged on tape. Of these, we estimate that we will reconstruct approximately $3.7x10^4$ dimuons from double semileptonic decay. If no information is required from the microvertex detector (see non-vertex method below), the sample size would increase to $5.1x10^4$. There are two possibilities for studying B^0 mixing using this sample of data. The first method makes use of those events that have two identified secondary vertices, while the second method uses the larger sample of data without vertex information.

Vertex Method

Assume a tracked muon can be associated with each of two identified secondary vertices in an event. One can then compute the component of muon momentum p_t which is transverse to the line of flight of the particle producing the secondary vertex. When the two secondary vertices are produced by the B pairs, a cut requiring $p_t > 1.0$ GeV/c for each muon will reduce the semileptonic dimuon sample to $1.8x10^4$ events. This cut is designed to exclude charm decay.

To study B mixing, one should exclude second generation decays (b->c->μ) relative to first generation decays (b->μ). An additional cut requiring the dimuon mass $M_{\mu\mu} > 3.2$ GeV/c^2 will produce a dimuon sample in which 90% of the events have both muons decaying by first generation. This cut reduces the data sample to 5,150 events. Monte Carlo corrections for contamination of the sample by second generation decays, B^+B^-, and background muons will be necessary. The association of a muon with a secondary vertex which is required for this technique is estimated to be approximately 80% for either muon.

Non-Vertex Method

A simpler method for studying mixing is similar to experiments done previously by other groups. A cut is made on the transverse momentum p_t of each muon with respect to the proton beam axis. Each decay candidate must have $p_t > 1.5$ GeV/c. After this cut, approximately 8700 dimuon pairs will remain. In addition, the dimuon mass must be $M_{\mu\mu} > 3.2$ GeV/c^2. This final data sample will contain 6,300 first generation dimuon events together with about 1900 background pairs. Analysis of this sample will require Monte Carlo correction for second generation B decays, charm contamination, and muon background. The large size of the data sample insures that systematic errors will dominate the determination of the mixing parameter.

The number of pairs used in this measurement should be compared to that of other experiments that have studied mixing with semileptonic pairs in very different environments at different energies. For example, the OPAL[40], L3[41] and UA1[42] had at their disposal μ pair samples of 1011,1083, and 889 respectively and used methods similar to the non-vertex method to determine mixing at their energies in their experimental configurations.

IV.A.5.b. B^0_S Mixing from $B^0_S \rightarrow D^+_S + X$

The fixed target environment described in this proposal offers the possibility of measuring mixing in the B_S mesons by direct observation of the oscillation in the decay time distribution. For this purpose, we will exploit the high p_t semileptonic decay sample which will be collected during the 1994 run.

The muon from the beauty meson which triggers the event will serve as the tag for the other beauty meson produced in the event. This tag introduces a dilution factor which can be large. For example, the UA1 measurement obtained by observing the same sign di-lepton rate gave a value for the mixing in hadronically produced beauty of 0.158 ± 0.059. This would result in a dilution of the mixing signal for the time dependent decay of 0.316. So, in principle, we would not be required to reconstruct the tagging beauty hadron if we were willing to suffer such a factor.

However, we can, to some extent, reduce this dilution factor by reconstructing at least a part of the visible mass associated with the tagging muon and demanding it to be large. This cut reduces to an acceptable level the $b \rightarrow c \rightarrow \mu$ decays which lead to mistagging. Another way to exclude these decays is to perform a cut on the muon transverse momentum (measured ideally with respect to the parent direction). Since the p_t cut requires us to form a vertex and the visible mass cut requires at least one other charged particle other than the muon, we require tagging B decays in which the decay muon be accompanied by at least one other charged particle. The acceptances of Table III.C and the reconstruction efficiencies of Table III.D.2 include losses due to the extra track.

The accompanying B_S decay would be reconstructed partially by its decay into a D_S meson plus one or more charged particles. The D_S meson would be fully reconstructed by observing the charged decays listed in Section IV.A.5. As discussed earlier, most of these modes do not require any particle identification for their reconstruction. If particle identification is available, all the listed modes could be reconstructed to increase the signal. Moreover, a sufficiently accurate estimate of the B_S gamma factor can be obtained measuring the gamma associated with the visible mass at the B_S decay vertex. This is primarily due to the fact that the D_S takes a large fraction of the Bs momentum. As detailed in Section III, we expect approximately 310 tagged $B_S \rightarrow D_S$ decays whose charged decay products have been reconstructed, identified as forming a common vertex with each other and survived whatever particle id is necessary for the mode to be identified as a D_S.

With the majority of the D_S modes of Table IV.A.4, we will either be able to completely reconstruct the D_S or be able to unambiguously identify the D_S even with partial reconstruction (for example the Ds->ϕlν modes). Applying a vertex separation requirement that the D_S be $\Delta r \approx 60$ microns$\approx 3\sigma$ or $\Delta z \approx 1200$ microns from the primary will reduces this data sample to 260 events but reduce backgrounds to the reconstructed events. An exhaustive study of backgrounds has not been done. However, we have studied with Monte Carlo simulations what we believe will be the most serious background, B_d decays to D_d which are incorrectly reconstructed as D_S. We estimate that a feedthrough of less than a few percent will occur which would contribute a rather smooth background to the reconstructed D_S spectrum.

In addition to isolating the B->D events, we must reduce the tagging dilution factor due to backgrounds to B->μ decay from b->c->μ decays. Since we have identified a Bs in the event by this point, there should be little direct c->μ backgrounds to give a false tag. We have required in the acceptance calculations that the tagging beauty hadron produce not only a trigger muon but also one or more charged particles in the acceptance which are reconstructed. As stated above, we apply the same requirements to the b->c->μ and demand a large p_t and visible mass of the μ•hadron combination in order to reduce background. We estimate that a requirement of $p_t > 1.5$ GeV/c determined with respect to the beam direction will conserve approximately 60% of the B->μ decays leaving 160 B_S ->D_S decays, while reducing the b->c->μ false tag backgrounds by a factor of 3. A further cut on the visible mass associated with the muon vertex would reduce the backgrounds by another factor of 2 to 3 while further reducing the signal by a factor of 72% leading to a sample of 110 B_S for use in a determination of mixing. We have assumed equal b->μ and b->c->μ components in the trigger muon sample before the cuts and have, therefore, cut hard on visible mass and p_t to get the tagging contamination level to less than 1/5 of the signal level. Further study may either indicate other ways to insure proper tagging or that the level of b->c-μ relative to B-μ is less than assumed, thereby alleviating the need make the p_t and visible mass cuts so severe.

The B_S mixing would be measured by observing the time dependent decay distributions for the tagged B_S mesons. The decay oscillations should be quite evident, given our vertex resolution, for a reasonable range of values of the mixing parameter x around the Standard Model prediction of five.

IV.A.5.c. B^0_d Mixing from B^0_d->D^+_d+X

The B_d mixing can be studied in much the same manner as the B_S discussed above. We plan to detect the B_d and study its mixing by selecting B_d -> D_d X^- decays in which the D decays entirely into charged particles and the B^0_d are tagged by the trigger muon. In particular, we will use the D_d decay modes which result in K$\pi\pi$ final states. These modes have a combined branching ratio of approximately 8%. The yields of these events as discussed in Section III are considerably larger than in the case of the analogous B_S->D decays. We expect ≈1180 events in which the D_d is completely reconstructed and the tagging μ and at least one other charged particle from the other B are in the acceptance.

The backgrounds to these B_d decay modes due to B_S decay will be minor . From the hadronization and branching ratios considerations the B_S->KKπ is less than 10% or the B_d->K$\pi\pi$ even without K/π id. In spite of this, we have required positive K/π id in estimating the number of events available for this study.

On the other hand, the contamination of the tagging μ by b->c->μ decays will be similar. Assuming the same loss of signal is experienced as in the case of B_S, we will have approximately

400 B_d->D_d decays with which to directly observe oscillations and measure mixing. While decay oscillations may be less evident since the B_d tend to decay before they fully mix, the requirement on time resolution is somewhat less than for the B_s which presumably has a faster oscillation. This would be the first direct observation of oscillations in the B^0_d just as was the case for the B^0_s.

IV.A.6 Observation of b->u Transitions and Determination of V_{ub}

The transition amplitude V_{ub} is a crucial element of the CKM matrix since no CP violation can occur in the standard model if it is equal to zero. The semi-leptonic decays of B mesons into exclusive states containing light mesons (charmless decays) offers the possibility to extract a value for the CKM matrix element V_{ub}. Both ARGUS and CLEO have reported indirect determinations of V_{ub} from the shape of the inclusive leptonic momentum spectrum, but no direct evidence of b->u transitions has yet been observed with the possible exception of two events from the ARGUS experiment. There is a significant discrepancy between the CLEO and ARGUS results for V_{ub}.

As an alternative approach, we plan to use exclusive semi-leptonic modes to determine V_{ub}. We have considered two possible modes of the B->μ semi-muonic exclusive variety, B^0_d->$\pi^{\pm}\mu\nu$ and $B^{\pm}_u$->$\rho^0\mu\nu$. The former mode has not yet been observed. The latter has been reported[20] by ARGUS to have a branching fraction of $1.03\pm0.36\pm0.25\times10^{-3}$. However, there is a disagreement on this observation between ARGUS and CLEO since CLEO quotes[21] a upper limit of 0.43×10^{-3} for this mode. We have used 4×10^{-4} in estimating yields of this decay mode. This number is at the low end of the range of theoretical estimates[22] (2.5×10^{-4} to 10×10^{-4}) for the branching ratio.

According to the Section III, we will have a sample of 300 reconstructed $B^{\pm}_u$->$\rho^0\mu\nu$ decays with which to extract Vub. Additional cuts must be applied to this sample to reduce charm and beauty backgrounds. The extra criteria applied to our sample of $B^{\pm}_u$->$\rho^0\mu\nu$ include:

1. Three charged particles are required to originate in a common vertex separated from the primary vertex by 3σ = 60 microns in Δr or 3σ = 1200 microns in Δz where Δr, Δz are the primary and secondary vertex separations transverse and parallel to the beam direction.

2. The visible mass of the charged tracks is required to be greater than 2 GeV/c^2. This cut eliminates possible background from charm semi-leptonic decays such as D->K$\pi\mu\nu$ and D->$\rho\mu\nu$.

3. The two non-muon charged particles are required to have opposite sign and an invariant mass consistent with a ρ mass ($\pm$200 MeV/c^2).

4. The μ is required to have $\geq$1.6 GeV/c transverse momentum relative to the B direction. This cut eliminates much of the background from b -> cμ semileptonic decays. (For example, only 5% of the B^+ -> $D^0\pi^+\mu^+\nu$ muons pass this cut). The optimal value of the cut is still under study.

We have estimated the effects of these cuts by Monte Carlo studies. Summarizing the estimated yields of events passing these additional criteria (beyond the criteria imposed in the triggering and reconstruction process described in Section III), we find

1. Additional Vertexing Criteria	0.85
2. $M_{visible} > 2$ GeV/c^2	0.86
3. ρ mass ($\pm$200 MeV/c^2)	0.92
4. $p_t > 1.6$ GeV/c	0.34
Overall Additional Efficiency	0.23

leading to a net sample of $B^{\pm}_u \rightarrow \rho^0 \mu\nu$ for analysis of approximately 70 events.

The direction of the decaying B for these events is known if the primary and secondary vertices are observed and are measured reasonably well ($\pm$2 mrad on average). Therefore, using four momenta conservation at the secondary vertex for the $B^{\pm}_u \rightarrow \rho^0 \mu\nu$ decays (or $B^0_d \rightarrow \pi\mu\nu$ as the case may be), the missing neutrino momentum can be calculated. There is a two-fold ambiguity in the calculation, but under the hypothesis that the parent particle is a B, each solution can be weighted with the probability (derived from the expected shape of the neutrino momentum spectrum in this semi-leptonic decay) that it is the correct value. In the special case where the minimum mass of the decay products, including the assumed neutrino, equals the mass of the B meson, a unique solution is determined. Thus, to this level the B decay can be said to be completely reconstructed and the proper time (and lifetimes) can be calculated for these decays.

Backgrounds from charm semileptonic decays (such as D -> $\rho\mu\nu$) are eliminated by the visible mass cut and the requirement of substantial transverse momentum of the muon. The major backgrounds will come from B decays resulting in three charged prong topologies. Decays of the type B -> D where the D decays semileptonically are eliminated by the observation that the two charged partners of the muon have the same sign charge. D decays which result in a final state charged kaon are eliminated by the kinematic cuts outlined above as well as the RICH particle identification. The most serious remaining backgrounds are B -> DμX decays where the D decays into a neutral Kaon and one or more pions. A few such decay modes with the potential largest composite branching ratios are given in Table IV.A.5 below.

Table IV.A.5
Background to $B^{\pm}_u \rightarrow \rho^0 \mu\nu$

Background Decays	BR	Combined BR
$B^{\pm} \rightarrow D^0 \mu^{\pm} \nu$	0.016	
$D^0 \rightarrow K^0 \pi^- \pi^+$	0.054	9×10^{-4}
$D^0 \rightarrow K^0 \rho$	0.006	1×10^{-4}
$B^+ \rightarrow D^0 \pi^+ \mu^+ \nu$	*	
$D \rightarrow K^0 \pi^-$	0.026	*

*Branching ratio not yet known

Since these decays have similar topologies and signatures to the $B^{\pm}_u \rightarrow \rho^0 \mu\nu$, a comparison of the relative branching ratios for the combined decays to that of the $B^{\pm}_u \rightarrow \rho^0 \mu\nu$ decay (4×10^{-4}) gives the first level of comparison of the background rates of the other B decays. The kinematic cuts described above reduce these backgrounds by a factor of three (relative to the signal) in the worst case ($B^+ \rightarrow D^0 \pi^+ \mu^+ \nu$) and much more in general. Many of these decays can be separated out by direct observation of the tertiary D decay vertex. For those events where the D decay vertex is not

separable, the requirement that the three charged tracks come from a common vertex gives a large rejection.

The extraction of V_{ub} from the data must be done in a model dependent way. An unambiguous measurement of V_{ub} requires a measurement of the form factors and angular distribution of the $B^{\pm}_u \to \rho^0 \mu \nu$ decay . Even with the small number of events obtained, theoretical uncertainties will still dominate the calculation of Vub. These uncertainties are at the level of a factor of four[22] due to uncertainties in the B form factors.

Finally, we have not yet considered fully the $B^0_d \to \pi^{\pm} \mu \nu$ decay which can also be used to determine V_{ub}. Since it is a two prong topology, it is more prone to backgrounds (such as $B^0 \to D^+ \mu \nu \to K^0 \pi^+ \mu \nu$ with a composite branching ratio of 5×10^{-4}) and it has a lower net yield. Using cuts similar to the ones described for $B^{\pm}_u \to \rho^0 \mu \nu$ we expect to obtain a small sample of events ($\approx$ 15 to 20). However, in view of the scarcity of experimentally observed b->u decays, this is still worthwhile.

IV.A.7. Observation of Λ_b Baryons

We intend to search for B baryon production in the single muon inclusive triggers. We give a single specific example of a baryon decay that we could hope to see. We plan to search for the Λ_b reported by ALEPH[43] and by OPAL[44] in the mode $\Lambda_b \to \Lambda^0 \mu \nu + X^0$ where the $\Lambda^0 \to p \pi^-$ and more recently by ALEPH[45] in the mode

$$\Lambda_b \to \Lambda_c \mu \nu X^0$$

$$p K^- \pi^+$$

The overall branching ratio for the second decay sequence is 0.096% according to the ALEPH experiment. This ratio includes the fraction of b quarks hadronizing into Λ_b in e^+e^- interactions as well as the branching ratio $\Lambda_c \to pK\pi$. If we make the assumption that the same hadronization fraction is present in hadronic reactions and, since from Table III.A.2 we expect 3.5×10^7 b pairs to be produced during the 1994 data taking, this will result in production of 2.1×10^6 $\Lambda_b \to \Lambda_c \mu \nu X^0$ decays.

We do not consider other possible decays of the Λ_b's other than the $\Lambda_b \to \Lambda_c \mu \nu X^0$ mode, although we will search for them and they will contribute to our ability to make Λ_b measurements. The strategy that we choose to employ to detect Λ_b's will then rest on our ability to detect the Λ_c's. Examining the various possibilities, we list in Table IV.A.7 below several exclusive Λ_c modes which have large branching ratios and result in only charged particles. Once again, this is not an inclusive list.

Table IV.7
Selected Λ_c Decay Modes

Λ_c Decay	Topology	Composite BR	Ref.	Yield
$\Lambda_c \to pK^-\pi^+$	3 prong	3.2%	47	67,200
$\Lambda_c \to p\overline{K}^0 \to p\pi^+\pi^-$	1 prong + V	1.1%	"	23,100
$\Lambda_c \to p\overline{K}^0\pi^+\pi^- \to p\pi^+\pi^-\pi^+\pi^-$	3 prong + V	1.2%	"	25,200
$\Lambda_c \to \Lambda\pi^+\pi^-\pi^+ \to p\pi^+\pi^-\pi^+\pi^-$	3 prong + V	1.3%	"	27,300

We consider, first, the simpler three prong decay topology. The Λ_b->$\Lambda_c\mu\nu$ followed by Λ_c->$pK^-\pi^+$ decay chain is "self triggered" with a 1994 trigger•live time•acceptance (of the $pK\pi$ for those events in which the single muon trigger has been satisfied) efficiency of 3.5% and an estimated composite reconstruction efficiency of ≈45% giving an overall yield of reconstructed decays of this sort of approximately 1050 events.

These events must be subjected to various cuts to eliminate backgrounds. If we consider the topology, we require the reconstructed $pK^-\pi^+$ to be at the proper mass and to intersect the muon track somewhere between the primary vertex and the Λ_c vertex itself. The Λ_c vertex does not have to be separated from the muon track so we do not apply a tertiary vertex separation criteria. However, in order to reduce combinatorial backgrounds, we will require the Λ_c vertex (or its composite with the muon) to be well separated from the primary vertex. Since this is a tertiary decay vertex, it will have the combination of both Λ_b and Λ_c lifetimes so we expect to lose less than the expected 15% of the events (see Appendix A) if we applied a $\Delta r \geq 3\sigma \approx 60$ micron or $\Delta z \geq 3\sigma \approx 1200$ cut (assuming the Λ_b life time is some what comparable to the B meson lifetimes).

A major background will be B->μ +X semi-muonic decays of one sort or another. For example, the decays B->$D^+_{d(s)}\mu\nu$ ->$K\pi$ (K)$\pi\mu\nu$ decay sequence has the same topology. However, with particle id we can separate these decay from Λ_b->$\Lambda_c\mu\nu$ on the basis of reconstructed mass by properly identifying the protons and the K's in the respective decays. Since the Cerenkov counter can only separate protons from K's above 12 GeV/c, we will only be able to positively identify that fraction of the total number of Λ_c->$pK^-\pi^+$ decays in which E_{proton}>12 GeV/c. We expect a second loss of events due to the particle id inefficiency which will be suffered for two of the three particles in order to properly accomplish π/K/p id for the $pK\pi$ final state. Combining these three loss factors,

1. Vertex cut	.85
2. Proton Energy	.60
3. K/π/p id	.77
Total	.39

we expect to obtain 410 identified Λ_b->$\Lambda_c\mu\nu$ followed by Λ_c->$pK^-\pi^+$ decays. This is very adequate for cross section, lifetime and relative branching ratios (provided other Λ_b modes such as those in Table IV.7 can be identified) determinations . For the semi-exclusive decays with only a missing neutrino, $\beta\gamma$ can be reasonably calculated using the visible energy and mass. As a final comment, it is worthwhile to note that the charge of the muon is correlated with the charge of the Λ_c, i.e. if the muon is negative the Λ_c must have positive charge and decay eventually into a proton which will typically have the largest momentum of the decay products. Backgrounds can be suppressed to some extent , therefore, without recourse to particle id by demanding that the charge of the highest momentum particle have the correct sign correlation with respect to the muon. This tends to suppress the topologically similar background from B->D+x->K$\pi\pi$ +x since the K charge has the opposite correlation with the muon charge as the proton form the Λ_b->Λ_c->p sequence. The technique of demanding proper charge correlations is generally useful (modulo mixing and b->c contamination) and can be applied in several other studies we are proposing. The effectiveness of this background suppression strategy is under study on a case by case basis.

As far as other Λ_c decays are concerned, although three prong plus V topologies have lower acceptance (more particles and the Λ,K^0 flight path losses) and lower individual branching ratios, they have the advantage that the presence of Λ and K^0 decays eliminate the requirement for

We consider, first, the simpler three prong decay topology. The $\Lambda_b \to \Lambda_c \mu\nu$ followed by $\Lambda_c \to pK^-\pi^+$ decay chain is "self triggered" with a 1994 trigger•live time•acceptance (of the $pK\pi$ for those events in which the single muon trigger has been satisfied) efficiency of 3.5% and an estimated composite reconstruction efficiency of ≈45% giving an overall yield of reconstructed decays of this sort of approximately 1050 events.

These events must be subjected to various cuts to eliminate backgrounds. If we consider the topology, we require the reconstructed $pK^-\pi^+$ to be at the proper mass and to intersect the muon track somewhere between the primary vertex and the Λ_c vertex itself. The Λ_c vertex does not have to be separated from the muon track so we do not apply a tertiary vertex separation criteria. However, in order to reduce combinatorial backgrounds, we will require the Λ_c vertex (or its composite with the muon) to be well separated from the primary vertex. Since this is a tertiary decay vertex, it will have the combination of both Λ_b and Λ_c lifetimes so we expect to lose less than the expected 15% of the events (see Appendix A) if we applied a $\Delta r \geq 3\sigma \approx 60$ micron or $\Delta z \geq 3\sigma \approx 1200$ cut (assuming the Λ_b life time is some what comparable to the B meson lifetimes).

A major background will be $B \to \mu + X$ semi-muonic decays of one sort or another. For example, the decays $B \to D^+_{d(s)}\mu\nu \to K\pi\ (K)\pi\mu\nu$ decay sequence has the same topology. However, with particle id we can separate these decay from $\Lambda_b \to \Lambda_c \mu\nu$ on the basis of reconstructed mass by properly identifying the protons and the K's in the respective decays. Since the Cerenkov counter can only separate protons from K's above 12 GeV/c, we will only be able to positively identify that fraction of the total number of $\Lambda_c \to pK^-\pi^+$ decays in which $E_{proton} > 12$ GeV/c. We expect a second loss of events due to the particle id inefficiency which will be suffered for two of the three particles in order to properly accomplish $\pi/K/p$ id for the $pK\pi$ final state. Combining these three loss factors,

1. Vertex cut	.85
2. Proton Energy	.60
3. K/π/p id	.77
Total	.39

we expect to obtain 410 identified $\Lambda_b \to \Lambda_c \mu\nu$ followed by $\Lambda_c \to pK^-\pi^+$ decays. This is very adequate for cross section, lifetime and relative branching ratios (provided other Λ_b modes such as those in Table IV.7 can be identified) determinations . For the semi-exclusive decays with only a missing neutrino, $\beta\gamma$ can be reasonably calculated using the visible energy and mass. As a final comment, it is worthwhile to note that the charge of the muon is correlated with the charge of the Λ_c, i.e. if the muon is negative the Λ_c must have positive charge and decay eventually into a proton which will typically have the largest momentum of the decay products. Backgrounds can be suppressed to some extent , therefore, without recourse to particle id by demanding that the charge of the highest momentum particle have the correct sign correlation with respect to the muon. This tends to suppress the topologically similar background from $B \to D+x \to K\pi\pi + x$ since the K charge has the opposite correlation with the muon charge as the proton form the $\Lambda_b \to \Lambda_c \to p$ sequence. The technique of demanding proper charge correlations is generally useful (modulo mixing and $b \to c$ contamination) and can be applied in several other studies we are proposing. The effectiveness of this background suppression strategy is under study on a case by case basis.

As far as other Λ_c decays are concerned, although three prong plus V topologies have lower acceptance (more particles and the Λ, K^0 flight path losses) and lower individual branching ratios, they have the advantage that the presence of Λ and K^0 decays eliminate the requirement for

K/π/p particle id capability. In spite of lower over all yields, we will be able to reconstruct appreciable number of Λ_b in those modes. In order to enhance statistics, we have also considered the inclusive Λ_b->Λ +x that ALEPH employed in the detection of the Λ_b. We have made a preliminary estimate that of order 1000 Λ_b can be identified in these inclusive mode.

Finally, we have not yet considered searching for Λ_b exclusive modes such as Λ_b ->ΨpK. This mode is thought to have a composite branching ratio of $\approx 5 \times 10^{-5}$ (quite accessible) for the $\mu\mu$pKπ final state and has a quite obvious signature with good trigger qualities. We would expect some 20 golden reconstructed events in such a mode.

IV.B Hidden Charm Physics

As described in Appendix B and Ref. 1, 2 and 5, in Fermilab Experiment E705 we have examined final states in which there was a J/Ψ or a Ψ' to both measure the production of the J/Ψ, Ψ' and χ states and search for previously unobserved hidden charm or four quark states. In the 1994 run we will be able to study the J/Ψ, χ and Ψ' production and decay in 800 GeV/c pN interactions with much higher statistics than were available to E705 at 300 GeV/c.

In addition, we made tentative observations with low statistics of two enhancements at 3.827 GeV/c^2 (decaying into J/$\Psi\pi^+\pi^-$) and 3.525 GeV/c^2 (decaying to J/$\Psi\pi^0$). These enhancements have been respectively interpreted as the $^3D_2$ and $^1P_1$ states of charmonium. The $^1P_1$ state has been previously reported[4] by Fermilab experiment E760 while the $^3D_2$ state has not previously been observed.

However, the level of the statistics in E705 made these observations inconclusive and did not allow adequate studies to be made to completely rule out other possible explanations such as four quark states. With the greatly increased statistics expected from the 1994 run (a factor of ≈100 more events containing reconstructed J/Ψ's than were obtained in E705), we expect to confirm or reject the observations and be able to make more sophisticated studies to ascertain the origin of the enhancements. We would also be able to inspect the various Ψ' mass combinations with other final state particles in order to search for other hidden charm final states.

IV.B.1. Measurements of Aspects of J/Ψ,Ψ', and χ Production and Decay

As discussed in Appendix B and Ref. 2 and 5, we performed measurements of several aspects of J/Ψ,Ψ', and χ production and decay in Fermilab Experiment E705 . We have scaled up from these measurements, assuming that the relative ratio of Ψ' and χ production to J/Ψ production is the same as in 300 GeV/c interactions. We have ignored improvements in reconstruction efficiencies in making these estimates. It is obvious from Table III.E.2 that a great deal more statistics for these states can be accumulated in the 1994 run.

The greater statistics will allow us to perform studies which were limited by the size of the data sample in E705. In addition, we will be making measurements of all facets of J/Ψ,Ψ', and χ production in 800 GeV/c pN interactions, a different energy regime. Among these studies are searches for other "new" states which decay into either Ψ' or χ. We will also be able to be more selective in choosing data samples for our χ studies, given the larger statistics. Our E705 photon data indicates that selection of higher quality, better resolution photons (those of higher energy or which do not overlap with other photons in the event) together with the better resolution expected in the electromagnetic calorimeter due to improvements in the ADC system[48] to eliminate pedestal shifts can improve the $\gamma\Psi$ mass resolution from 30 MeV/c^2 to better than 20 MeV/c^2. These factors will allow a better separation of χ_1 to χ_2 and a better determination of the χ_1 to χ_2 ratio for proton induced processes, a quantity which still remains very poorly determined.

The greater statistics and better photon resolution will also permit measurements of the $d\sigma/dx$, $d\sigma/dp_t$ and the decay angular distributions for the individual χ states. In particular, the angular distribution of the photon[49] with respect to the beam direction in the center of mass of the χ is sensitive to the details of the processes that can contribute to χ production.

IV.B.2 Confirmation of Charmonium States/Searches for Other Hidden Charm States

We have used the results[1] from E705 to estimate the yields of the 3.827 and 3.525 GeV/c^2 enhancements in a 1994 run. In the E705 experiment we reconstructed a total of 24,440 $J/\Psi \rightarrow \mu\mu$ decays with 12,470, 5560 and 6090 events from the π^-N, π^+N and pN data respectively. The level of the 3.827 GeV/c^2 enhancement seen in the π^- data was 74±22 events with a signal to background ratio of approximately 1/3. Scaling up by the ratio of the number of reconstructed $J/\Psi \rightarrow \mu\mu$ expected in the 1994 run to the number of reconstructed $J/\Psi \rightarrow \mu\mu$ in E705, we obtain the yields of the enhancements shown in Table III.E

In this process, we have, once again, assumed that the yield of the enhancements and the backgrounds to those enhancements will be the same as was observed in E705 in 300 GeV/c $\pi^{\pm}$ and pN interactions. No allowance has been made for the expected improvement in the reconstruction efficiencies for the additional charged pions (as in the case of $^3D_2$ decay into $J/\Psi\pi^+\pi^-$) relative to those of the E705 run.

Finally, the much larger statistics gives us the chance to look for other charmonium states that have not to date been observed. In addition, more exotic phenomena such as four quarks states can be searched for. With these statistics, we will have the opportunity to apply tests which may distinguish between such hypotheses and mundane charmonium explanations for any state observed (including the 3.827 and 3.525 GeV/c^2 objects).

V. 1994 Experimental Setup

The basic configuration of the spectrometer with which we plan to accomplish the objectives outlined in Section I and II, is shown in Fig. 1 in Section I. The configuration remains essentially the same as that of E771 except for the addition of a RICH counter (Appendix E). We plan, however, to make the following modifications and additions to enhance the capability of the detectors that are already in place:

1. Full instrumentation of the E771 silicon microvertex detector as outlined in Appendix C. Because of the late completion of the fast readout electronics for the silicon detector only ≈10K of the 17.5K channels planned for the E771 detector were delivered and installed in 1991. Approximately 4K channels of these were instrumented with prototype electronics which must be upgraded or replaced. The final 7.5K channels which are required for the 1994 run will be used to complete the instrumentation of the beam measurement system and to instrument two x and y planes (K type) in the silicon tracker as shown in Fig. C1. The university participants will take responsibility for monitoring of the production and execution of testing process, thereby relieving Fermilab of the burden of production engineering. It is expected that Fermilab will provide the funds for the completion of the instrumentation of this detector.

2. Addition of a second level trigger as discussed in Appendix D. In the 1991 run, we successfully operated our first level muon triggers at interaction rates averaging

approximately $2x10^6$ interactions per second and live times of 60%. We plan in the 1994 run to add this second level in order to go to higher rates ($\geq 5x10^6$ interactions per second) and accommodate larger trigger acceptance/efficiency while increasing our live time to ≥80%.

3. Completion of several smaller miscellaneous hardware projects to prepare the spectrometer for operation at higher rates. Included in this ensemble of tasks is the modification of pad chamber readout, adding one shots to selected large area, large capacitance pads to eliminate signals from earlier interactions. Also as discussed in Appendix D there are several upgrades to the muon detector required to enhance the efficiency and acceptance of the first level trigger.

4. Addition of a RICH Counter as described in Appendix E.

The cost of these upgrades and the expected funding sources as well as the institutional responsibilities are outlined in Appendix F

VI. Summary

We propose in the 1994 run to continue the work started in E771 and E705 to study beauty and charm phenomena associated with high p_t single muons and high mass dimuons from B and J/Ψ decay. The numbers of B->J/Ψ->μμ and B->μ that can be recovered (i.e. triggered on and reconstructed partially or totally for physics) for the various physics objectives are very competitive with that expected from other types of B physics experiments. An increase in data of a factor of approximately 100 is expected over the data accumulated in our short E771 data taking.

We expect to make measurements of the B hadroproduction cross sections at 800 GeV/c to better than 10% and measurements of the charged and neutral lifetimes to approximately 10%. We will measure $B^{\pm}_d$, B^0_d, B^0_s production (and to level of knowledge of branching ratios, the associated hadronization fractions), lifetimes and mixing. We will make a measurement of V_{ub} via the exclusive decay modes, $B^0_d \to \pi^{\pm}\mu\nu$ and $B^{\pm}_u \to \rho^0\mu\nu$. Finally, we plan to measure B baryon (specifically the Λ^0_b) production and lifetimes. We expect to accumulate reconstructed data samples for these studies ranging from the level of millions of J/Ψ->μμ, hundreds of thousands of inclusive B->μ, thousands of reconstructed B->J/Ψ->μμ inclusive decays down to several tens of reconstructed $B^{\pm}_u \to \rho^0\mu\nu$ decays.

We also expect to accumulate by far the largest number of directly produced J/Ψ decays of any experiment to date and to study those events for evidence of charm states decaying into J/Ψ + photons or pions that are presently, at best, only marginally measured because of limited statistics. As a measure of our sensitivity to such states, we estimate our reconstructed J/Ψ->μμ sample to be of order two million, a factor of ≈100 greater than previously obtained in E705.

The major upgrades required to accomplish this experiment include full instrumentation of the silicon detector, improvements to the existing muon detector and implementation of the second level trigger. In addition, although all these studies can be performed to some level with no π/K/p identification, the addition of the RICH detector enhances both statistics (making certain modes accessible) but also offers the opportunity to reduce backgrounds significantly for modes such as $\Lambda_b \to \Lambda_c\mu\nu \to pK\pi\mu\nu$ which contain strange particles in non resonant states.

In conclusion, we have a wealth of opportunity in the 1994 run to collect significant data samples for various B decay modes in our fixed target experiment which will be hard to obtain in

other experimental configurations. We can also greatly increase our charmonium statistics over what we have previously obtained. The upgrades to the existing E771 spectrometer needed to do this are relatively modest.

Appendix A
The 1991 E771 Run

In our 1991 run, we successfully implemented and tested our muon trigger system and determined the various efficiencies of both triggers and detectors. In addition, in spite of the late and partial delivery of our silicon detector electronics[50], we managed to accumulate 110 million dimuon triggers and 60 million single muon triggers in approximately three weeks of operation in December of 1991. At the time of this writing, we have only just begun bulk processing of our 1991 data. We present in this and the following appendices preliminary studies of approximately 1.1 million dimuon triggers representing a fraction (≤1%) of the data taken in the 1991 run.

Based on the dimuon data accumulated, we have been able to perform the "meaningful test" (J. Peoples, December 14, 1991 Letter) suggested by the Laboratory and Fermilab PAC (B. Cox, October 1, 1990 Letter; T. Yamanouchi, October 15, 1990 Letter; B. Cox, October 29 Letter) which was intended to prepare for a significant 1994 data taking run. We have used the small portion of our data thus far analyzed to investigate the technical issues concerning performance of the experiment and feel, with some confidence, that we can extrapolate to the performance we can achieve in a 1994 run.. The performance of the two critical detector components, the silicon detector and the muon detector/trigger system have been studied. The silicon vertex detector 1991 performance is discussed in this appendix. The configuration and the extrapolated 1994 performance of the completely instrumented configuration is presented in Appendix C. The 1991 performance of the muon trigger system has been evaluated in some detail and is presented in Appendix D along with the expected 1994 performance figures..

In Fig. A.1 we show the dimuon spectrum from a small fraction of the 1991 data. A clear J/Ψ signal (resolution of 45 MeV/c^2) is seen with very little background (estimated to be less than 10% of the signal).

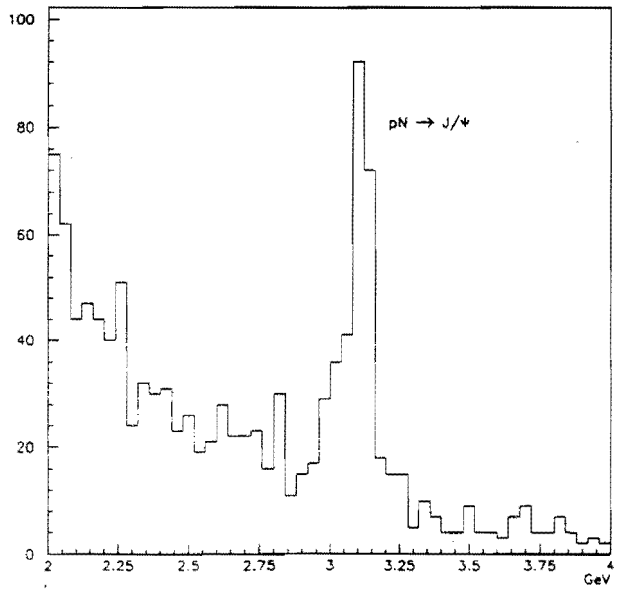

Fig. A.1
Dimuon Mass Spectrum From ≈0.3% of the 1991 E771 Data

We have calculated a preliminary cross section for J/Ψ->μμ production in pN interactions at 800 GeV/c. Using 0.22% of the 1991 data (a live beam of 6.6×10^{10} protons) in this determination of the cross section and the pertinent 1991 trigger and reconstruction efficiencies as discussed in Section III of the proposal, we obtain a cross section of 435± 70 nb per nucleon. To scale from the Si cross section to the nucleon cross section, we have used an A dependence of $A^{0.92}$. This is in reasonable agreement at this preliminary stage of the analysis with the Lyons parameterization (Section III.A.1) which predicts 509 nb/nucleon.

Silicon Detector Efficiencies

Given all of the difficulties with the silicon detector installation in the 1991 run, we were still able to begin our physics studies and gain valuable experience with the partially instrumented devices. Even though the smaller instrumented region of the beam and microvertex detectors forced operation with a smaller beam ($\sigma_x \approx 2.3$ mm , $\sigma_y \approx 1.8$ mm) than desirable from a radiation damage standpoint, we were able to achieve the efficiencies indicated in Fig. A2.

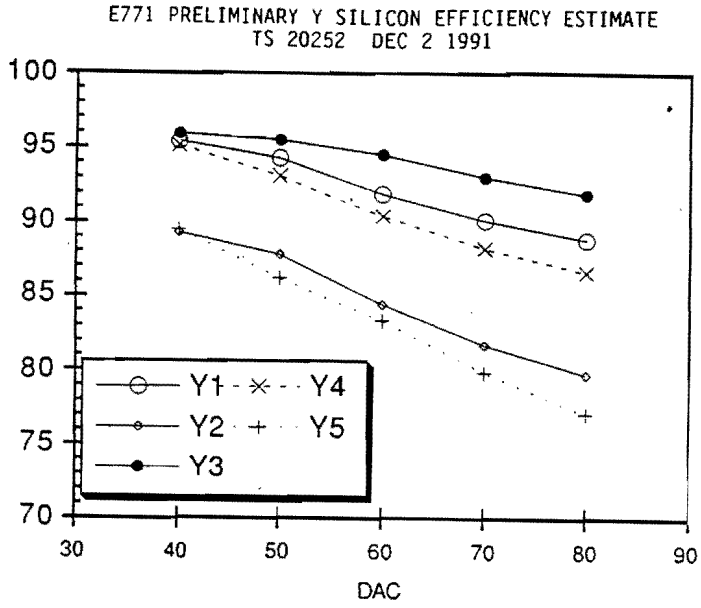

Fig. A2
1991 Silicon Detector Efficiencies

These efficiencies are not optimized since time was short in the 1991 run for complete tuning of the silicon detector performance (noise, timings, thresholds settings and other parameters should be studied under different operating conditions). In addition, if time had permitted, some of the lower efficiency silicon planes would have been replaced. However, the efficiencies were stable with time and radiation dose as will be seen in the discussion of radiation damage effects below.

Silicon MVD Resolutions

We have analyzed general dimuon triggers and J/Ψ->μμ decays from the data, as well as Monte Carlo J/Ψ->μμ superimposed on real 800 GeV/c interactions from the data to study the resolutions and efficiencies of the silicon detector. The overlaid Monte Carlo J/Ψ->μμ have been generated in a GEANT simulation of the 1991 silicon detector containing delta rays, strip width resolution effects, charge sharing, multiple scattering, etc. as well as the observed individual efficiencies of the silicon planes. The first crucial issue involving the resolutions of silicon detector (as well as the spectrometer wire chamber ensemble up stream of the analysis magnet) is the ability to match tracks in the silicon detector to spectrometer tracks. In Fig. A3 we show the observed matching in the slope and intercept in the x and y projections for the J/Ψ->μμ muon tracks in the spectrometer to the tracks in the silicon as evaluated at the z position intermediate between the silicon detector and spectrometer PWC system, which is optimal for matching resolution.

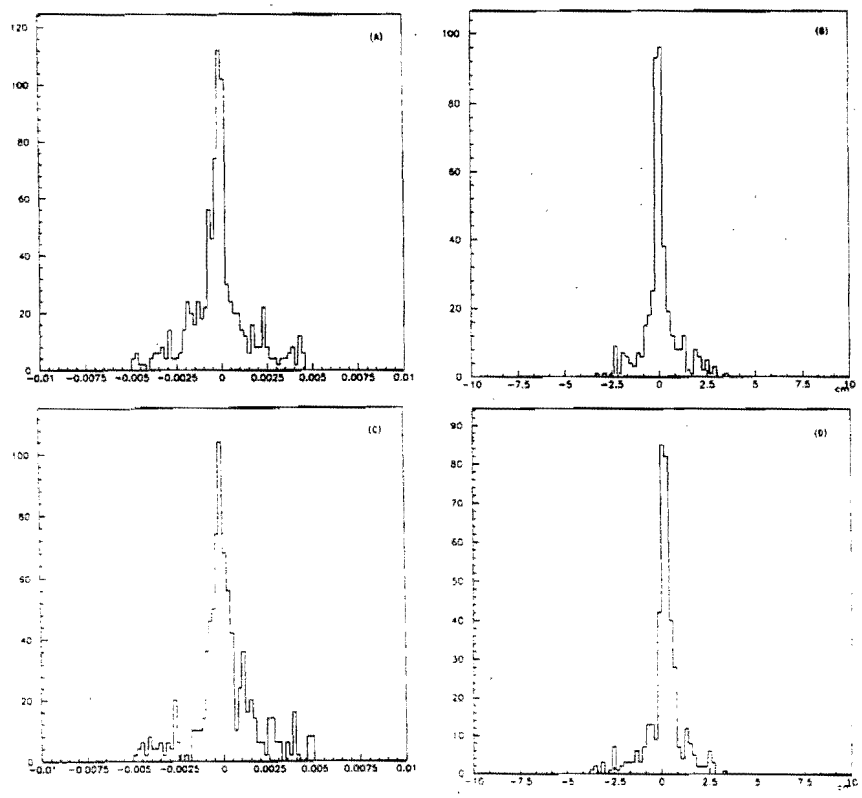

Fig. A3
Matching Distributions Between Silicon Tracks and Spectrometer Tracks
a) x slope matching b) x intercept matching
c)y slope matching d) y intercept matching

The matching resolutions observed for the muon tracks are $\sigma_{x'} \approx 0.47$ mrad, $\sigma_{y'} \approx .52$ mrad for the slopes and $\sigma_x \approx 0.30$ cm and $\sigma_y \approx 0.36$ cm for the intercepts, in reasonable agreement with Monte Carlo expectations. These results are dominated by the spectrometer front chamber track resolutions. The discrepancy between x and y is expected since the front chamber PWC system is a small angle (16.7°) system in which the y coordinate is not as well measured as the x.

The resolution of the primary vertex is important for all facets of B physics. We have determined the resolution of our partially instrumented vertex detector from the data taken in the 1991 run. In Fig. A4a we show the difference between the x position of the primary vertex as determined from the silicon tracker and the x position of the incident beam as measured by a 25 micron silicon plane. From this distribution, we extract a $\sigma \approx 15$ microns for the primary vertex resolution (after correction for the resolution of the beam plane measurement; $\sigma \approx 19$ microns). This is to be compared to the Monte Carlo prediction of 14 microns. In Fig. A4.b we show the z distribution of the primary vertices. This distribution clearly shows the twelve 2 mm silicon foils (and even a small peak due to interactions in the first 300 micron plane of the silicon tracker). Unfolding the z resolution of the primary vertex determination from observation of the edges of the foils, we obtain an average z resolution of 350 microns of the primary vertex (compared to the Monte Carlo expectation of 300 microns). The average z resolution for each of the foils is shown in Fig. 4.c

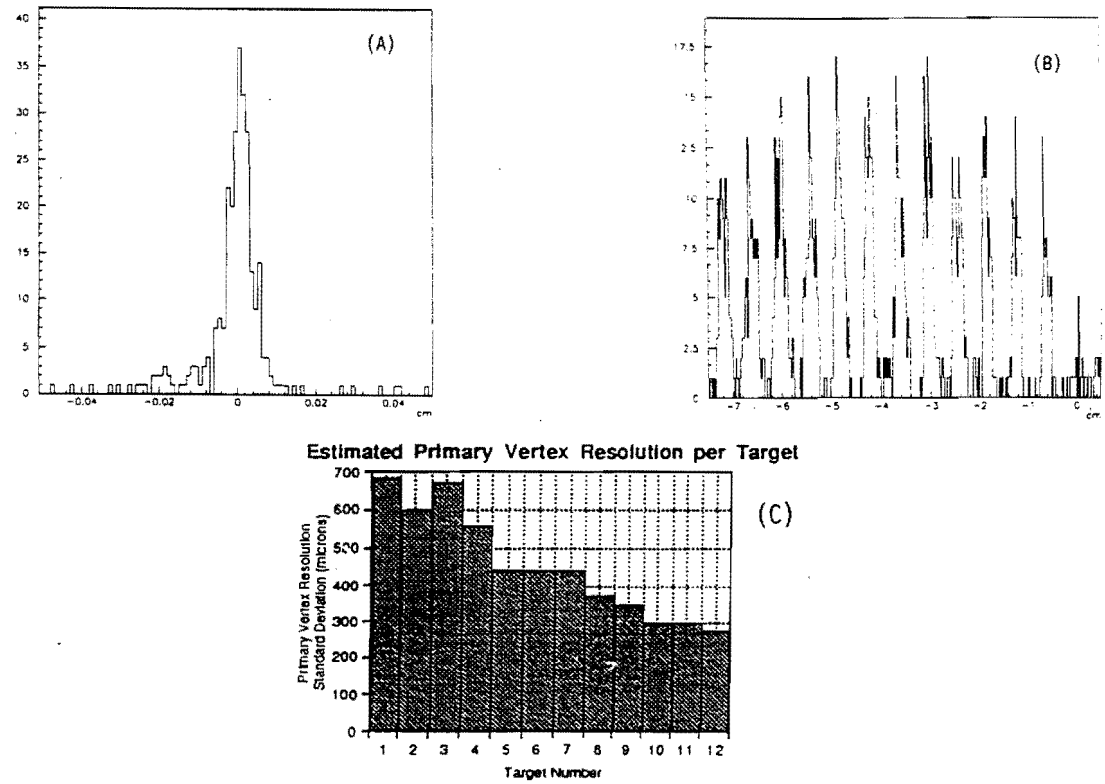

Fig. A4
a) x Silicon Primary Vertex - x Beam Silicon
b) z Vertex Distribution of Primary Vertices in Dimuon Triggers
c) z Vertex Resolutions for Each Foil

The resolution of the distance of closest approach of single tracks to the primary vertex (impact parameter) is a critical parameter for the analysis of the B->μ data and the separation of these decays for backgrounds Fig. A.5 shows the distribution of distance of closest approach of silicon microvertex tracks in the x projection to a primary vertex as calculated from the ensemble of all silicon tracks in a sample of dimuon triggers. This can be considered as a preliminary determination of a single track impact parameter resolution ($\sigma \approx 18$ microns to be compared with a Monte Carlo prediction of 16 microns).

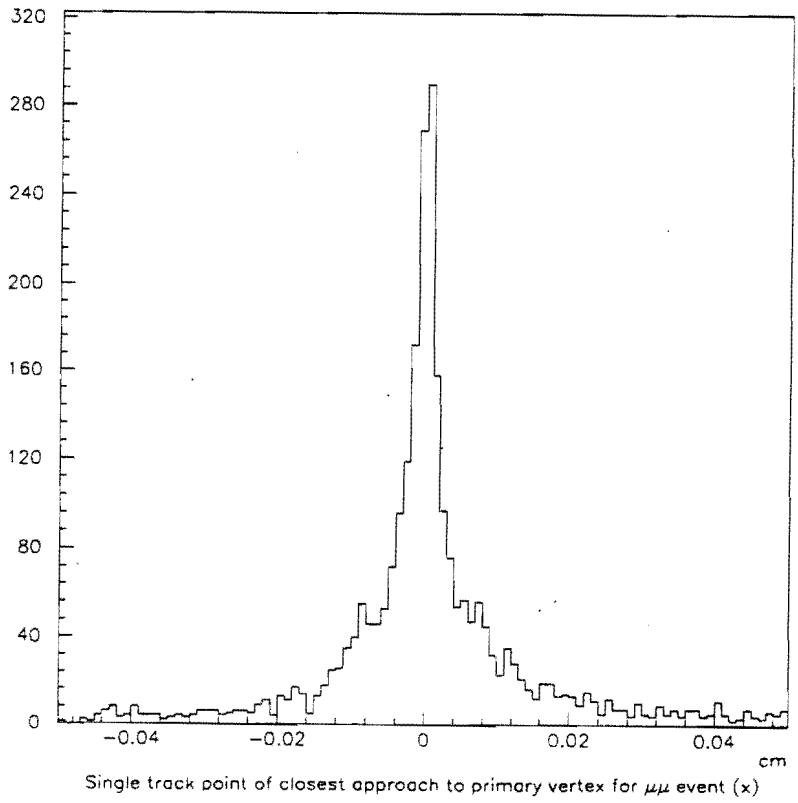

Fig. A.5
Distance of Closest Approach of Tracks in x Projection to Primary Vertices

The resolution for determining that two particle are emanating from the same vertex has been obtained from our data with a study of the distance of closest approach of the two muons from J/Ψ decays. We have also extracted these resolutions from the overlaid Monte Carlo J/Ψ-

>μμ. The determination of the distance of closest approach from the sample of primary vertex J/Ψ is perhaps a worst case result because of the many hits from primary tracks in the vicinity of the muon pair. Even though the resolutions for assigning a track to a given vertex will become better as the number of charged tracks from the secondary vertex increases, we have taken the two track resolutions as a worst case when applying the vertex resolution criteria in Section IV. In Fig. A6a and b we plot the distance of closest approach of matched muon tracks from J/Ψ->μμ decays in the x and $r=\sqrt{x^2+y^2}$ projections respectively.

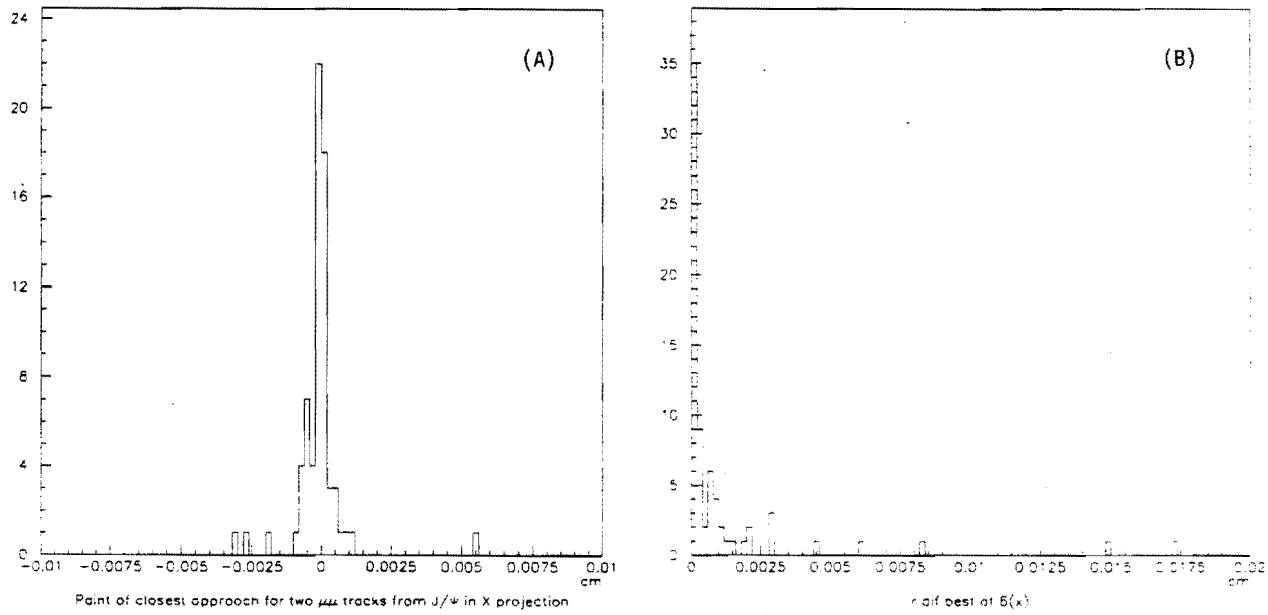

Fig. A6
a) Δx ; Distance of Closest Approach of Muons from J/Ψ->μμ
b) Δr ; Distance of Closest Approach of Muons from J/Ψ->μμ

The widths of these distributions ($\sigma_X \approx$ 7.0 microns, $\sigma_r \approx$ 8.5 microns) match Monte Carlo estimates based on superimposed J/Ψ Monte Carlo.

Finally, we have considered the secondary vertex resolution (the position of the vertex as determined from the midpoint of the distance of closest approach relative to its true position) which is the second component in determining the capability for separating primary and secondary vertices. Using the superimposed J/Ψ sample, we find a slightly poorer resolution (as expected) for secondary vertices (constructed from two tracks) than we did for the primary vertex (constructed from many tracks). The resolutions are $\sigma_x \approx$ 16 microns, $\sigma_r \approx$ 18 microns and $\sigma_z \approx$ 400 microns). Our cuts to define two track vertices (based on these resolutions) retain 85% of the J/Ψ's from the data (as compared to 86% of the overlaid MC J/Ψ's).

We have compiled the various vertexing resolutions in Table A. Based on these preliminary primary and secondary resolutions, we estimate the resolution of primary and secondary vertex separations in the three coordinates x, r and z for the 1991 run to be 23 microns, 24 microns and 530 microns respectively.

Table A
Silicon Vertex Detector Resolutions
(all lengths in microns)

Type of Resolution	Data			MC		
	Δx	Δr	Δz	Δx	Δr	Δz
Primary Vertex	15	18	350	14	17	300
Track Impact Parameter	18	22	500	16	19	400
Distance of Closest Approach	7.0	8.5	-	7.5	8.5	-
Secondary Vertex	*	*	*	16	18	400

*work in progress on extracting results from data

In the 1994 run, we expect to improve these resolutions, given the upgrades of the silicon detector that are contemplated. First, the primary vertex resolution will no longer be determined from tracks outgoing from the primary vertex. With the completely instrumented beam silicon discussed in Appendix C, we will determine the transverse position of the primary vertex from the incoming beam track to ≤ 7 microns. The secondary vertex resolution will also improve because of the additional measurement planes. Because of the limited number of planes for the 1991 run we were forced to accept 3 hit tracks. With 7 planes we will be able to increase our requirements to at least four hits and perhaps five leading to ≈25% improvements in secondary vertex resolutions. This leads us to expect vertex separation resolutions of <20 microns in r and ≈400 microns in z in the 1994 run compared to ≈23 and 530 microns in 1991.

Having determined the vertex separation resolutions, we can compare them to the expected decay lengths of the B decays. We show in Fig. A.8.a , b and c a Monte Carlo of the expected x, r and z decay length distributions for 800 GeV/c pN interactions for B decays based on the average of the latest measurements of B lifetime, 1.40±0.045ps, from the LEP experiments[21].

While, as stated in Section III.D, the separation criteria needed to insure distinguishable primary and secondary vertices are mode dependent, if we arbitrarily set a criteria of either $\Delta r=\sqrt{\Delta x^2+\Delta y^2} \geq 60$ microns ($\approx 3\sigma$) or $\Delta z \geq 1.2$ mm ($\approx 3\sigma$), we would retain $\approx 85\%$ of the decays. We would choose to set the criteria for adequate impact parameters somewhat greater ($\Delta r \geq 100$ microns) because of single track resolution.

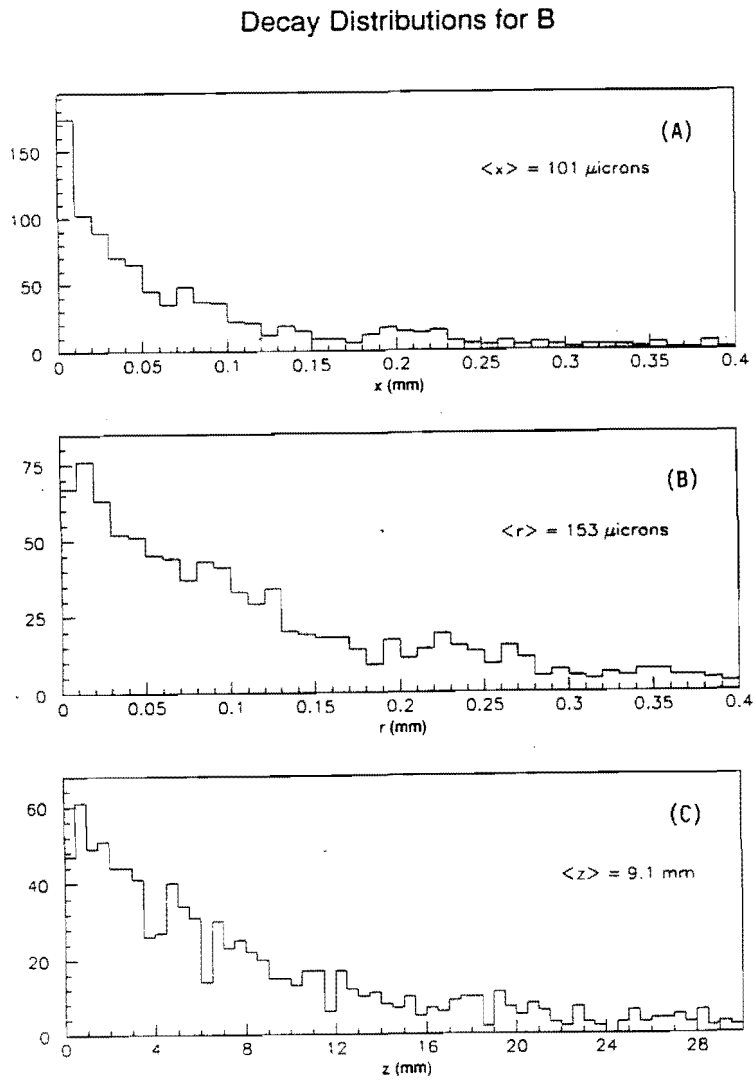

Fig. A.7
a) Separation of Primary and B Secondary Vertices in x
b) Separation of Primary and B Secondary Vertices in $r=\sqrt{x^2+y^2}$
c) Separation of Primary and B Secondary Vertices in z

Radiation Damage

The operation with a small beam size ($\sigma x \approx 2.3$ mm, $\sigma y \approx 1.8$ mm) forced us to accumulate a total 1991 exposure[51] of $\approx 3.3 \times 10^{14}$ minimum ionizing particles per cm^2 in the beam region of our silicon detector. This had the hidden advantage of proving that the detector could withstand radiation levels approaching those expected in the 1994 run. As shown in Fig. A.8.a below, while leakage currents increased very appreciably during the 1991 run, efficiencies determined from triggering on beam particle (Fig. A.8.b) measured before and after the major exposure do not indicate an appreciable decrease of performance. Since the E771 silicon amplifier was designed with large current capacity (>1μA/strip or ≈700μA per plane), the increase in leakage current can be accommodated.

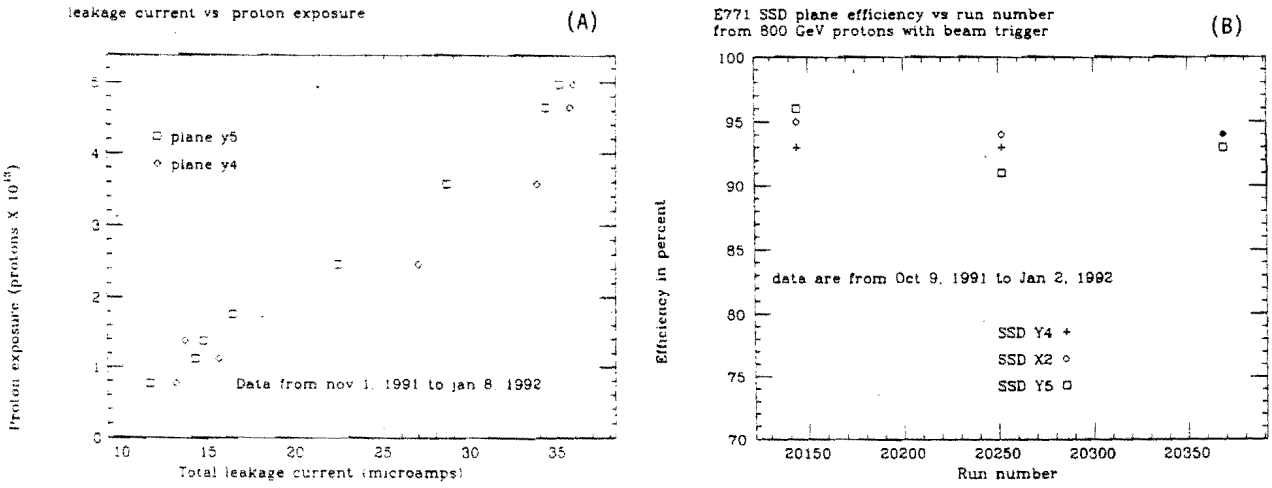

Fig. A.8
a) 1991 Integrated Silicon Plane Leakage Current as a Function of Radiation Exposure
b) Silicon Plane Efficiencies Before and After Major Exposure

The period in which the data of Fig. A.8 were accumulated corresponds to last three months of the Fermilab fixed target run when the bulk of the exposure to beam was experienced.

Because we can operate in the 1994 with a fully instrumented detector, we will be able to use a larger beam ($\sigma \approx 4$ mm). This should permit the much greater integrated beam flux (of order a factor of 8 greater) than was acquired in 1991.

Appendix B
Hidden Charm Results
from Fermilab Experiment E705

In 1988, we completed data taking in Fermilab Experiment E705. In this experiment we reconstructed 24,000 J/Ψ->μμ decays produced in 300 GeV/c $\pi^{\pm}$, proton and antiproton interactions. Since we expect to reconstruct over $2x10^6$ J/Ψ->μμ in the 1994 run, it is natural to continue the E705 study of the hidden charm physics associated with J/Ψ and Ψ' with much higher statistics with 800 GeV/c pN interactions.

In Fig. B.1 we show the composite dimuon spectrum obtained in E705. J/Ψ and Ψ' signal can be seen in this spectrum.

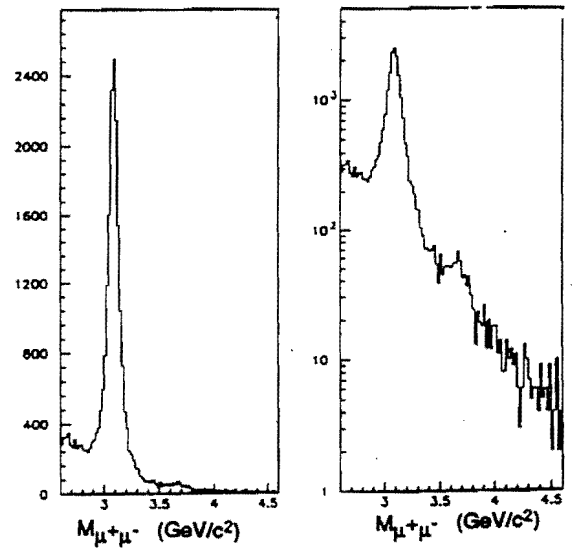

Fig. B.1
E705 Dimuon Mass Spectrum

The J/Ψ and Ψ' events were examined in a search for heavy quark states which decay into either charmonium state plus photons or pions.

The E705 search for hidden charm states[1,2] decaying into a photon or a π^0 was facilitated by the E705 electromagnetic detector[52] which had the ability to detect and measure with reasonable resolution photons with energies down to 2 GeV even in the presence of pedestal shifts in the ADC's at higher rate. The pedestal shift problem has since been rectified and the upgraded EM detector electronics[49] should allow somewhat better resolution in a 1994 run. As an example of the resolutions which were achieved at interaction rates over 2 MHz with this detector, we show in Fig. B.2.a an E/p spectrum for electrons from 300 Gev/c interactions and in Fig. B.2.b a γγ mass spectrum.

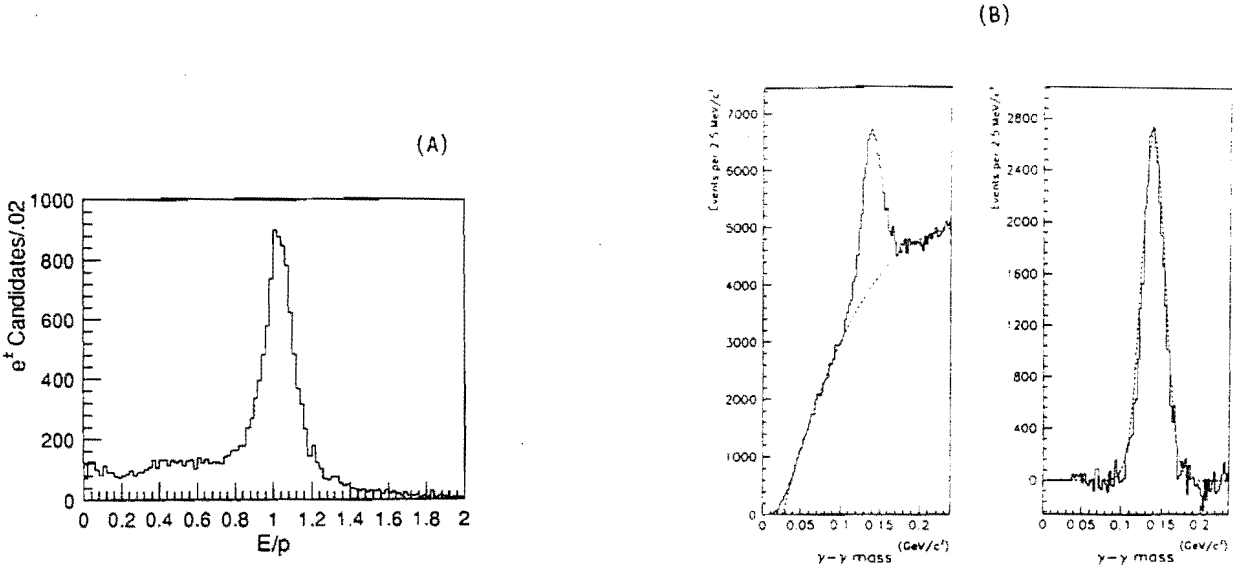

Fig. B.2
a) E/p for Electrons from 300 GeV/c Interactions
b) γγ Mass Spectrum from 300 GeV/c Interactions

The γΨ mass spectra from the 24,000 J/Ψ events accumulated in E705 is shown in Fig. B.3a and B.3.b below. Fig. B.3.b shows the a background subtracted γΨ mass spectrum where the background is constructed from combinations of photons from one Ψ event with Ψ dimuons from another event.

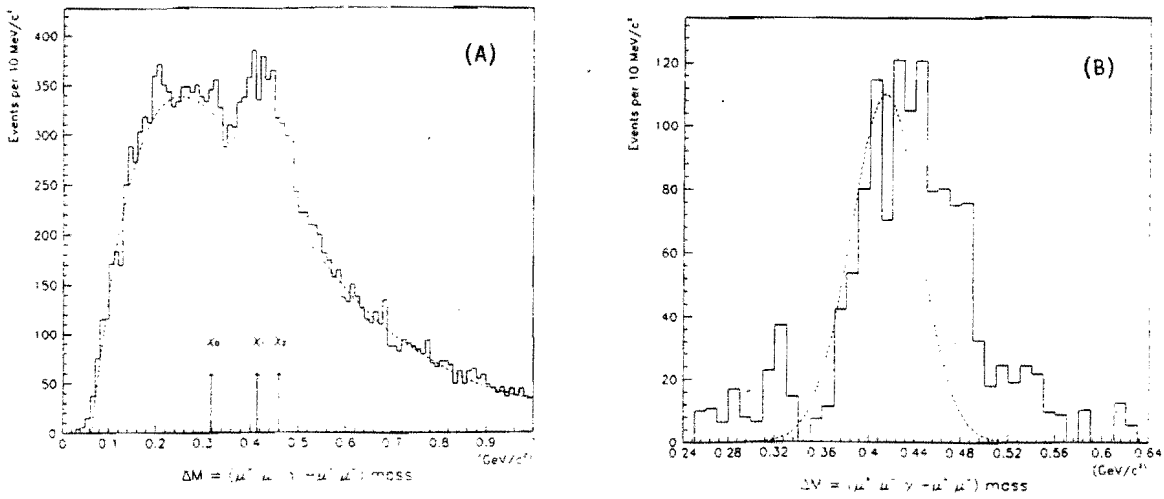

Fig. B.3
a) E705 γΨ Mass Spectra
b) Background Subtracted γΨ Mass Spectra

From these observation of the decay of the χ_1 and χ_2 states into $\gamma\Psi$ we have been able to extract the ratio of Ψ production from χ decay, determine the cross sections for direct J/Ψ production (correcting for the portion observed to proceed through χ or Ψ' decay), and measure the ratio of χ_1 to χ_2 production. Due to lack of statistics the latter of these measurements was limited in precision, especially for the case of production by protons. In addition, the investigation of the decay angular distributions of the photons to determine the χ production mechanisms could not be examined with any real significance because of statistics. All of these physics issues will be addressed with much more certainty with the better photon resolution and statistics a factor of 100 greater than available in the E705 run.

In addition to the observation of the χ_1 and χ_2 states, we searched in E705 for other states that might decay into either charged or neutral pions. We observed an enhancement at 3.837 GeV/c^2 in the J/$\Psi\pi^+\pi^-$ mass spectrum from our 300 GeV/c π^-N data as shown in Fig. B.4.a which we have tentatively identified as being due to the $^3D_2$ state of charmonium. The same spectrum shows a peak at 3.685 GeV/c^2 which is due to the Ψ'. Also shown in Fig. B.4.b is the J/$\Psi\pi^\pm\pi^\pm$ mass spectrum which shows no significant evidence for peaking.

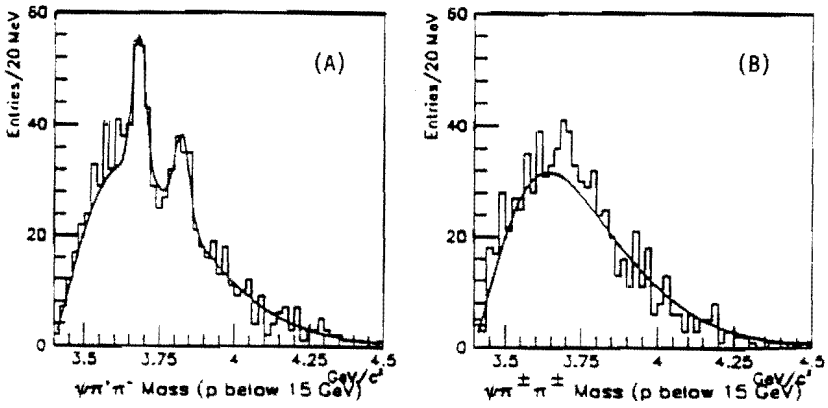

Fig. B.4
a) J/$\Psi\pi^+\pi^-$ Mass Spectrum
b) J/$\Psi\pi^\pm\pi^\pm$ Mass Spectrum

However, both the actual observation as well as the interpretation remain tentative since we are very limited by statistics. As shown in Table F.2 and Fig. B.3.a the effect is approximately 3.5 σ over a substantial background. We cannot definitely confirm the existence of the enhancement or rule out alternative explanations such as a four quark resonance. We need more statistics to examine the shape of the dipion mass spectrum and to search for $J/\Psi\pi^0\pi^0$ manifestations of the state.

We also were able to examine with low statistics the $J/\Psi\pi^0$ mass spectrum in E705. This spectrum is shown in Fig. B.5.a along with the π^0 spectrum from the J/Ψ events in Fig. B.5.b. As can be seen, a 2.5 σ enhancement appears at 3.525 GeV/c^2 near the expected position of the $^1P_1$ state of charmonium.

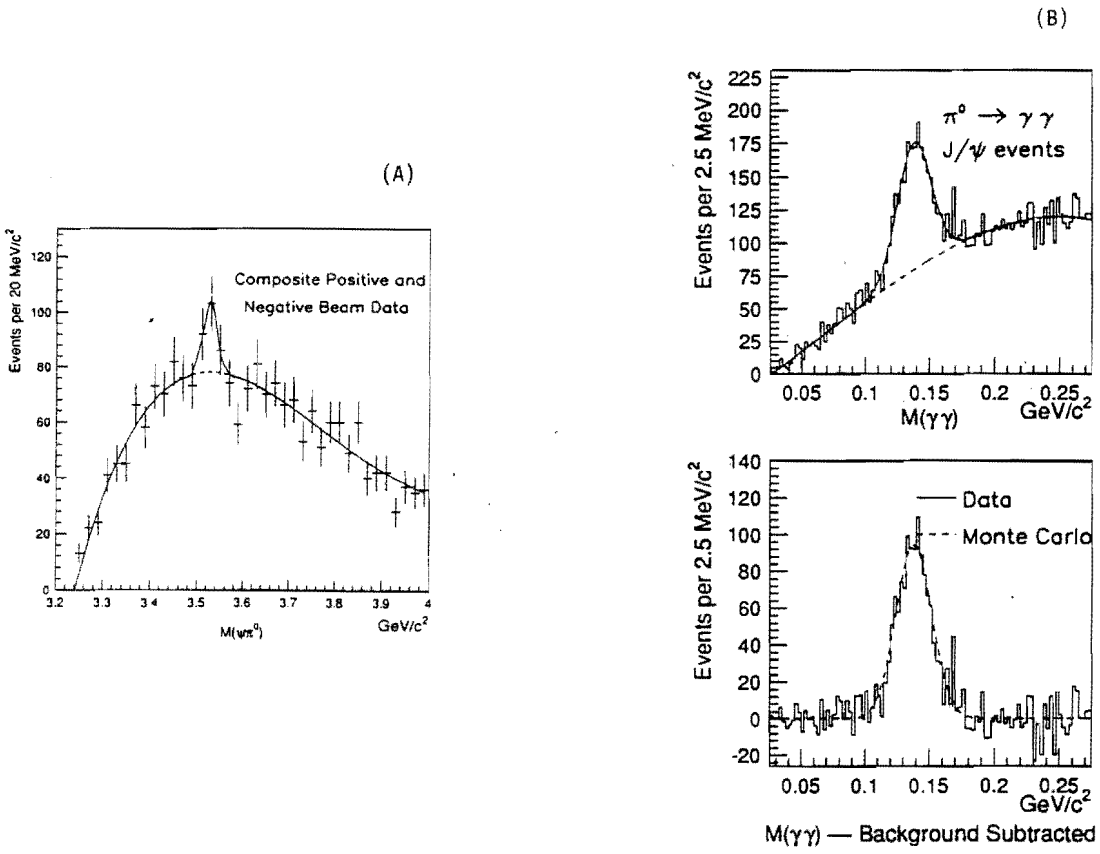

Fig. B.5
a) E705 $J/\Psi\pi^0$ Mass Spectrum - Sum of Positive and Negative Beam Data
b) E705 $\gamma\gamma$ Mass Spectrum - E705 J/Ψ Events

The production of this state followed by decay into $J/\Psi\pi^0$ has been previously reported[4] by Fermilab experiment E760 in proton-antiproton formation at the Fermilab antiproton accumulator. This observation was also low in statistics ($\approx 4\sigma$). A high statistics confirmation of our observation would be made in the 1994 run.

Appendix C
Completion of the Silicon Beam and Microvertex Detectors for the 1994 Run

We were able to achieve only a partial instrumentation of the E771 silicon microvertex and beam detectors and that only at the very end of the 1991 run. This resulted both in a limited number of planes per projection that could be instrumented and even in some case only partial instrumentation of those planes. Given the limited number of channels of silicon detector electronics and the late delivery of the same, we chose in our 1991 run to partially instrument our silicon microvertex detector with five planes in the orthogonal x and y projections and two u and v planes. The situation with the silicon beam detectors was even more marginal with only a single precision measurement per projection on a portion of the incoming beam. The late arrival of the bulk of the delivered electronics also resulted in very little time to check out and optimize the performance of all planes. The result of these factors was a less efficient system with a more limited solid angle and resolution than we had planned for.

In the 1994 run with the full complement of electronics and adequate time to insure optimal functioning, we will be able to increase the efficiency of each detector and improve the pattern recognition and track resolution with respect to the 1991 run. In Fig. C.1 we show the configuration of the planes planned for the 1994 run.

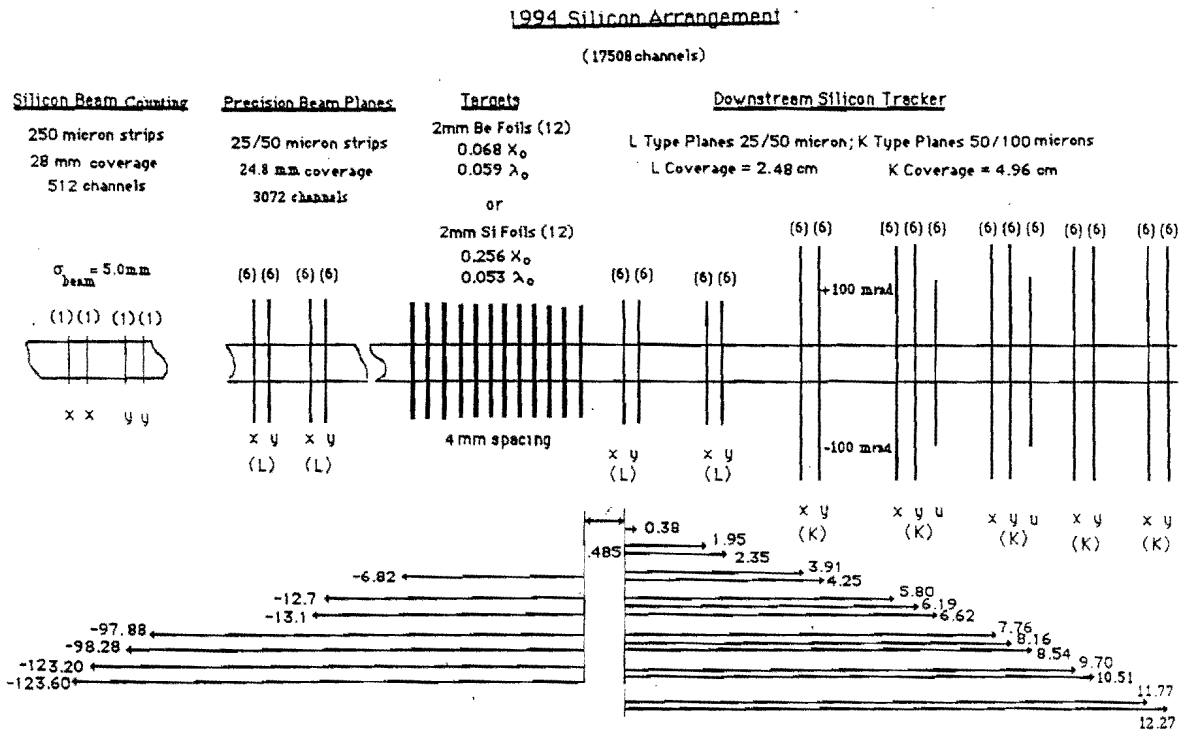

Fig. C.1
1994 Configuration of the Silicon Beam and Microvertex Detector

The completion of instrumentation of the E771 silicon detector will require an additional 7.5K channels of silicon electronics (increasing the total silicon electronics from 10K to 17.5K). With this extra electronics, we plan to:

1. Complete instrumentation of a new set of x,y "precision" beam planes (Micron Type L), increasing the number of precision (25/50 micron resolution) measurements of the beam to two per projection.

2. Complete the instrumentation of the u,v planes installed in the 1991 run to enhance 3D track reconstruction in the silicon tracker.

3. Add two new set of x,y planes (Micron Type K) to the tracker, increasing the number of measurements per x or y projection to seven thereby both improving the track finding efficiency and allowing some leeway for radiation damage at the higher integrated beam expected in 1994.

Adequate FASTBUS crates and smart crate controllers are already installed in the E771 spectrometer for the implementation of this scheme. In addition, adequate electronic components are on hand to construct the requisite number of channels of post amp comparator and delay encoder electronics. The major cost and work associated with this plan is the preparation, stuffing and testing of the post amp/comparator and delay encoder boards and the purchase of four new Type K planes from Micron. Adequate type L planes are already on hand to implement the beam detector. In addition to the new electronics, it may also be necessary to upgrade two existing crates of silicon PC/DE electronics which contain prototype versions of the final electronics. These modules were used only when it became clear that the silicon electronics delivery schedule would not permit adequate channels of the final design to be ready.

Appendix D
1994 Muon Detector
and Trigger Improvements

The overall efficiency times acceptance for the basic level of the E771 muon trigger system is given by

Dimuon: $\varepsilon_{2\mu\ \text{total}} = (\varepsilon_{DET})^2 \cdot A^{2\mu}_{GEO} \cdot \varepsilon_{2\mu\ \text{trigger}}$

Single Muon: $\varepsilon_{1\mu\ \text{total}} = (\varepsilon_{DET}) \cdot A^{1\mu}_{GEO} \cdot \varepsilon_{1\mu\ \text{trigger}}$

During the 1991 run, ε_{DET} was given by $(\varepsilon_{RPC})^3$ where ε_{RPC} was the efficiency of an individual Resistive Plate Counter (RPC) plane, A is the geometric acceptance for either one or two muons and $\varepsilon_{n\mu\ \text{trigger}}$ is the composite efficiency/acceptance for particular trigger strategies for single or dimuon events. This composite efficiency for the trigger includes a 6 to 10 GeV/c minimum energy requirement on the muons imposed by the steel and copper absorber of the muon detector.

We have made an examination of each of these factors using the data accumulated in the 1991 run. Based on that experience, several improvements in the E771 muon detector and the configuration of the associated trigger electronics are planned for the 1994 run. The improvements fall into three categories corresponding to the three factors in the expression for overall muon trigger/detector efficiency given above.

1. Improvement in the overall efficiency of the RPC system.

2. Increase in the acceptance, $A^{n\mu}_{GEO}$, of the RPC detector system

3. Changes in the configuration of RPC pad electronics to increase $\varepsilon_{n\mu\ \text{trigger}}$ by allowing more leeway for multiple scattering of muons and more projectivity of the triple coincidences of Resistive Plate Counters to the E771 target.

As will be seen, these improvements, which are minor compared to the scale of the original construction of the RPC muon detector system and its associated trigger electronics, will increase the overall acceptance times efficiency for dimuons by a factor of 4.1.

D.1. RPC Efficiency

In the 1991 run of E771, the single muon trigger condition required the simultaneous response of all three RPC planes. For the dimuon trigger the trigger condition, therefore, required 2x3=6 RPC signals to be present. Therefore as indicated above, the overall trigger efficiency was proportional to the third (1μ) or sixth (2μ) power of the individual RPC efficiency. In order to avoid such a strong dependence, we plan to install a fourth plane of RPC's, and to define a muon as the coincidence of any three out of the four planes. Moreover, we also plan to install a second layer of RPC in the central region of the muon detector for planes 1 and 2 and to OR the signals with the existing planes to increase overall efficiency of these planes. With these improvements,

we estimate that ε_{DET} will increase from 61% to 99% (and correspondingly ε_{DET}^2 from 38% to 98%).

D.2. Acceptance of the Muon Detector

The acceptance for wide angle muons is limited in the present E771 muon detector by the size of the second and third RPC plane. The present plan is to add twelve additional panels of RPC to preserve the wide angle muons which are an easier subset of the data to reconstruct. The dimuon acceptance $A^{2\mu}_{GEO}$ of the enhanced RPC system will be increased from 35% to 39% by this change.

D.3. Rearrangement of Pad Electronics

Based on the data from the 1991 run and various Monte Carlo studies, the efficiency of the dimuon system will be increased from 60% to 86% by a reconfiguration of the wiring of the RPC electronics to allow for more multiple scattering of muons and to increase the projectivity of the trigger to the target.

D.4. Summary of Improvements in Signal Retention by Level 1A Trigger for 1994 Run

Assuming all of these independent improvements are done, we expect to see the improvements in single and dimuon trigger efficiencies as given in Table D1 below:

Table D.1
Single and Dimuon Trigger Efficiencies for Level 1A

	1991 Run		1994 Run	
	B->J/Ψ->2 μ	B-> μ	B->J/Ψ->2 μ	B-> μ
$(\varepsilon_{DET})^n$	0.38	0.61	0.98	0.99
$A^{n\mu}_{GEO}$	0.35	0.56	0.39	0.59
$\varepsilon_{n\mu\ trigger}$	0.57	0.75	0.86	0.93
$\varepsilon_{n\mu\ total}$	0.08	0.25	0.33	0.54

As can been seen, the planned improvements and tuning of the muon detector and trigger will increase the efficiency of the 1A muon trigger for B->J/Ψ->2 μ by a factor of 4.1. The efficiency of single semi-muonic 1A trigger for B-> μ events will also increase by a factor of 2.2 relative to the yield/interaction of the 1991 run. It should be noted that the improvements in the trigger efficiency generated by these changes will be accompanied by an increase in the 1A trigger rate (see Tables D.2 and D.3). Moreover, we are planning to operate at a higher interaction rate. As described in the following sections, the 1B and Level 2 triggers will be used to contain the overall muon trigger rates to an acceptable level.

D.5. The 1B High Transverse Momentum Muon Trigger for 1994

In addition to recognizing the presence of one or more muons by means of the 1A coincidences among RPC planes, the E771 trigger system also imposes a cut on the transverse momentum of the candidate muons. This is accomplished by the 1B trigger[30], consisting of a large number of coincidences between two planes of pad chambers located between the magnet and the muon absorber and the first plane of muon detectors. Out of the many millions of possible pairs of

pads, only the ones consistent with a track of large transverse momentum (numbering about 40,000) are combined to form the 1B trigger coincidence set. During the E771 1991 run, the electronics to provide full coverage for the 1B trigger were built and tested: measurements of the resulting rates showed that the system provided rejections consistent with the expectations in the outer part of the spectrometer aperture (i.e. for |vertical angle|>23 mrad). Fig. D.1 below shows the effect of the 1B trigger on the single muon pt spectrum from the 1991 data, clearly demonstrating the cut at 0.8 GeV/c.

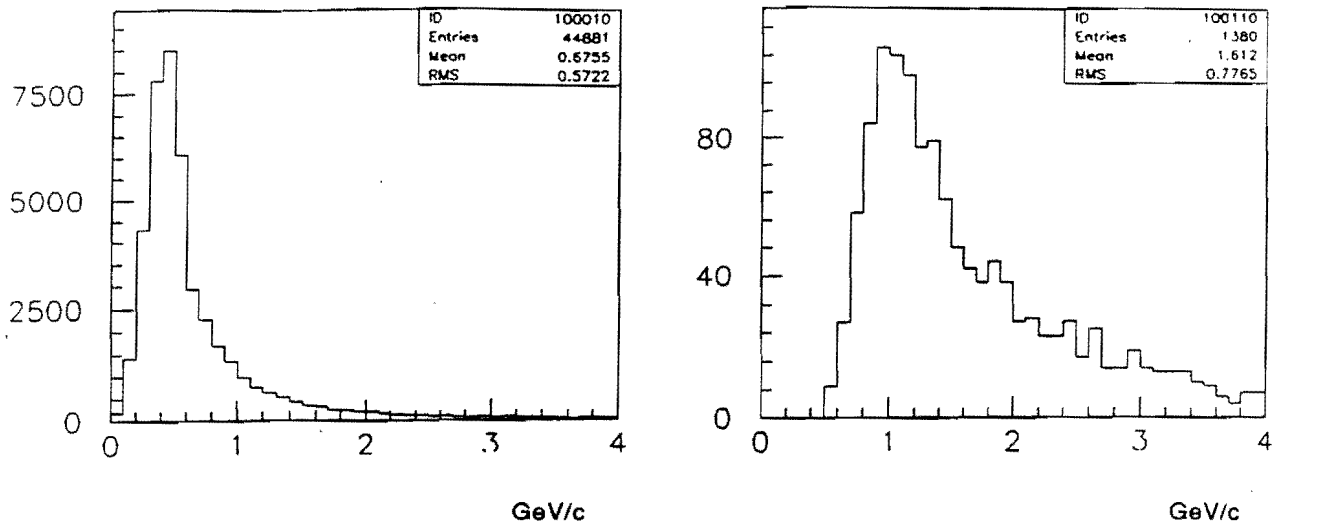

E771 Muon P_t Spectrum 1A Trigger Only

E771 Muon P_t Spectrum 1A * 1B Trigger
(0.8 GeV/c P_t Threshold 1B Trigger - Out Benders Only)

Fig. D.1
Functioning of Single Muon P_t Trigger

In the inner sections the rates were considerably larger because of a high rate of accidental combinations in the more congested part of the detector. Because of this, in the 1991 run the 1B trigger for single muons was activated only in the outer region of the detector, corresponding to a coverage of 65% of the spectrometer solid angle, and expected to contain 45% of the muons from B decay. It was also decided not to apply the 1B condition to the dimuon trigger, since its rate was brought to an acceptable level (Table D.2) by the application of the 1A condition alone, and it was desired to avoid additional signal losses due to the possible low efficiency of the pad chambers involved in the 1B trigger.

For the '94 run, the increase of 1A trigger rate induced by the higher signal acceptance, combined with the increase in interaction rate, will require to apply the 1B pt condition to the 1A

dimuon trigger; preliminary results from the '91 run indicate that a p_t cutoff at 1 GeV would conserve more than 95% of the Ψ->$\mu\mu$ signal, while providing an additional rejection of up to a factor of 10. Concerning the single muon trigger, preliminary studies indicate that we might be able to increase the B->μ acceptance form 45% to 66% while still containing the trigger rate within an acceptable level. Detailed tuning of the trigger will answer this question. The equipment necessary to accomplish this is already in place. This choice might be improved after we complete ongoing studies aimed at understanding the actual source of higher rates in the inner regions and possible ways to decrease it. As shown from tables D.2 and D.3, the expected rates after the first level (1A and 1B) triggers are still too high to be accommodated by our Data Acquisition system, capable of accepting up to a few hundred events per second with a reasonable dead time. We are then planning to impose a next level of selection, based upon the presence of secondary vertices, as described in the next section.

D.6. Implementation of a Level 2 Trigger for 1994

In order to go to higher rates and to minimize dead time in the 1994 run, we have begun to implement a second level of trigger for the spectrometer using associative memories[33]. Since our level 1A and 1B triggers have practically exhausted the possibilities for rejection of background triggers by use of the muons signatures, we are basing our Level 2 strategy on a completely independent method relying on detection of secondary vertices in the silicon MVD.

A block diagram for the Level 2 trigger is shown below in Fig. D.2:

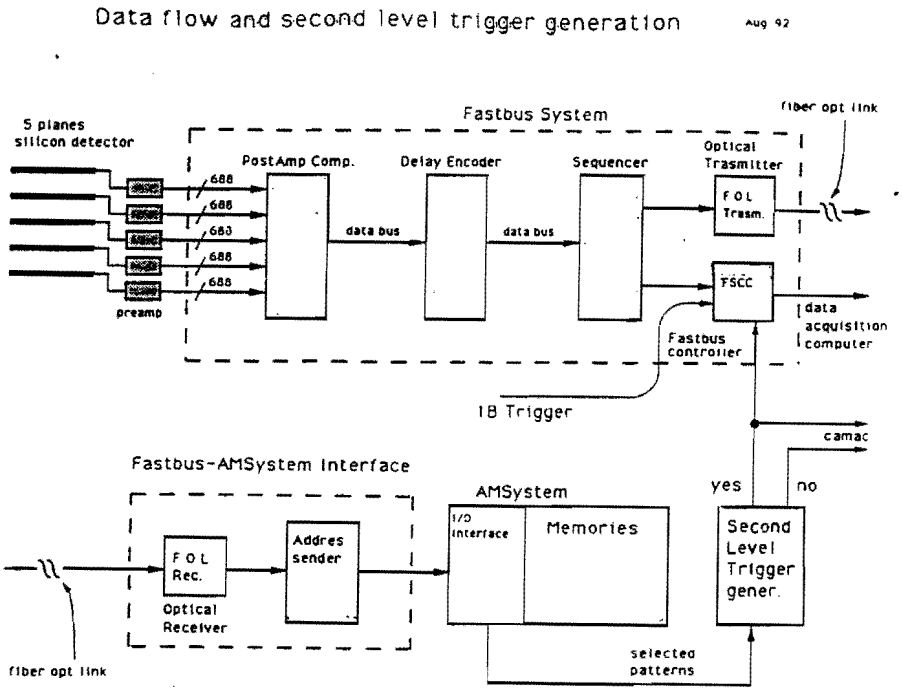

Fig. D.2
Block Diagram of the Level II Secondary Vertex Trigger Processor

The encoded list of hits from five x (and possibly five y) silicon tracker planes is sent from the FASTBUS electronics located near the vertex detector to the Level 2 electronics by means of a fast fiber optics link. The "brain" of the Level 2 system is a set of Associative Memories, pre-loaded with the list of all possible five hit patterns corresponding to valid (both primary and secondary) tracks in the silicon planes themselves. When presented with the hit lists relative to a given event, the Associative Memories will produce within a few microseconds, i.e. in the time it takes to load them with the event data, a complete list of valid tracks that can be formed with the hits from the event under question. The next step is to make a decision on the likelihood that the event contains several vertices, also keeping in mind that we have to contend with a non-negligible (about 20%) probability of re-interactions. We have been studying several different algorithms and the corresponding hardware implementation to process the list of tracks provided by the Associative Memories. Fig. D.3 shows the expected performance, both in terms of signal retention and of background rejection, of a given algorithm, based upon the shape of the impact parameter distribution for minimum bias, charm and B events.

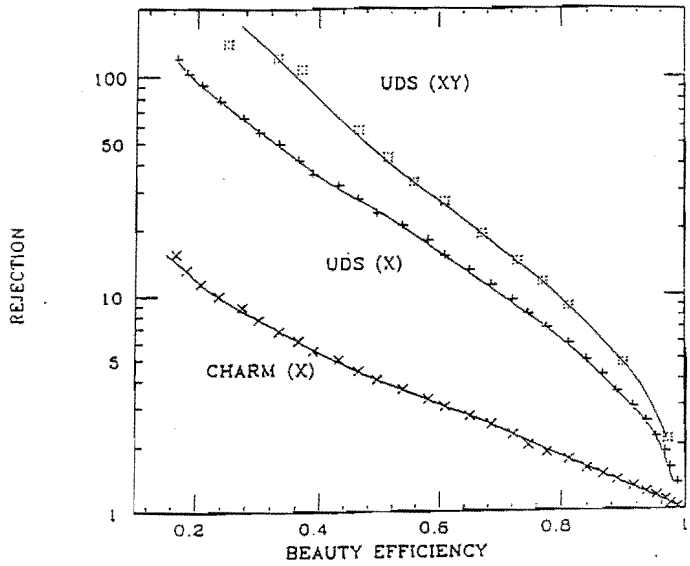

Fig. D.3
Anticipated Second Level Trigger Performance

The projected trigger figures in Tables D.2 and D.3 were derived from this result. At the moment of writing, a conceptual or actual design exists for all the components of the Level 2 system, with the exception of the very last stage, performing the final event selection on the basis of the track

information. This final choice will be made at the conclusion of the software simulations which are in progress, and could also be based upon the analysis of actual events recorded during the 1991 run.

D.7. Single Muon and Dimuon Trigger Rates for the 1994 Run

Given the combinations of trigger levels discussed above, we have estimated the 1994 single and dimuon trigger rates. These projections are obtained, wherever possible, by analyzing the 1991 data, otherwise from Monte Carlo simulations.

Table D.2
Dimuon Trigger Rates

	1991	1991	1994
	Expected	Observed	Expected
Raw Interaction Rate*	2.5×10^{6} Int/sec	2.5×10^{6} Int/sec	5×10^{6} Int/sec
Level 1A 2μ Trigger Reduction	8.8×10^{-5}	9.6×10^{-5}**	4.8×10^{-4}
Level 1A*1B 2μ Trigger Reduction	-	-	4.8×10^{-5}
Level 1A*1B*Level 2 2μ Trigger Red.	-	-	1.6×10^{-5}
2μ Trigger Rate	220/sec	240/sec	80/sec

Table D.3
Single Muon Trigger Rates

	1991	1991	1994
	Expected	Observed	Expected
Raw Interaction Rate	2.5×10^{6} Int/sec	2.5×10^{6} Int/sec	5×10^{6} Int/sec
Level 1A 1μ Trigger Reduction	1.8×10^{-2}	9.6×10^{-3}**	2.0×10^{-2}
Level 1A*1B 1μ Trigger Reduction	2.5×10^{-4}	9.8×10^{-5}	3.0×10^{-4}
Level 1A*1B*Level 2 μ Trigger Red.	-	-	1.5×10^{-5}
1μ Trigger Rate	625/sec	245/sec	75/sec

*For comparison of the expectations for the 1991 run trigger performance and the actual performance, we have quoted observed trigger rates at an interaction rate of 2.5×10^{6} interactions per second, the "normal intensity" condition for E771 at the end of the 1991 run.

**The observed rates include the effect of the less than 100% detector efficiency. For efficiency equal to 100%, the rates would extrapolate to 2.5×10^{-4} and 1.5×10^{-2} for the indicated 1A double and single muon rates respectively, and to 2×10^{-4} for the 1A*1B rate.

D8. Dead Time Losses for the 1991 Run and Estimated Losses for the 1994 Run

During the 1991 run, the number of triggers sent to the Data Acquisition system ranged between 5 to 600 events per second. In spite of the fact that the basic DA system would have been able to accommodate such a rate gracefully, our overall dead time was dominated by the very long conversion and digitization time intrinsic to our antiquated set of ADC's and TDC's, inducing an average read-out time of about 800 μsec/event. In turn, this generated an average dead-time of

40%. Because of financial considerations, we propose to replace our ADC and TDC system (in spite of the appeal of such a replacement) only if equipment becomes available from PREP at no new cost. If more modern ADC's and TDC's become available we estimate that we could decrease our readout time to ≤300 μsec/event, thereby allowing us to decrease trigger restrictions and decrease still further the dead time to increase yields.

As explained above, we are planning to strengthen the event selectivity at trigger level, as discussed in the previous sections. This will not come completely for free, since the extra levels of triggers will induce both an additional loss of good events, as detailed in chapter III and in this same Appendix D, as well as their own contributions to the overall dead-time. On the basis of the rate projections presented in Tables D.2 and D.3, we expect contributions to the dead time of 2 %, 3.5 % and 12.5 % originating respectively from the 1A/1B, Level 2 and event acquisition.

Another severe limiting factor encountered during the 1991 run was the very large non-uniformity of the beam structure. A concerted effort was begun at the end of the 1991 run by the Fermilab Accelerator Division to make the beam more uniform both from the standpoint of decreasing deadtime and to decrease the number of additional beam tracks that load our silicon detector. Improvements continued to be made up to the end of the run but, for purposes of the overall yield estimates, we assume that the structure in the 1994 run will be similar.

Appendix E
Proposed 1994
RICH Detector Addition

While a majority of the physics described in this proposal can be performed to some substantial level without K/π identification, a Ring Imaging Cerenkov counter (RICH) would significantly enhance the capabilities for achieving the B_S and Λ_b physics goals described in Section IV and, in general, give cleaner results due to the increased capacity for rejecting backgrounds. For example, most of the decay modes discussed in this proposal were purposely chosen so that. in principle, particle ID might not be necessary. However, the addition of a RICH would make those strategies more robust against, as yet uncertain, backgrounds and also increase the signal substantially by making more modes accessible. As an example, consider the decay $\overline{B_S}^0$ ->D^+_S π^- where D^+_S-> $K^-K^+\pi^+$ and its B_d analog. If the D vertex is resolvable from the first generation π^-, then one could assign the K mass to the negative track at the D vertex. There is ambiguity however on assignments to the remaining positive tracks. Figure E.1.a shows the reconstructed mass of a D^+ coming from a $\overline{B}^0$ decaying into Kππ when one of the pions is assigned the K mass. The mass peak is moved nearly on top of where the D_S is expected. Fig. E.1.b shows a similar effect in the reflected decay D_S->KKπ when the like signed K is assigned the π mass. Finally, Fig. E.1.c shows the resulting ambiguity if the π mass is assigned to all final particles in these two decays.

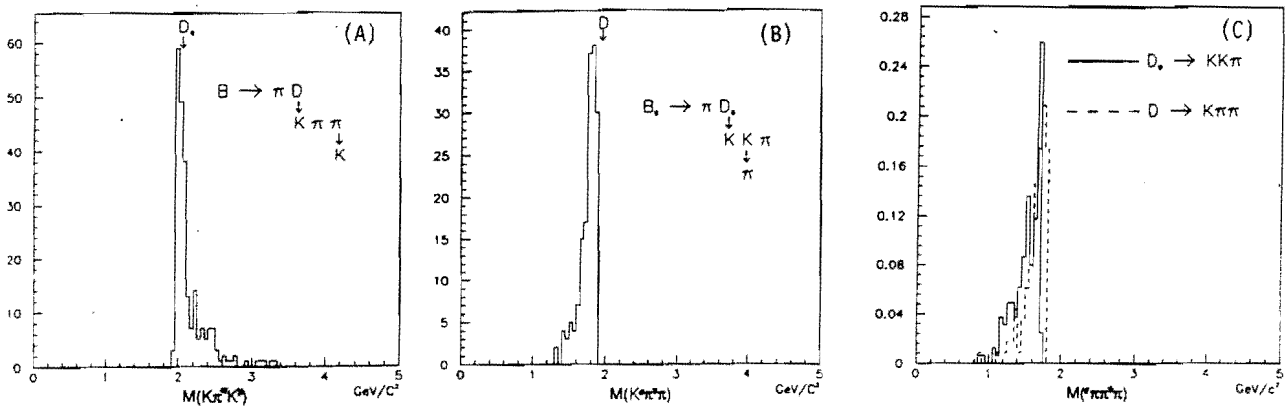

Fig. E.1
D Mass Peak Confusion due to K/π Misidentification
a) D^+_d->Kππ Decay; One π Assigned K Mass
b) D^+_S->KKπ Decay ; Like Sign K Assigned π Mass
c) D^+_d->Kππ and D^+_S->KKπ Decays; All Particles Assigned π Mass

In addition to these reconstruction issues, the RICH would also benefit flavor tagging. A potential tag for the B_S is to look for an associated charged K from the primary vertex as described in Section IV.A.6 . Unlike a lepton tag, these methods are not susceptible to mixing-type dilution. The use of the RICH would range from very useful in the first method to crucial in the second.

The choice of using a RICH rather than multiple segmented threshold counters is based on the need to preserve the acceptance of the E771 spectrometer. A 2.5m long radiator placed between the CC2 and DC5 chambers could be accommodated without significantly limiting the aperture of the spectrometer and the acceptance for B decays (see fig E.2). Threshold counters would require at least 10m for the same momentum range coverage as a 2.5m long RICH.

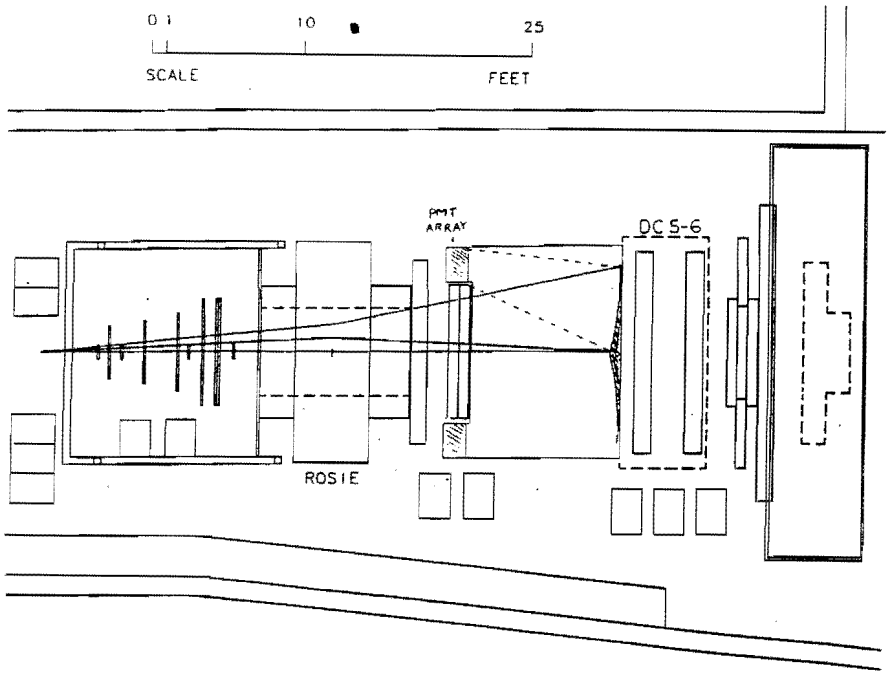

Fig. E.2
1994 RICH Layout

The RICH would use-off axis imaging as indicated in figure E.2. This allows the photon detectors to be placed outside of the aperture at the cost of increased geometrical aberration. The focal length F=3m was chosen slightly longer than the radiator length to accommodate the off axis imaging. We have tentatively chosen CF_4 (γthreshold=32) for the radiator gas although C_2F_6 (γthreshold=25) could be used if a lower threshold is needed. To register the rings from particles having momenta as low as 10 GeV/c will require each of the two photon detectors to have 75x75 cm^2 area. Other operational requirements and geometrical considerations for the RICH can be found in Ref. 53.

The hit multiplicity in an efficient RICH photon detector would be 10-20 times higher than that found in a tracking chamber. Thus, in a high rate environment such as the 1994 run, the time resolution of the RICH photon detector must be comparable to the RF bucket spacing and it should provide a pixel-based, rather than projective, position measurement. None of the already existing gaseous photo cathode detectors have these properties and also high efficiency. In Ref. 53, we proposed an array of multianode photomultiplier tubes placed along the mirror focal plane as a solution to these requirements. Due to the high cost of that solution we have been investigating the use of an array of miniature single channel photomultiplier tubes instead.

In July 1992, we tested a several types of photomultiplier tubes in a small prototype RICH at BNL. The photons were detected by two clusters of 1.5cm diameter tubes (MELZ FEU68), one cluster of 2cm tubes (Amperex P1911) and a 7.5cm square Multianode tube (Hamamatsu R2489MOD). The distribution of the PMTs along the focal plane, with the superimposed hit pattern from an event, is shown in figure E.3.

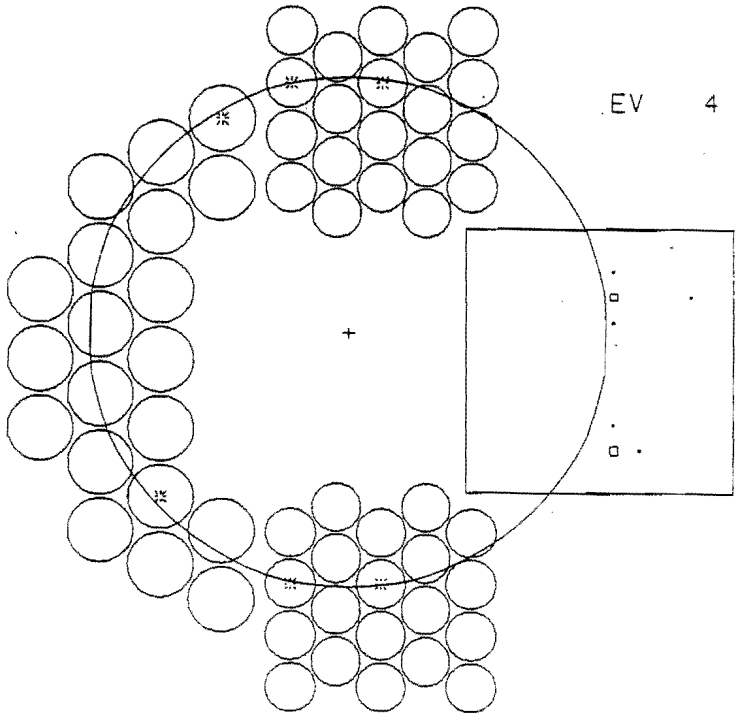

Fig. E.3
Results from July 1992 BNL Test

Experiment E781 has tested a much larger prototype device using similar miniature phototubes during the 1991 fixed target run[54]. To improve the geometrical packing fraction we propose to use for the E771 RICH 1.5cm square photomultiplier tubes which are currently being developed by MELZ in Moscow. Each detector array would require 2500 tubes. Samples of these tubes will be available in October of 1992 at a fraction of the cost of any other supplier.

In practice the geometrical packing fraction and quantum efficiency play a large role in determining the quality factor N_0;

$$N_0 \approx (370\ eV^{-1}\ cm^{1}) \cdot \langle QE \rangle \cdot \Delta E * \varepsilon$$

where <QE> is the average quantum efficiency over the full photon-energy bandwidth ΔE and ε is an additional loss factor. The tube entrance window will either be a UV glass or coated with a film of pTP to extend the sensitivity to the range 600-200nm (ΔE=4eV). If we assume a packing fraction of 45% (for square tubes) , optical efficiency of 80% and <QE> = 0.1, then we expect N_0 = 53/cm. In Ref. 54, N_0=66/cm was obtained with a somewhat better packing fraction that we had in our prototype.

For a gaseous radiator, where the dispersion is expected to be small, the average number of detected photons is given by

$$\langle N_{ph} \rangle = N_0 \cdot L \cdot \sin(\Theta)^2 \ ,$$

where L is the radiator length and $\Theta = \cos^{-1}(1/n\,\beta)$ is the Cherenkov angle. For $\beta \to 1$ particles $\Theta \to 1/\gamma_{threshold}$ and for a CF_4 radiator $\langle N_{ph} \rangle \sim 13$.

Given the track direction, each detected photon provides an independent measurement of the Cherenkov angle. There are several contributions to the error in this measurement.

* The geometric aberrations due to tracks having non zero impact parameter relative to the mirror center of curvature contribute $\Delta\Theta/\Theta = 1\%$.

* The chromatic dispersion of CF_4 contributes $\Delta\Theta \approx 0.13$mrad over the range 200-600nm.

* As usual these effects are smaller than the error due to finite PMT position resolution given by

$$\Delta\Theta = s/(F \cdot \sqrt{12}) = .96 \text{ mrad}$$

for a 1cm photocathode.

The contributions due to tracking errors and multiple scatter are expected to be $\approx$ 3 times smaller. The error for an entire ring is given by adding in quadrature the above contributions and dividing by $\sqrt{(N_{ph})}$.

The above result can be used to estimate the efficiency for identifying a K of a given momentum. In the calculation, the expected π/K ratio must be specified to optimize the Cherenkov angle cut. We have chosen two values; $\pi/K = 3$ which might be expected for tracks stemming from secondary vertices and $\pi/K = 10$ which should be more appropriate for primary tracks. The result of the calculation is shown in figure E.4.

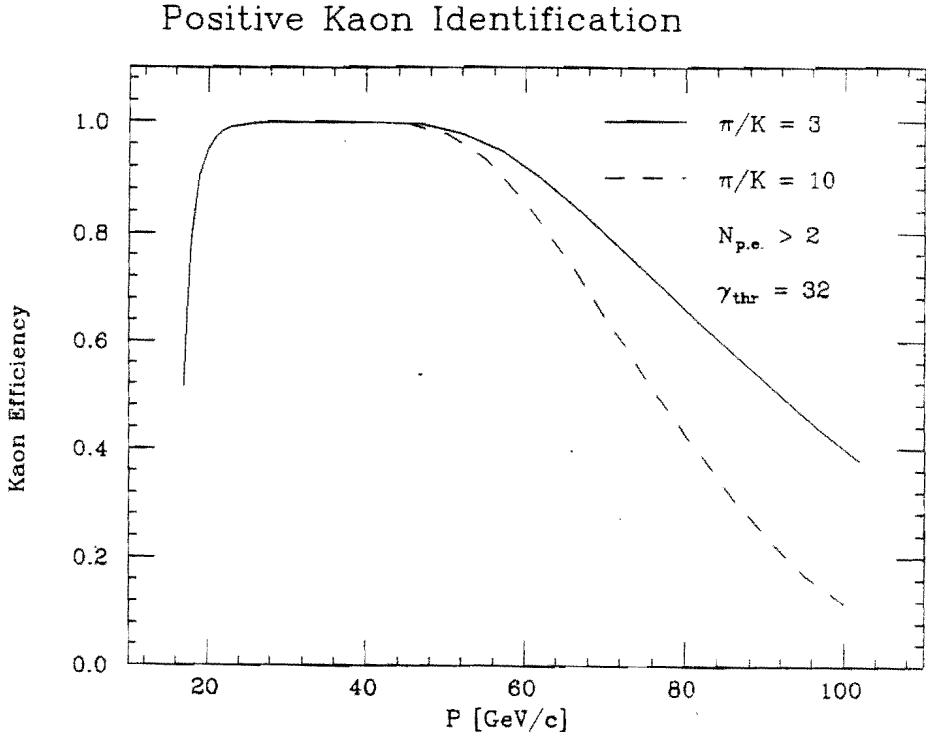

Fig. E.4
K Identification Efficiency as a Function of Energy

The loss in efficiency at low momenta is due to a requirement that at least 2 photons are detected since the K ceases to radiate in CF_4 below ≈ 16 GeV/c. Of course, if the proton contribution in this momentum range is negligible then one can still distinguish between K and π down to ~7 GeV/c . Alternatively a lower threshold radiator such as C2F6 could be used if necessary.

As an example, in Fig.E.5.a and b we show the momentum spectra for K from the decays

$$B^0_d \rightarrow \pi D_d$$
$$\rightarrow K \pi \pi$$

and

$$B_S \rightarrow \pi D_S$$
$$\rightarrow \phi \pi \rightarrow K K \pi$$

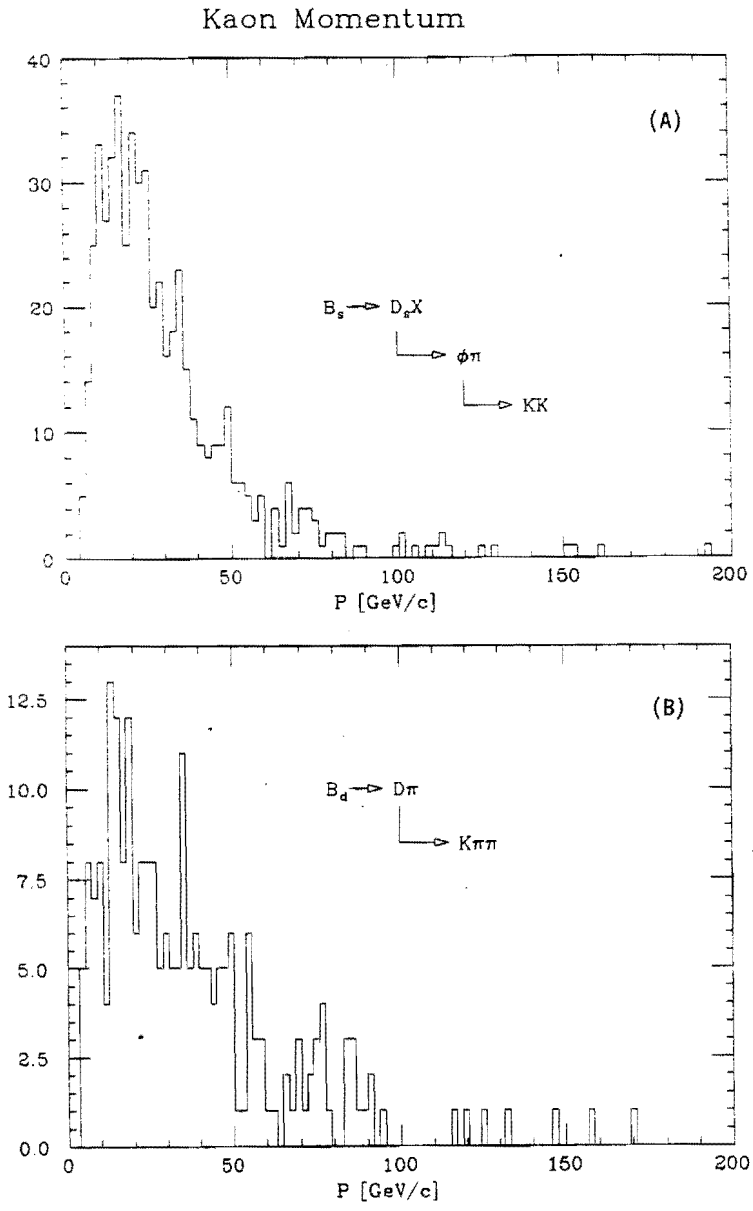

Fig. E.5
a) Momentum Spectrum for B^0_d --> πD_d -> K π π
b) Momentum Spectrum for B^0_S --> πD_S -> K π π

All particles are required to be in the spectrometer aperture and the recoil B must satisfy the 1B trigger. Monte Carlo studies are in progress to determine how much of the low momentum part of these spectra will be suppressed when a secondary vertex cut is applied to the events. Nevertheless, if we can ignore protons at low momentum, we expect ≥90% efficiency for identifying the K for $p_K > 7$ GeV/c and ≥80% efficiency when the entire momentum spectrum is considered.

For detection of the Λ_b, the RICH would be used to identify the protons from the secondary vertices. Figure E.6 shows the proton momentum spectra in semileptonic Λ_b decays in which two decay modes of the daughter Λ_c are considered;

$$\Lambda_c \text{ -> } p\ K_S \text{ and } \Lambda_c \text{ -> } p\ K\ \pi.$$

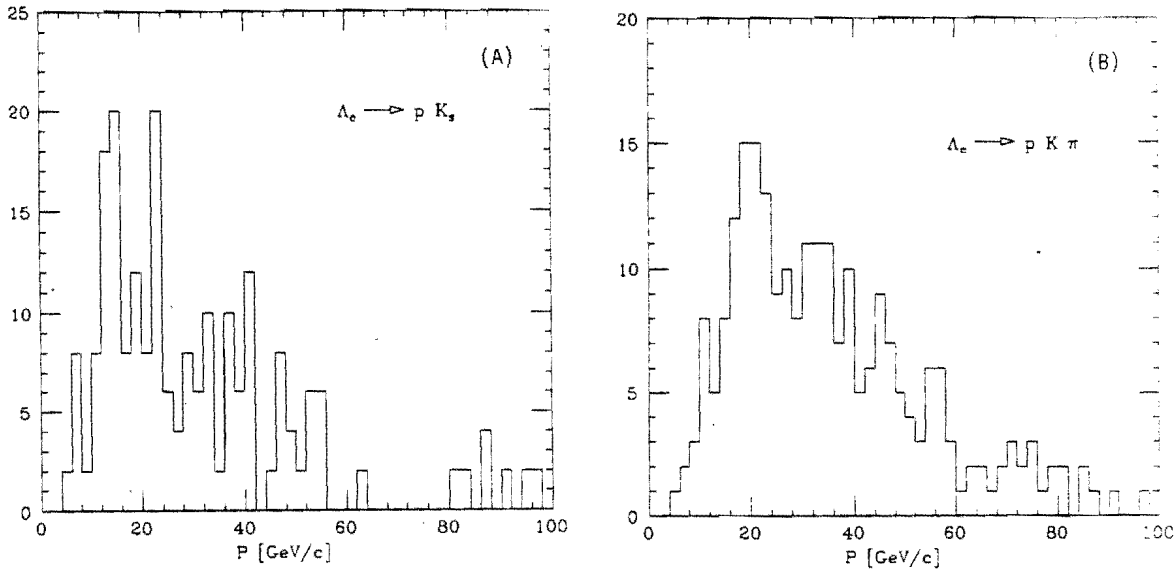

Fig. E.6
a) Momentum spectrum of the proton from Λ_c -> p K_S
b) Momentum spectrum of the proton from Λ_c -> p K π

Again only acceptance cuts have been performed on the final state particles. No vertex separation cut has been made. The relatively low momentum peak suggests using C2F6 as the radiator gas to distinguish between K and proton as low in momentum as possible. In this case we would expect an efficiency of 85% for identifying the proton. This efficiency is driven primarily at the low end ofthe spectrum by the threshold for radiation since the proton ring remains well separated from the K ring up to ~100 GeV/c.

In the above estimates no account has yet been taken of reconstruction inefficiencies due to overlapping rings. Certainly with adequate photon statistics one can afford to throw out ambiguous photon assignments. Also the background from pair production in the upstream material has not been taken into account. Detailed MC simulation of the detector is in progress to investigate these issues.

Finally, Table E contains the estimated cost of the device. Several caveats on these costs are included in the footnotes to the table.

Table E
Estimated Cost of the RICH Detector

Item	Cost
PMTs and Bases (5,000)	\$175K*
Power Supplies	--- **
Readout Electronics	\$ 20K***
Mirrors	\$ 60K****
Radiator Vessel (Material \$20K) (Labor *****) (Engineering \$10 K)	\$ 30K
Gas System	\$ 20K
Total	\$305K

* The FEU68 PM tubes which we have purchased for the prototype RICH test cost \$25 each plus a base cost of \$10. The gain of these tubes is low requiring use of sensitive amplifiers with a threshold of approximately 10^4 electrons. The newer, square tube should have higher gain and require less performance for the electronics.
** This assumes the PM HV supplies are available from PREP.
*** The bulk of the electronics is presumed to be supplied by Dubna. \$20K is the cost of adapting it to the RICH readout requirements.
**** Full cost is listed. Substantial reduction may be possible if Dubna can supply the mirrors
***** This presumes free or heavily subsidized time in the UVa and Berkeley shops. Otherwise approximately \$10K.

Appendix F

Preliminary Division of Effort/Cost Estimate for 1994 Run

We expect to obtain funding from three basic sources, Fermilab, DOE University Division and INFN. The totals from each source, as reflected in the Table below are, $285K from Fermilab, $465K from DOE University Division and $450K from INFN. The Fermilab RD costs assume that ASIC's and D/E memories previous purchased are still available and that costs of components are similar to 1990 costs.

Project	Institution	Estimates	Funding Source
Silicon MVD Completion	Fermilab*	$285K	Fermilab RD
Pad Chamber Electronics Mods	Wisconsin	$ 40K	DOE University
RICH Detector	UVa,UCLA,Berkeley	$305K	DOE University
RICH Detector Electronics*	UVa,Dubna+	$ 20K	DOE University
2nd Level Trigger	UVa	$ 75K	DOE University
Silicon Beam Detector	Duke/Houston/UVa	$ 25K	DOE University
Sub Total DOE University		$465K	
2nd Level Trigger/RPC Elect.	Pavia	$250K	INFN
Muon Detector Improvements	Lecce/Pavia	$200K	INFN
Sub Total INFN		$450K	

While no major upgrades are expected in the existing E771 Spectrometer equipment in the following categories, personnel from the listed institutions will take responsibility for bringing on line the particular components. There will be small costs associated with this.

PWC/Drift/Pad Chambers	FNAL/HoustonShandong/Nanjing+	--	Fermilab Physics
EM Detector	USA/UVa	--	DOE University
1st Level Trigger	Penn/UVa	--	DOE University
DA**	Prairie View	--	DOE University

* Dubna expects to supply electronics which must be modified to fit the E771 system. If the Dubna electronics are not available, then the additional cost for the RICH detector will be ≈ $100K .

+ Support will be required from either the DOE University Division or Fermilab to support Russian and PRC physicists during their stay in US to participate in E771 second run.

** SSC Lab personnel have shown an interest in participating in the next run of E771. If they are allowed to do so, they would work with the E771 DA and trigger systems.

References

1. L. Antoniazzi et al., E705 Collaboration, "A Search for Hidden Charm Resonance States Decaying into J/Ψ or Ψ' Plus Pions", in preparation.
2. L. Antoniazzi et al., E705 Collaboration, "Production of J/Ψ via Ψ' and χ Decay in 300 GeV/c Proton and $\pi^{\pm}$ Nucleon Interactions", FERMILAB-Pub-92/140-E, submitted to Physical Review Letters; L. Antoniazzi et al., E705 Collaboration, "Production of χ States via 300 GeV/c Proton and $\pi^{\pm}$ Interactions on a Lithium Target", in preparation.
3. A. Carroll et al., Phys. Lettr. **80B**, 319(179).
4. T.A. Armstrong et al., E760 Collaboration, "Observation of the 1P1 State of Charmonium", submitted to Physical Review Letters.
5. L. Antoniazzi et al., E705 Collaboration, "A Measurement of J/Ψ and Ψ' Production in 300 GeV/c Proton, Antiproton and $\pi^{\pm}$ Interactions with Nuclei", FERMILAB-Pub-92/141-E, submitted to Physical Review.
6. Y. Lemoigne et al., Phys. Lett. **113B**, 509(1982).
7. L. Lyons, Progress in Particle Physics **7**, 169(1981).
8. D. Coffman et al., "A Direct Measurement of the J/Ψ Leptonic Branching Fraction", SLAC-PUB-5992, (1991).
9. E. Berger, "Heavy Flavor Production", QCD Hard Hadronic Processes, NATO ASI Series B: Physics Vol. 197, 501(1987).
10. "Review of Particle Properties", Phys. Rev. **D45**, VII.145, (1992).
11. "Review of Particle Properties", Phys. Rev. **D45**, VII.153, (1992).
12. "Review of Particle Properties", Phys. Rev. **D45**, VII.88, (1992).
13. "Review of Particle Properties", Phys. Rev. **D45**, VII.153, (1992).
14. N. Isgur, private communication (Aug., 1992).
15. "Review of Particle Properties", Phys. Rev. **D45**, VII.144, (1992).
16. "Review of Particle Properties", Phys. Rev. **D45**, VII.23, (1992).
17. "Review of Particle Properties", Phys. Rev. **D45**, VII.144, (1992).
18. "Review of Particle Properties", Phys. Rev. **D45**, VII.144, (1992).
19. "Review of Particle Properties", Phys. Rev. **D45**, VII.144, (1992).
20. Danilov, Proceedings of the Joint International Lepton-Photon Symposium and Europhysics Conference of the High Energy Physics, Vol 2, 333(1991).
21. P. Drell, "Weak Decays, Rare Decays, Mixing and CP Violation", XXVI International Conference on High Energy Physics, Dallas, TX, (1992).
22. N. Isgur, D. Scora, B. Grinstein and M.B. Wise, Phys. Rev. Letters 56, 298(1986); M. Wirbel, B. Stech, and M. Bauer, Z. Phys. C29, 637(1988); J.G. Kornes and G.A. Schuler, Z. Phys, C38, 511(1988); J.M. Cline and W.E. Palmer, DESY 89-429(1989).
23. V. Sharma, "Evidence for B_S Meson and Lifetimes of B_S and Λ_b at LEP", XXVI International Conference on High Energy Physics, Dallas,TX, (1992).
24. K. Berkelman and S. Stone, Ann. Rev. Nucl. Part. Sci., Vol **41**, 1(1991).
25. "Review of Particle Properties", Phys. Rev. **D45**, VII.138, (1992).
26. "Review of Particle Properties", Phys. Rev. **D45**, VII.145, (1992).
27. "Review of Particle Properties", Phys. Rev. **D45**, VII.116, (1992).
28. "Review of Particle Properties", Phys. Rev. **D45**, VII.138, (1992).
29. R. Santonico et al., NIM **187**, 337(1981); R. Santonico et al., NIM **A263**, 20(1988); M. Bertino et al., NIM **A283**,654(1989).

30. S.N. Zhang et al., "A High Pt Muon Trigger Processor", IEEE Nuclear Science Symposium and Medical Imaging Conference Proceedings, Vol 1, 551(Nov,1991).
31. S. Conetti, Proceedings of the First Annual Conference on Electronics for Future Colliders, LeCroy Corp., Chestnut Hill, N.Y., 207(May, 1991); M. Dell'Orso and L. Ristori, NIM **A278**, 436(1989).
32. P. Drell, "Weak Decays, Rare Decays, Mixing and CP Violation", XXVI International Conference on High Energy Physics, Dallas, TX, (1992).
33. M. Binkley et al., E537 Collaboration, "Ψ Production in $\bar{p}$ N and π^- N Interactions at 125 GeV/c and a Determination of the Gluon Structure Functions of the $\bar{p}$ and the π^-, FERMILAB-Pub-90/63-E.
33. K. Abe et al., Physical Review D **33**,1(1986):
34. G. P. Yost, NIM **224**, 489(1984).
35. DELPHI Collaboration, "Evidence for B^0_S Meson Production in Z_0 Decays", XXVI International Conference on High Energy Physics, Dallas TX (1992).
36. D. Bartlett et al., NIM **A260**, 55(1987);
37. Tagged Photon Spectrometer Collaboration, Phys. Rev. Lett. **58**, 1818(1987).
38. Frabatti et al., E683 Collaboration, FERMILAB-Pub-90/258-E.
39. A. Ali and D. London, DESY 92-075 (1992).
40. Phys. Lett. **B276**, 379(1992).
41. Phys. Lett. **B252**, 703(1990).
42. Phys. Lett. **B262**, 171(1991).
43. ALEPH Collaboration, Phys. Lettr. B **278**, 209(1992).
44. OPAL Collaboration, Phys. Lettr. B **281**, 394(1992).
45. ALEPH Collaboration, "Observation of the Semileptonic Decays of B_S and Λ_b Hadrons at LEP", CERN-PPE/92-73, (May,1992), submitted to Phys. Lettrs. B.
46. "Review of Particle Properties", Phys. Rev. **D45**, VIII.60, (1992).
47. "Review of Particle Properties", Phys. Rev. **D45**, VII.114, (1992).
48. S. Delchamps et al., "Precision Charge Sensitive Amplification and Digitization System for a Scintillating and Lead Glass Array", IEEE Nuclear Science Symposium, (Nov, 1988).
49. B.L. Ioffe, Phys. Rev. Lett. **39**, 1589(1977).
50. A. McManus et al., "Performance of a Silicon Microstrip Detector in A Very High Rate Environment", Proceedings of the 1991 IEEE Nuclear Science Symposium and Medical Imaging Conference, Vol. 1, 298(Nov. 1991), to be published in IEEE Transactions on Nuclear Science; D. Christian et al., "Status of the Fermilab Designed E771 Silicon Strip Readout System", FERMILAB Report (April-June, 1991); C. Swoboda et al., "A High-Rate FASTBUS Silicon Strip Readout System" , IEEE NS 37, No. 2; T. Zimmerman et al. "A High Speed, Low Noise ASIC Preamplifier for Silicon Strip Detectors", Proceedings of the 1989 IEEE Nuclear Science Symposium.
51. A. McManus et al., "Effects of High Energy Protons on the E771 Silicon Microstrip Detector", Proceedings of the International Conference on the Effects of Radiation Damage on Scintillators and Detectors, Tallahassee, FA (May, 1992).
52. B. Cox et al., " A Measurement of the Response of an SCG1-C Scintillation Glass Shower Detector to 2 GeV to 17.5 GeV Positrons", NIM **219**, 487(1984); B. Cox et al., " High Energy Electromagnetic Shower Position Measurement by a Fine Grained Scintillation Hodoscope", NIM **219**, 487(1984); B. Cox et al., "A Measurement of the Response of an SCG1-C Scintillation Glass Array to 4 GeV to 14 GeV Pions", NIM **A238**, 321(1985); D. Wagoner et al., "A

Measurement of the Energy Resolution and Related Properties of an SCG1-C Scintillation Glass Shower Counter Array for 1 GeV to 25 GeV Positrons", NIM **A238**, 315(1985); C.M. Jenkins et al., "Results from the E705 Electromagnetic Shower Position Detector", IEEE Nuclear Science Symposium, Nov 9-11, 1988; R.Rameika et al., "Measurement of Electromagnetic Shower Position and Size with a Saturated Avalanche Tube Hodoscope and a Fine Grained Scintillator Hodoscope", NIM **A242**, 215(1986); L. Spiegel et al., "Performance of a Lead Radiator, Gas Tube Calorimeter", IEEE Nuclear Science Symposium, Nov 9-11, 1988; L. Antoniazzi et al., "The Experiment 705 Electromagnetic Shower Calorimeter", in preparation, to be submitted to NIM.

54. K.S. Nelson, "Design Calculations for the E771 RICH", UVa Internal Memo (Jan. 92).
55. M. P. Maia et al., " A Phototube RICH Detector", FERMI-PUB-92/155.

Proposal P867
December, 1993 Revision

A Proposal to Continue the Study of Beauty and Charm States in 800 GeV/c pN Interactions

T.Alexopoulos[20], M.Arenton[19], S.Bagdasarov[21], C.Ballagh[1], H.Bingham[1], M.Block[12], G.Bonomi[14], J.Budagov[3], Z.L. Cao[19], G. Cataldi[9], D.Chapman[1], T.Y.Chen[11], I.Chirikov-Zorin[3], G.Chlachidze[7], K.Clark[16], D.Cline[2], S.Conetti[19], M.Cooper[19], G.Corti[19], B.Cox[19], P.Creti[9], W. Davis[13], D.Djincharadze[7], A. Dolgert[19], C.Dukes[19], C.Durandet[20], V. Elia[9], M.Emery[13], A.Erwin[20], V.Flyagine[3], T.Gabriel[13], V.Geger[3], V.Glagolev[3], C. Glover[13], V.Golovatyuk[19], E.Gorini[9], F.Grancagnolo[9], M.Haire[15], K.Hagan-Ingram[19], P.Hanlet[19], M.Jenkins[16], J.Jennings[20], M.He[17], G.Introzzi[14], D.J.Judd[15], D.Khubua[7], A.Kurilin[6], V.Kushpil[3], A.Lanza[14], K.Lau[5], T.Lawry[19], A.Ledovskoy[19], G.Liguori[14], Y. Lomakin[3], J.Lys[1], G.Massey[19], N.Malakhov[3], S.Maliukov[3], P.O.Mazur[4], A.McManus[19], I.Minashivili[7], S.Misawa[1], G.H.Mo[5], C.T.Murphy[4], K.S.Nelson[19], M.Panareo[9], P.Pistilli[9], V.Pogosyan[19], S.Ramachadran[2], S.Ratti[14], A. Razinkov[3], M. Recagni[19], J.Rhoades[2], V.Rumiantsev[6], N. Russakovich[3], A. Semenov[3], R.P.Smith[4], L.Spiegel[4], J.G.Sun[19], S.Tokar[8], P.Torre[14], J.Trischuk[10], V.Timofeev[3], E.Tsyganov[3], L.Turnbull[15], I.Tzamouranis[19], A.Volodko[3], W.Yang[4], N.Yao[11], D.E.Wagoner[15], C.R.Wang[17], N.J.Zhang[17], N.Zhuravlev[3]

(1) University of California at Berkeley, Berkeley, CA 94720
(2) University of California at Los Angeles, Los Angeles, CA 90024
(3) Joint Institute for Nuclear Research, Dubna, Russia
(4) Fermilab, Batavia, IL 60510
(5) University of Houston, Houston, TX 77204-5504
(6)Institute of Physics, Belarus Academy of Science, Minsk, Belarus
(7) IHEP, Tbilisi State University, Tbilisi, Georgia
(8)J.A. Komensky State University, Bratislava, Slovakia
(9) University of Lecce/INFN, Lecce, Italy
(10) McGill University, Montreal, Canada, PQ H3A 2T8
(11) Nanking University, PRC
(12) Northwestern University, Evanston, IL 60208
(13) Oak Ridge National Laboratory, TN 37831-6369
(14) University of Pavia/INFN, Pavia, Italy
(15) Prairie View A&M University, Prairie View, TX 77446-0355
(16) University of South Alabama, Mobile AL 36688
(17) Shandong University, PRC
(18) Vanier College, Montreal, Canada PQ H3A 2T8
(19) University of Virginia, Charlottesville, VA 22901
(20) University of Wisconsin, Madison, WI 53706
(21)Yerevan State University, Yerevan, Armenia

Contact: B. Cox Dept. of Physics
Univ. of Virginia
804-982-5377

Table of Contents

I. Introduction

In the brief test run of E771 in 1991, we began the process of studying hadronic interactions which contain either beauty or charm with the open geometry E771 spectrometer. Although the E771 experimenters and the Laboratory management had hoped that E771 would reach a state of preparedness that would allow some B data taking, it was recognized before the run by both the PAC and the Laboratory[1] that the schedule for preparation of the microvertex electronics would allow little time for actual data taking. Therefore, while some B data was taken by E771, the main objective of the 1991 run as set by the PAC was to test aspects of the experiment for the next fixed target run.

Since 1991, significant B physics has been accomplished in CDF, CLEO and LEP. In that context, we have revisited both the objectives and the techniques of P867 to take into account the experiences of E771 and new heavy flavor data. Based on this re-evaluation, we have chosen to direct our efforts toward B physics difficult to accomplish in a collider environment as well as to point out the hidden and open charm potential of the experiment.

We plan modifications to our spectrometer and trigger/DA system which will allow us to

- accumulate 6 million B decays on tape making possible measurements of total and differential cross sections at 800 GeV/c, branching ratios and B_u, Bd, Bs lifetimes, B_d and B_s mixing, V_{cb} and various form factors, b->u transitions, and Λ_b production cross sections and lifetimes

- accumulate 290 million open charm decays on tape dominated by muonic decay channels allowing form factor measurements using $D^{\pm}\to K^{*0}\mu\nu$, $D^0\to K^{*-}\mu\nu$, $D_s\to\phi\mu\nu$ and searches for the decays $D^{\pm}\to\pi\mu\mu$, $D^0\to\mu\mu$.

- accumulate 170,000 $J/\Psi\to\mu\mu$ on tape, increasing by a factor of ≈4-8 our present E705 charmonium data and permitting the confirmation the E705 observation[2] of the $^1P_1$ and $^3D_2$ states of charmonium and to increase significantly the present level of statistics of our measurements[3] of χ state production.

II. P867 Operating Conditions

Table 1 summarizes the running conditions which we anticipate for P867 compared to those of E771. The interaction lengths for the E771 Si targets and the P867 Fe target have been calculated using an inelastic total cross section σ_T(pN) of 32 mb at 800 GeV/c and an A dependence[4] of $A^{0.71}$ to obtain σ_T(pSi) = 342 mb and σ_T(pFe) = 557 mb. This results in the interaction lengths given in Table 1.

The number of seconds of beam estimated for P867 is based on prorating the ≈ one month of E771 data taking period to 7.5 months total data taking out of the anticipated 10 months 1995-96 fixed target run. We estimate that 2.5 months for tuning of the spectrometer will be sufficient given the 1991 operation of E771, and the fact that the P867 experiment is simplified from the E771 configuration. While this running time is longer than our E771, by increasing the beam size we will reduce the total exposure per unit area in P867 by a factor of ≈three relative to that received in E771. In addition, operation of the silicon detector at lower temperatures[5] is planned. This, coupled with more efficient manipulation of the bias voltage as described in Appendix C, should give a comfortable margin of safety for operation in the 1995-96 run, allowing us to avoid radiation damage problems.

Table 1
E771 vs. P867 Run Conditions

	E771 1991 Run	P867 1995 Run
Proton Beam Momentum	800 GeV/c	800 GeV/c
Running Time	6.6×10^5 seconds	5.1×10^6 seconds
Spill Length	≈22 sec. every 57 sec.	≈22 sec. every 57 sec.
Target Material	2 mm Si foils (12)	7 mm Fe foil
Target Radiation Length	25.6%	39.8%
Target Interaction Length from σ_T(pA)	4.10%	3.41%
Average Interactions/Second in Target	1.9×10^6	2.5×10^6
Beam/Second on Target	4.6×10^7	7.3×10^7
Beam σ_x,σ_y	0.40 cm, 0.28 cm	1.24 cm, 1.24 cm
Total Integrated Useful Beam	3.0×10^{13}	3.7×10^{14}
Estimated Total Integrated m.i. /cm^2	1.6×10^{14}/cm^2†	5.1×10^{13}/cm^2
Total Integrated Interactions in Target	1.6×10^{12}	0.5×10^{13}
Available Triggers	1μ, 2μ	1μ, 2μ, E_γ, Mj, SV

† We have used our estimated 1991 total exposure of the E771 silicon target/tracker to beam of 6.0×10^{13} protons to estimate the number of minimum ionizing particles per cm^2 including both beam and interaction secondaries for 1991 fixed target run.

III. P867 Spectrometer

The physical configuration of P867 spectrometer as shown in Fig. 1 will remain essentially the same as that used in the E771 run. The major changes (save for the possible addition of a Cerenkov counter as discussed in Appendix E) include the full instrumentation of silicon microvertex detector, improvements to the RPC μ detector, changes to the muon triggers, addition of different types of triggers and changes to the data acquisition system. These changes will

- improve both resolutions and acceptances for B and C decays.

- allow the removal of the E771 front PWC/Drift chamber set to decrease the readout time.

- improve the efficiency of our muon triggers

- provide a system of three parallel triggers, hadronic, 1μ and 2μ by forming suitable combinations of μ, E_γ, multiplicity jump and secondary vertex trigger, thereby improving considerably the yields of B and C events logged compared to E771

* increase the bandwidth and live time of the DA system

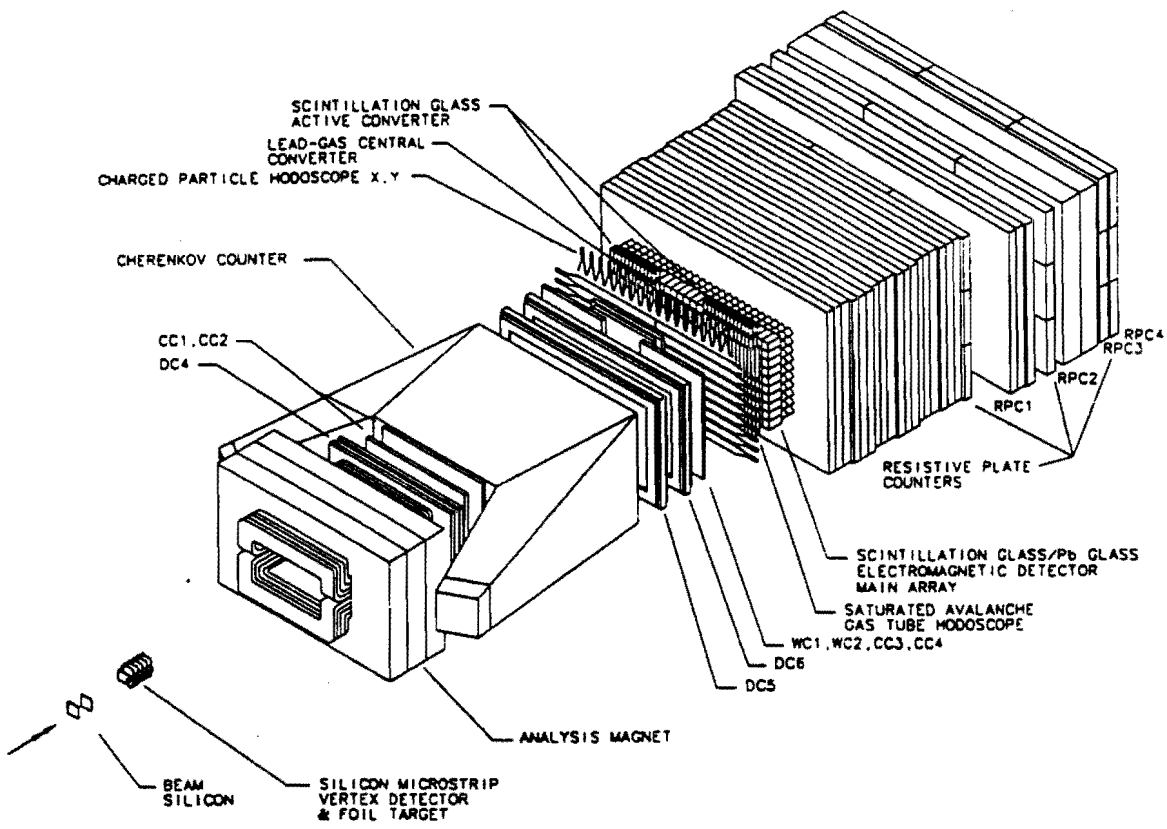

Fig. 1
P867 Spectrometer Configuration

With the contemplated changes to the trigger and the DA system and the longer running time anticipated, we are able to greatly increase the sensitivity of P867 for beauty and charm relative to E771 while operating at 2.5 MHz, a rate comparable to the E771 average of 1.9 MHz.

P867 DA System

In spite of the fact that the E771 DA system had the potential for high performance, an antiquated set of ADC's and TDC's have been a major restriction on our ability to accumulate heavy flavor data. The limited DA speed per event has forced the use of tight muon trigger requirements with an attendant loss of trigger efficiency. In the new version of P867, the readout time per event is decreased from 900 μsec, as experienced in E771 to 300 μsec, corresponding to 700 event/second capability with an 80% live time. This is achieved by eliminating the wire chambers upstream of the analysis magnet and increasing the number of parallel readout channels from six to twelve.

The 700 trigger per second capability does not require major modifications of the E771 DA. The addition of more parallel readout channels carries only a moderate cost. An even greater level of DA capability of 3000 events per second could also easily be attained by replacing 4K channels of slow TDC's and 1.5 K channels of ADC's with modern fast versions. However, we do not propose this upgrade unless the relatively small number of channels required is available to P867 from existing PREP stock.

P867 Triggers

The P867 trigger system consists of combinations of single and dimuon triggers, E_γ trigger, and multiplicity jump triggers at the first level followed by a second level secondary vertex trigger. The combinations presently planned for use in P867 are given in Table 2.

Table 2
P867 Triggers

	"1μ trigger"	"2μ trigger"	"Hadronic Trigger"
Level I	1μ•E_γ•Mult. Jump	2μ•Mult. Jump	E_γ•Mult. Jump
Level II	-	-	Secondary Vertex
Trig/sec	625 events/sec	60 events/sec	190 events/sec

The total trigger rate sums to 875 events/sec, matching the 700 event/sec DA capability when the expected 80% readout live time is taken into account.

The various triggers are discussed fully in Appendix D. Briefly, the 1μ or 2μ triggers are formed by requiring one or two tracks penetrating a thickness of steel and shielding concrete equivalent to between 6 and 10 GeV/c. The muons which penetrated the steel and concrete must generate triple coincidences between combinations of pads (called Super ORs) in three planes of Resistive Plate Counters[6] (RPC's) which are positioned at varying depths in the steel.

The E_γ trigger is formed from the sum of the energy of each individual scintillating and Pb glass block in the main array of the P867 electromagnetic calorimeter appropriately weighted by a resistive factor to account for the angle of the block with respect to the beam direction in the non bend plane (y projection). Ey is used, rather than transverse energy, to implement this trigger in order to avoid ambiguities due to magnet bending. Heavy quark production and decay, especially B's, generate a significantly different transverse distribution compared to minimum bias events, allowing an E_γ trigger to discriminate against the total cross section interactions. This rather simple and inexpensive trigger can be formed quickly and will operate at the first level.

The multiplicity jump trigger is formed from the difference of the pulse height of a pair of 2mm thick quartz counters separated by 4.2 cm and positioned just downstream of the 7mm Fe target (see Fig. C1, Appendix C). The decays of charm and beauty in the gap between the quartz generate a multiplicity jump leading to a difference in pulse height between the upstream and downstream counter. This trigger can be formed rapidly and will operate at Level I.

The third trigger addition is a Level II secondary vertex trigger[7] that will be implemented using associative memories to detect the presence of secondary vertices in the interaction. The secondary vertex trigger is the most complicated trigger since it depends on formation of tracks segments in the silicon microvertex detector in two projections using associative memories for fast tracking. Following track segment formation, the algorithm presently being tuned detects B and C events by forming crossings of tracks segments downstream of the primary target.

Cerenkov Counter

Finally, we have discussed the desirability of adding a Cerenkov counter to the P867 spectrometer for K,π,p particle ID. Since, as discussed in Section VI, most of the physics of P867 can be accomplished without a Cerenkov counter, we do not think it absolutely essential. However, K,π, p particle ID would add a unique capability to P867 that is currently not present in

collider experiments and would lead to improved statistics and reduced backgrounds for some B_S modes, Cabibbo suppressed decays, etc.. We indicate in the discussion of the physics objective of P867 in Section VI where the Cerenkov counter is considered to be valuable.

IV. P867 Trigger Efficiencies for Beauty and Charm

In E771, hampered by a limited DA, we were forced to accept small efficiencies when relying entirely on single and dimuon triggers. With the greater bandwidth DA and the new triggers, we are able to relax the criterion for the original E771 muon triggers to obtain greater efficiency. In addition, the combination of the E_T trigger, multiplicity jump and secondary vertex provides the capability of triggering on beauty and charm decays that do not contain muons. With these three triggers we collect B and C decays containing 1μ, 2μ or all hadronic final states.

Table 3 shows our preliminary estimates of efficiencies and trigger rates for the envisioned combinations of triggers (1μ, 2μ, E_T, Mj ≡ Multiplicity jump, and SV ≡ Secondary Vertex). The required performance in the three parallel triggers the appropriate Ey and/or Mj threshold for each specific condition. The various rejection or retention factors for each trigger are given in the B, C and σ_T rejection columns together with the overall rejection or retention factor.

Table 3
Trigger Efficiencies: 2.5 MHz Operation - 700 Trigger/sec DA

	Trigger	B Retention	C Retention	σ_T Rejection	Trig/sec
h	E_T * Mj*SV	.32*.60*.77=.148	.021*.19*.40=.0016	.005*.09*.17=6.0x10^{-5}	190/sec
1μ	1μ*E_T*Mj	.57*.85*.55=.267	.29*.42.*16=.019	.020*.17*.073=2.5x10^{-4}	625/sec
2μ	2μ*Mj† (X->μμ)	.37*.37=.137	.165*.092=.015	.00048*.042=2.0x10^{-5}	60/sec
	2μ*Mj (X->μ-X'->μ)	.27*.37= .10	.065*.092=.006		

†The retention factor in the C column is the average of that for D->μμ (0.18) and D->πμμ (0.15)

As indicated, there are different efficiencies for decays of the form B->μ•B->μ and D->μ•D->μ compared to B->J/Ψ->μμ or D->μμ. The direct J/Ψ->μμ decays necessary for the hidden charm objectives of the experiment are collected with the 2μ*Mj trigger because of the inefficiency of the Mj trigger. We expect approximately 4.2% of the J/Ψ->μμ to survive this trigger leading to an overall efficiency of the 2μ*Mj trigger of ≈1.6%. The 1μ and 2μ trigger total cross section rejection factors shown in Table 3 and discussed in Appendix D are derived from those observed in E771. The charm retention versus minimum bias rejection ratios for the E_T trigger that has been estimated using PYTHIA/GEANT Monte Carlo of the P867 EM detector is consistent with the ratios observed in previous charm data[8] for various E_T cuts. In addition, the preliminary B candidates from the E771 data agree with the signal retention vs. total cross section rejection predicted by Monte Carlo. The behavior of the P867 multiplicity jump trigger as calculated using GEANT simulations of the P867 target and quartz radiator configuration agrees with the results of test[9] of a similar multiplicity jump trigger by E791 in the last fixed target run.

V. P867 B, C, and J/Ψ->μμ Trigger Yields

During the 5.1x10^6 second P867 run, beauty, charm and J/Ψ decays will be accumulated in three different trigger categories - 1μ, 2μ and all hadronic decays - by the three planned triggers.

We have used the B hadroproduction cross section estimates of Berger[10] and a dependence of $A^{1.0}$ to obtain a $B\bar{B}$ production cross section of 950 nb in 800 GeV/c pFe interactions and 2.2×10^7 $B\bar{B}$ events produced in the P867 run, a fraction of which will satisfy the "hadronic trigger". Moreover, the 10.7% branching ratio[11] for B->μ semimuonic decays results in 4.62×10^6 B->μ and 5.1×10^5 B->μ•B->μ events produced during the P867 run, some of which will be contained in the 1μ and 2μ trigger samples. Using the B->J/Ψ +x branching ratio[12] of 1.12% and a J/Ψ->μμ branching ratio[13] of 5.91%, we expect to produce 2.9×10^4 B->J/Ψ+x ->μμ +x inclusive B decays which will also contribute to the 2μ trigger sample. It should be kept in mind that the value for the inclusive B->J/Ψ rate could be different in P867 due to contributions from B^0_s and B baryon decays not present in the ARGUS and CLEO experiments.

For charm production we have used $A^{1.0}$ together with a pN->D or $\bar{D}$ inclusive production cross section[14] of 32.4 μb at 400 GeV/c to obtain a pFe->D+x, inclusive production cross section of 1.81 mb at 800 GeV/c. This will result in production of 4.1×10^{10} $D\bar{D}$'s in P867 ignoring a possible energy dependence. Using an average over $D^{\pm}$ and D^0, 13.9%[15] of the produced D's will decay muonically. Therefore, we estimate 1.1×10^{10} D->μ and 1.6×10^9 D->μ•D-->μ decays will be produced in the P867 run.

Finally, we have used an updated "Lyons parameterization"[16], $\sigma(pN\to J/\Psi)=798\ e^{-15.3\sqrt{\tau}}$ nb ($\sqrt{\tau} = M_{\mu\mu}/\sqrt{s}$), to estimate the cross section of 234 nb for pN->J/Ψ production over all x_f in 800 GeV/c interactions. This updated parameterization of the σ(pN->J/Ψ + x), which is discussed in Appendix A, incorporates new measurements which were not available at the time of the original Lyons parameterization including the E771 preliminary result for pSi->J/Ψ + x production. We use an A dependence of $A^{0.92}$ to scale this cross section to an Fe target, obtaining 9.48 μb and an expect production of 2.2×10^8 J/Ψ during the run. Using the J/Ψ->μμ branching ratio quoted above results in an expected production of 1.3×10^7 J/Ψ->μμ decays in P867.

Using the retention factors given in Table 4 and the expected numbers of events produced in the various trigger categories, we expect to accumulate on tape the number of beauty, charm and J/Ψ->μμ shown in Table 4.

Table 4
Number of B's, C's and J/Ψ to Tape in the P867 Run

	General Decay Category	Number Produced††	Trigger Combination	Trigger Efficiency	# of Decays to Tape†
B	B->hadronic	4.4×10^7	Ey *Mj*SV	14.8%	5.2×10^6
	B->μ	4.6×10^6	1μ*Ey*Mj	26.7%	9.8×10^5
	B->μ•B->μ	4.8×10^5	2μ*Mj	10.0%	3.8×10^4
	B->J/Ψ->μμ	2.9×10^4	2μ*Mj	13.7%	3.2×10^3
C	D->hadronic	8.2×10^{10}	Ey *Mj*SV	0.16%	1.1×10^8
	D->μ	1.1×10^{10}	1μ*Ey*Mj	1.90%	1.7×10^8
	D->μ•D->μ	1.6×10^9	2μ*Mj	0.60%	5.4×10^6
	D->πμμ or ->μμ	-	2μ*Mj	1.52%	-
J/Ψ	J/Ψ->μμ	1.3×10^7	2μ*Ev*Mj*SV	1.6%	1.7×10^5

† The 80% live time has been taken into account in the number of events written to tape
†† B or D decay decaying to a state that could possibly satisfy given trigger

The 6 million B's, 290 million C's and 170,000 J/Ψ->μμ events written onto tape are part of a total data sample of 3.6×10^9 events expected to be logged during the P867 run. This is an

imposing number of events but is only 20% of charm experiment E791 already performed at Fermilab and less than 7% of P829. In addition, the processing of the muons triggers which form the bulk of the trigger sample (550 out of 700 triggers per second or ≈ 80% of all triggers are muon triggers) is quite rapid. The E771 data processing is proceeding at 3000 events per second with the present E771 computing resources. This speed is expected to increase by more than a factor of 2 with improvements already underway in the E771 reconstruction code.

VI. P867 Beauty and Charm Physics

The 6 million beauty and 290 million open charm triggers on tape in P867 offer many different possibilities for extraction of beauty and charm physics. We plan to measure both differential and total cross sections, lifetimes, mixing, and branching ratios for charged and neutral B's as well as for the $B^{\pm}_u$, B^0_d and B^0_s and the Λ_b. In addition, we plan to measure Vcb and Vub.

The particular modes and trigger combinations that we will use to address the various B physics issues are:

- determination of the $B^{\pm}$ and B^0 cross sections and lifetimes using the inclusive modes B->J/Ψ->μμ and B->μ decays. (1μ and 2μ triggers).

- observation and measurement of branching ratios of exclusive B->J/Ψ->μμ modes (2μ trigger).

- measurement of V_{cb} and B^0_d and $B^{\pm}$ lifetimes from decays such as B^0_d->$D^{*-}\mu^+\nu$ and B^+->$D^{0*}\mu^+\nu$. (1μ trigger)

- determination of the mixing of the neutral $B^0_d + B^0_s$ using the double semi-muonic decays of the B pairs (2μ trigger).

- observation of B^0_s and determination of B^0_s production cross sections, lifetimes and mixing via the inclusive channels, B^0_s->D^+_s + x and the exclusive channel, B^0_s->$D^-_s\mu\nu$ where the D^-_s decays into all-charged modes (1μ and hadronic triggers).

- search for semi-muonic decay modes $B^{\pm}_u$->$\rho^0\mu\nu$, B^0_d->$\pi^{\pm}\mu\nu$, and other b->u transitions such as B^0_d->$a^+\pi^-$->4 π with the subsequent measurement of Vub (1μ and hadronic trigger)

- measurement of Λ_b production and lifetime (hadronic, 1μ and 2μ triggers).

The open charm contribution of P867 is contained mainly in the muonic triggers. The physics topics which will be addressed include:

- measurement of form factors using the D modes D^+->$K^{0*}\mu\nu$ and D^0->$K^-\mu\nu$ and D^+_s->$\phi\mu\nu$ (1μ trigger).

- searches for $D^{\pm}$->$\pi^{\pm}\mu\mu$ and D^0->μμ (2μ trigger)

The hidden charm sector (accessible via observation of charmed states decaying into final states containing J/Ψ or Ψ') contains many interesting physics issues, including:

- measurements with higher statistics and better resolutions of the production of Ψ, Ψ' and χ total and differential cross sections to extract information about the heavy flavor production processes (2μ trigger).

- confirmation of tentatively observed charmonium states such as the $^1P_1$ and $^3D_2$ states of the $c\bar{c}$ system and search for 4 quark or exotic states (2μ trigger).

VI.A. Beauty Physics

VI.A.1 Cross Sections, Lifetimes and Branching Ratios from B->J/Ψ-> μμ and B->μ

Total and differential cross sections and lifetimes for charged and neutral B production in 800 GeV/c pN interactions can be obtained with good statistical accuracy from the 3,200 B->J/Ψ->μμ decay and ≈1 million B->μ inclusive decays accumulated on tape in P867. The total cross section measurements are important for understanding beauty quark production mechanisms in pN interactions in an energy regime where few if any results exist at the moment. In addition, with these data, we can achieve a precision of measurements of charged and neutral B lifetimes comparable to or better than those of the LEP or Fermilab Collider experiments[17] with quite different backgrounds and systematic errors. Indeed, one strength of the P867 fixed target hadroproduction configuration is the excellent time resolution afforded by the combination of long decay lengths ($\langle\Delta z\rangle \approx 9.1$ mm and $\langle\Delta r\rangle \approx 150$ μm) coupled with good resolution on primary-secondary vertices separation (σ_{Sep}=340 μm) resulting in the ratio of $\langle\Delta z\rangle/\sigma_{Sep} \approx 27$.

The technique for extraction of the total and x_F and p_t differential cross sections and lifetimes from B->J/Ψ->μμ or the B->μ decays is indirect since we measure only the muons and other charged particles from the vertex. In this indirect process, distributions of the observed quantities, e.g., the primary to decay vertex distance, the momentum of the charged B decay products, the visible invariant mass of the decay, the impact parameters of any decay product with respect to the primary vertex etc. are compared with predictions of detailed Monte Carlos calculated using a range of values of the production parameters and lifetime of the B's.

The technique, which we have used before in a different context[18], is to Monte Carlo B->J/Ψ and B->μ decays with different choices for the shapes of the x_F and p_t distributions of the B's. By comparing and adjusting the resulting x_F and p_t of the daughter J/Ψ and single μ's to the data, we can extract the parameters of the parent distributions. Preliminary evaluations of the systematic errors involved in this technique indicate that the cross section and lifetime determined by this indirect technique are not particularly sensitive to the input parameters of the Monte Carlo's. Moreover, because of the number of inclusive muonic B decays accumulated in P867, the event selection criteria can be tuned to minimize improper assignments of tracks to vertices, and to eliminate events where the missing neutrals carry most of the momentum or mass, etc. to reduce the systematic uncertainty of the measurements.

In addition, clean subsamples of fully or nearly fully reconstructed events are available as monitors of the effectiveness of the procedures used to determine cross sections or lifetimes from the inclusive decays. The almost fully reconstructed samples can also be used in a manner similar to that possible for exclusive decays to measure the charged and neutral lifetimes. Specifically, we

estimate that ≈10% of the B->J/Ψ->μμ + $x_{charged}$ +$x_{neutral}$ will be missing at most a soft π^0 or photon. For these, the proper flight time can be estimated well by the quantity:

$$\tau_{effective} = L_{effective} \cdot M_{visible} / (c \cdot p_{visible})$$

where $L_{effective}$ is the distance between the decay point and the point along the potential flight path where an event of this topology and configuration would have first passed all our cuts. $M_{visible}$ is the invariant mass of all the observed decay particles and $p_{visible}$ is the vector sum of their momenta. How good an estimate $\tau_{effective}$ is of the true proper flight time can be determined by a comparison of Monte Carlo with the data. Experience from previous experiments[18,19] suggests that we can take out any bias in $\tau_{effective}$ well enough to measure the separate lifetimes to a few percent. This is true even when only the outgoing muons are identified, i.e., all outgoing charged particles are considered to be pions. Similarly, an unbiased sample of several thousand B->μ+ $x_{charged}$ +$x_{neutral}$, where there is only a neutrino or a neutrino accompanied by a soft π^0 or photon, can be selected. The same technique should permit a second determination of the separate lifetimes to a few percent.

Our own experiences with indirect measurements of total and differential cross sections lead us to believe that we can make measurements of cross sections to better than 5%. In addition, while this indirect method might be thought to contribute some error in the shape parameters of the p_t and x_F distributions, our previous experience indicates that such errors are negligible in the extraction of parameters such as the exponent α of gluon structure function, $xG(x)=\beta\cdot(1-x)^{\alpha}$. The experience of other experiments that have reported indirect measurements of charm and beauty lifetimes convinces us that we can measure the average B lifetimes to better than 5% with the P867 data. Such a measurement will serve as an interesting contrast to the measurements made at e^+e^- or hadron colliders. Discrepancies could yield interesting information on the relative contributions of B^0_S, B^0_C, or B baryons to the indirect measurements in each experimental configuration.

Finally, it is worth mentioning that the large B->J/Ψ and B->μ inclusive data samples will lend themselves to many "engineering studies" for future experiments. For example, studies of tagging efficiencies for future CP violation proposals can be performed using the B->J/Ψ->μμ sample since among the ≈ 3200 B->J/Ψ decays on tape, approximately 18% will contain a lepton (e or μ) from the decay of the other B within the spectrometer acceptance. From this sub-sample tagging efficiencies useful to future experiments could be determined with reasonable accuracy.

VI.A.1.a Charged and Neutral B Cross Sections and Lifetimes from Inclusive B->J/Ψ-> μμ

Based on the present E771 analysis, we require that the dimuons satisfy the four criteria

- both muons must be in the acceptance of the spectrometer magnet and muon detector and be reconstructed fully in the spectrometer

- reconstruct to a J/Ψ mass with 2.9 GeV/c^2 <Mμμ<3.3GeV/c^2

- have a distance of closest approach of the μ's (≤15 microns in $r=\sqrt{x^2 + y^2}$; ≈ 3σ)

- the dimuon vertex in the decay region between the two quartz radiators and a distance Δz≥1mm ≈3 σ_z away from either radiator

to be designated as an inclusive B->J/Ψ-> μμ. Since we are triggering on the dimuon, both muons automatically satisfy the criterion of being in the acceptance of the spectrometer magnet and the muon detector so that the reconstruction efficiency•acceptance for the J/Ψ will be ≈50%. The mass criteria should lose a negligible fraction of the J/Ψ given the dimuon mass resolution of 33 MeV/c^2. The cut requiring the two muons to pass within 3σ is also loose enough that very few events are lost. Finally, though the B->J/Ψ-> μμ are already prejudiced by the multiplicity jump trigger to be between the two radiators, the offline requirement that the J/Ψ vertex be between the two radiators leads to an additional acceptance factor of 67%. We estimate an overall efficiency of ≈31% resulting in ≈1000 reconstructed B->J/Ψ->μμ decays useful for B cross section and lifetime determinations.

These events can be partitioned into neutral and charged B components by reconstruction of the remaining charged tracks associated with the dimuon vertex, a process which we estimate will introduce an additional efficiency of 65% together with background due to a missed or added charged track approximately 6% of the time (2% of the time an extra track is added, 5% of the time a track is lost). This contribution to the error in $B^{\pm}$ and B^0 cross sections and lifetimes is of the order of the statistical error of the B^0 and $B^{\pm}$->J/Ψ-> μμ reconstructed data sample(≈ 5%).

Among the other contributions to errors are the uncertainties in the efficiencies and acceptances. The experimental errors due to uncertainties in trigger, detector and reconstruction efficiencies can be determined by studies of the more copious direct J/Ψ->μμ production (≈ 170,000 events on tape) which provides a large signal with which to study efficiencies and resolutions. In addition to evaluations based directly on the data, we can also use the technique employed in E771, of superposition of GEANT Monte Carlo simulated B->J/Ψ->μμ on actual 800 GeV/c dimuon triggers to extract reconstruction efficiencies. Using both of these techniques, we expect a negligible contribution to the error in the cross sections due to uncertainties in the various efficiencies compared to the errors due to track misassignments..

There are errors due to backgrounds to the B->J/Ψ sample. The backgrounds for the strictly dimuon part of the B->J/Ψ->μμ inclusive decays arise mainly from mismeasured or multiple scattered dimuons from direct J/Ψ production at the primary or from J/Ψ production in secondary interactions where the reconstructed vertex appears to have been pulled downstream of its true position in the target material. Since we plan to restrict the B->J/Ψ->μμ data for the cross section measurements to the decay region between the two quartz radiators, we expect a negligible background contamination from false secondary vertices.

Finally, there is the contribution to the error due the measurements of live beam. This error is, of course, common to all cross section determinations in P867 but should not contribute directly to the error in the lifetime measurements. We expect to monitor the beam flux in several different ways as we did in E771 and expect a negligible contributions to the overall error.

We estimate that we will be able to make <5% measurement of the total B production cross section and lifetime using the B->J/Ψ->μμ inclusive decays. The measurements of the individual charged and neutral cross sections will be determined to <10% with the main errors coming errors in track assignments to secondary vertices. The lifetimes should be determined to better than 10% in all cases.

VI.A.1.b Charged and Neutral B Cross Sections and Lifetimes from Inclusive B->μ

The large trigger sample of 980,000 B->μ inclusive decays can be used to extract the cross sections and lifetimes also in much the same way as the B->J/Ψ->μμ inclusive decays. However,

the B->μ trigger sample is more contaminated by backgrounds, in particular C->μ, and therefore the final B->μ analysis sample must satisfy the criteria given below:

- complete reconstruction of the muon
- impact parameter greater than 75 μm (≈ 5 σ_{impact})
- p_t of the muon with respect to the parent particle >1.5 GeV/c
- potential B->μ vertices in the decay region between the quartz radiators of the Mj trigger

We estimate that approximately 71% of the muons in the trigger sample will be reconstructed and that 85% of the B->μ and 60% of the D->μ will survive the impact parameter cut of 75 μm. The requirement that the muon p_t can be greater than 1.5 GeV/c with respect to the direction of the parent particle is a very effective cut with only 0.16% of the remaining charm background surviving while 62% of the B->μ signal is retained. The 367,000 remaining B->μ decays are estimate to have a 20% residual background after these cuts, due mostly to D->μ decays. Studies are underway to further minimize the charm backgrounds.

This sample of B->μ can then be used to obtain a second determination of the B production cross sections and lifetimes by the indirect methods discussed above. The B data is partitioned into neutral and B decays by reconstruction of the remaining charged tracks from forming a consistent vertex with the muon. Should additional cleanliness be required, there are many additional handles that can be applied to these events (for example, visible mass at the muon vertex or the presence of a secondary vertex in the event or harder p_t cuts on hadrons as well as muons) that could further eliminate contamination while preserving significant numbers of B->μ events. Overall, the major errors should still be the misassignments of tracks to the secondary vertices but the additional statistics should permit cross sections and lifetimes for charged and neutral B's to be measured to better than 5%.

VI.A.1.c Exclusive B->J/Ψ->μμ Decays

The observation of B->J/Ψ exclusive decays will suffer from small statistics but have lower systematic errors and negligible backgrounds. Some of the exclusive modes that we can observe have not yet been reported or have large errors on branching ratios. With the 3,200 B->J/Ψ->μμ in the 2μ trigger sample we should be able to reconstruct enough events in several exclusive channels to improve the branching ratio measurements. In addition, the exclusive modes have the advantage that the B is totally reconstructed and the lifetime, x_F and p_t distributions are directly observable. Therefore, the small number of the completely reconstructed B->J/Ψ exclusive decays serve as a useful check on the higher statistics inclusive procedure.

We have chosen a few exclusive J/Ψ modes to demonstrate the ability of the P867 experiment to study such decays. Accessible B^0_d->J/Ψ decay modes include B^0_d->ΨKπ with a composite branching ratio[20] of 5.9×10^{-5} for the final state $\mu\mu K^+\pi^-$. Another interesting example is B^0_d->Ψ'K*(890) with a composite branching ratio[20] of 2.7×10^{-5} for the μμππKπ (when the Ψ'->Ψππ) .

$B^{\pm}_u$ modes accessible to P867 include $B^{\pm}_u$ ->Ψ$K^{\pm}$ with a composite branching ratio[21] of 4.55×10^{-5} for the final state μμ$K^{\pm}$. A second example is the decay $B^{\pm}_u$->Ψ$K^{\pm}\pi^+\pi^-$ with a

composite branching ratio[21] of 6.5×10^{-5} to decay into $\mu\mu K^{\pm}\pi^{+}\pi^{-}$. An interesting aspect of this last decay mode would be the investigation of the possible resonance structure for the $K\pi\pi$ system.

Finally, we will search for the B^0_s meson via its decay into $\Psi\phi$. We will be able to reconstruct the ϕ without particle ID by using tracks from a resolvable secondary vertex. The signal would consist of a secondary vertex containing the two J/Ψ muons and two closely correlated tracks. The branching ratio for the $B^0_s\to\Psi\phi$ decay should be approximately equal[22] to that of the $B^{\pm}_u\to\Psi K^*$ decay, measured[21] to be 1.4×10^{-3}. Using this and the $\phi\to K^+K^-$ decay branching ratio[23] of 0.49, we obtain a composite branching ratio of 4.1×10^{-5} for the $B^0_s\to\Psi\phi\to\mu\mu K^+K^-$ sequence. We also intend to search for B^0_s decay modes of the type $B^0_s\to\Psi\,\phi$ plus charged pions which should contribute a significant number of B^0_s decays to add to the $\Psi\phi$ data.

Collecting the information about these modes, we show in Table 5 then numbers of these particular modes that we expect to collect with the dimuon trigger. We have used the hadronization ratios $B^{\pm}_u/B^0_d/B^0_s/\Lambda_b = 0.38/0.38/0.14/0.10$ to obtain these yields.

Table 5
Numbers of Various B->J/Ψ Exclusive Decay on Tape

	Composite BR	# On Tape
$B\to J/\Psi\to\mu\mu$	6.6×10^{-4}	3200
$B^0_d\to\Psi K^+\pi^-\to\mu\mu K\pi$	5.9×10^{-5}	105
$B^0_d\to\Psi' K^*(890)$	2.7×10^{-5}	50
$\to\Psi\pi^+\pi^- K^+\pi^-\to\mu\mu\pi\pi K\pi$		
$B^0_s\to\Psi\phi\to\Psi K^+K^-\to\mu\mu KK$	4.1×10^{-5}	30
$B^{\pm}_u\to\Psi K^{\pm}\to\mu\mu K$	4.6×10^{-5}	90
$B^{\pm}_u\to\Psi K^{\pm}\pi^+\pi^-\to\mu\mu K^{\pm}\pi^+\pi^-$	6.5×10^{-5}	120

These ≈400 B decays are required to meet the additional criteria that:

- both muons and all other charged decay products be must fully reconstructed
- the dimuon must reconstruct to a J/Ψ mass with $2.9\ \mathrm{GeV/c^2} < M\mu\mu < 3.3\ \mathrm{GeV/c^2}$
- all charged decay products have a distance of closest approach at the secondary vertex point with $\Delta r \le 15\ \mu m$ ($\approx\sigma_{\Delta r}$; $(r=\sqrt{x^2+y^2})$
- the charged decay products must reconstruct to a B mass
- The secondary vertex must be separated from the primary vertex by a distance $\Delta z \approx 1.7$mm ($\approx 5\sigma_{\Delta z}$)

The composite effect of these requirements varies from mode to mode but, on average. yields an efficiency of 16%. Summing over all B->J/Ψ modes, we expect to have available of order one to two hundred completely reconstructed exclusive decays. These events will serve as a useful check on the B->J/Ψ inclusive measurements. For these fully reconstructed events, the proper flight time is measured directly from the decay length (suitably corrected for efficiency and

resolution of the measurement of the secondary vertex) and the momentum of the B as determined from its decay products. The backgrounds for these exclusive modes are expected to be negligible.

VI.A.2 B^0 Mixing from Double Semileptonic Decays

In the P867 run, we will have approximately 38,000 double semimuonic triggers on tape. Two methods will be used for studying B^0 mixing using the double semileptonic decays. The first method ("non vertex") makes use of a larger sample of data without using vertex information while the second method (vertex) requires two identified secondary vertices.

VI.A.2.a Non-Vertex Method

The "non vertex method" for determining average B mixing is similar to that used previously by other groups, comparing same sign to opposite sign dimuon rates. To eliminate backgrounds in this data, cuts are made on the transverse momentum with respect to the beam direction and on the mass of the dimuon pair. Approximately 8700 of the 38,000 B->μ•B->μ events survive the requirements that both muons be reconstructed, the dimuon mass be greater than 3.2 Gev/c^2 and the p_t of each muon be greater than >1.5 GeV/c^2. The background to the double semimuonic B decays due to muon pairs from double semileptonic charm decays, charged B decays and b->c->μ decays that survive to this point totals approximately 2600 muon pairs. Analysis of this sample will require Monte Carlo correction for these backgrounds which will contribute to the same sign signal and dilute the actual mixing effect. The large size of the data sample insures that systematic errors will dominate the determination of the mixing parameter.

The number of pairs available for this measurement is quite substantial when compared to that of other experiments that have studied mixing with semileptonic pairs in very different environments at different energies. For example, the OPAL[24], L3[25] and UA1[26] had at their disposal μ pair samples of 1011, 1083 and 889 respectively and used methods similar to the non-vertex method to determine mixing at their energies in their experimental configurations.

VI.A.2.b Vertex Method

Out of the 38,000 B->μ•B->μ event trigger sample, approximately 14,000 double semimuonic B decays survive the requirements that both muons are reconstructed, have impact parameters greater than 75 μm and the lowest p_t muon >0.5 GeV/c. Additional requirements including that each muon be associated with an identified secondary vertex and the muon p_t with respect to direction of the parent B decay > 1.0 GeV/c for each muon, reduces the number of events to approximately 12,400 with less than 6% background. The p_t cut is designed to exclude double charm decay. The mass cut rejects second generation decays (b->c->μ) relative to first generation decays (b->μ). Monte Carlo corrections for contamination of the sample by second generation decays, charged B decays, and background muons will be necessary. This technique will provide an alternative measurement with different (and presumably lower) backgrounds with which to compare the results of the "non vertex" method.

VI.A.3. B^0_S Cross Section, Lifetime and Mixing

We plan to detect the B^0_S and measure its parameters using the inclusive decays B^0_S->D^+_S +x decays (where x is all hadronic) or the exclusive decay B^0_S->D^+_Sμ ν semimuonic decay by reconstructing the associated D^+_S. The observation of the B^0_S by the detection of its D^+_S decays depends on our ability to reconstruct D^+_S mesons. We list "accessible" decay modes in Table 6:

Table 6
Accessible D^+_S Decay Modes
(Reference 27)

D_S Decay Mode	Composite BR	Topology
$D^+_S \rightarrow \pi^+ \pi^- \pi^+$	1.2%	3 prong
$D^+_S \rightarrow \phi \pi^+ \rightarrow K^+ K^- \pi^+$	1.4%	2 prong
$D^+_S \rightarrow \phi \pi^+\pi^- \pi^+ \rightarrow K^+ K^- \pi^+ \pi^- \pi^+$	0.6%	4 prong
$D^+_S \rightarrow \phi \mu^+\nu \rightarrow K^+ K^-\mu^+\nu$	0.8%	2 prong
$D^+_S \rightarrow \phi e^+\nu \rightarrow K^+ K^-e^+\nu$	0.8%	2 prong
$D^+_S \rightarrow K^+ \bar{K}^{*0} \rightarrow K^+ K^- \pi^+$	1.7%	3 prong
$D^+_S \rightarrow K^+K^-\pi^+$	0.8%	3 prong

We have considered in what follows only all charged D^+_S decay modes. In specifying the D^+_S decay chains resulting in ϕ and K^{*0}, we consider only $\phi \rightarrow K^+K^-$ and $\bar{K}^{*0} \rightarrow K^-\pi^+$ with branching ratios of 0.5 and 0.667 respectively.

Since any ϕ candidate track pair would be required to come from a secondary vertex, it may be possible that the first five modes can be reconstructed without particle identification. For example, at LEP, where particle identification is presently done by dE/dx, a $D_S \rightarrow \phi\pi$ (where $\phi \rightarrow K^+K^-$) signal has been seen[28,29] in a sample of secondary vertices without requiring particle identification on the tracks (the track separation is too small). The topology of two nearly overlapping charged tracks which point back to the decay vertex is a sufficiently distinct ϕ signature. In situations of higher multiplicity and/or ambiguous vertex assignments, K/π particle identification may become necessary. The Tagged Photon Laboratory Spectrometer has found[30,31] particle identification to be crucial in the study of charm decays containing the ϕ. By making strict vertex cuts, E687 has found[32] $\phi \rightarrow KK$ and $D \rightarrow K+n\pi$ (n=1,2,3) using a topological analysis without resorting to particle identification. In this sense particle id is used more for reducing background than initially finding signals. However, for the last two modes, particle identification would be necessary to distinguish them from the analogous D^+_d decays (e.g. $D^+_d \rightarrow \bar{K}^{*0}\pi^+$) and to reduce the combinatorial background.

It should be noted that the above modes are not unimpeachable D^+_S decays by particle composition alone since D^+_d decays into the same final states with a factor of approximately five (Cabibbo) suppression in all three cases. Thus a mass cut will be required to distinguish the D^+_d from the D^+_S. The mass resolution for a two body state in our spectrometer is of order $\sigma \approx 45$ MeV/c^2 to be compared to the D^+_d - D^+_S mass difference of 1969-1864 ≈ 100 MeV/c^2. Since we expect the mass resolution for ≥ 2 prong topologies to be better than the two body resolutions, the mass resolutions of the P867 spectrometer should be adequate to the task of separation.

We have considered two different types of decay modes for obtaining events containing B^0_S. Either the B_S may decay directly into a muon and provide the trigger (self triggered) or, alternatively, the B_S may decay into hadrons. We evaluate in the following sections our ability to observe B^0_S in two different decay types but have limited ourselves to our 1μ trigger sample. In principle, additional yields of tagged B_S decays are available from our hadronic trigger sample using electron or kaon tagging as well as muon tagging.

VI.A.3.a B^0_S Mixing from the B^0_S->D^+_S+x Inclusive Mode

The fixed target environment described in this proposal offers the possibility of measuring mixing in the B_S mesons by direct observation of the oscillation in the decay time distribution of the inclusive decays B^0_S->D^+_S+X. In order to separate the data into B^0s and $\bar{B}^0$s at production, we use the charge of the muon from the other B->μ decay in the event. The "other" B->μ decay will also provide the trigger for the event so we expect to find the B^0_S->D^+_S+x in the $9.8x10^5$ B->μ trigger sample accumulated in the P867 run.

In order to identify the inclusive B^0_S ->D^-_Sx decays, we require that the D^-_S decay into the channels listed in Table 6. Furthermore, we exclude the last two modes in Table 6 since a Cerenkov counter would be essential for them to reject backgrounds. This retains two thirds of the accessible decay chains. To estimate yields, we assume that the branching ratio for B^0_S ->$D^-_S x^+$ is the same as B^0_d ->$D^-_d x^+$, i.e., 30%. Summing the indicated D^-_S modes, we obtain a branching ratio of 4.8% for the "usable" D^-_S decays, leading to a composite branching ratio of 1.44%.

If we assume the hadronization fraction for B^0s production is 14%, then 140,000 of the B->μ decays on tape should be B^0s->μ decays. Approximately 2000 of these will be the desired B^0_S ->$D^-_S x^+$ followed by the required D^-_S decays. Using a GEANT Monte Carlo, we estimate a 15% acceptance times reconstruction efficiency (including the tagging μ) for the decay chains. This gives approximately 300 reconstructed tagged events with which to study mixing oscillations.

In this sample of events, the accompanying B_S decay is only partially reconstructed and recognized by its reconstructing its decay into a D_S meson plus one or more charged particles. A sufficiently accurate estimate of the B_S gamma factor can be obtained measuring the gamma associated with the visible mass at the B_S decay vertex. This is primarily due to the fact that the D_S takes a large fraction of the B_S momentum. If a vertex separation requirement must be applied to the D_S ($\Delta z \approx 1700$ μm$\approx 5\sigma_{\Delta z}$ separation from the primary vertex is more than adequate), the data sample is reduced to ≈ 285 events but backgrounds are significantly reduced.

We have studied with Monte Carlo simulations what we believe will be the most serious backgrounds to this procedure. The first background will be B_d decays to D_d which are incorrectly reconstructed as D_S. We estimate that this effect will appear as a few percent smooth background to the reconstructed D_S. A second important source of background are $B_{u,d}$ decays into D_S, observed to occur at a rate of about 10%. In a large fraction of these background events, the D_S will be accompanied by another D and the decay products of the D will not intersect the D_S line of flight. At the B vertex, certainly in the case of the B_S and often for $B_{u,d}$ decays, there will be more charged tracks, but the visible mass of any such track together with the reconstructed D_S will be in general much larger for B_S than for $B_{u,d}$ decays (due to the unobserved D). We have estimated with a Monte Carlo the reduction of this background achieved by requiring the charged track to be within 100 μm of the D_S flight path and to form , when combined with the reconstructed D_S, a visible mass > 2.4 GeV/c^2. We conclude that we can reduce the $B_{u,d}$ background to less than 10% of the B_S signal, while retaining more than 75% or ≈215 events.

The μ tag is diluted by processes which generate "wrong charge" muons such as b->c->μ decays and which must be minimized if possible. An unavoidable process is mixing of the tagging B processes if it is neutral. UA1 obtained by observing the same sign di-lepton rate a value for the overall or average mixing in hadronically produced beauty events of 0.158±0.059 at collider energies. This level of mixing (which depends on the ratios of beauty species u,d,s) would result in a mixing dilution of 0.316 which must be suffered if appropriate to our energies.

However, other dilution factors due to b->c->μ decays and other muon backgrounds can be minimized by reconstructing at least a part of the visible mass associated with the tagging muon and demanding it to be large. This cut will reduce to a negligible level the b->c->μ decays and other backgrounds which lead to mistagging (Alternatively, if we recognize the charm->μ decay by the presence of a distinct tertiary vertex, we can make the proper tagging assignment to the event). Another way to exclude these b->c->μ decays is to perform a cut on the muon transverse momentum measured with respect to the parent direction. The p_t cut requires us to form a vertex and the visible mass cut requires that we reconstruct at least one other charged particle from the tagging B decay. This requirement on the tagging B decays reduces our data sample to approximately 140 events.

Since we have identified a B_S in the event by this point, there should be little background from direct charm production followed by D->μ decay. We have required in the acceptance calculations that the tagging beauty hadron produce not only a trigger muon but also one or more charged particles in the acceptance which are reconstructed. As stated above, we apply the same requirements to the b->c->μ and demand a large p_t and visible mass of the μ•hadron combination in order to reduce background. We estimate that a requirement of p_t for the tagging muon >1.0 GeV/c determined with respect to the parent particle direction will conserve approximately 85% of the B->μ decays leaving 120 B_S ->D_S decays, while reducing the b->c->μ false tag backgrounds by a factor of 3. A further cut on the visible mass associated with the muon vertex would reduce the backgrounds by another factor of 2 to 3 while further reducing the signal by a factor of 85% leading to a sample of ≈ 100 B_S for use in a determination of mixing. These cuts reduce the b->c->μ tagging contamination level to less than 20% of the signal level. These yields, as has been pointed out above, can be significantly increased if the hadronic trigger sample is utilized.

All cuts discussed above are by no means optimized nor is it clear that they are all needed. Further study will certainly indicate other ways to identify the B^0_S and insure proper muon tagging with less loss of events. In fact, each event at the level of the final data sample of a few hundred candidates will be treated to individual inspection so the global analysis scheme outlined above will be optimized on an event by event basis depending on the topology observed.

The B_S mixing would be measured by observing the time dependent decay distributions for the tagged B_S mesons in the final data sample. The decay oscillations should be quite evident, given our vertex resolution, for a reasonable range of values of the mixing parameter x around the Standard Model prediction of ten.

VI.A.3.b B^0_S Observation using the Exclusive Decay B^0_S-> $D^+_S \mu^- \nu$

The semi-inclusive decay mode B^0_S->D^+_S $\mu^-\nu$->$\pi^+K^+K^-\mu^-\nu$ is a prime candidate for observing and measuring the cross section and lifetime of the B^0_S. A preliminary measurement[28] of the inclusive BR(B_S -> D_S μ x) = 8% has been reported. This measurement, which is obtained from B's produced in e^+e^- interactions, assumes a hadronization fraction of 0.2 for the B_S. If we take the vector-to-pseudoscalar decay ratio to be ≈3 and the fraction of the semileptonic rate into either $D_S l\nu$ or $D^*_S l\nu$ to be 54% (similar to B^0_d->D^{*+} $\mu^-\nu$ to B^0_d->D^+ $\mu^-\nu$ and neglecting a 14% contribution from higher excited states[33]), then 16% of the B_S->$D_S\mu x$ branching ratio should be due to the exclusive mode B_S -> D_S μν . This means an overall branching ratio of 1.3% for B_S -> D_S μν. Finally, using a branching ratio of 3.9% for the D^+_S->$\pi^+K^+K^-$ decay (see Table 7), we obtain a composite branching ratio of 4.2×10^{-4} for the chain.

These decays will be found in the 9.8×10^5 1μ triggers on tape. Assuming a hadronization fraction of 14% for B_S, we would expect to have approximately 550 such decays on tape. Based

on a full tracking studies using a complete GEANT Monte Carlo simulation of the P867 spectrometer, we expect to have a 19% acceptance•reconstruction efficiency for the B^0_S->D^+_S $\mu^-\nu$->$\pi^+K^+K^-\mu^-\nu$ resulting in approximately 100 completely reconstructed decays when just considering the single exclusive D^+_S decay into $K^+K^-\pi^-$. Inclusion of all the other $D^{\pm}_S$ decay modes listed in Table 7 would approximately double the size of the sample. For these decays, the B momentum is ambiguous due to the unobserved neutrino. However, since the D_S carries a large fraction of the B_S momentum, one can correct by the appropriate Monte Carlo the visible momentum at the secondary vertex. As discussed in Section IV.A.2, even with incomplete knowledge of the parent B momentum, a sample containing ≈ 50 events will allow a lifetime determination to better than 20%. The size of the sample increases substantially if we include decays of the type B_S->$D^*_S\mu\nu$, where the D* decays into D_S accompanied by an undetected gamma.

We anticipate that the primary source of background will be from B-> $D_S\bar{D}$ +x where $\bar{D}$ -> μ^-+X. The background can be reduced by making a cut on the visible mass at the secondary vertex and requiring a muon p_t higher than the one already applied by the trigger. At this point, a preliminary estimate is that the B_S signal will be retained with an efficiency of 70% or better, while the background will be reduced to less than 10% of the signal.

VI.A.4 $B^{\pm}_u$ Cross Section, Lifetime, BR's and Form Factors

The $B^{\pm}_u$->D^0+x decays where the D^0 decays presents us with an opportunity to measure production cross sections, branching ratios, lifetimes, and form factors because of the relative large branching ratios for b->c decays even in exclusive channels. The identification of the charged and neutral D's forms the heart of these measurements.

VI.A.4.a Cross Section, BR, and Lifetime from the Exclusive Decay $B^{\pm}$->$D^0\pi^{\pm}\pi^+\pi^-$

To demonstrate our ability to measure $B^{\pm}$ cross sections, BR and lifetimes using exclusive modes, we choose as one example the mode $B^{\pm}$->$D^0\pi^+\pi^+\pi^-$which has a definitive vertex topology and is less prone to background contamination from other B decays. This mode has a measured branching ratio[21] of 1.1±0.4% (which we note has an error of order 40%). The "accessible" decays of the daughter D^0's that provide decay chains which can be totally reconstructed and have been consider in this study are listed in Table 7 .

Table 7
Accessible D^0 Decay Modes
(Reference 35)

D^0 Decay Mode	BR
D^0 -> $K^-\pi^+$	3.65±0.21%
D^0 -> $K^-\pi^+\pi^+\pi^-$	7.5±0.5%
Total BR	11.15%

The $B^{\pm}$->$D^0\pi^+\pi^+\pi^-$ decay plus the two D^{*-} decay chains of Table 8 will result in a four prong B decay vertex plus either a two or four prong D decay vertex, will had a composite branching ratio of 1.2×10^{-3}. These events will be part of the 5.8 million B's in the hadronic triggers on tape, approximately 38% of which will be $B^{\pm}$. With an average acceptance times track reconstruction

efficiency times vertexing efficiency for these events determined by a full tracking GEANT Monte Carlo to be approximately 6.9%, we estimate a yield of approximately 180 events in these particular exclusive decay chains available for cross section and lifetime measurements. When other exclusive $B^{\pm}$-> D's chains are considered, we expect to have few hundred completely reconstructed $B^{\pm}$'s available for lifetime and cross section measurements. The statistics should allows us to improve considerably on the present level of branching ratio measurement precision.

VI.A.4.b $B^{\pm}$ Form Factor from $B^{\pm}\to D^0\mu\nu_{\mu}$

The semimuonic exclusive mode $B^+\to\bar{D}^0\mu^+\nu$ can be used to extract from factor information and make measurements of V_{cb}. The $B^+\to\bar{D}^0\mu^+\nu$ branching ratio[21] is 0.8±0.35% if half of the measured $B^+\to\bar{D}^0l^+\nu$ branching ratio is due to muonic decay. If, as in Section VI.A.5.a, we restrict ourselves to the D^0 decay modes of Table 8, we obtain a composite branching ratio from "accessible" decay chains of 8.9×10^{-4}. This channel is part of the 980,000 B->μ events on tape. Allowing that 38% of the these B->μ decays will be due to $B^{\pm}$, we expect approximately 3200 $B^{\pm}\to D^0\mu\nu$ with the $D^0\to K\pi$ or $K\pi\pi\pi$ among them. The composite efficiency for this mode which is part of the 1μ trigger sample when averaged over the different D decays is ≈17.6% resulting in 560 events in the exclusive decay channel for extraction of form factor information.

VI.A.5 B^0_d Cross Section, Lifetime, BR's and Mixing and Form Factors

As in the case of the $B^{\pm}$->D decays, the B^0_d->D+x decays where the D^-_d decays into a recognizable final state provides good opportunities for measurements of production cross sections, branching ratios, lifetimes, form factors and, most particularly, mixing.

VI.A.5.a B^0_d Cross Section, Lifetime and BR from $B^0_d\to D^{*-}\pi^+\pi^+\pi^-$

As one example of our ability to measure B^0d cross sections and lifetimes, we choose the mode $B^0_d\to D^{*-}\pi^+\pi^+\pi^-$. This mode has a measured branching ratio[20] of 1.41±0.34% (approximately 20% errors). The D* decay in to $D^0\pi^+$ with a measured branching ratio[36] of 55±4% followed by the D^0 decays listed in Table 8 in Section VI.A.5 provide decay chains which can be totally reconstructed.

The $B^0_d\to D^{*-}\pi^+\pi^+\pi^-$ decay followed by the $D^*\to D^0\pi^+$ -> two indicated D^0 decays of Table 8 will result in a four prong B decay vertex plus either a two or four prong D decay vertex with a total composite branching ratio of 8.6×10^{-4}. The $B^0_d\to D^{*-}\pi^+\pi^+\pi^-$ decays are part of the 5.8×10^6 B's in the P867 hadronic trigger sample on tape, 38% of which are B^0_d, leading to an estimate of approximately 1900 such decays on tape. The average acceptance times track reconstruction efficiency times vertexing efficiency for these events has been determined by a full tracking GEANT Monte Carlo to be approximately 4.3%, resulting in a yield of approximately 80 events in this particular decay modes available for cross section and lifetime measurements. When different exclusive B^0_d-> decays into D's are considered, we expect to have between one and two hundred completely reconstructed B^0_d's available for lifetime and cross section measurements. There should be negligible backgrounds to this exclusive decay

VI.A.5.b B^0_d Cross Section Lifetime and Mixing Using Inclusive $B^0_d\to D^+_d+x$

The B^0_d mixing can be studied in much the same manner as the B^0_s mixing discussed above. We plan to detect the B^0_d and study its mixing by selecting B^0_d -> D^-_d+x inclusive decays in which the D decays entirely into charged particles or the semi-leptonic final state Kπlν. The D^-_d -> Kππ decays give a particularly obvious signature and are therefore relatively background free. We

tag the particle-antiparticle nature of the B^0_d at production by the muonic decay of the other B in the event.

Table 8
Accessible $D^{\pm}_d$ Decay Modes
(Reference 37)

D^+ Decay Mode	BR
$D^+ \rightarrow K^- \pi^+\pi^-$	8.0±0.8%
$D^+ \rightarrow K^- \pi^+\pi^+\pi^-\pi^+$	0.6±0.15%
$D^+ \rightarrow K\pi l\nu$	7.6±1.6%
Total BR	16.2%

To obtain the inclusive branching ratio for $B^0_d \rightarrow D^-_d+x$, we have used the measurement[20] of the $B_{u,d} \rightarrow D^{\pm}+x$ branching ratio (22.7%) in which the charge of the B is not determined. If we assume that the $B^{\pm}_u$ decays exclusively into D^0_u or D^{*0}_u in distinction to the B^0_d which decays predominately into $D^{\pm}_d$ or $D^{*\pm}_d$, we infer an inclusive branching ratio for $B^0_d \rightarrow D^-_d+x$ of approximately 45%. This branching ratio would be reduced to approximately 30% if we were to assume a 30% probability for the B^0_d to decay into the "wrong sign" D (e.g. the $B^-_u \rightarrow D^0_d e^-$ branching ratio of $1.3\pm0.6\times10^{-2}$ as compared with $B^-_u \rightarrow D^+\pi^-\pi^-$). Using the total "accessible" $D^{\pm}_d$ branching ratio of 16.2% results in a ≈5% composite branching ratio for $B^0_d \rightarrow D^-_d+x$ where the D decays into a recognizable final state. As a subset of the various all-charged decays, the $D^-_d \rightarrow K^-\pi^+\pi^-$ has been considered as a particular clean signature. Once again using a $B^0_d \rightarrow \rightarrow D_d+x \approx$ 30% and the measured branching ratio of 8.0% for the $D^- \rightarrow K^-\pi^+\pi^-$ mode, we obtain an overall branching ratio of 2.4% for this particular chain, almost half of the total branching ratio.

Since we are requiring the muon from the other B decay for the tagging of the B^0_d, the neutral B decays will be included mainly (but not entirely) in the ≈ one million 1μ triggers on tape. Using the 5% composite branching ratios leads to an estimate of 19,000 such decays in the 1μ sample (taking into account the hadronization fraction of B^0d) with topologies which include B vertex at least one charged track plus a charged D and a three or five prong D vertex. The average acceptance times track reconstruction efficiency times vertexing efficiency for these events has been determined by a full tracking GEANT Monte Carlo to be approximately 15%, resulting in 2900 tagged inclusive $B^0_d \rightarrow$charged D decays in which the D_d and the tagging μ are "completely" reconstructed and at least one other charged particle from the other B are is the acceptance.

The backgrounds to these B_d decay modes due to B_s decay will be minor . From the hadronization and branching ratios considerations the $D_s \rightarrow KK\pi$ is less than 10% of the $D_d \rightarrow K\pi\pi$ even without K/π ID. On the other hand, the contamination of the tagging μ by b->c->μ decays will be similar. Assuming the same loss of signal is experienced as in the case of B_s when cuts are done to eliminate the b->c->μ contamination, we estimate that approximately 1000 $B_d \rightarrow D_d$ decays with which to directly observe oscillations and measure mixing. While decay oscillations may be less evident since the B_d tend to decay before they fully mix, the requirement on time resolution is somewhat less than for the B_s which presumably has a faster oscillation. This would be the first direct observation of mixing oscillations in the B^0_d time distributions just as was the case for the B^0_s.

As a final remark, these B^0_d->charged D decays obviously offer an opportunity to measure lifetimes and cross sections with the indirect methods discussed in Section VI.A.1

VI.A.6.c B^0_d Form Factor from B^0_d->$D^{*-}\mu^+\nu$.

We can accumulate enough data in semileptonic B^0_d->$D^{*-}\mu^+\nu$ to study the detailed kinematics of the semileptonic decays b->c decays to extract form factor information and make measurements of V_{cb}. The B^0_d->$D^{*-}\mu^+\nu$ branching ratio[20] is 2.45% making the usual assumption that half of the B^0_d->$D^{*-}l^+\nu$ branching ratio is due to muonic decay. If, as in Section VI.A.6.a, we restrict ourselves to D*(2010) decays to $D^0\pi^\pm$ followed by the decays into $K\pi$ and $K\pi\pi\pi$ of Table 8, we obtain a composite branching ratio from "accessible" decay chains of 1.5×10^{-3} as before. Using the hadronization fraction of 38% we expect to find 5300 such decays in the 1 million B->μ decays on tape. The composite efficiency for this mode which is part of the 1μ trigger sample when averaged over the different D decays is ≈12%. The combination of branching ratios and efficiency results in 640 reconstructed events in this exclusive decay channel for use in a form factor study.

VI.A.7 b->u Transitions and V_{ub} from B^0_d->$\pi^\pm\mu\nu$ and $B^\pm_u$->$\rho^0\mu\nu$

The transition amplitude V_{ub} is a crucial element of the CKM matrix since no CP violation can occur in the standard model if it is equal to zero. The semi-leptonic decays of B mesons into exclusive states containing light mesons (charmless decays) offers the possibility to extract a value for the CKM matrix element V_{ub}. Both ARGUS and CLEO have reported indirect determinations of V_{ub} from the shape of the inclusive leptonic momentum spectrum, but no direct evidence of b->u transitions has yet been observed with the possible exception of two events from the ARGUS experiment. There is a significant discrepancy between the CLEO and ARGUS results for V_{ub}.

As an alternative approach, we plan to use exclusive semi-leptonic modes to determine V_{ub}. We have considered two possible modes of the B->μ semi-muonic exclusive variety, B^0_d->$\pi^\pm\mu\nu$ and $B^\pm_u$->$\rho^0\mu\nu$. The former mode has not yet been observed. The latter has been reported by ARGUS[38] to have a branching fraction of $1.03\pm0.36\pm0.25\times10^{-3}$. However, there is a disagreement on this observation between ARGUS and CLEO since CLEO quotes[39] a upper limit of 0.43×10^{-3} for this mode. We have used 4×10^{-4} in estimating yields of this decay mode. This number is at the low end of the range of theoretical estimates[40] (2.5×10^{-4} to 10×10^{-4}) for the branching ratio.

We expect these decays to be part of the 980,000 event B->1μ trigger sample. Using hadronization fractions of 38% for $B^\pm_u$, we estimate approximately 1430 $B^\pm_u$->$\rho^0\mu\nu$ decays will be on tape. Based on GEANT Monte Carlos, this mode will have ≈30% acceptance•reconstruction efficiency, resulting in approximately 420 reconstructed events with which to extract Vub. Additional cuts must be applied to this sample to reduce charm and beauty backgrounds. The extra criteria applied to our sample of $B^\pm_u$->$\rho^0\mu\nu$ include:

1. Three charged particles are required to originate in a common vertex separated from the primary vertex by 1700 μm in Δz (≈5σ) where Δz is the separation of the primary and secondary vertices parallel to the beam direction.

2. The visible mass of the charged tracks is required to be greater than 2 GeV/c^2. This cut eliminates possible background from charm semi-leptonic decays such as D->K$\pi\mu\nu$ and D->$\rho\mu\nu$.

3. The two non-muon charged particles are required to have opposite sign and an invariant mass consistent with a ρ mass ($\pm$200 MeV/c^2).

We have estimated the effects of these cuts by Monte Carlo studies. Summarizing the estimated yields of events passing these additional criteria, we find

1. Additional Vertexing Criteria	0.86
2. $M_{visible} > 2$ GeV/c^2	0.86
3. ρ mass ($\pm$200 MeV/c^2)	0.92
Overall Additional Efficiency	0.67

leading to a net sample of $B^{\pm}_u$->$\rho^0\mu\nu$ for analysis of approximately 280 events.

The direction of the decaying B for these events is known if the primary and secondary vertices are observed and are measured reasonably well ($\pm$2 mrad on average). Therefore, using four momenta conservation at the secondary vertex for the $B^{\pm}_u$->$\rho^0\mu\nu$ decays (or B^0_d->$\pi\mu\nu$ as the case may be), the missing neutrino momentum can be calculated. There is a two-fold ambiguity in the calculation, but under the hypothesis that the parent particle is a B, each solution can be weighted with the probability (derived from the expected shape of the neutrino momentum spectrum in this semi-leptonic decay) that it is the correct value. In the special case where the minimum mass of the decay products, including the assumed neutrino, equals the mass of the B meson, a unique solution is determined. Thus, to this level the B decay can be said to be completely reconstructed and the proper time (and lifetimes) can be calculated for these decays.

Backgrounds from charm semileptonic decays (such as D->$\rho\mu\nu$) are eliminated by the visible mass cut and the requirement of substantial transverse momentum of the muon. The major backgrounds will come from B decays resulting in three charged prong topologies. Decays of the type B->D where the D decays semileptonically are eliminated by the observation that the two charged partners of the muon have the same sign charge. D decays which result in a final state charged kaon are eliminated by the kinematic cuts outlined above (as well as the Cerenkov particle identification if available). The most serious remaining backgrounds are B -> Dμx decays where the D decays into a neutral kaon and one or more pions. A few such decay modes with the potential largest composite branching ratios are given in Table 9 below.

Table 9
Backgrounds to $B^{\pm}_u$->$\rho^0\mu\nu$

Background Decays	BR	Combined BR
$B^{\pm}$->$D^0\,\mu^{\pm}\,\nu$	0.016	
D^0->$K^0\pi^-\pi^+$	0.054	9×10^{-4}
D^0->$K^0\rho$	0.006	1×10^{-4}
B^+ -> D^- ->$\pi^+\mu^+\nu$	Br not Known	-
D^- -> $K^0\pi^-$	0.026	

Since these decays have similar topologies and signatures to the $B^{\pm}_u \to \rho^0 \mu \nu$, a comparison of the relative branching ratios for the combined decays to that of the $B^{\pm}_u \to \rho^0 \mu \nu$ decay (4×10^{-4}) gives the first level of comparison of the background rates of the other B decays. The kinematic cuts described above reduce these backgrounds by a factor of three (relative to the signal) in the worst case ($B^+ \to D^- \pi^+ \mu^+ \nu$) and much more in general. Many of these decays can be distinguished by observation of the tertiary D decay vertex. For those events where the D vertex is not separable, the criterion that the three charged tracks are from a common vertex gives a large rejection.

The extraction of V_{ub} from the data must be done in a model dependent way. An unambiguous measurement of V_{ub} requires a measurement of the form factors and angular distribution of the $B^{\pm}_u \to \rho^0 \mu \nu$ decay . Even with the small number of events obtained, theoretical uncertainties will still dominate the calculation of Vub. These uncertainties are at the level of a factor of four[22] due to uncertainties in the B form factors.

Finally, other decays such as $B^0_d \to \pi^{\pm} \mu \nu$ and $B^0_d \to a^+ \pi^-$ can also be used to determine V_{ub}. Since $B^0_d \to \pi^{\pm} \mu \nu$ is a two prong topology, it is more prone to backgrounds (such as $B^0 \to D^+ \mu \nu \to K^0 \pi^+ \mu \nu$ with a composite branching ratio of 5×10^{-4}) and it has a lower net yield. Assuming a branching ratio of 10^{-4}, and using cuts similar to the ones described for $B^{\pm}_u \to \rho^0 \mu \nu$ we expect to obtain a small sample of events (≈70). However, in view of the scarcity of experimentally observed b->u decays, this is still worthwhile.

Equally, interesting, would be the observation of $B^0_d \to a^+ \pi^-$ (current limit $< 6 \times 10^{-4}$), an important mode for future CP violation studies as well as a b->u transition. In this case, we would find this inclusive mode in the 5.8 million B->hadronic decays on tape. With a branching ratio of 10^{-4} and a hadronization fraction of 38%, we would expect 220 events on tape. The acceptance times reconstruction efficiency for this mode is estimated to be ≈17% so we might hope to obtain ≈40 reconstructed events of this type in the P867 run.

VI.A.8. Λ_b Baryon Cross Section and Lifetime

We will search for B baryon production in the single muon inclusive triggers. We give a single specific example of a baryon decay that we could hope to see. We plan to search for the Λ_b reported by ALEPH[41] and by OPAL[42] in the mode $\Lambda_b \to \Lambda^0 \mu \nu + X^0$ where the $\Lambda^0 \to p \pi^-$ and more recently by ALEPH[43] in the mode

$$\Lambda_b \to \Lambda_c \mu \nu X^0$$
$$\longrightarrow p K^- \pi^+$$

We do not consider other possible decays of the Λ_b's other than the $\Lambda_b \to \Lambda_c \mu \nu X^0$ mode, although we will search for them and they will contribute to our ability to make Λ_b measurements.

The overall branching ratio for the second decay sequence is 0.48% according to the ALEPH experiment. This ratio includes the branching ratio for $\Lambda_c \to pK\pi$. We expect to find this decay sequence in our 980,000 1μ triggers. Assuming a hadronization fraction of 10% in 800 GeV/c interactions, we would expect to find 4800 $\Lambda_b \to \Lambda_c \mu \nu X^0 \to pK\pi\mu\nu X^0$ decay sequences on tape if the inclusive branching ratio for $\Lambda_b \to \mu$ is approximately 10% like the B mesons.

The $\Lambda_b \to \Lambda_c \mu \nu$ followed by the simple three prong decay $\Lambda_c \to pK^-\pi^+$ decay is "self triggered" with a reconstruction efficiency • acceptance estimated to be approximately 19%. This results in an overall yield of reconstructed decays of this sort of approximately 910 events.

These events must be subjected to various cuts to eliminate backgrounds. If we consider the topology, we require the reconstructed $pK^-\pi^+$ to be at the proper mass and to intersect the muon track somewhere between the primary vertex and the Λ_c vertex itself. The Λ_c vertex does not have to be separated from the muon track so we do not apply a tertiary vertex separation criteria. However, in order to reduce combinatorial backgrounds, we will require the Λ_c vertex (or its composite with the muon) to be well separated from the primary vertex. Since this is a tertiary decay vertex, it will have the combination of both Λ_b and Λ_c lifetimes so we expect to lose less than the expected 10% of the events if we apply a $\Delta z \geq 5\sigma \approx 1700$ cut (assuming the Λ_b life time is comparable to the B meson lifetimes).

A background will be B->μ +X semi-muonic decays of one sort or another. For example, the decays $B\to D^+_{d(s)}\mu\nu \to K\pi\ (K)\pi\mu\nu$ decay sequence has the same topology. However, although it is not absolutely necessary, with particle ID we can separate these decays from $\Lambda_b \to \Lambda_c\mu\nu$ on the basis of reconstructed mass by properly identifying the protons and the K's in the respective decays. Since the Cerenkov counter can only separate protons from K's above 12 GeV/c, we will only be able to positively identify that fraction of the total number of $\Lambda_c \to pK^-\pi^+$ decays in which $E_{proton}>12$ GeV/c. We expect a second loss of events due to the particle ID inefficiency which will be suffered for two of the three particles in order to properly accomplish π/K/p ID for the pKπ final state. Combining these three loss factors,

1. Vertex cut	.85
2. Proton Energy	.60
3. K/π/p id	.77
Total	.39

we expect to obtain 360 identified $\Lambda_b \to \Lambda_c\mu\nu$ followed by $\Lambda_c \to pK^-\pi^+$ decays. This is very adequate for cross section, lifetime and relative branching ratios (provided other Λ_b modes such as those in Table IV.7 can be identified) determinations . For the semi-exclusive decays with only a missing neutrino, $\beta\gamma$ can be reasonably calculated using the visible energy and mass. As a final comment, it is worthwhile to note that the charge of the muon is correlated with the charge of the Λ_c, i.e. if the muon is negative the Λ_c must have positive charge and decay eventually into a proton which will typically have the largest momentum of the decay products. Backgrounds can be suppressed to some extent , therefore, without recourse to particle id by demanding that the charge of the highest momentum particle have the correct sign correlation with respect to the muon. This tends to suppress the topologically similar background from B->D+x->K$\pi\pi$ +x since the K charge has the opposite correlation with the muon charge as the proton form the $\Lambda_b \to \Lambda_c \to p$ sequence. The technique of demanding proper charge correlations is generally useful (modulo mixing and b->c contamination) and can be applied in several other studies we are proposing. The effectiveness of this background suppression strategy is under study on a case by case basis.

Finally, we can search for other Λ_b exclusive modes such as $\Lambda_b \to \Psi pK$. This mode is thought to have a composite branching ratio of $\approx 5\times10^{-5}$ for the $\mu\mu$pKπ final state and has a quite obvious signature with good trigger qualities. We would expect some 30 events on tape and 5->10 golden reconstructed events in such a mode. Other all hadronic modes could contribute significantly to the final Λ_b sample.

VI.B Charm Physics

Competitive open and hidden charm physics opportunities are available to P867 because of the 1μ and 2μ triggers. While P867 is not competitive with an dedicated charm experiment for charm decaying into hadronic final states, the muon triggers give us special sensitivity for muonic decays. The large 170 million single D->μ sample collected by our single muon trigger should allow high statistics studies of D form factors. In addition, the dimuon trigger sample contains 170,000 J/Ψ->μμ decays with which to continue the study of charmonium physics begun in E705 with higher statistics.

VI.B.1 Open Charm Physics

In this section, we briefly address the issue of yields of semimuonic channels accessible to P867 without discussion of the extraction of physics parameters. Studies are underway to determine how to best perform a form factor analysis given the large numbers of events available.

VI.B.1.a $D^{\pm}$ and D^0 Form Factor from $D^+ \to K^{*0}\mu\nu$ and $D^0 \to K^-\mu\nu$

The $D^{\pm} \to K^{*0}\mu\nu$, with a branching ratio[15] of 1.8% inclusive of the K^{*0} decaying to $K^-\pi^+$, is a definitive signature. The 170 million D->μ triggers should, estimating the relative production of charge D to total D be 35%[14], include approximately 1.1×10^6 such decays (neglecting $D^{\pm}_s$ production). We estimate from Monte Carlo studies that our reconstruction efficiency•acceptance for this self trigger mode is ≈29%, yielding approximately 3.1×10^5 of these decays reconstructed before cuts to eliminate backgrounds and purify the sample. Anticipated cuts on vertex separation, Kπ mass, the requirement that the decay occur in the decay volume, and various kinematic cuts to insure identity of the mode will produce a relatively background free sample with at worst a 30% efficiency. Therefore, we should retain approximately 94 thousand such events in our physics sample.

The $D^0 \to K^-\mu\nu$ has a branching ratio[15] of 2.9%. The 170 million D->μ triggers should be 65%[14] D^0 and, therefore, should include approximately 3.2×10^6 such decays. We estimate from Monte Carlo studies that our reconstruction efficiency•acceptance for this self trigger mode is ≈46%, yielding approximately 1.5×10^6 reconstructed decays. With additional (more restrictive than the $D^{\pm}$ cuts because of the less definitive signature) cuts, we would expect more than 150 thousand such decays for physics analysis.

For comparison, we note that E791 projects a final data sample of 2,500 $D^{\pm} \to K^{*0}\mu\nu$ decays and ≈ 1000 $D^0 \to K^{\pm}\mu\nu$ decays. The expectation for the new P829 experiment in the Tagged Photon Laboratory is to increase this sample to 50K and 20K events respectively.

VI.B.1.b D_s Form Factor from $D^{\pm}_s \to \phi\mu\nu$

The $D^{\pm}_s \to \phi\mu\nu$ (with the $\phi \to K^+K^-$) has a composite branching ratio[27] of 0.8%. If we assume that the $D^{\pm}_s$ production in 800 GeV/c interactions is approximately 18% of the charged D production as in π^-N at 230 GeV/c[55], we expect 2.5×10^5 such decays in our 1μ triggers. The reconstruction efficiency for the self trigger events is ≈29% leading to an initial analysis data sample of 72K decays before final cuts. The additional cuts on vertex separation, decay region among others should retain 30% of the events, yield a final sample for physics of 22K decays.

VI.B.1.c Search for $D^0 \to \mu\mu$ and $D^{\pm} \to \pi\mu\mu$

The muonic D decay modes $D^{\pm} \to \pi^{\pm}\mu\mu$ and $D^0 \to \mu\mu$ present opportunities to search for flavor changing neutral weak currents (FCNC) in the heavy quark decay. We have conducted such

a search using to date approximately a quarter of the E771 dimuon trigger sample to establish a preliminary upper limit[44] of 1.1×10^{-5} for the $D^0 \rightarrow \mu\mu$. We expect to be able to extend this and a comparable search for $D^{\pm} \rightarrow \pi^{\pm}\mu\mu$ to much lower limits in P867 than heretofore possible.

As shown in Section III we expect to produce approximately 8.2×10^{10} D's. We expect from measurements of the inclusive D cross sections[14] that the neutral D's would be approximately 65% of the total D production. If $D^0 \rightarrow \mu\mu$ were present with a branching ratios of 5×10^{-8}, given trigger efficiency for $D \rightarrow \mu\mu$ of ≈1.5%, we would expect ≈60 events in the dimuon trigger sample. With an estimated acceptance•reconstruction efficiency of 50% for $D^0 \rightarrow \mu\mu$, we would expect to see peaks of 30 events in the $\mu\mu$ mass spectra at the D^0 mass. Additional cuts such as requiring a secondary vertex in the decay region between the M_j radiators and tight vertex requirements to assure the identity of these events may be required to reduce backgrounds, giving us a handful of $D^0 \rightarrow \mu\mu$ events. Following the same steps for the $D^{\pm} \rightarrow \pi^{\pm}\mu\mu$ with 35% of the D's charged and 32% acceptance• reconstruction efficiency, we would get approximately 15 events. This level of signal would probably be adequate to insure observation of a signal since we expect backgrounds to be negligible.

We have not yet studied extensively the backgrounds that may be present at this level. Because of the requirement of $\mu\mu$ and $\pi\mu\mu$ secondary vertices of the right charge signature reconstructing to a D mass, these backgrounds would have to be rather exotic pathologies of the reconstruction programs or arise from B or C decays themselves. We are investigating potential sources such as $B \rightarrow \mu + D$ + all neutrals where the D decays very promptly into μ plus all neutrals or one charged pion. Such a decay sequence would produce a two or three prong topologies, $\mu\mu$ or $\pi\mu\mu$, which might have a reconstructed mass in the 1.86-1.87 GeV/c^2 region.

VI.B.2 Hidden Charm Final States

Since P867 will reconstruct approximately 85,000 $J/\Psi \rightarrow \mu\mu$ in pN interactions as compared to Fermilab Experiment E705[46] in which we reconstructed a total of 24,440 $J/\Psi \rightarrow \mu\mu$ decays with 12,470, 5560 and 6090 coming from π^-N, π^+N and pN interactions respectively, the 1995-96 J/Ψ and Ψ' data should permit a much more detailed investigation of several interesting physics topics, in particular for proton interactions.

We show in Table 8 the yields of the various interesting hidden charm final states expected in the P867 run extrapolating the numbers of events for the $^1P_1$ and $^3D_2$ candidates, the Ψ' and various χ states reconstructed in E705 in the 300 GeV/c^2 data (See Section VI.B.1 and VI.B.2). Since each of the final states in question is associated with a $J/\Psi \rightarrow \mu\mu$ decay, this method takes into account A dependence and increase of cross sections due to increased beam energy, provided the ratio of production of the various states to overall J/Ψ production does not change. In making this extrapolation, we have assumed that the ratio of production of other hidden charm states to J/Ψ production is the same for 800 GeV/c protons as it was for the 300 GeV/c beams used in E705, neglecting the differences between $\pi^{\pm}$ and proton production of the various states for purposes of this crude scaling. We point out that we did observe differences (for example, χ_1 production in protons vs. χ_1 production with $\pi^{\pm}$). In addition, for some states (for example, the 3.837 GeV/c^2 observation), we were not been able to measure production with protons in the E705 due to lack of statistics. Finally, we have not allowed for better efficiencies, resolutions and rejection of backgrounds that we expect in P867 in making these estimates.

The expected P867 yields with these assumptions and caveats are:

Table 8
Yields of Reconstructed Hidden Charm States

	E705 Yields	P867 Yields
$J/\Psi \to \mu\mu$	2.4×10^4*	8.5×10^4
3.837 GeV/$c^2 \to J/\Psi\pi^+\pi^- \to \mu\mu\pi\pi$	74±22**	5.1×10^2
3.525 GeV/$c^2 \to J/\Psi\pi^0 \to \mu\mu\gamma\gamma$	42±17***	1.6×10^2
$\Psi' \to \mu\mu$	540±48	2.0×10^3
$\Psi' \to J/\Psi\pi^+\pi^- \to \mu\mu\pi^+\pi^-$	68±16**	4.7×10^3
$\chi \to J/\Psi\gamma \to \mu\mu\gamma$	1140±85***	4.1×10^3

*Sum of $\pi^\pm$ and proton beam data.
**Signal from π^- beam data
***Signal from sum of all beam types

VI.B.2.a Measurements of Aspects of J/Ψ,Ψ', and χ Production and Decay

As discussed in Appendix B and Ref. 2 and 46, we performed measurements of several aspects of J/Ψ,Ψ', and χ production and decay in Fermilab Experiment E705 . We have scaled up from these measurements, assuming that the relative ratio of Ψ' and χ production to J/Ψ production is the same as in 300 GeV/c interactions. We have ignored the P867 improvements in track reconstruction efficiencies in making these estimates. It is obvious from 8 that a great deal more statistics for these states can be accumulated in P867.

The greater statistics will allow us to perform studies which were limited by the size of the data sample in E705. In addition, we will be making measurements of all facets of J/Ψ,Ψ', and χ production in 800 GeV/c pN interactions, a different energy regime. Among these studies are searches for other "new" states which decay into either Ψ' or χ. We will also be able to be more selective in choosing data samples for our χ studies, given the larger statistics. Our E705 photon data indicates that selection of higher quality, better resolution photons (those of higher energy or which do not overlap with other photons in the event) together with the better resolution expected in the electromagnetic calorimeter due to improvements in the ADC system[47] can improve the $\gamma\Psi$ mass resolution from 30 MeV/c^2 to better than 20 MeV/c^2. These factors will allow a better separation of χ_1 to χ_2 and a better determination of the χ_1 to χ_2 ratio for proton induced processes, a quantity which still remains poorly determined.

The greater statistics and better photon resolution will also permit measurements of the $d\sigma/dx$, $d\sigma/dp_t$ and the decay angular distributions for the individual χ states. In particular, the angular distribution of the photon[48] with respect to the beam direction in the center of mass of the χ is sensitive to the details of the processes that can contribute to χ production.

VI.B.2.b Confirmation of Charmonium States/Searches for Hidden Charm States

Of particular interest is the tentative low statistics observations[2,45] of the $^1P_1$ state of charmonium via its decay into $J/\Psi\pi^0$. In addition, we have observed in E705 a possible new charmonium state[2], the $^3D_2$ in the decay mode $\Psi\pi^+\pi^-$. The level of the 3.827 GeV/c^2 enhancement ($^3D_2$) seen in the π^- data was 74±22 events with a signal to background ratio of approximately 1/3. The level of the $^1P_1$ was 42±17 summed over all beam types. Scaling up by the ratio of the number of reconstructed $J/\Psi \to \mu\mu$ expected in P867 to the number of reconstructed $J/\Psi \to \mu\mu$ in E705, we obtain the yields of the enhancements shown in Table 8.

In this process, we have, once again, assumed that the yield of the enhancements and the backgrounds to those enhancements will be the same as was observed in E705 in 300 GeV/c $\pi^{\pm}$ and pN interactions. No allowance has been made for the expected improvement in the reconstruction efficiencies for the additional charged pions (as in the case of $^3D_2$ decay into $J/\Psi\pi^+\pi^-$) or the improvement in photon resolution (which is critical to the $^1P_1$ measurement).

Finally, the higher level of statistics gives us the chance to look for other charmonium states that have not to date been observed. In addition, more exotic phenomena such as four quarks states can be searched for. With these statistics, we will have the opportunity to apply tests which may distinguish between such hypotheses and mundane charmonium explanations for any state observed (including the 3.827 and 3.525 GeV/c^2 objects).

VII. Summary

We propose in P867 to continue the work started in E771 and E705 to study beauty and charm phenomena with a more powerful set of trigger and DA. The numbers of B and C decays that can be recovered for the various physics objectives are very competitive with the expected from other types of beauty and charm physics experiments.

We expect to make measurements of the B hadroproduction cross sections at 800 GeV/c to better than 5% and measurements of the charged and neutral lifetimes to approximately 5%. We will measure $B^{\pm}_u$, B^0_d, B^0_s cross sections and lifetimes, some exclusive B branching ratios and determine hadronization fractions for the three meson species in 800 GeV/c pN interactions. We study the mixing of neutral B's and with specific strategies attempt an individual determination of B_s and B_d mixing, We will make a measurement of V_{ub} via the exclusive decay modes, B^0_d->$\pi^{\pm}\mu\nu$ and $B^{\pm}_u$->$\rho^0\mu\nu$. Finally, we plan to measure the Λ^0_b production and lifetimes. We expect to accumulate reconstructed data samples for these studies ranging from the level of a few hundred thousand inclusive B->μ, few thousand B->J/Ψ->$\mu\mu$ inclusive decays down to several tens of reconstructed $B^{\pm}_u$->$\rho^0\mu\nu$ decays.

This experiment also has a considerable sensitivity for open charm decays, especially in the modes which result in a muon in the final states. Modes like D^+->$K^{*0}\mu\nu$ and D^0->$K^-\mu\nu$ will be used to determine the form factors of the charged and neutral D. In addition, we plan to study the D_S via the D^+_s->$\phi\mu\nu$ decays. Finally, we will continue the search begun in E771 for FCNC currents by searching for D->$\mu\mu$ and D->$\pi\mu\mu$. We expect to lower the upper limit on the D->$\mu\mu$ branching ratio from 1.1×10^{-5} measured to date in E771 by approximately two orders of magnitude.

We also expect to accumulate a large number of J/Ψ->$\mu\mu$ decays to continue our studies of charmonium states decaying into J/Ψ + photons or pions. As a measure of our sensitivity to such states, we estimate our reconstructed J/Ψ->$\mu\mu$ sample to be of order of 85,000, leading to statistics for the various charmonium states to be studied a factor of ≈4 to 8 greater than previously obtained in E705.

The upgrades required to accomplish this experiment, full instrumentation of the silicon detector, improvements to the existing muon detector and implementation of new triggers are modest both in effort required to implement and cost. The addition of a Cerenkov counter which is discussed in the proposal, while desirable, is not essential for much of the P867 physics.

In conclusion, we have a wealth of opportunity in P867 to collect significant charm and beauty data samples in P867. The beauty and charm data that we can take in the next fixed target run would represent a significant increment to the world data that can be accumulated before the end of the decade.

References

[1] J. Peoples, December 14, 1991 Letter; B. Cox, October 1, 1990 Letter; T. Yamanouchi, October 15, 1990 Letter; B. Cox, October 29, 1990 Letter.

[2] L. Antoniazzi et al., E705 Collaboration, "A Search for Hidden Charm Resonance States Decaying into J/Ψ or Ψ' Plus Pions", Fermilab-Pub-92/265E, submitted to Phys. Rev. D.

[3] L. Antoniazzi et al., E705 Collaboration, Phys. Rev. Lett. **70**, 383(1993); L. Antoniazzi et al., E705 Collaboration, "Production of χ States via 300 GeV/c Proton and Interactions on a Lithium Target", Fermilab Pub-93/083E, submitted to Phys. Rev. Lett..

[4] A. Carroll et al., Phys. Lettr. **80B**, 319(179).

[5] C. Brown, E789 operating conditions and experiences, private communication.

[6] R. Santonico et al., NIM **187**, 337(1981); R. Santonico et al., NIM **A263**, 20(1988); M. Bertino et al., NIM **A283**,654(1989). **29**

[7] S. Conetti, Proceedings of the First Annual Conference on Electronics for Future Colliders, LeCroy Corp., Chestnut Hill, N.Y., 207(May, 1991); M. Dell'Orso and L. Ristori, NIM **A278**, 436(1989). **31**

[8] Fermilab Proposal P829, (October, 1993).

[9] A.M.Halling and S. Kwan, NIM **A333**, 324(1993).

[10] E. Berger, "Heavy Flavor Production", QCD Hard Hadronic Processes, NATO ASI Series B: Physics Vol. 197, 501(1987).

[11] "Review of Particle Properties", Phys. Rev. **D45**, VII.144, (1992).

[12] "Review of Particle Properties", Phys. Rev. **D45**, VII.145, (1992).

[13] D. Coffman et al., "A Direct Measurement of the J/Ψ Leptonic Branching Fraction", SLAC-PUB-5992, (1991).

[14] M.Aguilav-Benitez et al. LEBC-EMS, Phys. Lett 189B, 476(1987).

[15] "Review of Particle Properties", Phys. Rev. **D45**, VII.116, (1992); "Review of Particle Properties", Phys. Rev. **D45**, VII.125, (1992).

[16] L. Lyons, Progress in Particle Physics **7**, 169(1981).

[17] F. Abe et al., Phys. Rev. Lett. 71, 3421(1993); LEP lifetime measurements reference

[18] M. Binkley et al., E537 Collaboration, "Ψ Production in pN and $\bar{}$ N Interactions at 125 GeV/c and a Determination of the Gluon Structure Functions of the $\bar{p}$ and the $\bar{}$, FERMILAB-Pub-90/63-E, accepted for publication in Phys. Rev D.

[19] K. Abe et al., Physical Review D 33,1(1986).

[20] "Review of Particle Properties", Phys. Rev. **D45**, VII.153, (1992).

[21] "Review of Particle Properties", Phys. Rev. **D45**, VII.144, (1992).

[22] N. Isgur, private communication (Aug., 1992).

[23] "Review of Particle Properties", Phys. Rev. **D45**, VII.23, (1992).

[24] Phys. Lett. **B276**, 379(1992).

[25] Phys. Lett. **B252**, 703(1990).

[26] Phys. Lett. **B262**, 171(1991).

[27] "Review of Particle Properties", Phys. Rev. **D45**, VII.138, (1992).

[28] V. Sharma, "Evidence for B_S Meson and Lifetimes of B_S and Λ_b at LEP", XXVI International Conference on High Energy Physics, Dallas,TX, (1992).

[29] DELPHI Collaboration, "Evidence for B^0_S Meson Production in Z_0 Decays", XXVI International Conference on High Energy Physics, Dallas TX (1992).

[30] D. Bartlett et al., NIM **A260**, 55(1987);

[31] Tagged Photon Spectrometer Collaboration, Phys. Rev. Lett. **58**, 1818(1987).
[32] Frabatti et al., E683 Collaboration, FERMILAB-Pub-90/258-E.
[33] K. Berkelman and S. Stone, Ann. Rev. Nucl. Part. Sci., Vol **41**, 1(1991).
[34] A. Ali and D. London, DESY 92-075 (1992).
[35] "Review of Particle Properties", Phys. Rev. **D45**, VII.125, (1992).
[36] "Review of Particle Properties", Phys. Rev. **D45**, VII.134, (1992).
[37] "Review of Particle Properties", Phys. Rev. **D45**, VII.116, (1992).
[38] Danilov, Proceedings of the Joint International Lepton-Photon Symposium and Europhysics Conference of the High Energy Physics, Vol 2, 333(1991).
[39] P. Drell, "Weak Decays, Rare Decays, Mixing and CP Violation", XXVI International Conference on High Energy Physics, Dallas, TX, (1992).
[40] N. Isgur, D. Scora, B. Grinstein and M.B. Wise, Phys. Rev. Letters 56, 298(1986); M. Wirbel, B. Stech, and M. Bauer, Z. Phys. C29, 637(1988); J.G. Korner and G.A. Schuler, Z. Phys, C38, 511(1988); J.M. Cline and W.E. Palmer, DESY 89-429(1989).
[41] ALEPH Collaboration, Phys. Lettr. B **278**, 209(1992).
[42] OPAL Collaboration, Phys. Lettr. B **281**, 394(1992).
[43] ALEPH Collaboration, "Observation of the Semileptonic Decays of B_S and Λ_b Hadrons at B LEP", CERN-PPE/92-73, (May,1992), submitted to Phys. Lettrs. B.
[44] G. Mo, "Search for Flavor Changing Neutral Current Decay D^0-> + - Produced in 800 GeV/c Proton-Si Interactions", Doctoral thesis, University of Houston, (December, 1993).
[45] T.A. Armstrong et al., E760 Collaboration, Phys. Rev. Lett **69**, 2337(1992).
[46] L. Antoniazzi et al., E705 Collaboration, Phys. Rev. **D46**, 4829(1992).
[47] S. Delchamps et al., "Precision Charge Sensitive Amplification and Digitization System for a Scintillating and Lead Glass Array", IEEE Nuclear Science Symposium, (Nov, 1988).
[49] B.L. Ioffe, Phys. Rev. Lett. **39**, 1589(1977)
[50] A. McManus et al., "Performance of a Silicon Microstrip Detector in A Very High Rate Environment", Proceedings of the 1991 IEEE Nuclear Science Symposium and Medical Imaging Conference, Vol. 1, 298(Nov. 1991), to be published in IEEE Transactions on Nuclear Science; D. Christian et al., "Status of the Fermilab Designed E771 Silicon Strip Readout System", FERMILAB Report (April-June, 1991); C. Swoboda et al., "A High-Rate FASTBUS Silicon Strip Readout System" , IEEE NS 37, No. 2; T. Zimmerman et al. "A High Speed, Low Noise ASIC Preamplifier for Silicon Strip Detectors", Proceedings of the 1989 IEEE Nuclear Science Symposium.
[51] A. McManus et al., "Effects of High Energy Protons on the E771 Silicon Microstrip Detector", Proceedings of the International Conference on the Effects of Radiation Damage on Scintillators and Detectors, Tallahassee, FA (May, 1992).
[52] B. Cox et al., " A Measurement of the Response of an SCG1-C Scintillation Glass Shower Detector to 2 GeV to 17.5 GeV Positrons", NIM **219**, 487(1984); B. Cox et al., " High Energy Electromagnetic Shower Position Measurement by a Fine Grained Scintillation Hodoscope", NIM **219**, 487(1984); B. Cox et al., "A Measurement of the Response of an SCG1-C Scintillation Glass Array to 4 GeV to 14 GeV Pions", NIM **A238**, 321(1985); D. Wagoner et al., "A Measurement of the Energy Resolution and Related Properties of an SCG1-C Scintillation Glass Shower Counter Array for 1 GeV to 25 GeV Positrons", NIM **A238**, 315(1985); C.M. Jenkins et al., "Results from the E705 Electromagnetic Shower Position Detector", IEEE Nuclear Science Symposium, Nov 9-11, 1988; R.Rameika et al.,

"Measurement of Electromagnetic Shower Position and Size with a Saturated Avalanche Tube Hodoscope and a Fine Grained Scintillator Hodoscope", NIM A242, 215(1986); L. Spiegel et al., "Performance of a Lead Radiator, Gas Tube Calorimeter", IEEE Nuclear Science Symposium, Nov 9-11, 1988; L. Antoniazzi et al., "The Experiment 705 Electromagnetic Shower Calorimeter", accepted for publication by NIM.

[53] K.S. Nelson, "Design Calculations for the E771 RICH", UVa Internal Memo (Jan. 92).

[54] M. P. Maia et al., " A Phototube RICH Detector", FERMI-PUB-92/155.

[55] S.Kwan et al., Z. Phys. C49, 555(1991).

Appendix A

The 1991 E771 Run

In our 1991 run, we successfully implemented and tested our muon trigger system and determined the various efficiencies of both triggers and detectors. In addition, in spite of the late and partial delivery of our silicon detector electronics[50], we managed to accumulate 127 million dimuon triggers and 62 million single muon triggers in approximately three weeks of operation in December of 1991. We have developed the analysis scheme (which we plan to follow in P867) and begun bulk processing of our 1991 data. We present in this section and the following appendices preliminary studies of portions of the data processed so far. The data samples used do not exceed 5% of the 1991 data sample for any given study.

Based on the dimuon data accumulated, we have been able to perform the "meaningful test" (J. Peoples, December 14, 1991 Letter) suggested by the Laboratory and Fermilab PAC (B. Cox, October 1, 1990 Letter; T. Yamanouchi, October 15, 1990 Letter; B. Cox, October 29, 1990 Letter) which was intended to prepare for a significant 1994/95 data taking run. We have used the small portion of our data thus far analyzed to investigate the technical issues concerning performance of the experiment and feel, with some confidence, that we can extrapolate to the performance we can achieve in a 1995 P867 run.. The performance of the two critical detector components, the silicon detector and the muon detector/trigger system have been studied. The silicon vertex detector 1991 performance is discussed in this appendix along with the extrapolation to P867. The completely instrumented P867 silicon configuration is presented in Appendix C. The 1991 performance of the muon trigger system has been evaluated in some detail and is presented in Appendix D along with the expected improved P867 configuration. Finally we have begun to extract physics from the J/Ψ's in our data and have begun to extract our first B events. We show some of our results to date in this appendix.

In Fig. A.1.a below we show the dimuon spectrum from a small fraction of the 1991 data. A clear J/Ψ signal (resolution of 45 MeV/c^2; no silicon information has been used in track formation) is seen with a small background estimated to be less than 10% of the signal. As seen in Fig. A1, clear J/Ψ and Ψ'->μμ signals are observed and we have determined the cross section for production of both resonances. from this data.

Using the 1342±42±140 J/Ψ->μμ and 54±12±5 Ψ'->μμ of Fig. A1a and the pertinent 1991 trigger and reconstruction efficiencies as discussed in Section III of the proposal, we obtain J/Ψ and Ψ' cross sections of 339±10±74 nb and 72±16±16 nb per nucleon respectively for all x_f. To scale from the Si cross section to the nucleon cross section, we have used an A dependence of $A^{0.92}$. The observed ratio of Ψ'->μμ to J/Ψ->μμ decays is 2.74±0.61±0.61%. We also show in Fig. A.1.b the dN/dx_f and $p_t^{-1} \cdot dN/dp_t$ differential distributions for a portion of our J/Ψ sample. The distributions of Fig. A.1.b are not yet corrected for acceptances but it is obvious that the 800 GeV/c beam momentum enhances our ability to see the backward hemisphere of the J/Ψ production.

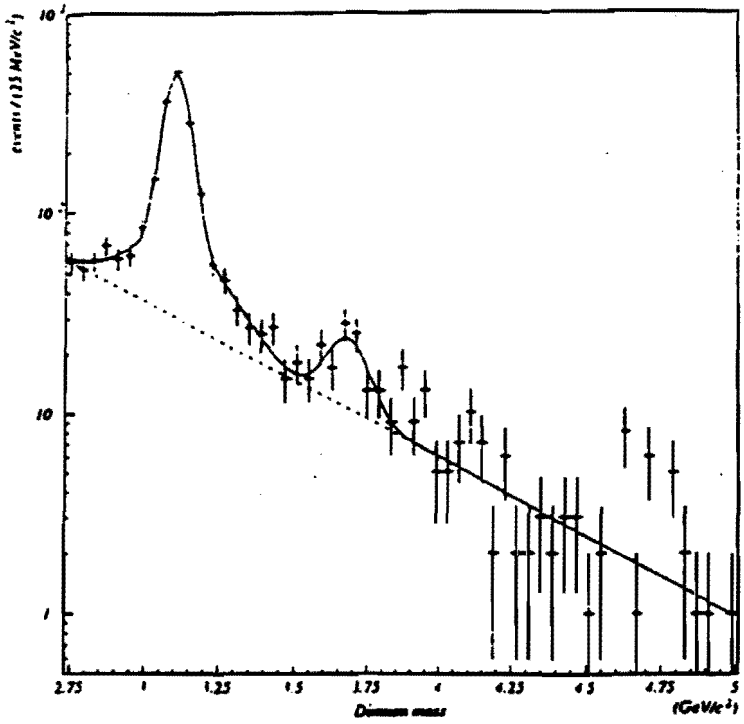

Fig. A.1.a
Dimuon Mass Spectrum From < 3% of the 1991 E771 Data

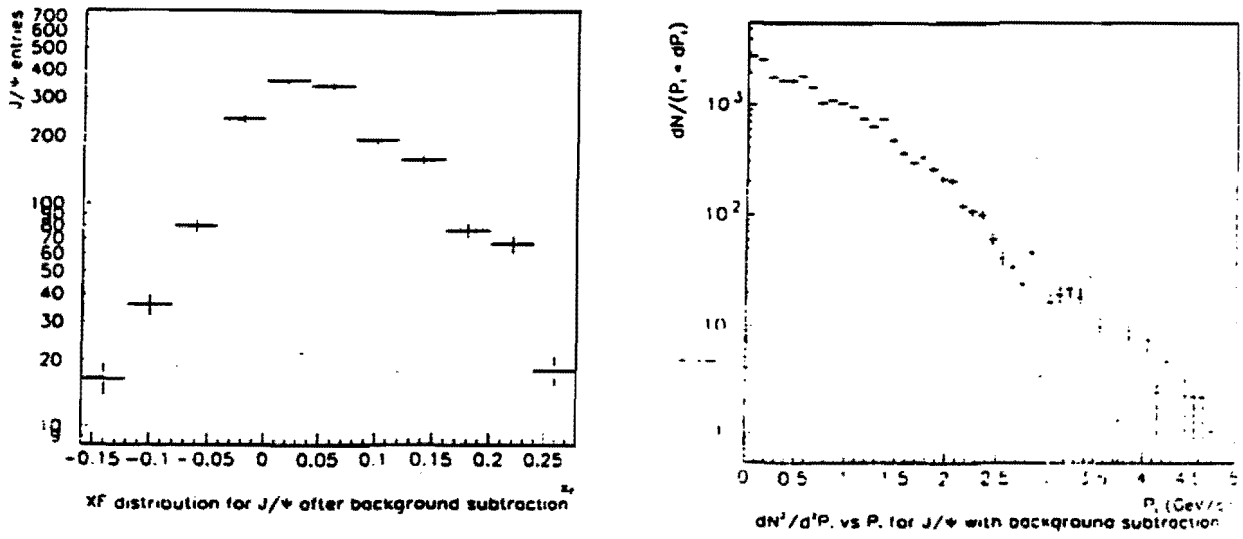

Fig. A.1.b
a) dN/dx_f b) $p_t^{-1} \cdot dN/dp_t$

To compare our preliminary results for J/Ψ cross section with other experiments, we have parameterized the energy dependence of the existing world data for pN interactions in the form of Lyons (Ref. 7). Since the original Lyons parameterization of pN data is over ten years old much new data has been accumulated since it was generated. We show in Fig. A2 below the complete data for pN interactions.

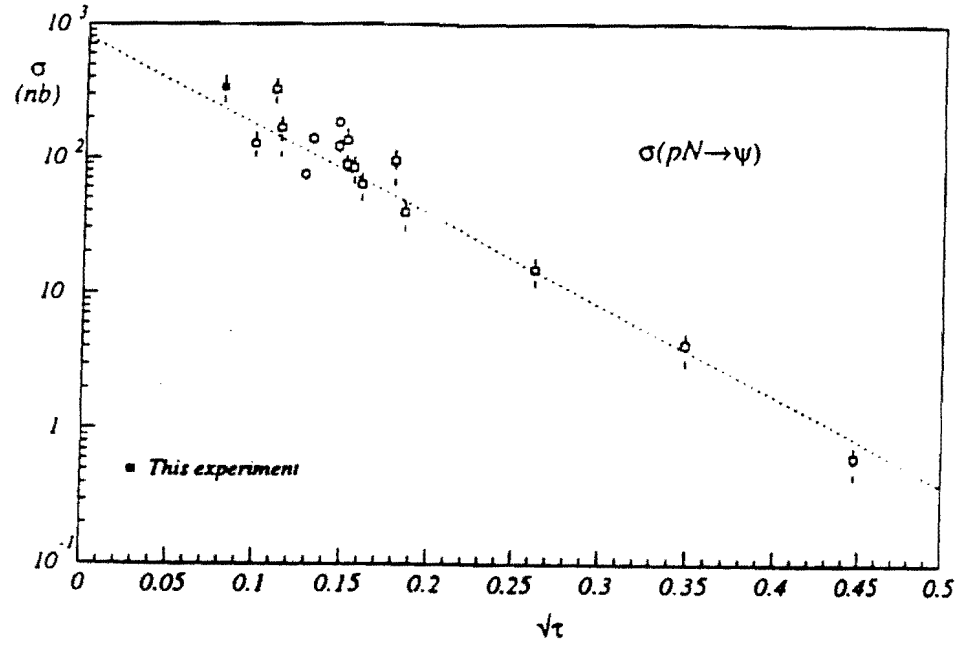

Fig. A2
E771 Reevaluation of the "Lyons Parameterization " of the
$\sigma(pN \rightarrow J/\Psi + x)$ all x_f

Using this data, our new evaluation of the Lyons parameterization results in

$$\sigma(pN \rightarrow J/\Psi + x) = 797.6\, e^{-15.3\sqrt{\tau}} \quad \text{(nb/nucleon)}$$

as compared to the old parameterization of $\sigma(pN \rightarrow J/\Psi + x) = 1985\, e^{-17\sqrt{\tau}}$, almost a factor of two difference in predicted cross section at 800 GeV/c. The preliminary E771 J/Ψ cross section is in reasonable agreement with our reevaluation of the Lyons parameterization shown in Fig. A.2 above which predicts 234±26nb nb/nucleon.

Silicon Detector Efficiencies

Even given the difficulties with the silicon detector installation in the E771 run, we were still able to gain valuable experience with the partially instrumented devices and actually take data. We were able to achieve the initial efficiencies indicated in Fig. A3 at the beginning of the run..

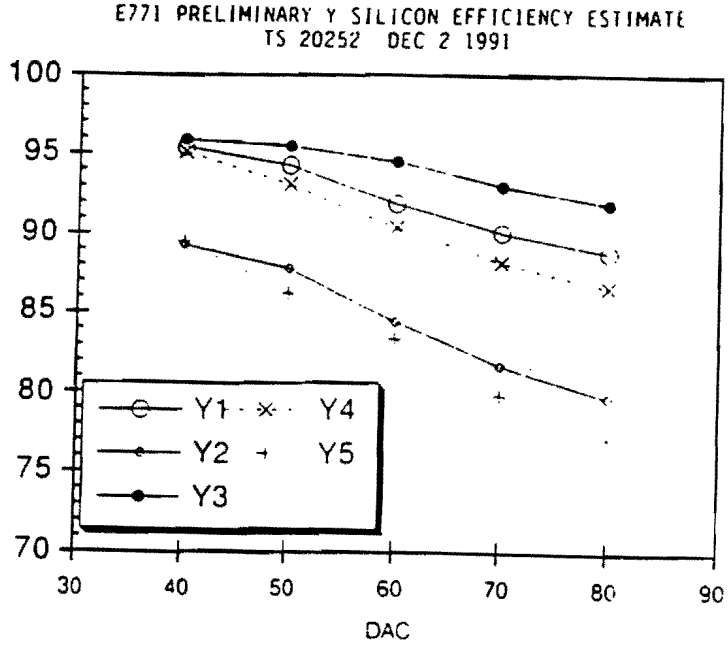

Fig. A3
Initial E771 Silicon Detector Efficiencies

These initial efficiencies are not optimized since time was short in the E771 run for complete tuning of the silicon detector performance (noise, timings, thresholds settings and other parameters should be studied under different operating conditions). In addition, if time had permitted, some of the lower efficiency silicon planes would have been replaced. Finally, as discussed below, these efficiencies degraded with radiation dose in the vicinity of the beam over the run period due to the small beam spot (σ_x=2.3 mm, σ_y=1.9 mm) which was necessitated by the partial instrumentation of the silicon detector for the E771 run. By the end of the run the efficiencies within one mm of the beam were below 50% in most of the planes.

Silicon MVD Resolutions

We have analyzed general dimuon triggers and J/Ψ->μμ decays from the data, as well as Monte Carlo J/Ψ->μμ superimposed on real 800 GeV/c interactions from the data to study the resolutions and efficiencies of the silicon detector. The overlaid Monte Carlo J/Ψ->μμ have been generated in a GEANT simulation of the 1991 silicon detector containing delta rays, strip width resolution effects, charge sharing, multiple scattering, etc. as well as the observed individual efficiencies of the silicon planes. The first crucial issue involving the resolutions of silicon detector (as well as the spectrometer wire chamber ensemble up stream of the analysis magnet) is the ability to match tracks in the silicon detector to spectrometer tracks. In Fig. A4 we show the observed matching in the slope and intercept in the x and y projections for the J/Ψ->μμ muon tracks in the spectrometer to the tracks in the silicon as evaluated at the z position intermediate between the silicon detector and spectrometer PWC system, which is optimal for matching resolution.

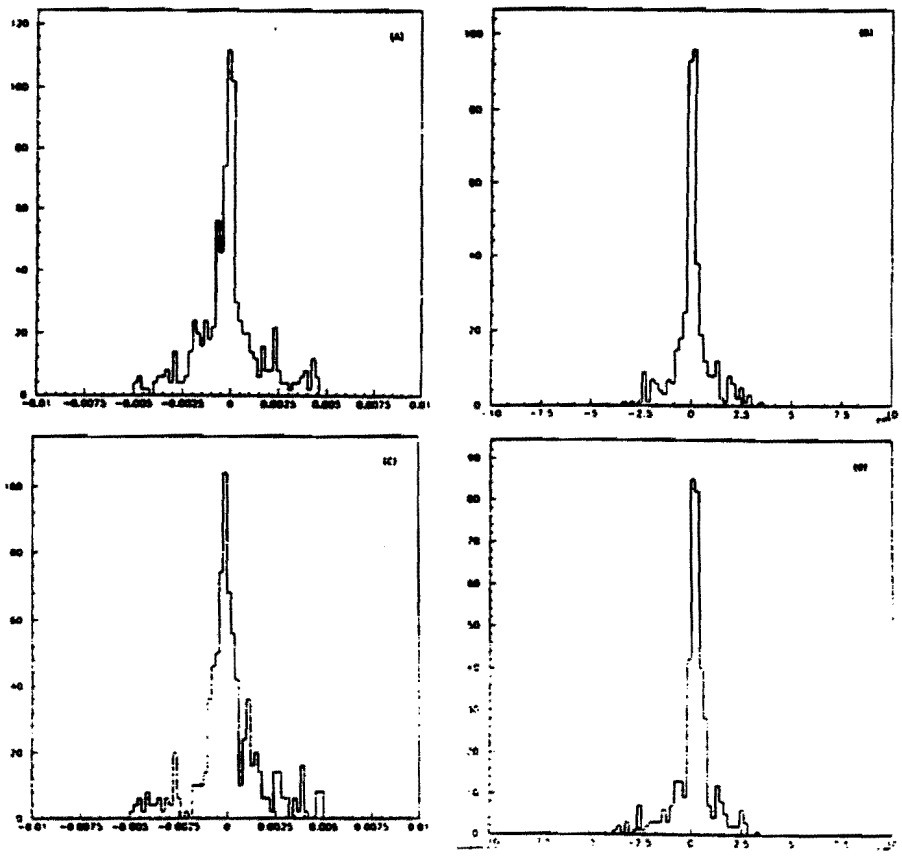

Fig. A4
Matching Distributions Between Silicon Tracks and Spectrometer Tracks
a) x slope matching b) x intercept matching
c)y slope matching d) y intercept matching

The matching resolutions observed for the muon tracks are $\sigma_{x'} = 0.47$ mrad, $\sigma_{y'} = .52$ mrad for the slopes and $\sigma_x = 0.30$ cm and $\sigma_y = 0.36$ cm for the intercepts, in reasonable agreement with Monte Carlo expectations. These results are dominated by the spectrometer front chamber track

resolutions. The discrepancy between x and y is expected since the front chamber PWC system is a small angle (16.7°) system in which the y coordinate is not as well measured as the x.

The resolution of the primary vertex is important for all facets of B physics. We have determined the resolution of our partially instrumented vertex detector from the data taken in the E771 run. In Fig. A5a we show the difference between the x position of the primary vertex as determined from the silicon tracker and the x position of the incident beam as measured by a 25 micron silicon plane. From this distribution, we extract a σ=15 microns for the primary vertex resolution (after correction for the resolution of the beam plane measurement; σ=19 microns). This is to be compared to the Monte Carlo prediction of 14 microns. In Fig. A5.b we show the z distribution of the primary vertices. This distribution clearly shows the twelve 2 mm silicon foils (and even a small peak due to interactions in the first 300 micron plane of the silicon tracker). Unfolding the z resolution of the primary vertex determination from observation of the edges of the foils, we obtain an average z resolution of 350 microns of the primary vertex (compared to the Monte Carlo expectation of 300 microns). The average z resolution for each of the foils is shown in Fig. A5.c

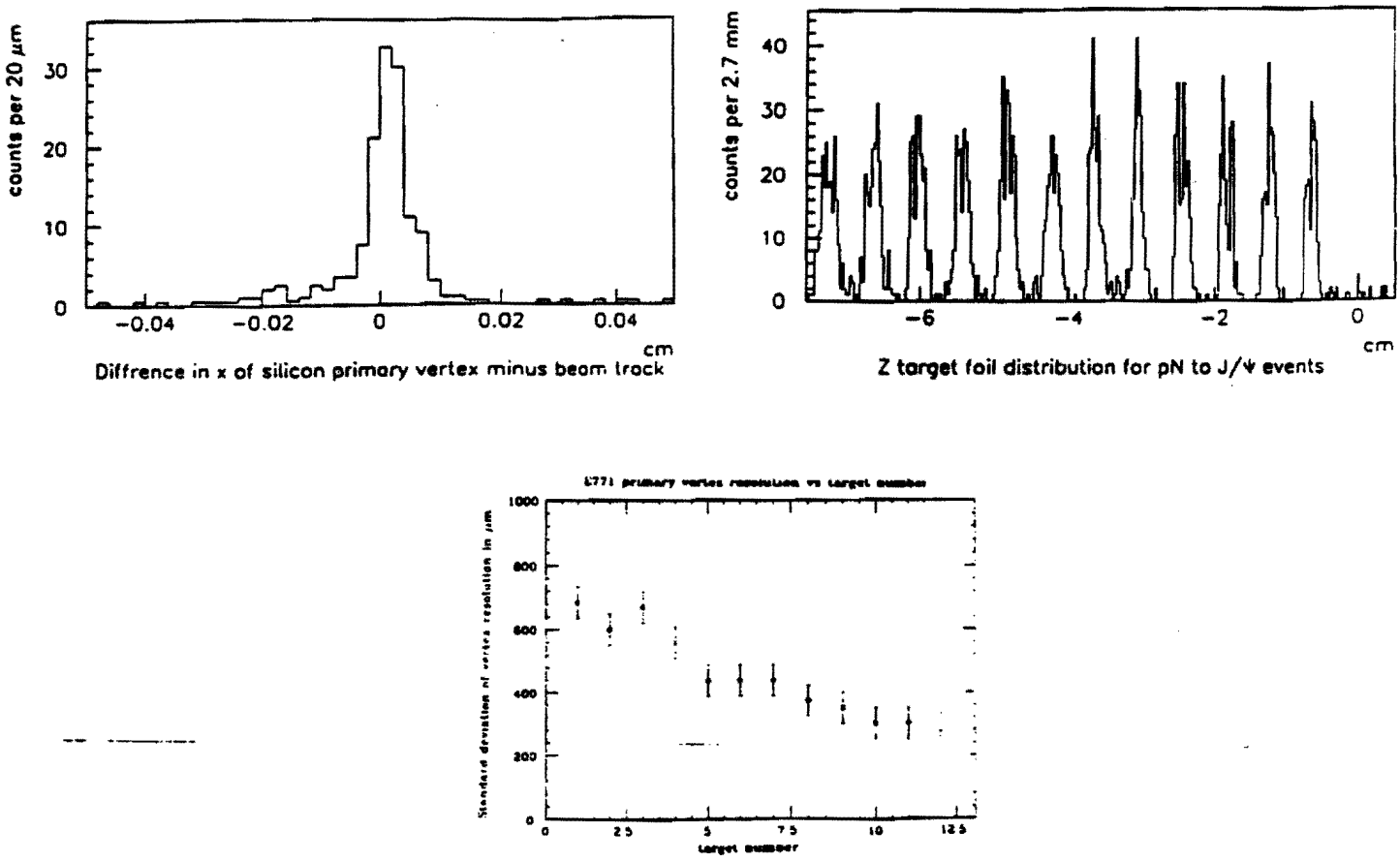

Fig. A5
a) x Silicon Primary Vertex - x Beam Silicon
b) z Vertex Distribution of Primary Vertices in Dimuon Triggers
c) z Vertex Resolutions for Each Foil

The resolution of the distance of closest approach of single tracks to the primary vertex (impact parameter) is a critical parameter for the analysis of the B->μ data and the separation of these decays for backgrounds Fig. A.6 shows the distribution of distance of closest approach of silicon microvertex tracks in the x projection to a primary vertex as calculated from the ensemble of all silicon tracks in a sample of dimuon triggers. This can be considered as a preliminary determination of a single track impact parameter resolution (σ=18 microns to be compared with a Monte Carlo prediction of 16 microns).

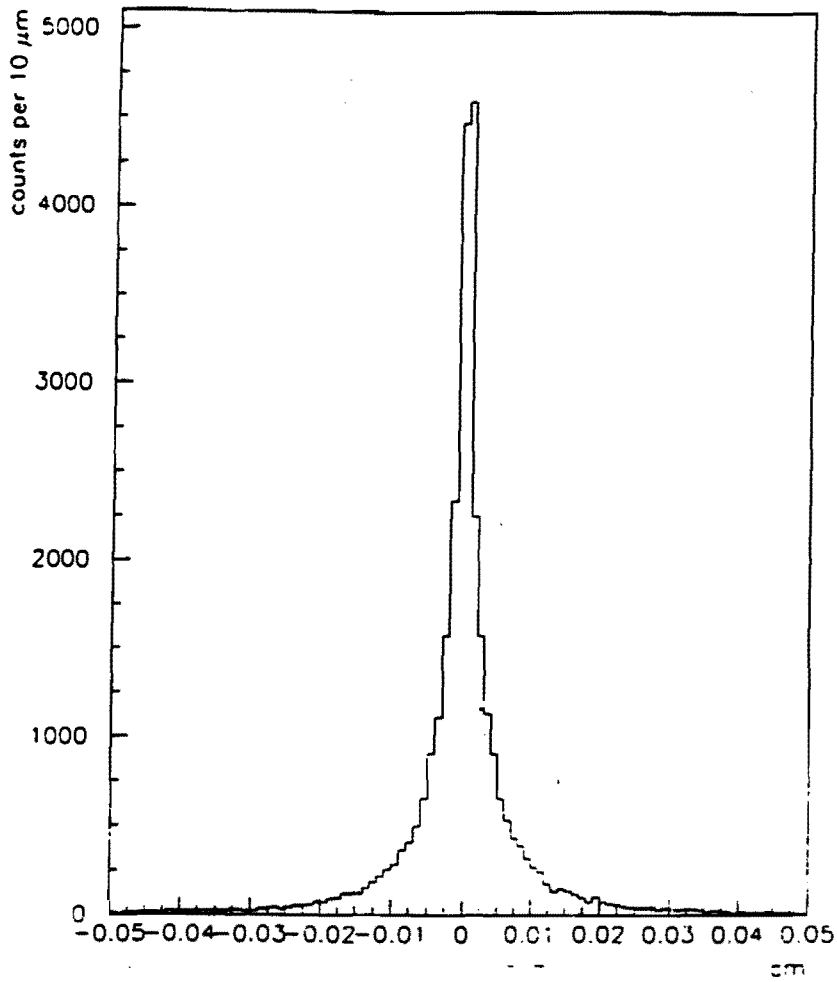

Fig. A.6
Distance of Closest Approach of Tracks in x Projection to Primary Vertices

The resolution for determining that two particle are emanating from the same vertex has been obtained from our data with a study of the distance of closest approach of the two muons from J/Ψ decays. We have also extracted these resolutions from the overlaid Monte Carlo J/Ψ-

>μμ. The determination of the distance of closest approach from the sample of primary vertex J/Ψ is perhaps a worst case result because of the many hits from primary tracks in the vicinity of the muon pair. Even though the resolutions for assigning a track to a given vertex will become better as the number of charged tracks from the secondary vertex increases, we have taken the two track resolutions as a worst case when applying the vertex resolution criteria in Section IV. In Fig. A7a and b we plot the distance of closest approach of matched muon tracks from J/Ψ->μμ decays in the x and $r=\sqrt{x^2+y^2}$ projections respectively.

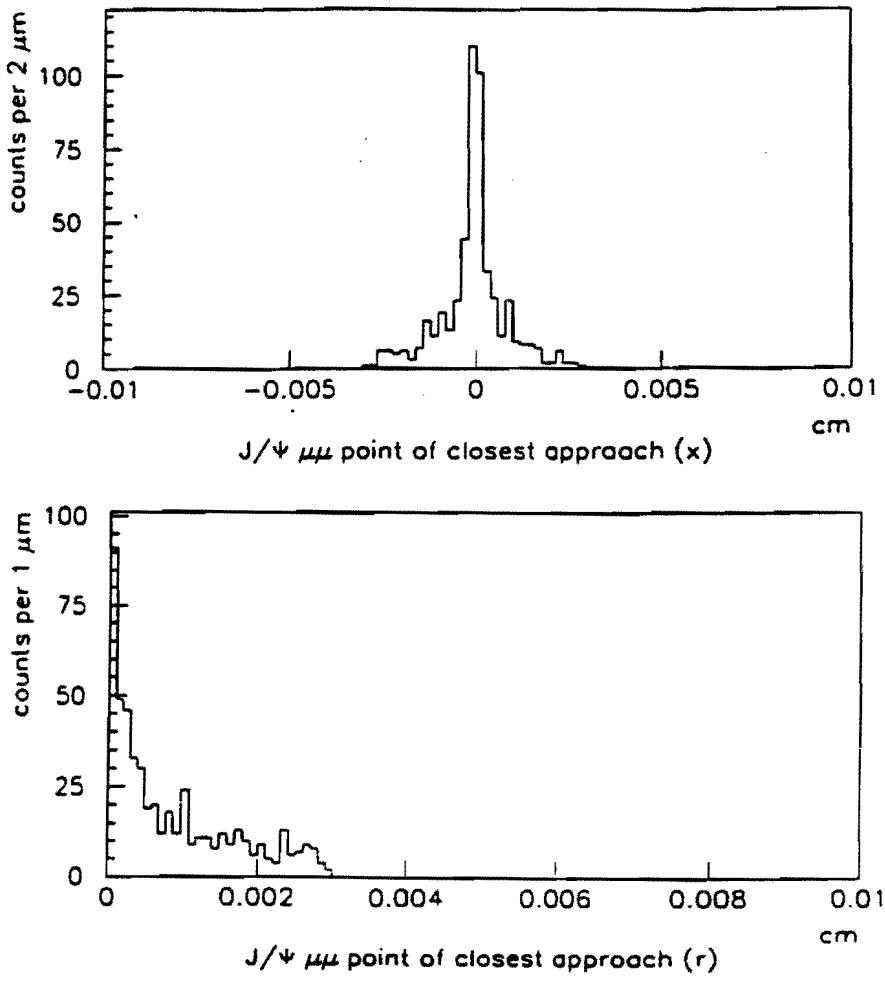

Fig. A7
a) Δx ; Distance of Closest Approach of Muons from J/Ψ->μμ
b) Δr ; Distance of Closest Approach of Muons from J/Ψ->μμ

The widths of these distributions (σ_x= 7.0 microns, σ_r= 8.5 microns) match Monte Carlo estimates based on superimposed J/Ψ Monte Carlo.

The most critical resolution for the J/Ψ events is that of the separation distance of the J/Ψ vertex, as determined from the distance of closest approach of the J/Ψ muons, and the primary vertex as reconstructed from all the other tracks in the event. Since the J/Ψ's are mainly directly produced we can both measure backgrounds and determine resolutions of the separation in x, r and z. We show in Fig. A8.a, b the x and z separations of the J/Ψ vertex. In Fig. A8.c we show the correlations between the transverse (r) and longitudinal (z) separations. We point out that no attempt has been made to eliminate pathological backgrounds from this plot so, by no means, are the J/Ψ's used for this plot background free or well measured.

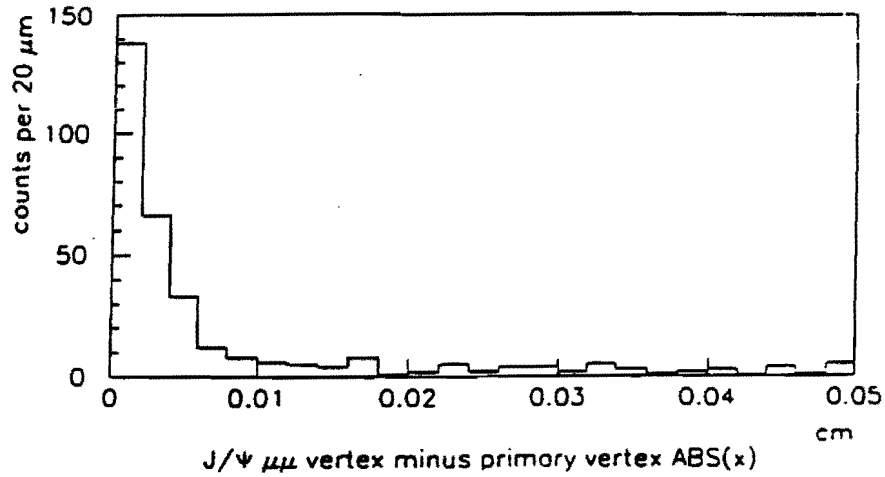

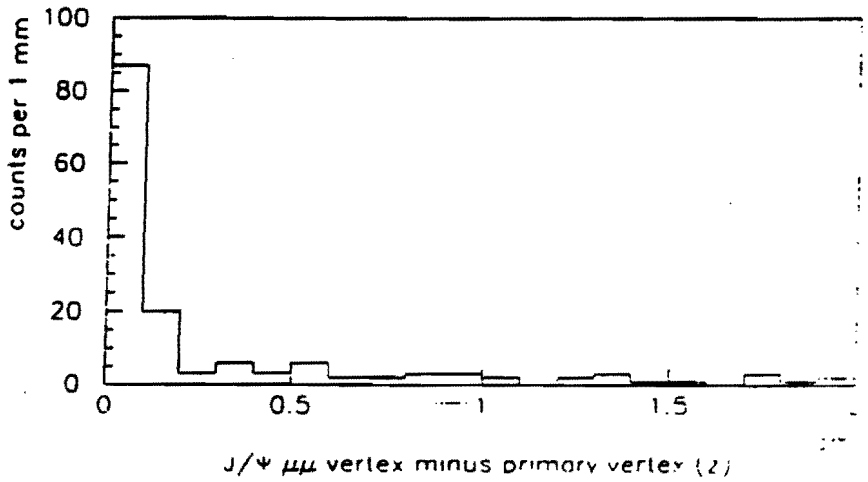

Fig. A8
a) Separation of primary and J/Ψ vertices in x
b) Separation of primary and J/Ψ vertices in z

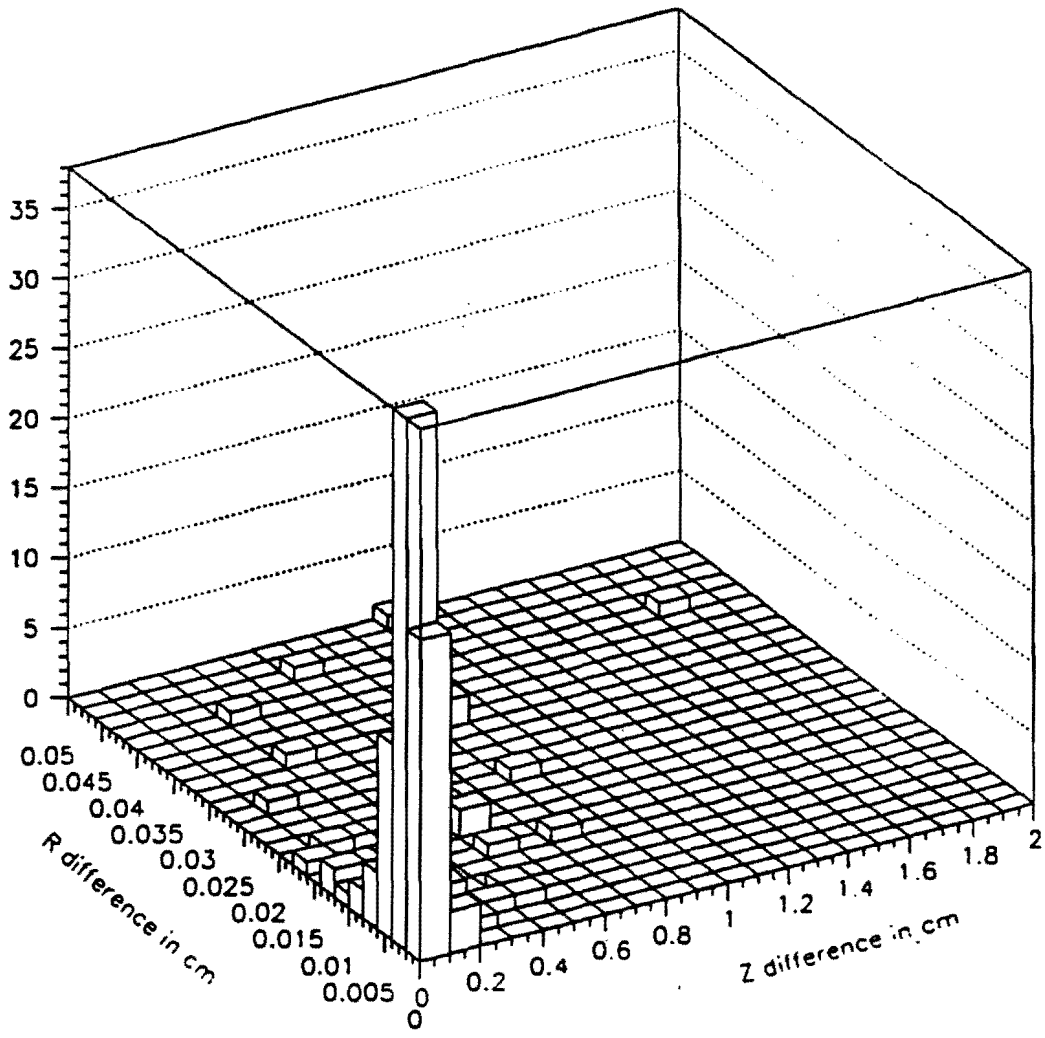

Fig. A8
c) Correlations between r and z separations

Finally, we have considered the secondary vertex resolution (the position of the vertex as determined from the midpoint of the distance of closest approach relative to its true position) which is the second component in determining the capability for separating primary and secondary vertices. Using the superimposed J/Ψ sample, we find a slightly poorer resolution (as expected) for secondary vertices (constructed from two tracks) than we did for the primary vertex (constructed from many tracks). The resolutions are $\sigma_x \approx$ 16 microns, $\sigma_r \approx$ 18 microns and $\sigma_z \approx$ 400 microns). Our cuts to define two track vertices (based on these resolutions) retain 85% of the J/Ψ's from the data (as compared to 86% of the overlaid MC J/Ψ's).

We have compiled the various vertexing resolutions in Table A.1 Based on these preliminary primary and secondary resolutions, we estimate the resolution of primary and secondary vertex separations in the three coordinates x, r and z for the E771 run to be 23 microns, 24 microns and 530 microns respectively.

Table A.1
Silicon Vertex Detector Resolutions
(all lengths in microns)

Parameter	E771 Data			E771 MC Estimates			P867 Estimates		
	Δx	Δr	Δz	Δx	Δr	Δz	Δx	Δr	Δz
Primary Vert.	15	18	350	14	17	300	5*	7*	190
Impact Par.	18	22	500	14	21	400	11	15	320
DCA**	7	9	-	7	9	-	5	7	-
Secondary Vert.	15	21	440	16	18	400	12	14	280
P-S Separation†	21	28	560	21	25	500	14	17	340

* Using the beam silicon for determination of the transverse primary vertex position
** Distance of closest approach of the muons
† Separation of primary and secondary vertices

As shown in Table A.1, we expect in P867 to improve the E771 resolutions, given the enhancements of the silicon beam tracker system due to the full instrumentation of Type L precision planes (which will provide the best measurements of the x and y of the primary vertex), the changes to the target foil configuration which will move the average primary and secondary vertex closer to the track measurements (thereby improving both distance of closest approach and vertex separation distance resolutions by improving vertex resolutions) and upgrades of the silicon detector by addition of more tracker planes (which will improve trajectory resolution and hence vertex resolution).

The vertex separation resolutions, as determined from the primary and secondary vertex resolutions of Table A.1, can be compared to the expected decay lengths of the B decays. We show in Fig. A9.a, b, c Monte Carlo simulations of the expected x, r and z decay length

distributions for 800 GeV/c pN interactions for B decays based on the average of the latest measurements of B lifetime, 1.40±0.045ps, from the LEP experiments[21]. While, as stated in Section III.D, the separation criteria needed to insure distinguishable primary and secondary vertices are mode dependent, a $\Delta z \geq 1600$ μm (≈4σ), would retain ≈ 85% of the decays. Similarly, an adequate criterion for impact parameters would be $\Delta r \geq 50$ μm (≈3σ).

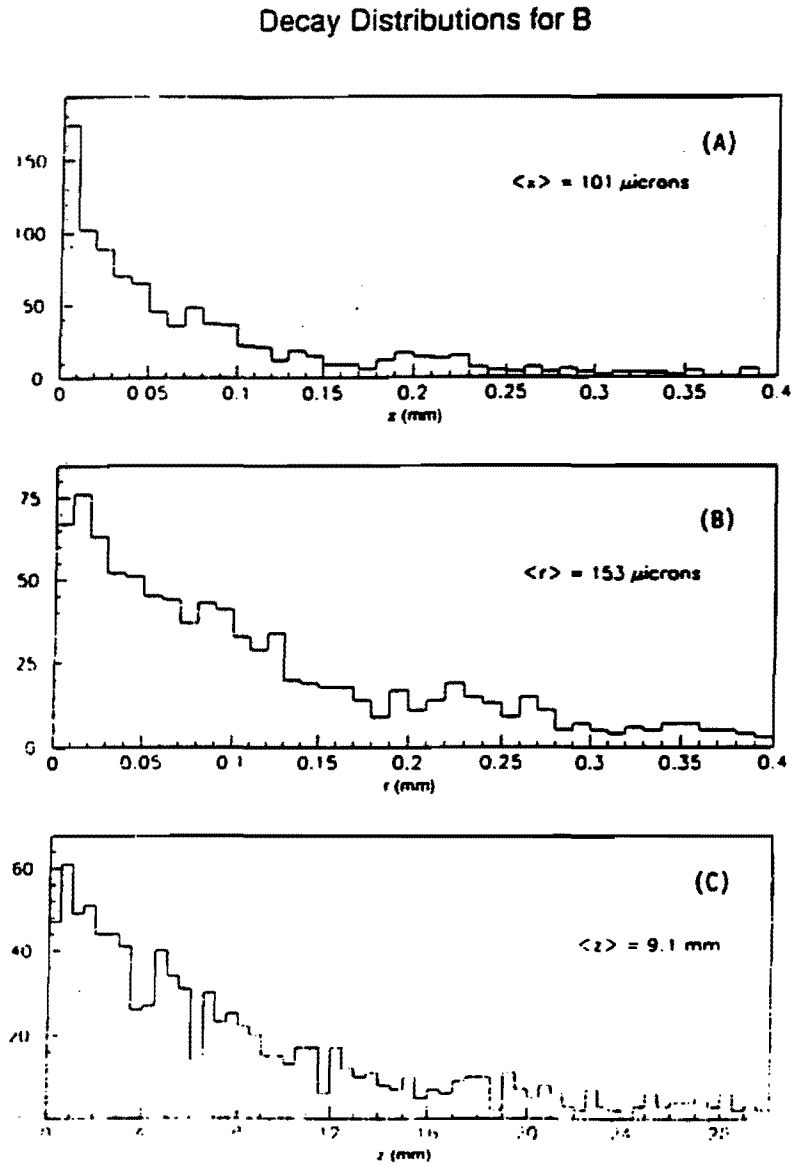

Fig. A9
a) Separation of Primary and B Secondary Vertices in x
b) Separation of Primary and B Secondary Vertices in $r=\sqrt{x^2+y^2}$
c) Separation of Primary and B Secondary Vertices in z

E771 Extraction of B's

At the time of the preparation of this proposal we have begun the Pass IV search for B events in the residue of both single and dimuon triggers which survive the first three passes of "purification". From a small sample of data, we presently have ten candidates for B->J/Ψ->μμ decays and four B->μ candidates. This number of events is consistent with expectations given the small numbers of events inspected thus far and still imprecise the knowledge of the efficiency for our Level IV scanning procedures.

We show one of our candidate B->J/Ψ->μμ decays in Fig. A10.a, b, c, d, e and f. What is shown in Fig. A10.a and b are the x and y projections of tracks from the primary production vertex of the event. At the left of these two figures, one can see the incoming beam tracks (this event had two such tracks). The tracks from B secondary vertex are not included in these event displays. Fig. A.8c and d shows on the same scale those secondary vertex tracks. Finally, Fig. A10.e and f show, on a larger scale, the relationship of the primary and the secondary vertices for this event. The upstream face of the various target foils are shown in these displays as the vertical lines. The primary vertex is well within the foil material. Although not necessary to our assignment of the B decay identity to this event, the secondary vertex lies outside the material of the foil by $>3\sigma_z$ for this event and is separated from the primary vertex by almost 7mm.

The various parameters for the individual tracks are shown in Table A.2 below:

Table A.2
Track Parameters for B->J/Ψ h_1 h_2 Event

Track	p (GeV/c)	θ_x (mrad)	θ_y (mrad)
Muon 1	74.2	-16.1	-3.3
Muon 2	25.6	-75.4	-42.4
Hadron 1	15.7	11.9	26.7
Hadron 2	0.98	161.8	174.9

Hadron 2 is at such a steep angle that it does not go through the spectrometer magnet so its momentum has been arrived at by using transverse momentum balance (assuming that the visible momentum perpendicular to the direction of the B is zero).

Using the momenta and directions of the tracks, this event has been fit under the assumption of a parent B to several hypotheses among which are:

$$B->J/\Psi\ K^*(890)->\mu\mu K\pi;$$

$$B->J/\Psi\ K\pi$$

$$B->J/\Psi\rho->\mu\mu\pi\pi$$

It is found that the event fits the B->J/Ψ Kπ hypothesis with a $\chi^2/DOF = 0.88$. Other fits are considerably worse.

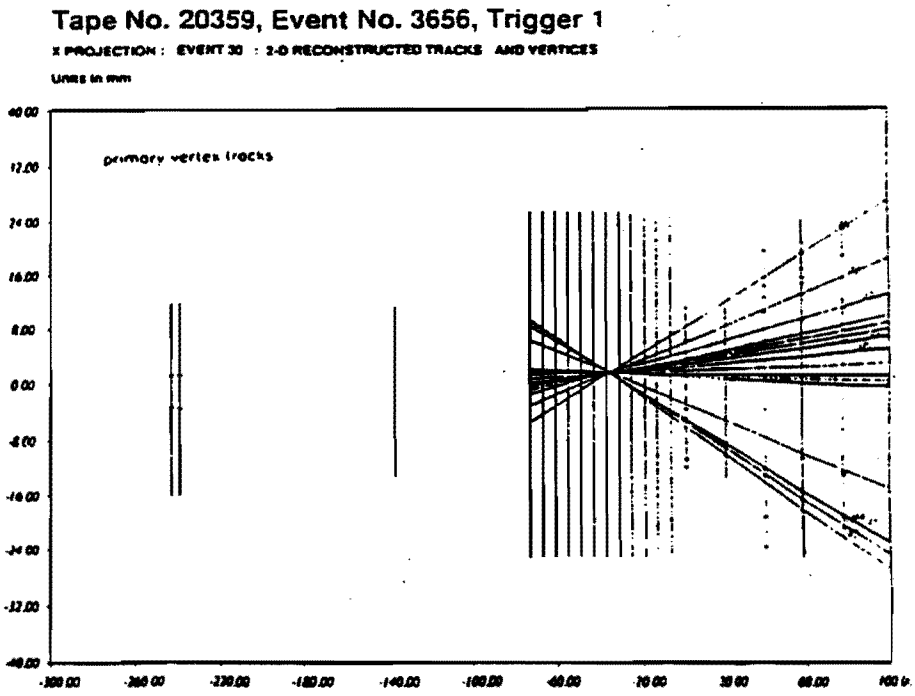

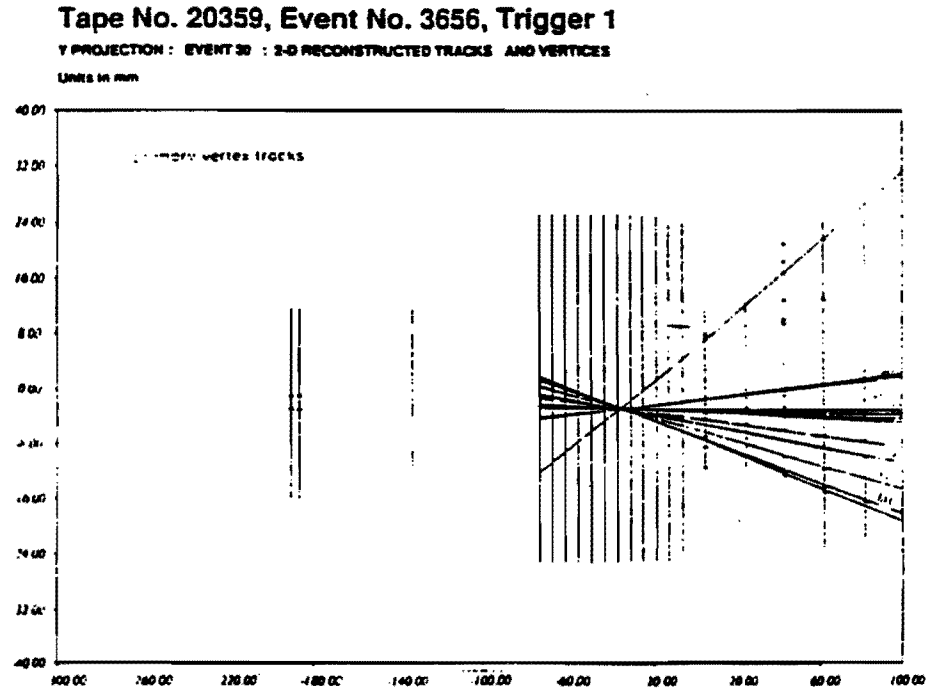

Fig. 10
"B" Decay: Event 3656 - Tapeset 20359
a)X projection: Primary Vertex Tracks Only
b) Y projection: Primary Vertex Tracks Only

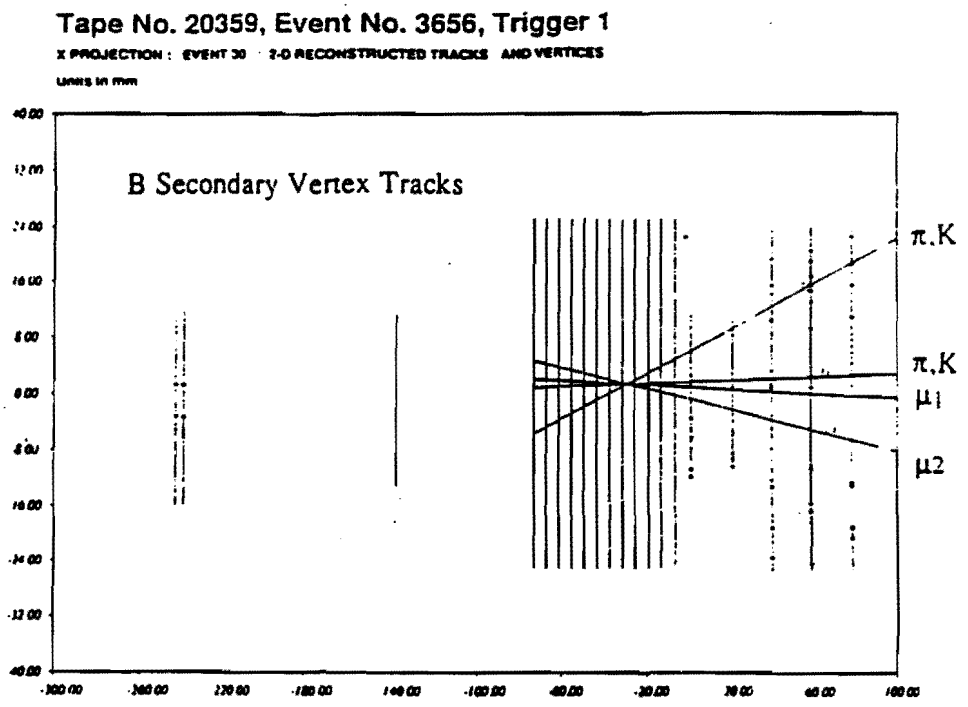

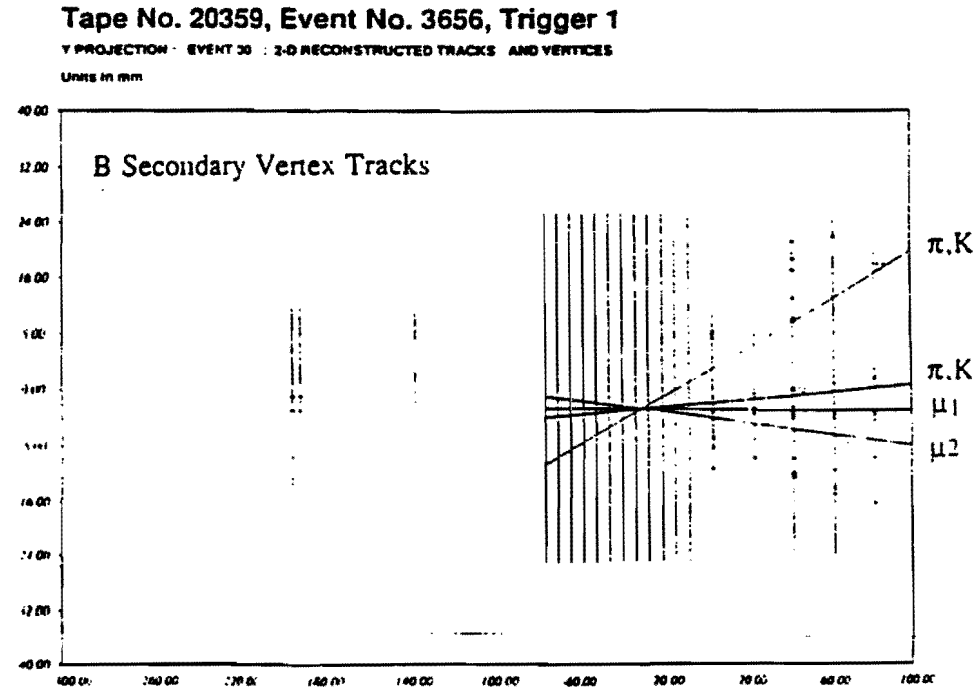

Fig. 10
"B" Decay: Event 3656 - Tapeset 20359
c) X projection: Secondary Vertex Tracks Only
d) Y projection: Secondary Vertex Tracks Only

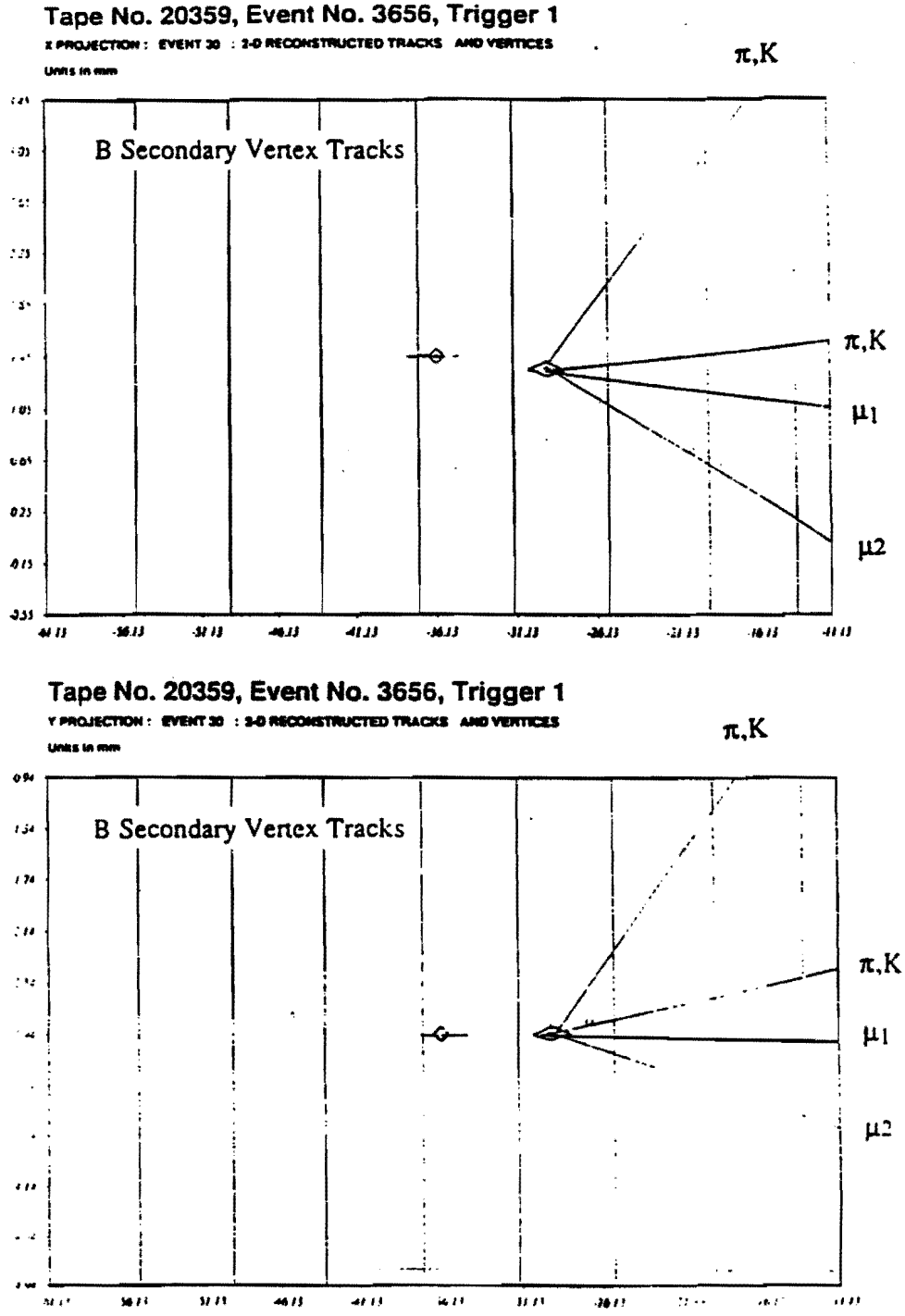

Fig. 10
"B" Decay: Event 3656 - Tapeset 20359 :
e) X projection of Secondary Vertex Tracks Expanded Scale
f) Y projection of Secondary Vertex Tracks Expanded Scale

The various parameters of this B decay shown in Fig. A10 are given in Table A3 below:

Table A3
Parameters of "B" Decay: Event 3656 - Tapeset 20359

"B" Parameters	
B Mass	5.278 GeV/c^2
Decay Time	1.096 ps
B Momentum	115.7 GeV/c
B Transverse Momentum	2.89 GeV/c
$M_{\mu\mu}$	3.096 GeV/c^2
$P_{\mu\mu}$	99.7 GeV/c
$Pt_{\mu\mu}$	3.39 GeV/c

Radiation Damage

The operation with a small beam size (σ_x=4.0 mm, σ_y=2.3 mm) forced us to accumulate a total 1991 exposure[51] of ≈ 1.6×10^{14} minimum ionizing particles per cm^2 in the beam region of our silicon detector compared to $0.52\times10^{14}/cm^2$ expected for P867).

As shown in Fig. A.11 below, leakage currents increased very appreciably during the 1991 run.

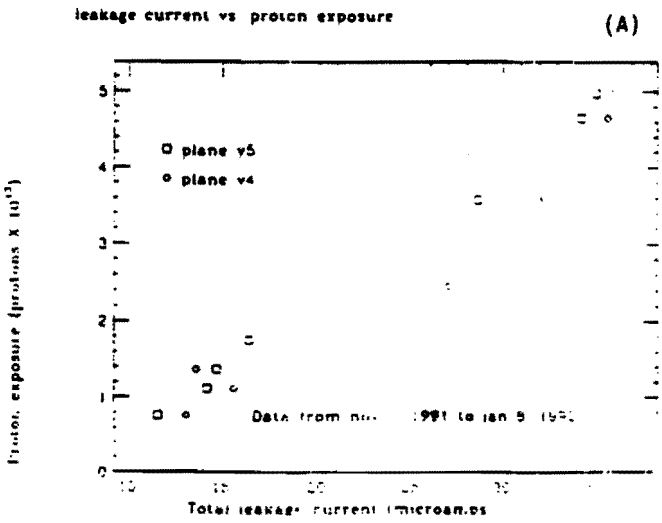

Fig. A.11
1991 Integrated Silicon Plane Leakage Current as a Function of Radiation Exposure

The increase in leakage current led to decreases in pre-amplifier gain over the course of the E771 run. The period in which the data of Fig. A.11 were accumulated corresponds to last three months of the Fermilab fixed target run when the bulk of the exposure to beam was experienced.

The decrease of signal level due to gradual conversion of the n type silicon to p type also led to loss of signal. Gradual increases of bias voltage and successive decreases of the threshold should allow us to compensate for this loss of signal. The exact effect on track reconstruction efficiency is still under evaluation but, because of the limited region of damage, we have been able to adopt strategies which recover most tracks.

Examining the radiation damage in the 2 mm beam region of the E771 SMVD detector experienced in the 1991 run has permitted us to determine the radiation limits (expressed in number of minimum ionizing particles/cm^2) allowable in P867 and to devise strategies to remain within those limits. Because we can operate in the P867 with a fully instrumented detector, we will be able to use a larger beam ($\sigma \approx 1.24$ cm). This increase in beam spot size for P867 (by almost a factor of 14 relative to E771) will reduce the worst case integrated number of minimum ionizing tracks per cm^2 by a factor of almost three relative to that experienced in E771, even with the increased running time. In addition, as discussed in Appendix C, a lower operating temperature ($\approx 0^0$C in P867 compared to 19^0C in E771) together with operation at higher bias voltages and more careful attention to exposure during spectrometer tuning will help keep the effects of radiation on the silicon microvertex detector in P867 to an acceptable level and permit the greater integrated beam flux of P867.

Appendix B

Hidden Charm Results from Fermilab Experiment E705

In 1988, we completed data taking in Fermilab Experiment E705. In this experiment we reconstructed 24,000 J/Ψ->μμ decays produced in 300 GeV/c $\pi^{\pm}$, proton and antiproton interactions. Since we expect to reconstruct over 600,000 J/Ψ->μμ in P867, it is natural to continue the E705 study of the hidden charm physics associated with J/Ψ and Ψ' with much higher statistics with 800 GeV/c pN interactions.

In Fig. B.1 we show the composite dimuon spectrum obtained in E705. J/Ψ and Ψ' signal can be seen in this spectrum.

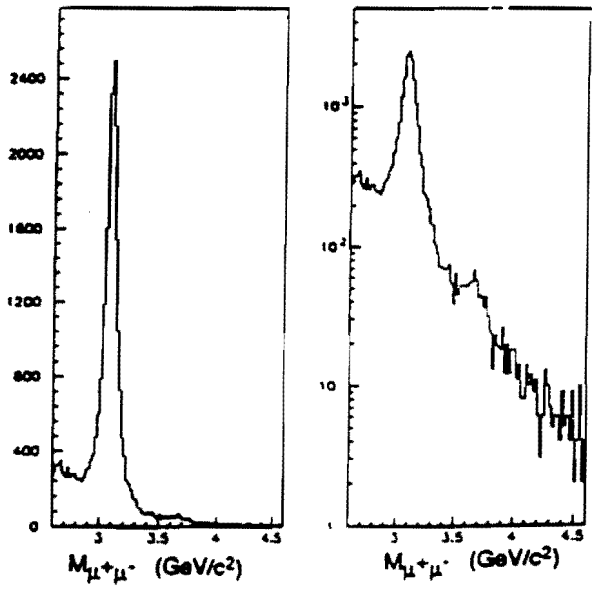

Fig. B.1
E705 Dimuon Mass Spectrum

The J/Ψ and Ψ' events were examined in a search for heavy quark states which decay into either charmonium state plus photons or pions.

The E705 search for hidden charm states[1,2] decaying into a photon or a π^0 was facilitated by the E705 electromagnetic detector[52] which had the ability to detect and measure with reasonable resolution photons with energies down to 2 GeV even in the presence of pedestal shifts in the ADC's at higher rate. The pedestal shift problem has since been rectified and the upgraded EM detector electronics[49] should allow somewhat better resolution in P867. As an example of the resolutions which were achieved at interaction rates over 2 MHz in E705, we show in Fig. B.2.a an E/p spectrum for $e^{\pm}$ from 300 Gev/c interactions and in Fig. B.2.b a $\gamma\gamma$ mass spectrum.

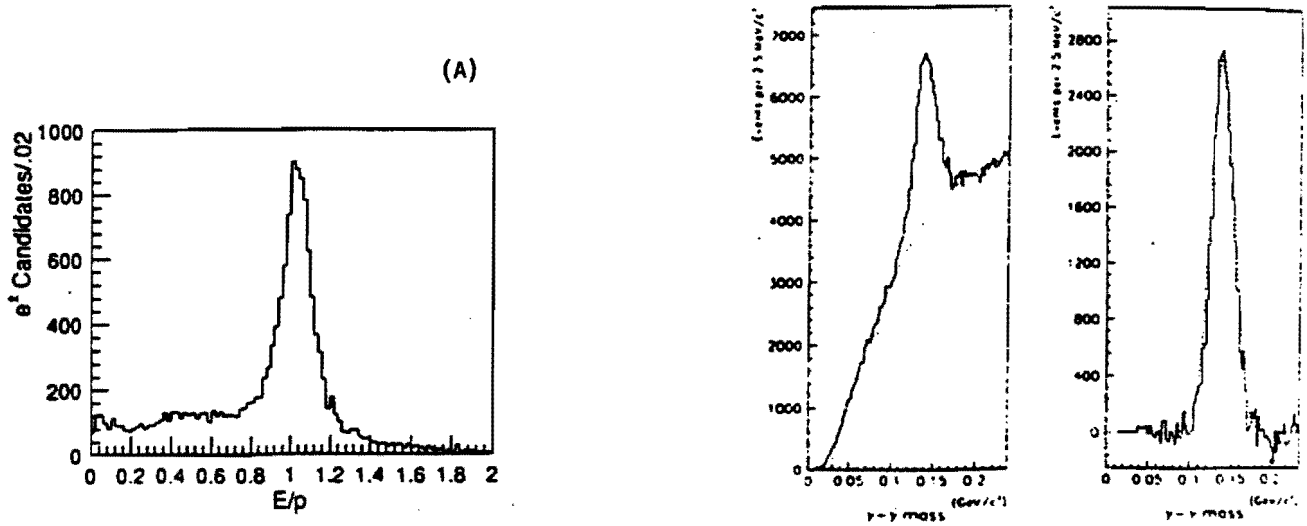

Fig. B.2
a) E/p for Electrons from 300 GeV/c Interactions
b) γγ Mass Spectrum from 300 GeV/c Interactions

The $\gamma\Psi$ mass spectra from the J/Ψ events accumulated in the $\pi^{\pm}$ E705 data is shown in Fig. B.3a. Fig. B.3.b shows the a $\gamma\Psi$ mass spectrum from the proton data. The backgrounds are constructed from combinations of photons from one Ψ event with Ψ dimuons from another event. The inserts on each plot are the background subtracted spectra fit to expected resolution functions for χ_1 and χ_2 states.

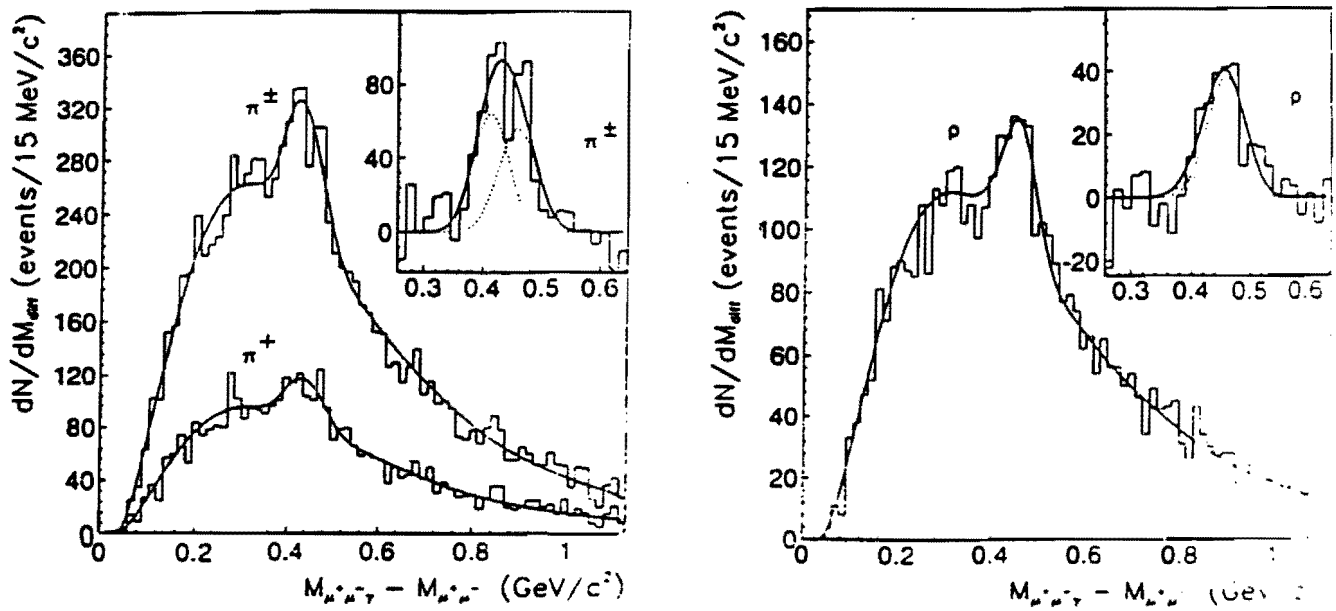

Fig. B.3
a) E705 $\gamma\Psi$ Mass Spectra from $\pi^{\pm}$ data
b) E705 $\gamma\Psi$ Mass Spectra from proton data

From these observation of the decay of the χ_1 and χ_2 states into $\gamma\Psi$ we have been able to extract the ratio of Ψ production from χ decay, determine the cross sections for direct J/Ψ production (correcting for the portion observed to proceed through χ or Ψ' decay), and measure the ratio of χ_1 to χ_2 production. Due to lack of statistics the latter of these measurements was limited in precision, especially for the case of production by protons. In addition, the investigation of the decay angular distributions of the photons to determine the χ production mechanisms could not be examined with any real significance because of statistics. All of these physics issues will be addressed with much more certainty with the better photon resolution and statistics a factor of 100 greater than available in the E705 run.

In addition to the observation of the χ_1 and χ_2 states, we searched in E705 for other states that might decay into either charged or neutral pions. We were able to examine the J/$\Psi\pi^0$ mass spectrum in E705 for both our pion and proton data. Fig. B.4 shows the $\gamma\gamma$ mass spectrum form our J/Ψ events showing clearly a good resolution π^0 peak. We point out that these π^0 photons are quite low enegy so we depend heavily on the ability of the E705 electromagnetic detector to reconstruct low energy photons in observing this π^0 signal.

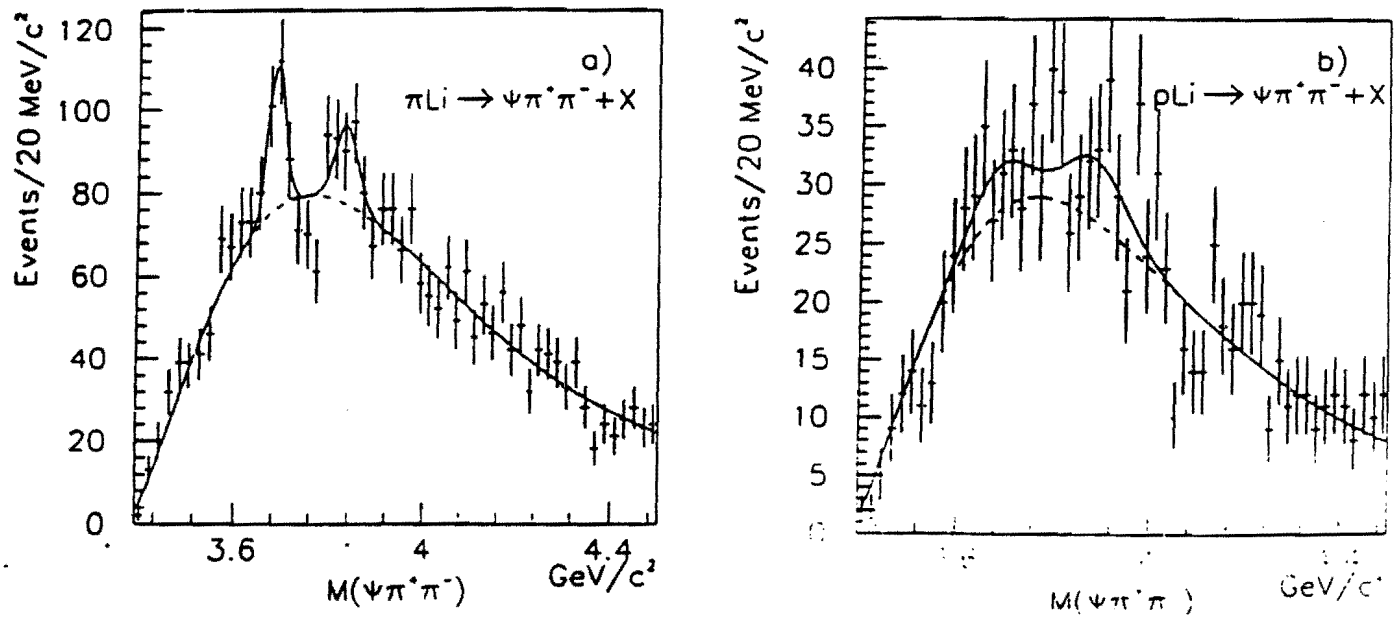

Fig. B4
a) J/Ψ $\pi^+\pi^-$ Mass Spectrum from $\pi^\pm$ Data
b)J/Ψ $\pi^+\pi^-$ Mass Spectrum from Proton Data

The composite $J/\Psi\pi^0$ mass spectrum for all our E705 as well as the individual spectra for the $\pi^{\pm}$ and proton data are shown in Fig. B.5.a, b and c. These spectra all show a 2.5 σ enhancement appears at 3.525 GeV/c^2 near the expected position of the $^1P_1$ state of charmonium.

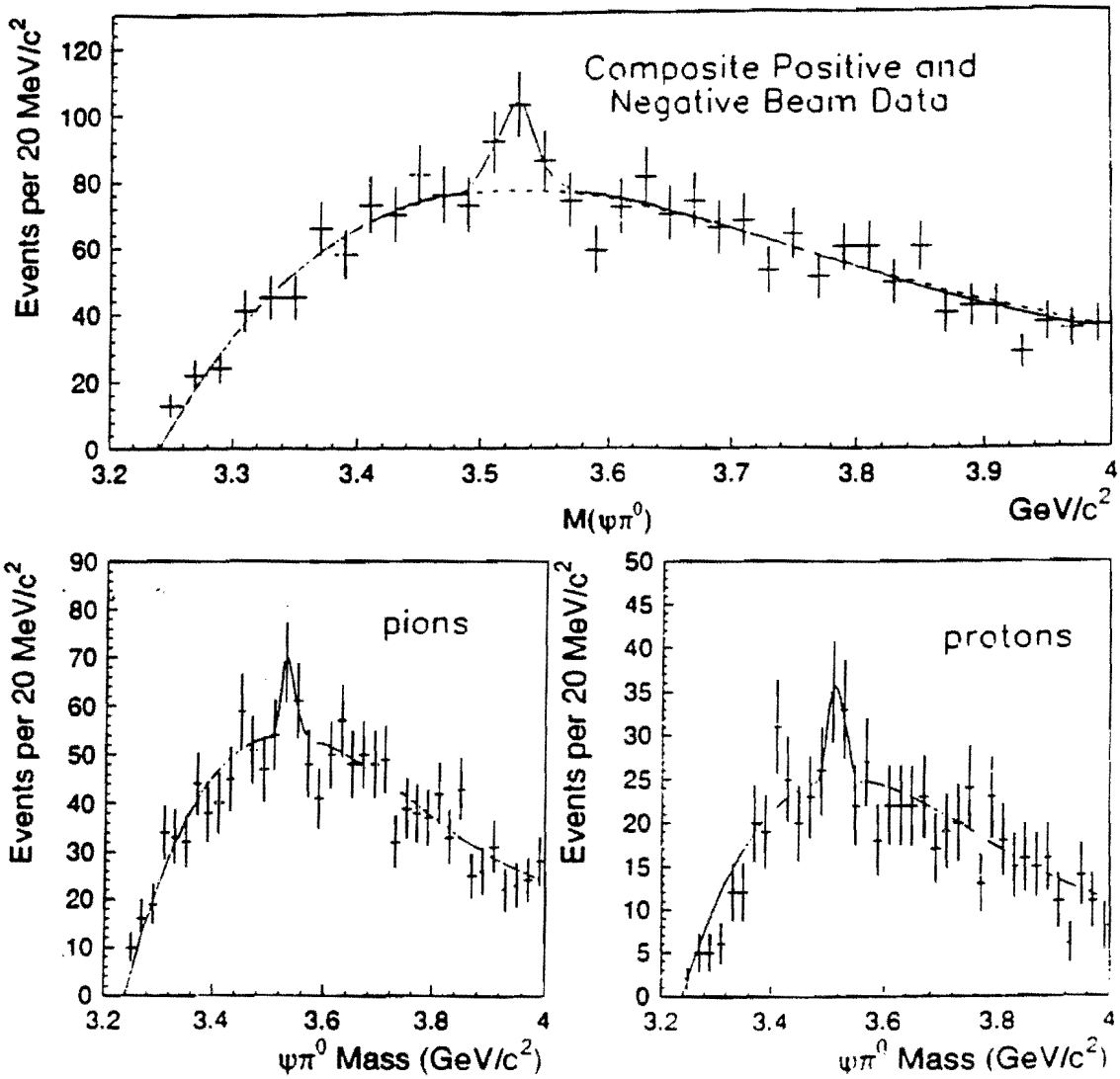

Fig. B.5
a) E705 $J/\Psi\pi^0$ Mass Spectrum - Sum of Positive and Negative Beam Data
b) E705 $J/\Psi\pi^0$ Mass Spectrum - $\pi^{\pm}$ Beam Data
c) E705 $J/\Psi\pi^0$ Mass Spectrum - Proton Beam Data

The production of this state followed by decay into $J/\Psi\pi^0$ has been previously reported by Fermilab experiment E760 in proton-antiproton formation at the Fermilab antiproton accumulator. This observation was also low in statistics (=4σ). A high statistics confirmation of our observation would be made in P867.

Appendix C

Completion of the P867 Silicon Beam and Microvertex Detectors

We were only able in the 1991 E771 run to achieve a partial instrumentation of the E771 silicon microvertex and beam detectors at the very end of the runnin gperiod. This resulted both in a limited number of planes per projection that were instrumented. In some case only partial instrumentation of those planes was possible. Given the limited number and late delivery of the silicon detector electronics, we chose in the 1991 run to partially instrument in the x and y projections five silicon detector planes and plus an additional u and v plane. The situation with the silicon beam detectors was even more marginal with only a single precision measurement per projection on a portion of the incoming beam. The late arrival of the bulk of the delivered electronics also resulted in very little time to check out and optimize the performance of all planes. The result of these factors was a much less efficient system with a much more limited solid angle and resolution than had been planned.

In P867, with the full complement of electronics and adequate time to insure optimal functioning, we will be able to increase the efficiency of each detector and improve the pattern recognition and track resolution with respect to the E771 run. In Fig. C.1 we show the configuration of the planes planned for P867.

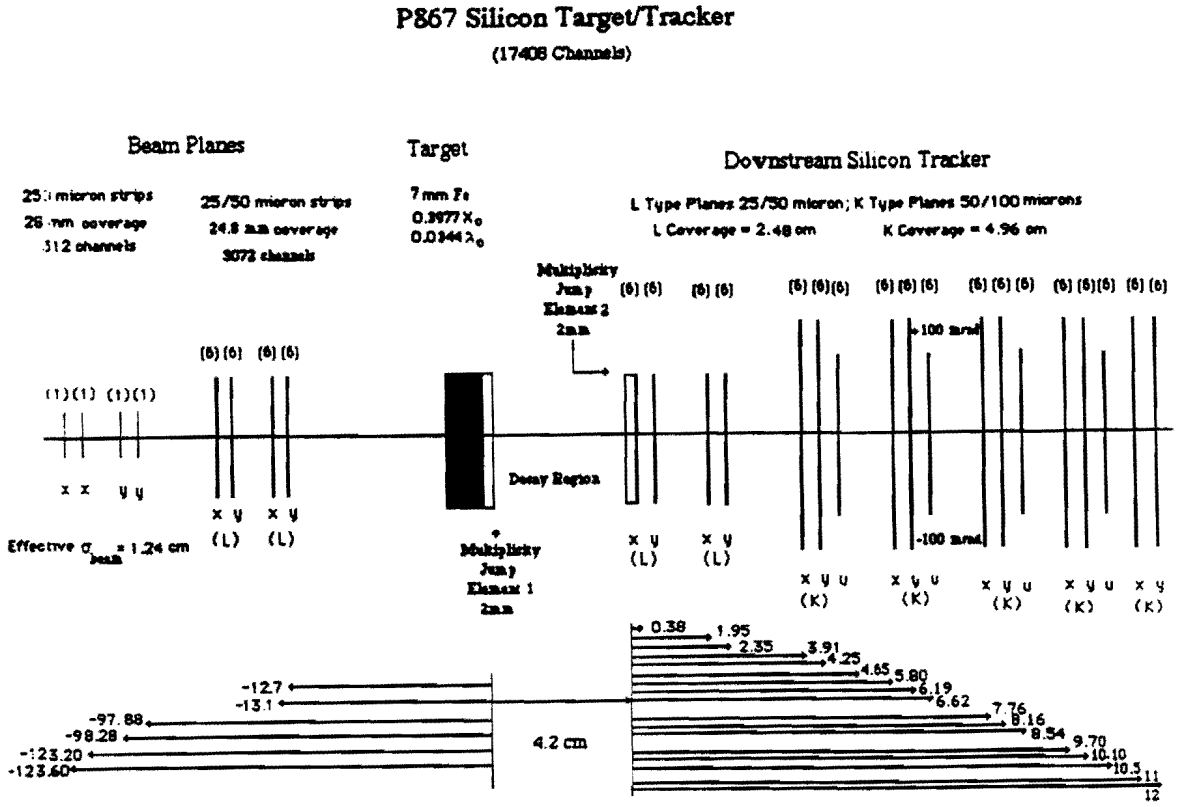

Fig. C.1
P867 Configuration of the Silicon Beam and Microvertex Detector

The completion of instrumentation of the E771 silicon detector will require an additional 7.5K channels (plus 10% spare channels) of silicon electronics (increasing the total silicon electronics from 10K to 17.5K). With this extra electronics, we plan to:

1. Complete instrumentation of previous installed x,y "precision" beam planes (Micron Type L), and add another x,y pair increasing the number of precision (25/50 micron resolution) measurements of the beam to two per projection.

2. Replace the existing u and v planes (Micron Type K) installed in the E771 run with 4 u planes to enhance 3D track reconstruction in the silicon tracker.

3. Add two new set of x,y planes (Micron Type K) to the tracker, increasing the number of measurements per x or y projection to seven thereby both improving the track finding efficiency and allowing some leeway for radiation damage at the higher integrated beam expected in 1994.

Adequate FASTBUS crates and smart crate controllers are already installed in the E771 spectrometer for the implementation of this scheme. In addition, adequate electronic components are on hand to construct the requisite number of channels of post amp comparator and delay encoder electronics. The major cost and work associated with this plan is the preparation, stuffing and testing of the post amp/comparator and delay encoder boards and the refurbishment of existing type L and K planes by Micron to replace radiation damaged wafers and increase the total number of type K planes. Micron has indicated that only new silicon strip wafers would be needed since they are able place new wafers in the existing wafer fanouts from E771. Adequate type L planes are already on hand to implement the beam detector.

In order to deal minimize radiation damage effects, three different strategies will be employed in P867. First and foremost, the beam size will be increased by a factor of almost 14. Second, the silicon detector will be continuously monitored to determine the adjustments of the bias voltage necessary to fully deplete the detector and operation at higher bias voltages is anticipated. Finally, the leakage current of the detector will be reduced by a factor of 10 by reducing the temperature of the detector to 0° C, minimizing the reduction of amplifier gain caused by the large leakage currents. The last two procedures are supported by data from E789[5] which used similar detectors and electronics. These two improvements should allow total fluences of $\approx 10^{14}$ particles/cm^2 without significant degradation of the performance of the silicon detector.

Appendix D

P867 Muon Detector and Trigger Improvements

The overall efficiency times acceptance for the basic level of the E771 muon trigger system is given by

Dimuon: $\varepsilon_{2\mu\ \text{total}} = (\varepsilon_{DET})^2 \cdot A^{2\mu}{}_{GEO} \cdot \varepsilon_{2\mu\ \text{trigger}}$

Single Muon: $\varepsilon_{1\mu\ \text{total}} = (\varepsilon_{DET}) \cdot A^{1\mu}{}_{GEO} \cdot \varepsilon_{1\mu\ \text{trigger}}$

During the E771 run, ε_{DET} was given by $(\varepsilon_{RPC})^3$ where ε_{RPC} was the efficiency of an individual Resistive Plate Counter (RPC) plane, A is the geometric acceptance for either one or two muons and $\varepsilon_{n\mu\ \text{trigger}}$ is the composite efficiency/acceptance for particular trigger strategies for single or dimuon events. This composite efficiency for the trigger includes a 6 to 10 GeV/c minimum energy requirement on the muons imposed by the steel and copper absorber of the muon detector.

We have made an examination of each of these factors using the data accumulated in the E771 run. Based on that experience, several improvements in the E771 muon detector and the configuration of the associated trigger electronics are planned for P867. The improvements fall into three categories corresponding to the three factors in the expression for overall muon trigger/detector efficiency given above.

1. Improvement in the overall efficiency of the RPC system.

2. Increase in the acceptance, $A^{n\mu}{}_{GEO}$, of the RPC detector system

3. Changes in the configuration of RPC pad electronics to increase $\varepsilon_{n\mu\ \text{trigger}}$ by allowing more leeway for multiple scattering of muons and more projectivity of the triple coincidences of Resistive Plate Counters to the E771 target.

As will be seen, these improvements, which are minor compared to the scale of the original construction of the RPC muon detector system and its associated trigger electronics, will increase the overall acceptance times efficiency for dimuons by a factor of 4.1.

D.1. RPC Efficiency

In the 1991 run of E771, the single muon trigger condition required the simultaneous response of all three RPC planes. For the dimuon trigger the trigger condition, therefore, required 2x3=6 RPC signals to be present. Therefore as indicated above, the overall trigger efficiency was proportional to the third (1μ) or sixth (2μ) power of the individual RPC efficiency. In order to avoid such a strong dependence, we plan to

install a fourth plane of RPC's, and to define a muon as the coincidence of any three out of the four planes. Moreover, we also plan to install a second layer of RPC in the central region of the muon detector for planes 1 and 2 and to OR the signals with the existing planes to increase overall efficiency of these planes. With these improvements, we estimate that ε_{DET} will increase from 64% to 97% (and correspondingly ε_{DET}^2 from 41% to 95%).

D.2. Rearrangement of Pad Electronics

Based on the data from the E771 run and various Monte Carlo studies, the efficiency of the dimuon system will be increased from 64% to 86% by a reconfiguration of the wiring of the RPC electronics to allow for more multiple scattering of muons and to increase the projectivity of the trigger to the target and to yield, correspondingly, better efficiency for the trigger, improving the overall $\varepsilon_{n\mu}$ from 41% to 74%.

D.3. Summary of P867 Improvements in Signal Retention by Level 1A Trigger

Assuming all of these independent improvements are done, we expect to see the improvements in single and dimuon trigger efficiencies as given in Table D1 below:

Table D.1
Single and Dimuon Trigger Efficiencies for Level 1A

	E771		P867	
	B->J/Ψ->2 μ	B-> μ	B->J/Ψ->2 μ	B-> μ
$(\varepsilon_{DET})^n$	0.41	0.64	0.95	0.97
$A^{n\mu}_{GEO}$	0.35	0.56	0.35	0.56
$\varepsilon_{n\mu\ trigger}$	0.41	0.64	0.74	0.86
$\varepsilon_{n\mu\ total}$	0.059	0.23	0.25	0.47

As can been seen, the planned improvements and tuning of the muon detector and trigger will increase the efficiency of the 1A muon trigger for B->J/Ψ->2 μ by a factor of 4.2. The efficiency of single semi-muonic 1A trigger for B-> μ events will also increase by a factor of 2.0 relative to the yield/interaction of the E771 run. It should be noted that the improvements in the trigger efficiency generated by these changes will be accompanied by an increase in the 1A trigger rate (see Tables D.2 and D.3). Moreover, we are planning to operate at a higher interaction rate. As described in the following sections, the 1B and Level 2 triggers will be used to contain the overall muon trigger rates to an acceptable level.

D.4 Single Muon and Dimuon Trigger Rates in P867

Given the muon trigger improvements discussed above, we have estimated the P867 single and dimuon trigger rates. These projections are obtained, wherever possible, by analyzing the E771 data, otherwise from Monte Carlo simulations.

Table D.2
E771 and P867 Single and Dimuon Trigger Rates

	E771	E771	P867
	Expected (1.9×10^6)*	Observed (1.9×10^6)*	Expected (2.5×10^6)
Level 1A 2μ Trigger Reduction	8.8×10^{-5}	9.6×10^{-5}	4.8×10^{-4}
Level 1A 1μ Trigger Reduction	1.8×10^{-2}	9.6×10^{-3}	2.0×10^{-2}

*"normal intensity" E771 condition at the end of the 1991 run.

The observed rates include the effect of the less than 100% detector efficiency. For efficiency equal to 100%, the rates would extrapolate to 2.5×10^{-4} and 1.5×10^{-2} for the indicated 1A double and single muon rates respectively.

D.5. The P867 Ey Trigger

The first new trigger that has been added to P867 is based on the transverse energy deposit of the event in the non-bend plane. The Ey trigger for the P867 spectrometer is formed from the signals from the 396 elements of the electromagnetic calorimeter main array suitably weighted in a resistive network multiply each pulse height by a factor proportional to $\sin\Theta_y$. Θ_y is the angle in the y or non-bend plane of the center of each calorimeter element with respect to the beam.

The effectiveness of this trigger has been estimated using a GEANT simulation of calorimeter performance which takes into account all the aspects of the P867 calorimeter. Beauty and charm signal retentions and rejection of minimum bias events are estimated using PYTHIA simulations together with the GEANT simulations of the Ey for each event. In addition, since PYTHIA may not replicate either the minimum bias or the structure underlying the heavy quark production, we have compared the correlation of retention of charm and beauty versus the expected rejection of total cross section wherever possible with data. We note that charm production itself is well reproduced by PYTHIA at these energies. In addition, the retention of charm when compared to the rejection of total cross section as predicted by PYTHIA matches that observed in 500 GeV/c π^-N interactions by E791. Finally, we have compared the retention of our own B->J/Ψ->μμ beauty candidates and rejection of interaction triggers from E771 to the predictions of PYTHIA and find very similar behavior over a wide range of Ey. So, we conclude, that even if the underlying structure (i.e. the minimum bias part of the event) is not well reproduced by PYTHIA, the Ey in both minimum bias events and heavy flavor events scale by similar factors so that the retention vs. rejection factors match those observed in the data.

The retention and rejection factors of Table VI (page 5) are obtained in the manner described above. The rejection power of the E_y trigger is significant while retaining very reasonable efficiencies of B decays. It is less effective for charm because the charm events are not very different in E_y structure from the total cross section events.

Finally, it is worth noting that this is a simple and very inexpensive trigger to implement. It is fast and will operate at Level 1 in our P867 trigger scheme.

D.6 The P867 Multiplicity Jump Trigger

The second new trigger that will be implemented for P867, a vertex trigger predicated on appearance of additional charged tracks just downstream of the P867 target is also relatively simple and inexpensive to implement. The multiplicity jump trigger (Mj) is based on the difference between the Cerenkov signals from two 2mm thick quartz radiators separated by 4.2 cm (see Figure C.1- Appendix C). This trigger is very similar to the trigger tested success fully in the TPL in the last fixed target run by M. Halling and S. Kwan[9].

We have estimated the effectiveness of this trigger for retaining charm and beauty signals and rejecting total cross section interactions using GEANT simulations of the Cerenkov radiator arrangement as would be positioned in P867. This simulation included secondary interactions, conversions, delta rays, the effects of Poisson statistics on the photoelectrons produced in the PM tubes as well as other physics effects such as production of K^0, Λ^0, etc. which decay in the volume between the quartz radiators, all of which tend to lower the efficiency and diminish the rejection power of such a trigger. However, we find that we can achieve rejection factors as great as 10 with such a trigger while maintaining reasonable efficiency for beauty. As expected, this trigger is more effective for beauty than for charm since the multiplicity jump is less in charm events than in beauty events

The estimated number of photoelectrons produced in the quartz radiators (≈9.5 per track) approximately matches the observations of Halling and Kwan. Other aspects of their test have been replicated in our simulations of the P867 multiplicity jump trigger. This trigger is also reasonably simple and inexpensive to implement and will operate at Level 1 in the P867 trigger scheme.

D.7. The P867 Level 2 Secondary Vertex Trigger

In order to go to higher rates and to minimize dead time in P867, we will implement a second level of trigger for the spectrometer using associative memories[7]. We are basing our Level 2 strategy on a method relying on detection of secondary vertices in the silicon microvertex detector.

An encoded list of hits from five x (and possibly five y) silicon tracker planes is sent from the FASTBUS electronics located near the vertex detector to the Level 2 electronics by means of a fast fiber optics link. The "brain" of the Level 2 system is a set of Associative Memories, pre-loaded with the list of all possible five hit patterns corresponding to valid (both primary and secondary) tracks in the silicon planes themselves. When presented with the hit lists relative to a given event, the Associative Memories will produce within a few microseconds, i.e. in the time it takes to load them with the event data, a complete list of valid tracks that can be formed with the hits from the event under question. The next step is to make a decision on the likelihood that the event contains several vertices. At this point in time, the electronic design of components of the Level 2 system has been completed by the UVa and Pavia groups with the exception of the final stage which implements the algorithm which processes the track list to detect the presence of secondary vertices. With complete GEANT simulations of the silicon tracker including the simulations of the hardware of the associative track finder and secondary vertex finder, we have been studying several different algorithms that could be used to

process the list of tracks provided by the Associative Memories. The performance projections of Table VI are based on the promising approach currently under study which identifies track crossings in the x and y projections downstream of the Fe target and correlates their z coordinates.

A block diagram for the Level 2 trigger is shown below in Fig. D.1.

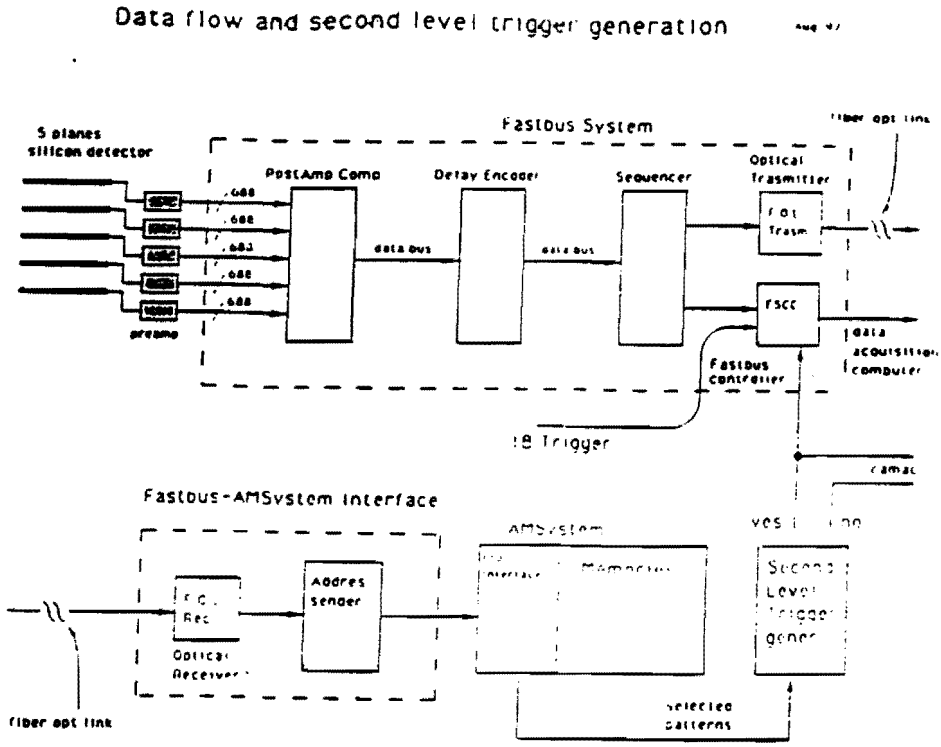

Fig. D.1
Block Diagram of the Level II Secondary Vertex Trigger Processor

Appendix E
Proposed 1994
RICH Detector Addition

While a majority of the physics described in this proposal can be performed to some substantial level without K/π identification, a Ring Imaging Cerenkov counter (RICH) would significantly enhance the capabilities for achieving the B_s and Λ_b physics goals described in Section IV and, in general, give cleaner results due to the increased capacity for rejecting backgrounds. For example, most of the decay modes discussed in this proposal were purposely chosen so that, in principle, particle ID might not be necessary. However, the addition of a RICH would make those strategies more robust against, as yet uncertain, backgrounds and also increase the signal substantially by making more modes accessible. As an example, consider the decay $\overline{B}_s^0$ $\rightarrow D^+_s \pi^-$ where $D^+_s \rightarrow K^-K^+\pi^+$ and its B_d analog. If the D vertex is resolvable from the first generation π^-, then one could assign the K mass to the negative track at the D vertex. There is ambiguity however on assignments to the remaining positive tracks. Figure E.1.a shows the reconstructed mass of a D^+ coming from a $\overline{B}^0$ decaying into Kππ when one of the pions is assigned the K mass. The mass peak is moved nearly on top of where the D_s is expected. Fig. E.1.b shows a similar effect in the reflected decay $D_s \rightarrow KK\pi$ when the like signed K is assigned the π mass. Finally, Fig. E.1.c shows the resulting ambiguity if the π mass is assigned to all final particles in these two decays.

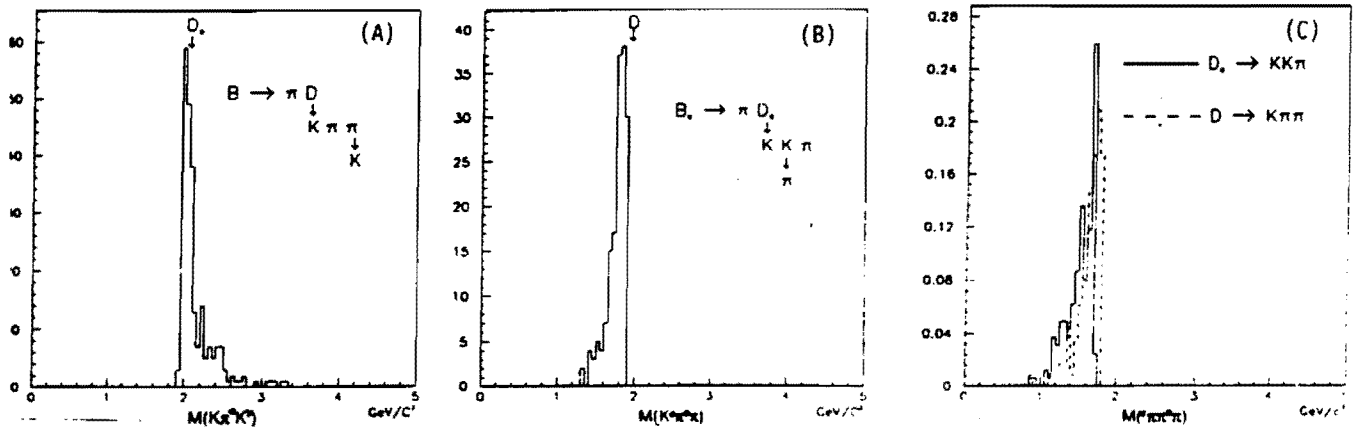

Fig. E.1
D Mass Peak Confusion due to K/π Misidentification
a) $D^+_d \rightarrow K\pi\pi$ Decay; One π Assigned K Mass
b) $D^+_s \rightarrow KK\pi$ Decay ; Like Sign K Assigned π Mass
c) $D^+_d \rightarrow K\pi\pi$ and $D^+_s \rightarrow KK\pi$ Decays; All Particles Assigned π Mass

In addition to these reconstruction issues, the RICH would also benefit flavor tagging. A potential tag for the B_S is to look for an associated charged K from the primary vertex as described in Section IV.A.6 . Unlike a lepton tag, these methods are not susceptible to mixing-type dilution. The use of the RICH would range from very useful in the first method to crucial in the second.

The choice of using a RICH rather than multiple segmented threshold counters is based on the need to preserve the acceptance of the E771 spectrometer. A 2.5m long radiator placed between the CC2 and DC5 chambers could be accommodated without significantly limiting the aperture of the spectrometer and the acceptance for B decays (see fig E.2). Threshold counters would require at least 10m for the same momentum range coverage as a 2.5m long RICH.

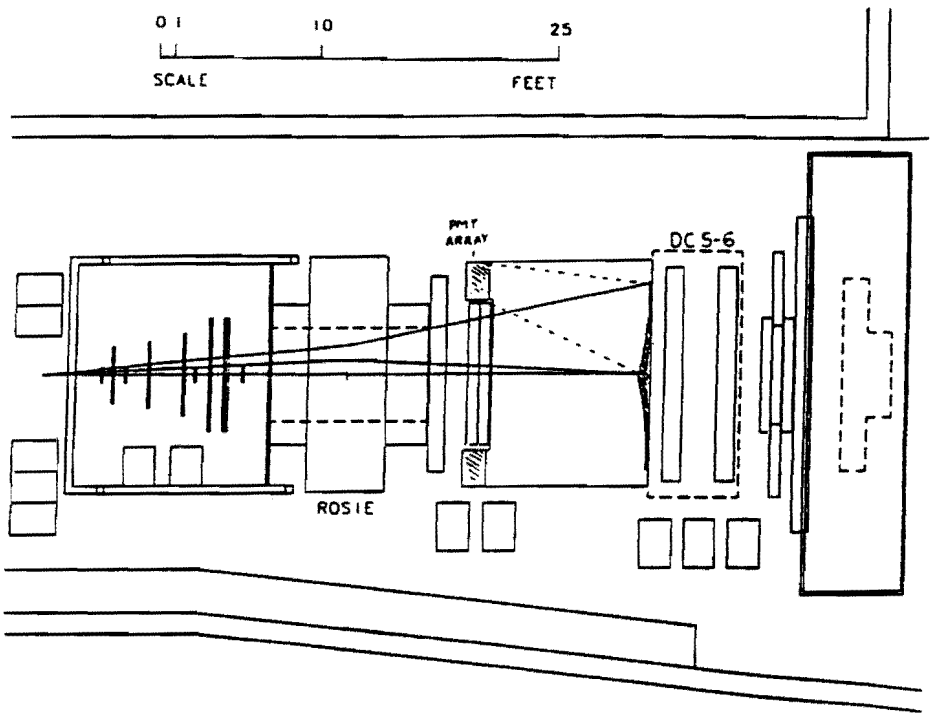

Fig. E.2
1994 RICH Layout

The RICH would use-off axis imaging as indicated in figure E.2. This allows the photon detectors to be placed outside of the aperture at the cost of increased geometrical aberration. The focal length F=3m was chosen slightly longer than the radiator length to accommodate the off axis imaging. We have tentatively chosen CF_4 (γthreshold=32) for the radiator gas although C_2F_6 (γthreshold=25) could be used if a lower threshold is needed. To register the rings from particles having momenta as low as 10 GeV/c will require each of the two photon detectors to have 75x75 cm^2 area. Other operational requirements and geometrical considerations for the RICH can be found in Ref. 53.

The hit multiplicity in an efficient RICH photon detector would be 10-20 times higher than that found in a tracking chamber. Thus, in a high rate environment such as the 1994 run, the time resolution of the RICH photon detector must be comparable to the RF bucket spacing and it should provide a pixel-based, rather than projective, position measurement. None of the already existing gaseous photo cathode detectors have these properties and also high efficiency. In Ref. 53, we proposed an array of multianode photomultiplier tubes placed along the mirror focal plane as a solution to these requirements. Due to the high cost of that solution we have been investigating the use of an array of miniature single channel photomultiplier tubes instead.

In July 1992, we tested a several types of photomultiplier tubes in a small prototype RICH at BNL. The photons were detected by two clusters of 1.5cm diameter tubes (MELZ FEU68), one cluster of 2cm tubes (Amperex P1911) and a 7.5cm square Multianode tube (Hamamatsu R2489MOD). The distribution of the PMTs along the focal plane, with the superimposed hit pattern from an event, is shown in figure E.3.

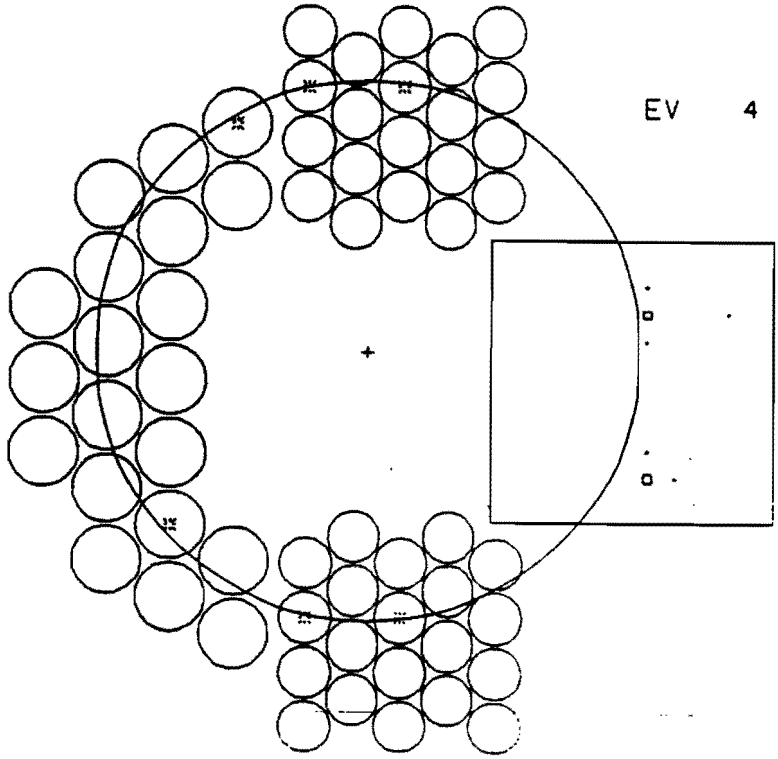

Fig. E.3
Results from July 1992 BNL Test

Experiment E781 has tested a much larger prototype device using similar miniature phototubes during the short E771 fixed target run[54]. To improve the geometrical packing fraction we propose to use for the E771 RICH 1.5cm square photomultiplier tubes which are currently being developed by MELZ in Moscow. Each detector array would require 2500 tubes. Samples of these tubes will be available in October of 1992 at a fraction of the cost of any other supplier.

In practice the geometrical packing fraction and quantum efficiency play a large role in determining the quality factor N_0;

$$N_0 \approx (370\ eV^{-1}\ cm^{1}) \cdot \langle QE \rangle \cdot \Delta E * \varepsilon$$

where <QE> is the average quantum efficiency over the full photon-energy bandwidth ΔE and ε is an additional loss factor. The tube entrance window will either be a UV glass or coated with a film of pTP to extend the sensitivity to the range 600-200nm (ΔE=4eV). If we assume a packing fraction of 45% (for square tubes) , optical efficiency of 80% and <QE> = 0.1, then we expect N_0 = 53/cm. In our prototype, we obtained N_0= 47/cm using round tubes while Ref. 54, which had somewhat better packign fraction, obtained N_0 = 66/cm.

For a gaseous radiator, where the dispersion is expected to be small, the average number of detected photons is given by

$$\langle N_{ph} \rangle = N_0 \cdot L \cdot \sin(\Theta)^2 \ ,$$

where L is the radiator length and $\Theta = \cos^{-1}(1/n\ \beta)$ is the Cherenkov angle. For $\beta \to 1$ particles $\Theta \to 1/\gamma_{threshold}$ and for a CF_4 radiator $\langle N_{ph} \rangle \sim 13$.

Given the track direction, each detected photon provides an independent measurement of the Cherenkov angle. There are several contributions to the error in this measurement.

* The geometric aberrations due to tracks having non zero impact parameter relative to the mirror center of curvature contribute $\Delta\Theta/\Theta$ = 1%.

* The chromatic dispersion of CF_4 contributes $\Delta\Theta \approx$ 0.13mrad over the range 200-600nm.

* As usual these effects are smaller than the error due to finite PMT position resolution given by

$$\Delta\Theta = s/(F \cdot \sqrt{12}) = .96 \text{ mrad}$$

for a 1cm photocathode.

The contributions due to tracking errors and multiple scatter are expected to be ≈ 3 times smaller. The error for an entire ring is given by adding in quadrature the above contributions and dividing by $\sqrt{(N_{ph})}$.

The above result can be used to estimate the efficiency for identifying a K of a given momentum. In the calculation, the expected π/K ratio must be specified to optimize the Cherenkov angle cut. We have chosen two values; π/K = 3 which might be expected for tracks stemming from secondary vertices and π/K = 10 which should be more appropriate for primary tracks. The result of the calculation is shown in figure E.4.

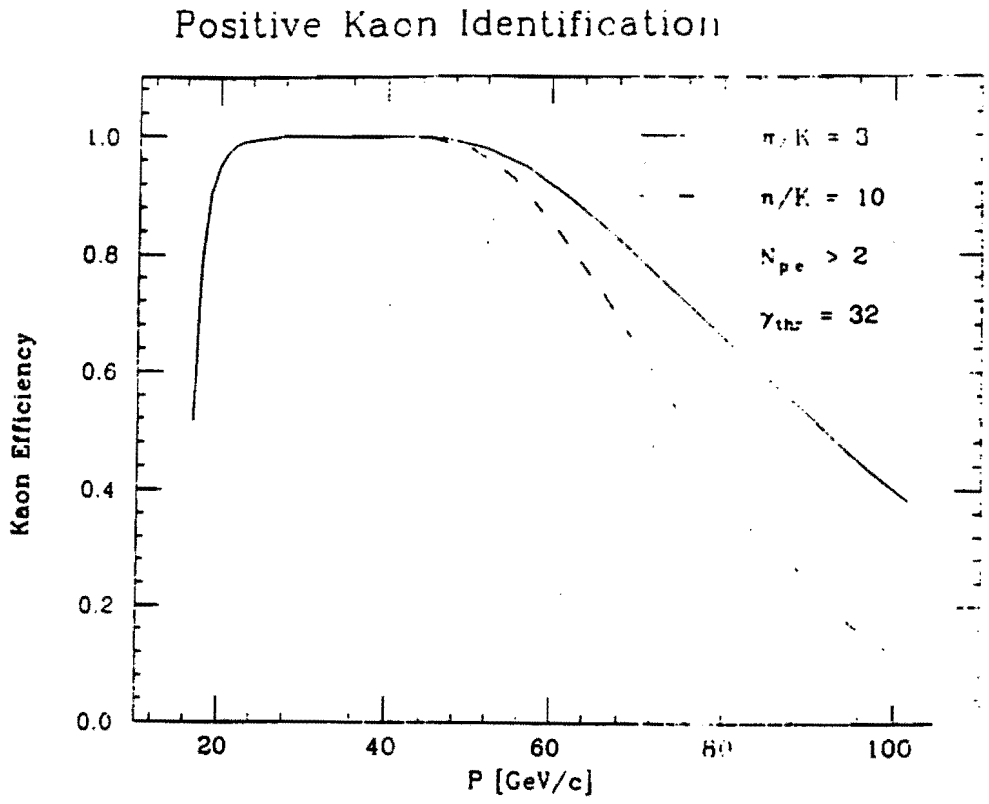

Fig. E.4
K Identification Efficiency as a Function of Energy

The loss in efficiency at low momenta is due to a requirement that at least 2 photons are detected since the K ceases to radiate in CF_4 below ≈ 16 GeV/c. Of course, if the proton contribution in this momentum range is negligible then one can still distinguish between K and π down to ~7 GeV/c. Alternatively a lower threshold radiator such as C_2F_6 could be used if necessary.

In addition to kaon efficiency, the Cerenkov angle cut also implies a background of pions which, because of the finite resolution, may pass the cut. Fig. E.5 shows the probability of misidentifying a K as a pion under two assumed π/K ratios. In general, if the track in question can be associated to a secondary vertex, then we expect a π/K background of less than 5% for P<60 GeV/c

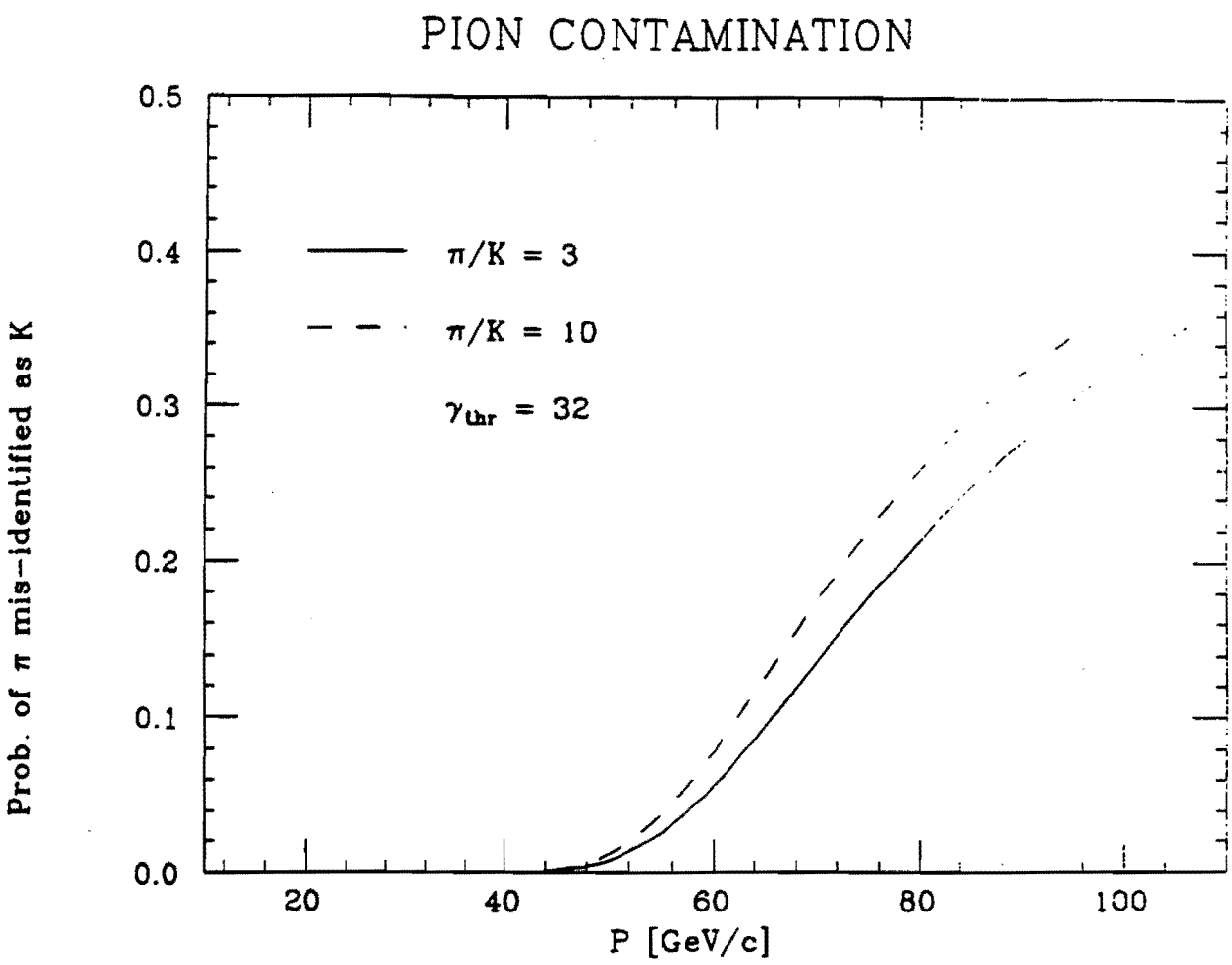

Fig. 5
Probablity of Misidenification of Pions as Kaons
as a Function of Momentum

As an example of the efficiency estimate, in Fig.E.6.a and b we show the momentum spectra for K from the decays

$$B^0_d \rightarrow \pi D_d \rightarrow K \pi \pi$$

and

$$B_s \rightarrow \pi D_s \rightarrow \phi \pi \rightarrow K K \pi$$

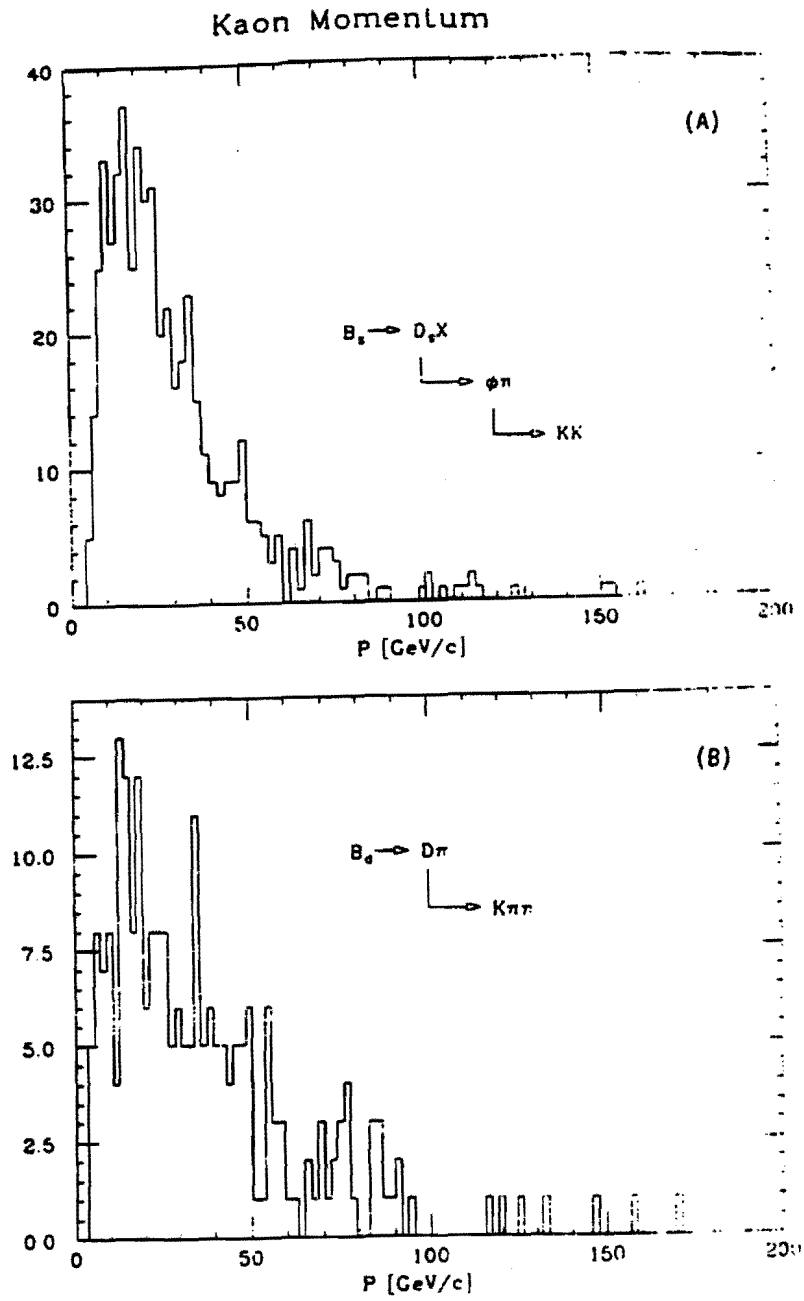

Fig. E.6
a) Momentum Spectrum for $B^0_d \to \pi D_d \to K\,\pi\,\pi$
b) Momentum Spectrum for $B^0_s \to \pi D_s \to K\,\pi\,\pi$

All particles are required to be in the spectrometer aperture and the recoil B must satisfy the 1B trigger. Monte Carlo studies are in progress to determine how much of the low momentum part of these spectra will be suppressed when a secondary vertex cut is applied to the events. Nevertheless, if we can ignore protons at low momentum, we expect ≥90% efficiency for identifying the K for $p_K > 7$ GeV/c and ≥80% efficiency when the entire momentum spectrum is considered.

For detection of the Λ_b, the RICH would be used to identify the protons from the secondary vertices. Figure E.6 shows the proton momentum spectra in semileptonic Λ_b decays in which two decay modes of the daughter Λ_c are considered;

$$\Lambda_c \rightarrow p\ K_S \text{ and } \Lambda_c \rightarrow p\ K\ \pi.$$

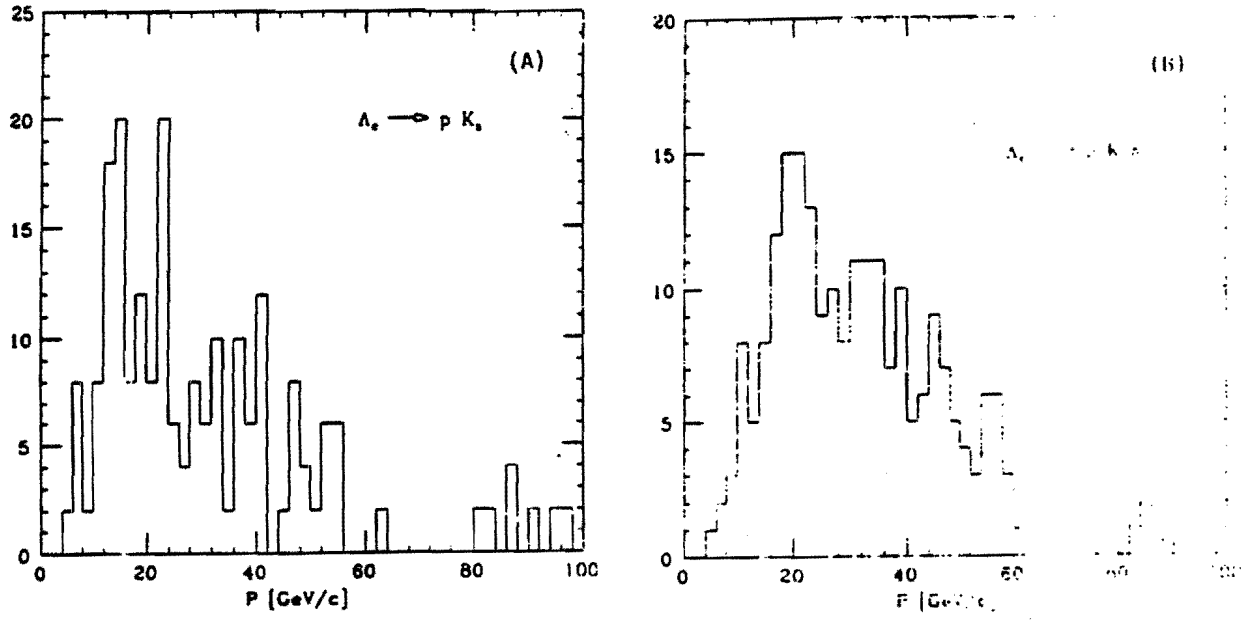

Fig. E.7
a) Momentum spectrum of the proton from $\Lambda_c \rightarrow p\ K_S$
b) Momentum spectrum of the proton from $\Lambda_c \rightarrow p\ K\ \pi$

Again only acceptance cuts have been performed on the final state particles. No vertex separation cut has been made. The relatively low momentum peak suggests using C_2F_6 as the radiator gas to distinguish between K and proton as low in momentum as possible. In this case we would expect an efficiency of 85% for identifying the proton. This efficiency is driven primarily at the low end of the spectrum by the threshold for radiation since the proton ring remains well separated from the K ring up to ~100 GeV/c.

In the above estimates no account has yet been taken of reconstruction inefficiencies due to overlapping rings. Certainly with adequate photon statistics one can afford to throw out ambiguous photon assignments. Also the background from pair production in the upstream material has not been taken into account. Detailed MC simulation of the detector is in progress to investigate these issues.

Finally, Table E contains the estimated cost of the device. Several caveats on these costs are included in the footnotes to the table.

Table E
Estimated Cost of the RICH Detector

Item	Cost
PMTs and Bases (5,000)	\$175K*
Power Supplies	--- **
Readout Electronics	\$ 20K***
Mirrors	\$ 60K****
Radiator Vessel (Material \$20K) (Labor *****) (Engineering \$10 K)	\$ 30K
Gas System	\$ 20K
Total	\$305K

* The FEU68 PM tubes which we have purchased for the prototype RICH test cost \$25 each plus a base cost of \$10. The gain of these tubes is low requiring use of sensitive amplifiers with a threshold of approximately 10^4 electrons. The newer, square tube should have higher gain and require less performance for the electronics.
** This assumes the PM HV supplies are available from PREP.
*** The bulk of the electronics is presumed to be supplied by Dubna. \$20K is the cost of adapting it to the RICH readout requirements.
**** Full cost is listed. Substantial reduction may be possible if Dubna can supply the mirrors
***** This presumes free or heavily subsidized time in the UVa and Berkeley shops. Otherwise approximately \$10K.

Appendix F

Preliminary Division of Effort/Cost Estimate for P867

The breakdown of preliminary funding requirements from five sources - Fermilab Research Division, Fermilab Computing, DOE University Division, INFN and the Fermilab Physics Section - is given below. The totals required from each source are $317K from Fermilab Research Division, $40K from Fermilab Computing, $155K from DOE University Division and $450K from INFN and $25K from Fermilab Physics Department. The Fermilab RD silicon electronics costs assume availability of previously purchased ASIC's and D/E memories.

Project	Institution	Estimates	Funding Source
Silicon MVD Completion	Fermilab	$317K	Fermilab RD
DA Readout	Fermilab	$ 40K	Fermilab Computing
PWC Elect. Rearrangements	Wisconsin Dubna	$ 15K	DOE University
Mj and Ey Trigger	UVa/Berkeley	$ 25K	DOE University
EM Detector Repairs	USA	$ 10K	DOE University
2nd Level Trigger	UVa/UCLA	$ 75K	DOE University
Silicon Beam Detector	Houston/PVAM	$ 30K	DOE University
Sub Total DOE University		$155K	
2nd Level Trigger/RPC Elect.	Pavia	$250K	INFN
Muon Detector Improvements	Lecce/Pavia	$200K	INFN
Sub Total INFN		$450K	
Beam Flux Measuring System	Fermilab	$ 10K	Fermilab Physics
Target /Tracker Mount	Fermilab	$ 15K	Fermilab Physics
Subtotal Fermilab Physics		$ 25K	

The RICH detector is still under discussion. Associated costs are found in Appendix E.